

Dissertation

An der Fakultät für Biologie

Der Ludwig-Maximilians-Universität München



**The tissue-specific action of FKBP51 in the
regulation of the acute stress response and
metabolism**



MAX-PLANCK-GESELLSCHAFT

Vorgelegt von

Alexander Häußl

München, Mai 2022

Dissertation eingereicht am: 19.05.2022

Mündliche Prüfung am: 24.11.2022

1. Gutachter: PD. Dr. Mathias V. Schmidt
2. Gutachter: Prof. Dr. Benedikt Grothe
3. Gutachterin: Prof. Dr. Angelika Böttger
4. Gutachter: Prof. Dr. Peter Geigenberger
5. Gutachter: Prof. Dr. Hans Straka
6. Gutachter: Prof. Dr. Christof Osman

Table of Contents

Table of Contents	i
List of abbreviations	iii
Summary	vi
Zusammenfassung	viii
1. General Introduction.....	1
1.1. The co-chaperone FKBP51	2
1.2. The biological concept of stress	3
1.2.1. Activation of the acute stress response.....	4
1.2.2. FKBP51 and the termination of the acute stress response.....	7
1.2.3. FKBP51 as a candidate in stress- and metabolic-related disorders	9
1.3. Obesity and the concept of energy homeostasis.....	11
1.3.1. Peripheral signals in the control of whole-body homeostasis	12
1.3.2. Mediobasal hypothalamic control of energy homeostasis.....	15
1.4. Autophagy	19
1.4.1. Importance of autophagy in metabolism	20
1.4.2. Autophagy regulation and core molecular mechanism	22
1.5. Aim of the thesis.....	25
2. Focus on FKBP51: A molecular link between stress and metabolic disorders	26
3. Research articles.....	39
3.1. Stress-responsive FKBP51 regulates AKT2-AS160 signaling and metabolic function.....	40
3.2. Mediobasal hypothalamic FKBP51 acts as a molecular switch linking autophagy to whole-body metabolism	77
3.3. The co-chaperone Fkbp5 shapes the acute stress response in the paraventricular nucleus of the hypothalamus of male mice	110
4. General discussion.....	137
4.1. FKBP51 in the control of metabolism.....	139
4.1.1. Total loss of FKBP51 improves metabolic health in mice.....	139
4.1.2. Hypothalamic FKBP51 manipulation affects food intake and body weight control.....	142
4.2. Underlying molecular mechanism regulated by FKBP51	145
4.2.1. FKBP51 regulates AKT in skeletal and adipose tissue	145
4.2.2. FKBP51 regulates autophagy by balancing AMPK and mTOR signaling.....	147
4.3. Translation to humans - FKBP51 a marker for psychiatric and metabolic disorders?	150

4.4. FKBP51 - a therapeutic option for stress-related and metabolic disorders?	152
4.5. Conclusion.....	153
5. References	154
Curriculum Vitae.....	171
List of Publications.....	173
Acknowledgement.....	176
Declaration of Contribution.....	178
Eidesstattliche Versicherung	181

List of abbreviations

α -MSH	Alpha-melanocyte stimulating hormone
AAV	Adeno-associated virus
ACTH	Adrenocorticotrophic hormone
AGRP	Agouti-related peptide
AKT	Protein Kinase B
AMBRA1	Beclin-1 regulated autophagy protein 1
AMPK	Adenosine monophosphate-activated protein kinase
ANS	Autonomic nervous system
ARC	Arcuate Nucleus
AS160	AKT substrate 160
ATG	Autophagy related gene
AVP	Arginine vasopressin
BAT	Brown adipose tissue
BBB	Blood-brain barrier
BMI	Body mass index
CART	Cocaine-and amphetamine regulated transcript
CCK	Cholecystokinin
CRH	Corticotropin-releasing hormone
CRHR1	Corticotropin-releasing hormone receptor 1
CMA	Chaperone-mediated autophagy
CNS	Central nervous system
Cort	Corticosterone
DFCP1	Zinc-finger FYVE domain-containing protein 1
DMH	Dorsomedial hypothalamic nucleus
FIP200	FAK family-interacting protein of 200 kDa
FK1	FK506 binding domain

FKBP	FK506 binding protein
FKBP51	FK506 binding protein 51
FKBP52	FK506 binding protein 52
FOXO1	Forehead box protein 1
GC	Glucocorticoids
GLP 1	Glucagon-like peptide 1
GR	Glucocorticoid receptor
GRE	GC response elements
GSK3 β	Glycogen synthase kinase 3 beta
HFD	High-fat diet
HPA axis	Hypothalamic-pituitary-adrenal axis
Hsp90	Heat shock protein 90
IR	Insulin receptor
JAK2	Janus kinase 2
KO	Knockout
LC3	Microtubule-associated protein 1 light chain 3
LepR	Leptin receptor
LH	Lateral hypothalamus
LKB1	Liver kinase B 1
MC2R	Melanocortin 2 receptor
MC3R & MC4R	Melanocortin receptor 3 & Melanocortin receptor 4
MD	Major depression
mRNA	Messenger RNA
MR	Mineralcorticoid receptor
mTOR	Mechanistic/mammalian target of rapamycin
NPY	Neuropeptide Y
NTS	Nucleus tractus solitarius
PAS	Phagophore assembly site

PE	Phosphatidylethanolamine
PGC-1 α	Peroxisome proliferator-activated receptor gamma coactivator 1-alpha
PHLPP	PH domain and leucine rich repeat protein phosphatase
PI3P	Phosphatidylinositol-3-phosphate
PPAR γ	Peroxisome proliferator-activated receptor gamma
PPIase	Peptidyl-prolyl <i>cis-trans</i> isomerase
PRDM16	PR domain containing 16
POMC	Pro-opiomelanocortin
PTSD	Post-traumatic stress disorder
PVN	Paraventricular nucleus of the hypothalamus
SAFit	Selective antagonist for FKBP51 induced fit
Ser	Serine
SF-1	Steroid factor 1
SHR	Steroid hormone receptors
SKP2	S-phase kinase-associated protein 2
SNP	Single nucleotide polymorphism
SNS	Sympathetic nervous system
SOCS3	Suppressor of cytokine 3
T2D	Type 2 diabetes
TEE	Total energy expenditure
Thr	Threonine
TPR domain	Tetratricopeptide repeat domain
TSC	Tuberous sclerosis complex
ULK1	Unc-51-like kinase 1
VMH	Ventromedial hypothalamic nucleus
VSP34	Class 3 phosphatidylinositol 3-kinase
WIPI	WD repeat domain phosphoinositide interacting protein
WT	Wild type

Summary

Obesity and stress related disorders are a major burden to modern societies and significantly impact public health worldwide. The FK506 binding protein 51 (FKBP51) has been identified as an essential regulator of signaling pathways associated with stress-related disorders and metabolic diseases. This thesis demonstrates further molecular and physiological evidence that FKBP51 acts in a tissue-specific manner to mediate the acute stress response, body weight control, and glucose metabolism.

In the first set of experiments, we investigated the role of global FKBP51 deletion on high-fat diet (HFD) exposure. We could show that FKBP51 knockout (KO) mice are protected from high-fat diet-induced weight gain, have improved glucose tolerance, and increased insulin signaling in skeletal muscle. Chronic treatment with a novel FKBP51 antagonist, SAFit2, recapitulated the effects of FKBP51 deletion on both body weight regulation and glucose tolerance. Mechanistically, we identified that FKBP51 regulates glucose uptake in muscle through the association between FKBP51 and AS160, a substrate of AKT2.

Next, we were interested in the role of FKBP51 in the hypothalamus, a key brain area involved in regulating whole-body metabolism. We investigated the impact of FKBP51 via hypothalamic-specific overexpression and deletion and observed an opposing phenotype compared to the global FKBP51 KO animals, which display a lean phenotype upon a high-fat diet. In fact, hypothalamic FKBP51 deletion strongly induced obesity on a regular chow diet, while its overexpression protected against HFD induced body weight gain. We further identified FKBP51 as a critical mediator for the LKB1/AMPK complex recruitment to WIPI4 and TSC2 to WIPI3, thereby regulating the balance between autophagy and mTOR signaling in response to metabolic challenges.

In the last study, we manipulated FKBP51 in the paraventricular nucleus of the hypothalamus (PVN) and investigated its role in the acute stress response. The study demonstrated that FKBP51 deletion dampens the acute stress response and increases GR sensitivity, while its overexpression results in a chronic hypothalamic-pituitary adrenal (HPA) axis overactivation. Furthermore, we identified a cell-type specific expression pattern of FKBP51 in the PVN and showed that FKBP51 expression is most upregulated in Crh⁺ neurons after acute stress. Interestingly, Crh-specific FKBP51 overexpression alters

Crh neuronal activity but only partially recapitulates the PVN-specific FKBP51 overexpression phenotype.

In summary, this thesis significantly extends the knowledge about the tissue-specific action of FKBP51 in the regulation of the acute stress response and whole-body metabolism and provides novel molecular binding partners of FKBP51.

Zusammenfassung

Adipositas und stressbedingte Erkrankungen stellen eine große Belastung für die moderne Gesellschaft dar und haben weltweit erhebliche Auswirkungen auf die Gesundheit der betroffenen Patienten. Das FK506-bindende Protein 51 (FKBP51) wurde als wesentlicher Mediator von Signalwegen identifiziert, die mit der Entstehung von stressbedingten Krankheiten und Stoffwechselerkrankungen in Verbindung gebracht werden. In der vorliegenden Arbeit wird gezeigt, dass FKBP51 die akute Stressreaktion, die Kontrolle des Körpergewichts und des Glukosestoffwechsel gewebespezifisch reguliert.

In der ersten Studie untersuchten wir die Rolle einer kompletten Deletion von FKBP51 während einer fettreichen Ernährung (HFD). Wir konnten zeigen, dass FKBP51-Knockout-Mäuse (KO Mäuse) vor einer fettreichen Diät-induzierten Gewichtszunahme geschützt sind, eine verbesserte Glukosetoleranz aufweisen und die Glukoseaufnahme im Muskel erhöht ist. Die chronische Behandlung mit dem neuen FKBP51-Antagonisten SAFit2 hatte ähnliche Effekte auf das Körpergewicht und den Glukosestoffwechsel wie in FKBP51 KO Mäusen. Mechanistisch haben wir festgestellt, dass FKBP51 die Glukoseaufnahme im Muskel durch eine Interaktion mit AS160 und AKT2 reguliert.

Als nächstes interessierten wir uns für die Rolle von FKBP51 im Hypothalamus, einer Schlüsselregion zur Regulierung des Ganzkörperstoffwechsels. Wir untersuchten die Auswirkungen einer hypothalamus-spezifischen Überexpression und Deletion und beobachteten einen gegensätzlichen Phänotyp im Vergleich zu den FKBP51-KO-Tieren. Die Deletion von FKBP51 im Hypothalamus führte bei normalem Futter zu einer Fettleibigkeit, während die Überexpression von FKBP51 vor der Gewichtszunahme durch eine HFD schützt. Darüber hinaus haben wir FKBP51 als wichtiges Bindeglied für die Rekrutierung des LKB1/AMPK-Komplexes an WIPI4 und TSC2 an WIPI3 identifiziert. Somit reguliert FKBP51 in Reaktion auf metabolische Veränderungen das Gleichgewicht zwischen Autophagie und mTOR-Signalwegen.

In der letzten Studie haben wir FKBP51 im Nucleus paraventricularis (PVN) manipuliert und seine Rolle bei der akuten Stressreaktion untersucht. Die Studie zeigte, dass die Deletion von FKBP51 die akute Stressreaktion dämpft und dabei die GR-Empfindlichkeit erhöht, während eine Überexpression zu einer chronischen Überaktivierung der Stressachse führt. Darüber hinaus haben wir ein

zelltypspezifisches Expressionsmuster von FKBP51 im PVN identifiziert und gezeigt, dass die FKBP51-Expression in Crh⁺-Neuronen nach akutem Stress am stärksten hochreguliert ist. Interessanterweise veränderte die Crh-spezifische Überexpression von FKBP51 die neuronale Aktivität von Crh, aber konnte nur teilweise den Phänotyp der PVN-spezifischen FKBP51-Überexpression wiederherstellen.

Diese Arbeit erweitert das Wissen über die gewebespezifische Funktion von FKBP51 bei der Regulierung der akuten Stressreaktion und des Ganzkörperstoffwechsels erheblich und zeigt dabei neue essentielle Bindungspartner von FKBP51 auf.

1. General Introduction

The corona pandemic interfered with the daily lives of billions of people, and measures to slow down the viral spread have caused economic and financial losses, loneliness, frustration and have substantially damaged adults' and children's emotional and psychological well-being¹⁻³. The subsequent long-term impact on mental health is still unclear, but researchers fear an upcoming wave of depressed and traumatized children and adults emerging from this pandemic³⁻⁶. It is estimated that about 4.4 % of the global population already suffer from depression, not considering undiagnosed cases⁷. The corona pandemic has further demonstrated the health risk of overweight and obesity worldwide. Studies have outlined that patients suffering from overweight or obesity are more likely to have a severe course of COVID-19 and a higher rate of hospitalization and death^{8,9}. In fact, obesity has emerged as a global pandemic itself, with a worldwide prevalence of 13 % of adults in 2016¹⁰. Thus, lack of mental stability and metabolic disorders represent two main health issues during a viral pandemic as well as in non-pandemic times. A growing body of literature indicates that mental and metabolic disorders are closely associated with each other, and research suggests that depressed patients display higher rates of obesity and related diseases, such as type 2 diabetes (T2D)^{11,12}. At the same time, people suffering from metabolic syndrome show increased rates of affective disorders¹³. Given its biological and physiological overlap¹⁴, it is crucial to untangle the underlying mechanism and gain a detailed understanding of molecules linking both disease groups. The last decades of intense research and advancing technology have revealed a plethora of molecules, signaling pathways, and organs involved in the development of both diseases. However, a molecular link between stress related and metabolic disorders remains still elusive. Human and animal studies have revealed the main protagonist of this thesis, the FK506 binding protein 51 (FKBP51), as a crucial regulator of the stress response and systemic metabolic control. This thesis aims to extend the existing knowledge about FKBP51 and explores its tissue-specific action in regulating the acute stress response and whole-body metabolism.

1.1. The co-chaperone FKBP51

Proteins are vital molecules, and their correct folding and functionality is essential for all biological processes maintaining every cell's life cycle. Therefore, protein quality control mechanisms, such as the regulation of protein synthesis, folding, unfolding, and turnover, are essential to avoid diseases or the aggregation of misfolded proteins. These processes are mediated by a plethora of diverse protein families, the chaperones and co-chaperones¹⁵. Molecular chaperones secure the functionality of proteins, especially in the recovery from stress conditions. The heat shock protein 90 (Hsp90) is the central chaperone mediating stress hormone signaling by efficiently loading steroids to steroid hormone receptors (SHRs). FKBP51 (encoded by the *FKBP5* gene) is a co-chaperone of Hsp90 and was first identified in complex with SHRs¹⁶. FKBP51 belongs to the highly conserved protein superfamily of immunophilins, which is defined by their ability to bind immunosuppressive drugs, such as FK506 (tacrolimus) and rapamycin (sirolimus)¹⁷.

Structurally, FKBP51 consists of three functional domains, facilitating multiple protein-protein interactions (Figure 1 A). The N-terminally located FK506 binding domain (FK1) confers peptidyl-prolyl *cis-trans* isomerase (PPIase) activity and is the primary regulatory domain for steroid receptor signaling and the binding domain of immunosuppressants¹⁸. The FKBP-like domain (FK2) shares structural similarity to the FK1 domain, but is catalytically inactive and does not bind immunosuppressive drugs¹⁹. Finally, the tetratricopeptide repeat (TPR) domain, a 34 amino acid sequence, is located at the C-terminus and facilitates Hsp90 binding to target proteins within steroid receptor complexes²⁰. The TPR domain has also been found to exhibit independent protein-folding activity²¹.

In addition to its function as a co-chaperone of the Hsp90 complex (see chapters 1.2.2 and 1.2.3), several studies have identified a diverse repertoire of kinases, transcription factors, and proteins as interaction partners of FKBP51 (Figure 1 B)^{22,23}. These multifaceted molecular abilities and interaction partners position FKBP51 as a promising target for therapeutic interventions in multiple disorders, such as cancer, depression, and obesity (discussed in chapter 2 and reviewed in-depth in^{19,24-26}). Interestingly, the development of antagonists specifically targeting FKBP51 proceeded rapidly during the last years,

offering new possibilities in FKBP51 research ²⁷. However, to fully establish FKBP51 as a drug target, it is of utmost importance to further investigate the molecular functions of FKBP51 in response to stress and metabolic challenges in detail.

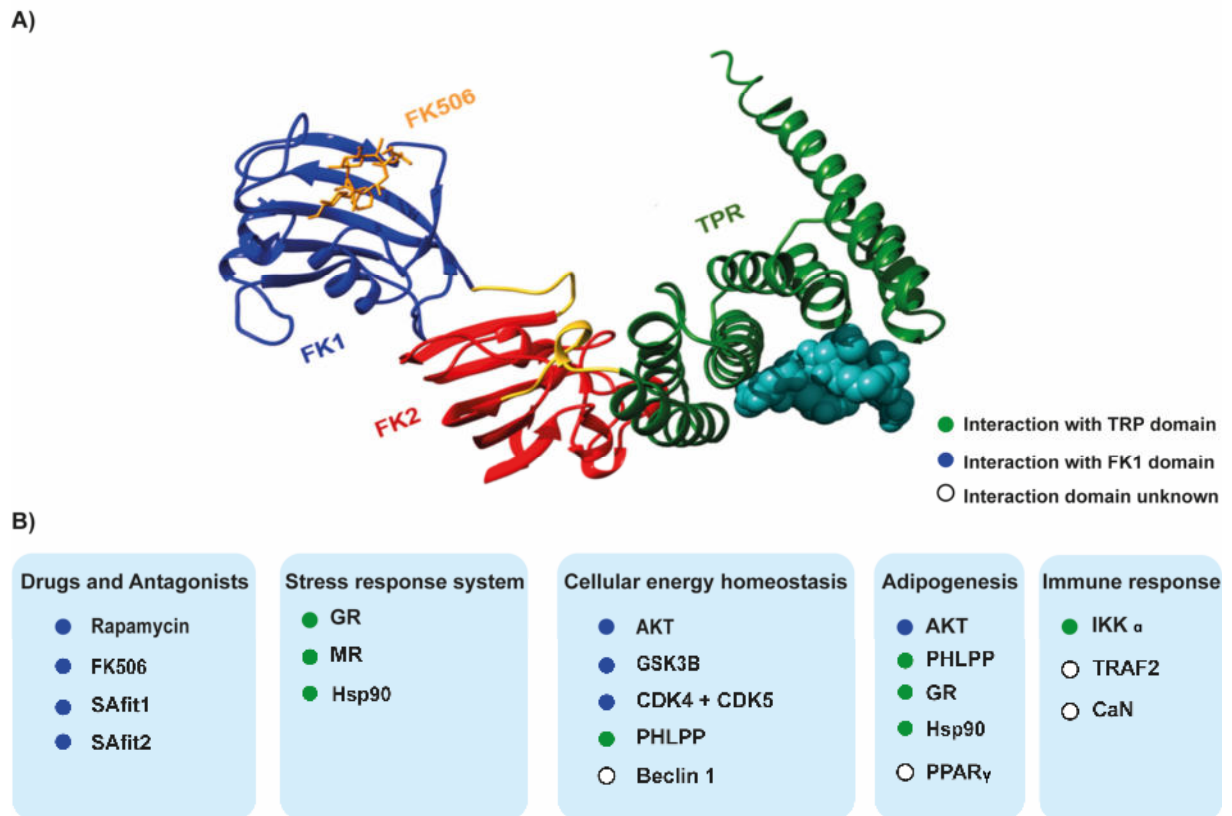


Figure 1: Structure and demonstrated binding partners of FKBP51. A) FKBP51 consists of three functional domains, including the tetratricopeptide (TRP) domain, the FK506 binding domains 1 (FK1) and 2 (FK2) (for detailed information, see text). B) FKBP51 interacts with multiple proteins, which are crucial in the regulation of the stress response, cell differentiation and homeostasis, and the immune response. Abbreviations: AKT, protein kinase B; Cort, corticosterone; CaN, calcineurin; CDK, cyclin-dependent kinase; GR, glucocorticoid receptor; GSK3 β , glycogen synthase kinase 3 beta; Hsp90, heat shock protein 90; IKK α , I κ B kinase α ; MR, mineralocorticoid receptor; PHLPP, PH domain and leucine rich repeat protein phosphatase; PPAR γ , peroxisome proliferator-activated receptor gamma; TRAF2, TNF receptor associated factor 2.

1.2. The biological concept of stress

Living organisms naturally strive to maintain stability for essential physiological parameters for survival, such as pH, blood pressure, and glucose levels. This process was initially described as homeostasis by Walter Cannon ³¹. Homeostasis can be disrupted by certain physical, psychological, or psychosocial events ^{32,33}, which are known as “stressors” and trigger physiological and behavioral

responses to reinstate homeostasis and prepare the body for future events. This so-called “stress” was firstly described by Hans Selye as the “general adaptation syndrome”, which he considered as an “emergency” and “fight or flight” response to a threat³⁴. He defined three distinct levels of which almost every organ system is affected. Upon stress, the organism first tries to restore homeostasis by the initiation of an alarm reaction. The resistance stage describes an status where adaptation to stress is optimally sustained. Finally, after prolonged exposure to stress, it comes to a stage of exhaustion, in which the organism is unable to respond sufficiently and this may eventually lead to illness³⁵. Peter Sterling and later Bruce McEwen built on Selye’s stress paradigm and introduced the term allostasis. In contrast to the “general adaptation syndrome”, allostasis is an ongoing process that describes the active adaptation to stressors and, more importantly, the anticipatory preparation for future events³⁵⁻³⁷. The ability to successfully adapt to stressful events depends heavily on the adequate activation of the stress response and the subsequent release of a non-linear network of stress mediators, such as neurotransmitters, peptides, and steroid hormones³⁶. This network of primary mediators involves an efficient and highly conserved set of interlocking systems with the brain as its central organ. Different regions in the brain (e.g., amygdala, hippocampus, and hypothalamus) perceive and integrate the information of internal and external stressors and adequately orchestrate biological mechanisms to reinstate homeostasis³³. The adaptation to stressors is a protective system and most valuable when it can be rapidly mobilized and turned off in times of no need. However, the activation of the stress response can not only protect but also damage the body. Prolonged exposure to stress or chronic activation of stress pathways can promote a dysregulated response system (=allostatic load/overload)³⁶, leading to an inadequate stress response, increased vulnerability, and ultimately growing risk for various metabolic, neurological, cardiovascular, and mental diseases^{38,39}.

1.2.1. Activation of the acute stress response

The stress response is primarily driven by mediators released of two critical systems, the short-lived response of the autonomous nervous system (ANS) and the slower long-term response of the hypothalamic-pituitary-adrenal (HPA) axis. The ANS innervates multiple peripheral tissues and is triggered within seconds following a stress exposure to initiate the “fight or flight” reaction, which is characterized by increased alertness, appraisal, and vigilance. The peripheral endings of the sympathetic

nervous system (SNS) enable a rapid secretion of catecholamines, such as noradrenaline and adrenaline. Both hormones facilitate energy mobilization to adjust to short-term needs³³.

The HPA axis is the second control module of the stress response in mammals. It is tightly regulated at three distinct levels: the hypothalamus, the pituitary, and the adrenal glands (Figure 2).

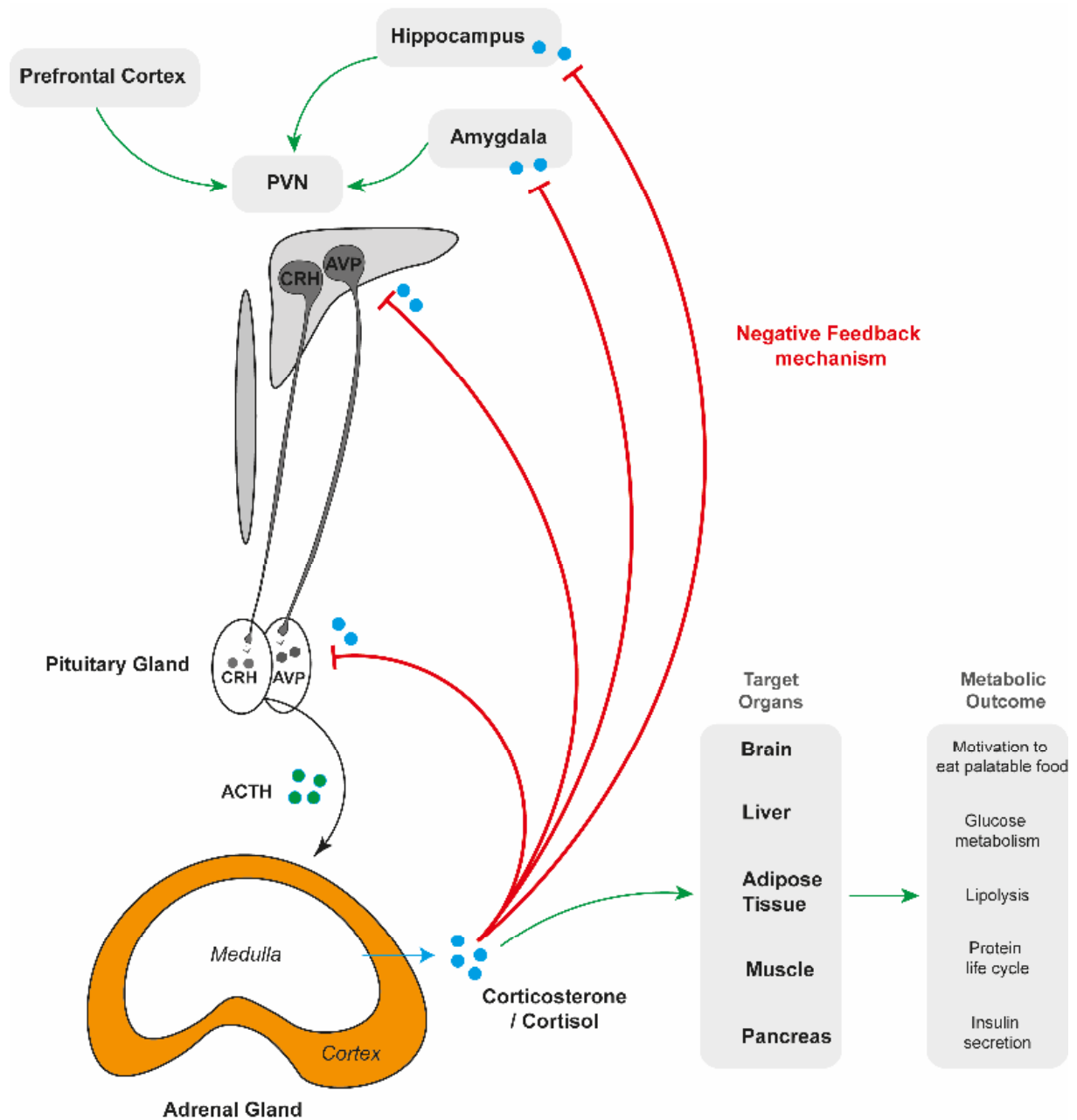


Figure 2: The hypothalamic-pituitary-adrenal axis: Upon stress exposure, a signaling cascade originating from higher brain areas leads to the secretion of corticotropin-releasing hormone (CRH) and vasopressin (AVP) in the paraventricular nucleus of the hypothalamus (PVN), which triggers the release of adrenocorticotropic hormone (ACTH, green circles) and finally results in the peripheral release of corticosterone (blue circles). Corticosterone is then transported to multiple target organs, such as muscle, brain, and adipose tissue, to stimulate metabolic

processes for energy mobilization. At the same time, corticosterone inhibits the continuous release of stress hormones by a negative feedback loop, which targets the pituitary and several nuclei within the central nervous system, such as the hippocampus, amygdala and PVN (red arrows).

Within the hypothalamus, the paraventricular nucleus of the hypothalamus (PVN) is crucial for an adequate activation of the HPA axis. The PVN consists of multiple neuronal subpopulations that integrate “stress information” of limbic brain regions and brainstem nuclei to initiate the HPA axis stress response. The corticotropin-releasing hormone (CRH or corticotropin-releasing factor [CRF]) and vasopressin (AVP) expressing neurons are the main neuronal populations initiating HPA axis activation. CRH and AVP neurons are located in the parvocellular subdivision of the PVN and project to the external layer of the median eminence³³. Upon stress, both are activated and rapidly release the neuropeptides CRH and AVP into the hypophyseal portal plexus of veins. Both neuropeptides then travel to the anterior part of the pituitary gland^{40,41}. At the level of the pituitary, CRH binds to corticotropin-releasing hormone receptor 1 (CRHR1) on corticotrope cells and thereby activates the adenylate cyclase to initiate the synthesis and release of pro-opiomelanocortin (POMC). POMC is immediately cleaved into ACTH by the prohormone convertase 1⁴². Via binding to AVP receptors (AVPR1), AVP works in conjunction with CRH and markedly potentiates the actions of CRH. However, AVP is not sufficient to drive significant ACTH release on its own⁴³⁻⁴⁵. After the release into the systemic circulation, ACTH circulates through the bloodstream and reaches the secretory cells of the *zona fasciculata* and the *zona reticularis* of the inner adrenal cortex. Within the adrenal cortex, ACTH acts on melanocortin 2 receptors (MC2R). ACTH binding to MCR2 causes a rapid increase in cholesterol biosynthesis and thereby the secretion of glucocorticoids (GCs, cortisol in humans, and corticosterone in mice/rats) as well as mineralocorticoids. GCs are the primary outcome of the HPA axis stress response and mobilize, redistribute, and conserve energy for energetic demands. Furthermore, GCs can have long-lasting effects on brain regions that prepare the body’s stress response to adapt to future stressful events⁴⁶. Notably, GCs are not only secreted after acute stress but are constantly released in a pulsatile manner following an ultradian rhythm under non-stressed conditions⁴⁷.

1.2.2. FKBP51 and the termination of the acute stress response

The recovery to baseline GC levels after a stressful situation is critical for effective stress coping and for reducing maladaptive effects on the body⁴⁶. The termination of the stress response heavily depends on functional GC signaling and involves both a fast non-genomic (“fast feedback”) and delayed genomic feedback (delayed feedback) mechanism⁴⁸. The negative feedback inhibition occurs in several brain regions, but primarily in the hypothalamus, hippocampus, and the pituitary gland (Figure 2). The so-called “fast feedback” occurs within minutes and is mediated by membrane-associated receptors of GC, which cause rapid synthesis and mobilization of endocannabinoids⁴⁹. The endocannabinoids bind CB1 receptors on presynaptic terminals, inhibiting glutamate release and thereby reducing CRH neurons' firing and reducing subsequent ACTH release⁵⁰.

GCs mediate its long-lasting genomic effects via two different types of steroid receptors, the mineralocorticoid receptor (MR) and the glucocorticoid receptor (GR). Both receptors are primarily cytosolic receptors and belong to the ligand-dependent transcription factor family⁴⁶. MRs have a high binding affinity to GCs and are thought to mediate GCs action during the nadir of the circadian rhythm⁴⁸. In contrast to the MR, the GRs have a ten-fold lower binding affinity. Thus, it is suggested that GRs are the receptors that mediate the response to GCs during acute stress and the circadian peak⁵¹. In the absence of GCs, both receptors are primarily localized in the cytoplasm. However, GR and MR can constantly cycle between the cytosol and nucleus by simple diffusion⁵² and the active transport of GR and MR is thought to function via a rapid dynein-dynactin mechanism²⁴. Both receptors are part of a multiprotein complex that includes the chaperone Hsp90 and various co-chaperones and molecules (depicted in Figure 3).

The co-chaperones, such as FKBP51, define the complex's conformation state and thereby regulate its ligand's binding capacity. Under low GC levels, the Hsp90 complex is primarily located in the cytosol and bound to FKBP51, which reduces the binding affinity of the complex to GC^{53,54}. Upon binding of GCs, FKBP51 is replaced by its closest homologue, FKBP52. FKBP52 shares 70% similarity to FKBP51, and both proteins compete for the Hsp90 binding site^{16,24}. In contrast to FKBP51, FKBP52 is able to bind the dynein-dynactin transport machinery via its PPIase domain. Thus, the replacement of

FKBP51 by FKBP52 actively mediates the translocation of GRs from the cytoplasm to the nucleus⁵⁵. In the nucleus, GR and MR form homo- and heterodimers that bind to the GC response element (GRE) of GC responsive genes to alter transcription and protein synthesis of various target genes. GR monomers can also directly regulate the activity of multiple transcription factors to diminish their transcriptional activity⁴¹. Interestingly, active GR and MR induce FKBP51 expression and thus initiate an ultra-short negative feedback to reduce its own activity (Figure 3)⁵⁶. Furthermore, high levels of FKBP51 were shown to disrupt the FKBP52-mediated recruitment of the dynein-dynactin complex and consequently attenuate the nuclear translocation of GR^{19,55}. Excess FKBP51-Hsp90 complexes mediate a conformational change of GR and reduced steroid-binding affinity^{53,54}. Loss of FKBP51, on the other side, increases GR sensitivity to GCs and thus increases the activity of GR⁵⁷.

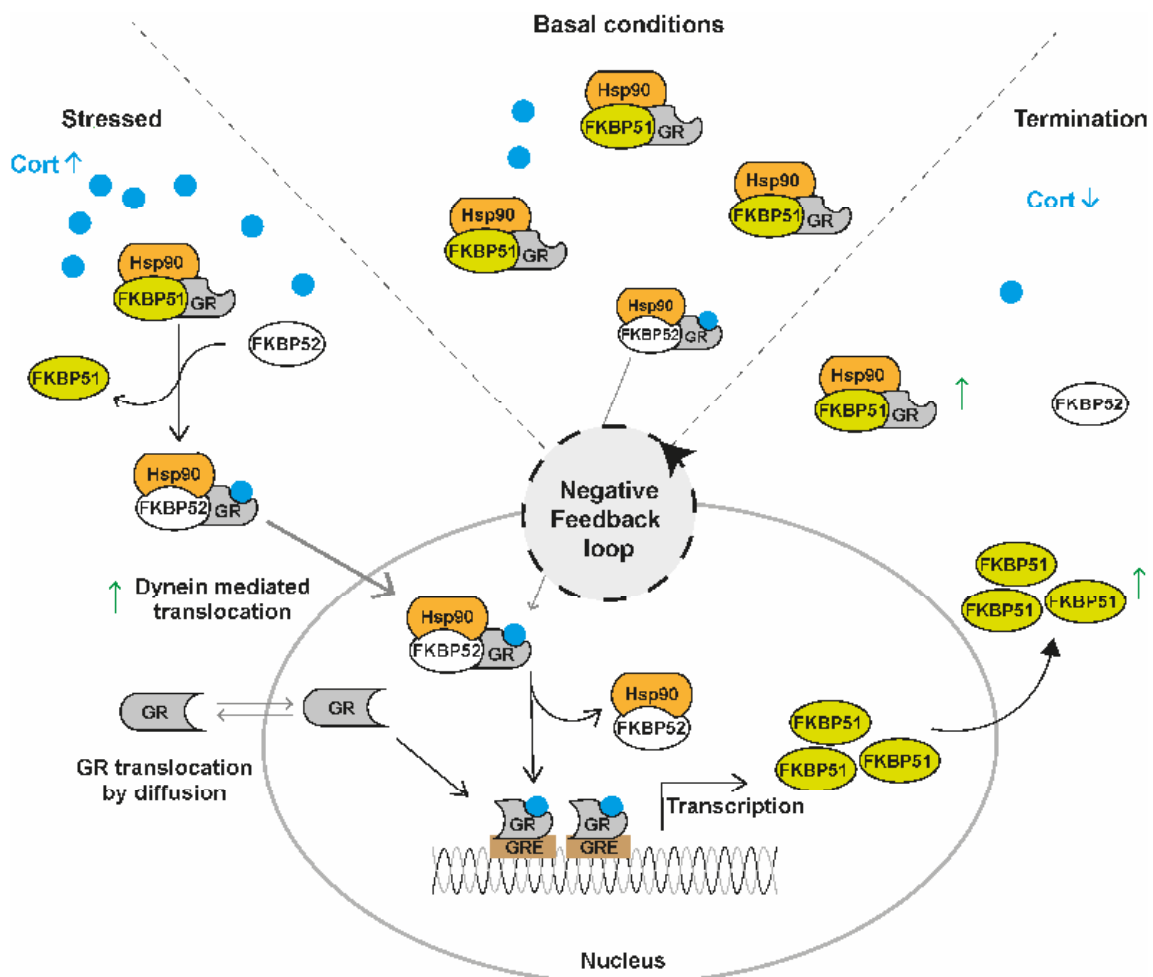


Figure 3: FKBP51 regulates GR sensitivity via an ultra-short negative feedback loop. Under basal conditions, FKBP51 is bound to the GR-complex via Hsp90 and consequently reducing the affinity of the receptor to corticosterone. Upon stress, corticosterone concentrations rise within the cytoplasm, which leads to a replacement of FKBP51 by FKBP52 and subsequent translocation of the FKBP52-Hsp90 complexes into the nucleus. Within 8

the nucleus, GR dissociates from the heterocomplex and binds to DNA binding sites to induce transcription of target genes. One target gene of GR is FKBP51 itself, and increased levels of FKBP51 reduce the cellular glucocorticoid responsiveness by an increased concentration of GR-FKBP51-Hsp90 complexes. Abbreviations: Cort, corticosterone; FKBP51, FK506 binding protein 51; FKBP52, FK506 binding protein 52; GR, glucocorticoid receptor; Hsp90, heat shock protein 90; GRE, glucocorticoid response elements.

Taken together, the FKBP51-Hsp90 complex functions as a short, negative feedback regulator of GR signaling to terminate stress hormone production and consequently the HPA axis response to acute stress. Notably, FKBP51-Hsp90 complexes regulate the GR and MR sensitivity to changes in basal and stimulated GC levels, and dysregulation of the FKBP51-Hsp90 complex is considered to increase the susceptibility to the development of mental disorders ^{56,58}.

1.2.3. FKBP51 as a candidate in stress- and metabolic-related disorders

A healthy response to an acute stressor requires both rapid activation and subsequent termination of the HPA axis to avoid maladaptive effects of excess stress hormones ³⁷. As already mentioned, dysregulation of the HPA axis is associated with several mood and metabolic disorders, such as depression and PTSD ⁴⁶, and the search for an appropriate marker and target for therapeutic intervention is still ongoing. FKBP51 is one of the most promising candidates with profound evidence for an association with stress-related disorders ^{19,25}.

Preclinical studies demonstrated that acute and chronic stress upregulates FKBP51 in stress-sensitive brain regions, such as the PVN and hippocampus ^{57,59,60}. In addition, a study by Touma and colleagues on FKBP51 deficient (FKBP51 KO) adult mice, demonstrated a better active stress-coping behavior of FKBP51 KO mice than their controls following a single stress exposure ⁶¹. Furthermore, FKBP51 KO mice subjected to three weeks of chronic social stress were less vulnerable with a reduced response to and enhanced recovery from acute stress episodes ⁵⁷. The improved stress resilient phenotype of FKBP51 KO mice is proposed to be due to an improved sensitivity of GCs to GR ⁵⁷.

In humans, research demonstrated the association of *FKBP5* polymorphisms or variants with stress-related disorders, such as bipolar disorders ⁶², suicidal events ^{63,64}, childhood trauma ⁶⁵, PTSD ⁶⁶, and depression ⁶⁷. The experimental data so far suggests that elevated expression of FKBP51 is accompanied with psychiatric disorders. In line with that notion, a study by Yehuda and colleagues has identified that

decreased levels of FKBP51 correlates with enhanced GR sensitivity in PTSD patients ⁶⁶. These data in human studies are in line with the abovementioned results from preclinical studies.

FKBP51 is ubiquitously expressed in stress responsive brain regions, with high expression patterns in the hippocampus and prefrontal cortex ⁶⁰. Other regions, such as the PVN and amygdala, show low FKBP51 levels under basal conditions but a strong induction of FKBP51 after acute stress ⁶⁰. These observations suggest a prominent role of FKBP51 in the acute stress response. Despite the stress-sensitive expression pattern of FKBP51, most of the current studies were performed on full knockout mice. Tissue and nuclei-specific studies, however, are still rare. In particular, the role of FKBP51 in the PVN is still hardly studied, despite its high mRNA induction after mild and moderate stress ⁶⁰. Thus, this thesis aims to develop the necessary technical tools, such as suitable mouse models, to further investigate the PVN-specific role of FKBP51 in regulating the acute stress response (see chapter 3.3).

1.3. Obesity and the concept of energy homeostasis

In most of the 7 million years of human evolution, the supply of food intake was not as stable as today and was characterized by constant foraging and hunting. Overeating and the accumulation of extra calories when food was available was essential for energy supply in times of metabolic needs to ensure survival. The mammalian body has developed a highly efficient system to stabilize body weight and food intake over a more extended period. For example, in a decline in adipose mass, the body activates anabolic systems to stimulate hunger and decreases energy expenditure to increase energy stores to previous levels. On the other hand, the body automatically reduces appetite and facilitates energy utilization when energy stores are sufficient⁶⁸. Hence, the body constantly tries to maintain a healthy balance between energy intake and energy expenditure. However, in our modern lifestyle of highly processed food with unlimited supply, the habit of frequent snack consumption, less physical exercise, and a work environment requiring little movement bears a high risk of the development of overweight (body mass index (BMI) > 25 kg per m²) and obesity (BMI ≥ 30 kg per m²)⁶⁹. Consequently, the worldwide prevalence of obesity has tripled since 1975 and emerged as one of the major health burdens, with more than 1.9 billion adults being overweight and 650 million obese in 2016^{70,71}. Individuals suffering from obesity are associated with an increased risk of insulin resistance, diabetes, cardiovascular disease, cancer, and decreased life expectancy^{72,73}. In the last decades, it became clear that many psychological factors, such as depression and anxiety, are highly associated with symptoms of the metabolic syndrome, such as obesity and diabetes. In fact, adverse effects of psychological stress, either chronic or early life stress conditions, affect food choices and physical activities and are a risk factor for the development of obesity⁷⁴. Notably, obese individuals develop a robust mechanism promoting weight gain and adapting their energy homeostasis system to protect their high body weight even under targeted weight-loss attempts, such as diets⁷⁵⁻⁷⁷. Thus, obesity is often seen as a chronic, relapsing progressive disease^{77,78}. Obesity is not only caused by “unhealthy” personal choices but rather by the relationship between personal behavior, individual energy expenditure levels, and environmental factors⁷⁶. Therefore, it is essential to identify new molecules and signaling pathways suitable for novel treatment avenues.

Whole-body energy homeostasis is highly regulated by a complex interplay between central and peripheral pathways in multiple organs and tissues, including the brain, adipose tissue, skeletal muscle, liver, and pancreas. This regulatory process can also be seen as an adaptive energy homeostasis system where the brain mediates changes in response to peripheral signals that circulate at concentrations proportionate to body fat in order to stabilize energy balance ^{79,80}.

1.3.1. Peripheral signals in the control of whole-body homeostasis

Peripheral signals have short-term and long-term effects and are secreted from metabolic active organs, being fat tissue, the gut, and the pancreas. While numerous environmental factors, such as stress, influence the initiation of food intake, satiety perception, and meal termination are biologically conserved processes triggered by internal peptides secreted from the gastrointestinal tract during meals⁸⁰. The most studied satiety factors are cholecystokinin (CCK) and glucagon-like peptide 1 (GLP1), which provide short-term energy information to the central nervous system (CNS). CCK and GLP1 signal via the vagus nerve from the gut to the brain to inhibit feeding and initiate meal termination. This information converges in the nucleus tractus solitarius (NTS), an area of the caudal brainstem that integrates sensory information ⁸¹. These satiety peptides are short-lived, and studies demonstrated that chronic injections of CCK decreased meal size but did simultaneously increase meal frequency and thus had minor effects on long-term body weight ⁸⁰. Just recently, the gut-brain axis and the composition of the microbiome have received increasing attention because of their profound impact on whole-body metabolism and psychiatric disorders ^{82,83}.

Long-term feedback signals, like leptin, adiponectin, and insulin, act on multiple tissues, such as the brain, to regulate the balance between food intake and energy expenditure over long periods of time ⁸⁰. Leptin is secreted by adipocytes of white adipose tissue in proportion to levels of internal triglyceride stores and can be seen as a “mirror” of the body’s energy status. Under normal physiological conditions, leptin acts as a signal of energy sufficiency by suppressing feeding and stimulating energy expenditure⁸⁴. Leptin deficiency is associated with hyperphagic individuals with decreased energy expenditure, which results in massive obesity in mice (e.g., *ob/ob* mouse) and humans ⁸⁵⁻⁸⁷. Interestingly, under a state of metabolic stress, such as obesity, leptin levels increase in proportion to the body fat mass but lose their

efficiency as anorexic hormones to reduce food intake⁸⁸. In line with that, administration of exogenous leptin reverses obesity only in individuals lacking leptin or the leptin receptor (LepR) and does not affect obese individuals with high leptin levels⁸⁸, which are thought to develop a state of leptin resistance. The detailed molecular mechanism of leptin resistance is largely unknown, but researchers suggest that leptin resistance might result from impaired intracellular signaling and defects in the transportation across the blood-brain barrier (BBB)⁸⁹.

Leptin mediates its action through the long form of the LepR, which is highly expressed in brain regions that are crucial in the control of energy balance, such as the hypothalamus⁹⁰ and a loss in LepR function (e.g. *db/db* mouse) causes massive obesity similar to *ob/ob* mice^{91,92}. The LepR is also expressed in other brain regions, such as the midbrain and hindbrain (e.g., NTS) with a suggested role in the signal transduction of gut-derived satiety signals, such as CCK⁹⁰. Mechanistically, leptin mediates its action by LepR binding and subsequent activation of the Janus kinase-2 (JAK2)/STAT3 pathway⁹³ (depicted in Figure 4 A). A critical regulator of leptin signaling is SOCS3 (suppressor of cytokine 3) that limits leptin signaling and is thought to play a key role in leptin resistance⁸⁹.

Insulin is secreted rapidly in response to feeding (or elevated blood glucose) by β -cells in the pancreas, and defects in insulin signaling are associated with type 1 and type 2 diabetes. Like leptin, insulin circulates at levels proportionate to body fat mass and acts tissue-specific to regulate peripheral and central glucose metabolism^{94,95}. In the periphery, insulin stimulates glucose uptake of skeletal muscle and adipose tissue and suppresses hepatic gluconeogenesis in the liver. Through its ability to cross the BBB, insulin profoundly affects the activity of a diverse set of neuron populations located in the hypothalamus regulating food intake and glucose metabolism⁹⁶. For instance, the acute administration of insulin directly into the CNS reduces feeding and body weight gain^{95,97}, and the inhibition of insulin signaling in the hypothalamus causes obesity and T2D⁹⁸.

Insulin mediates its effects through the insulin receptor (IR), expressed in various tissues throughout the body, including different brain regions⁹⁶. The IR is a highly conserved tyrosine kinase receptor with the PI3K (class III phosphoinositide 3-kinase)/AKT pathway as its primary downstream target (see Figure 4 B), mainly responsible for insulin's metabolic effects. Downstream of the PI3K/AKT cascade are

multiple signaling pathways, such as the forkhead box protein 1 (FOXO1) and mTORC1 (mechanistic/mammalian target of rapamycin complex 1) pathway⁹⁹. The critical signaling hub of these pathways is the serine-threonine (Ser/Thr) kinase, AKT, which has been shown to regulate those pathways directly¹⁰⁰. Interestingly, a study by Pei et al. has demonstrated that FKBP51 is able to interact with all three isoforms of AKT (AKT1, AKT2, and AKT3) via the phosphatase PHLPP to inhibit AKT signaling in cancer cells²⁸. Furthermore, AKT2 is the isoform most responsible for regulating glucose homeostasis in muscle and adipose tissue, in which FKBP51 shows its highest expression in the periphery¹⁰¹. Given the overlapping expression pattern and molecular action, it is worth investigating a possible novel role of peripheral and central FKBP51 in the control of glucose metabolism.

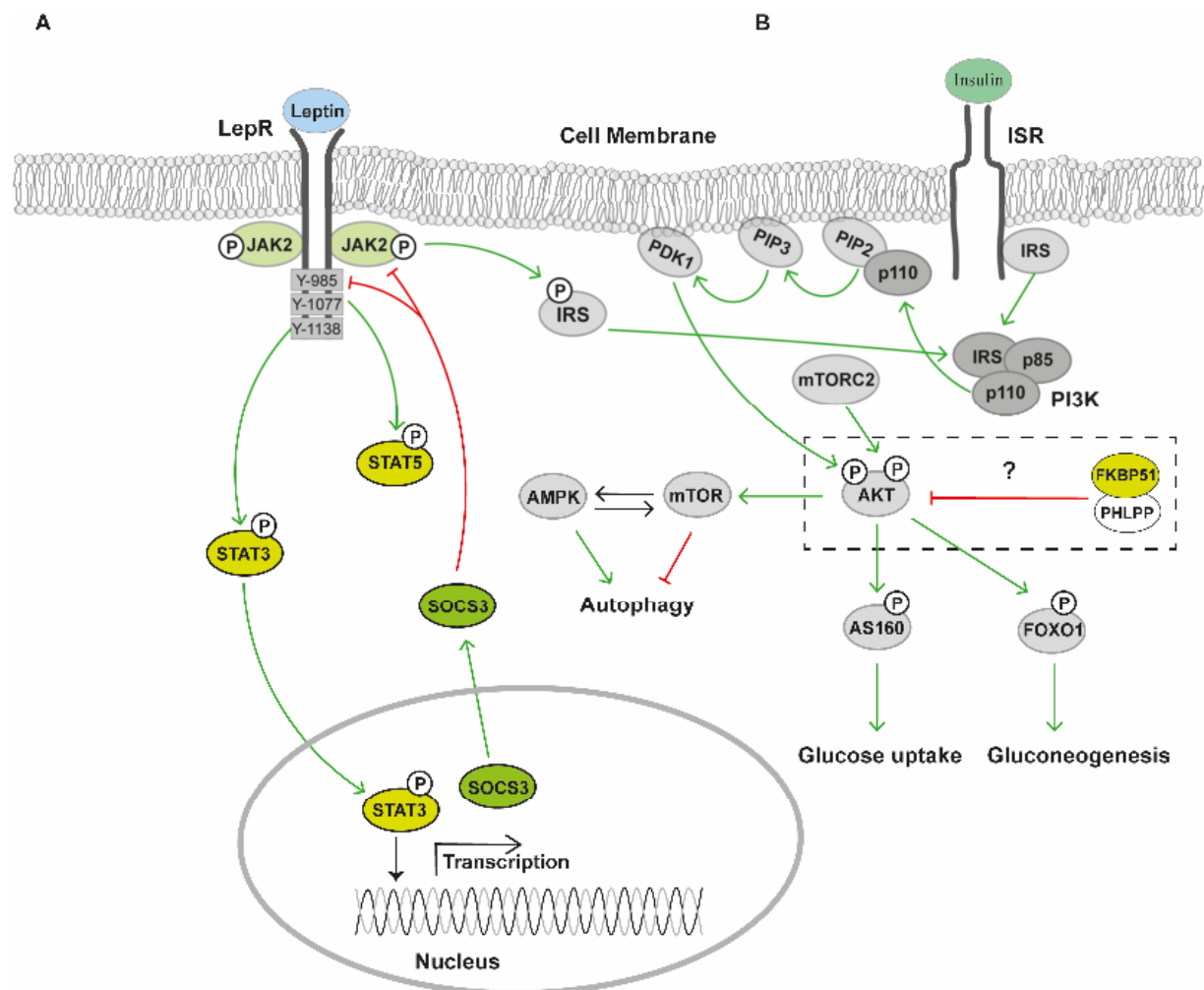


Figure 4: Insulin and leptin signaling pathways. A) Circulating leptin binds to its leptin receptor, which triggers the activation of the tyrosine-protein kinase JAK2. Activated JAK2 phosphorylates the LepR residues Y-985, Y-1077, and Y-1138, which triggers activation of the downstream targets STAT3, and STAT5, respectively. The induction of STAT3 induces the expression of SOCS3, which in turn binds to Y-985 to inhibit leptin signaling.

B) Insulin binds to its receptor to initiate the PI3K-dependent cascade which leads to the phosphorylation and activation of AKT. Activated AKT promotes glucose uptake via the phosphorylation of AS160. Both signaling pathways regulate AMPK and mTOR and thereby also autophagy signaling. A potential role of FKBP51 in insulin signaling pathway is not yet known, but FKBP51 was shown to negatively regulate AKT via PHLPP in cancer cells. Abbreviations: FOXO1, forkhead box protein 1; JAK2, Janus kinase 2; mTOR, mammalian target of rapamycin; PHLPP, PH domain and leucine rich repeat protein phosphatase; PI3K, phosphoinositide 3 kinase; SOCS3, suppressor of cytokine signaling 3; STAT5, signal transducer and activator of transcription 5.

1.3.2. Mediobasal hypothalamic control of energy homeostasis

The crucial role of the brain, especially of the MBH, in the regulation of feeding behavior was first demonstrated in the mid-20th century with lesion studies ^{102–104}. Since then, it was further revealed that the MBH, alongside nuclei in the hindbrain (such as the NTS), is the key brain region for integrating and processing incoming peripheral information to coordinate an appropriate physiological response to metabolic stressors, such as starvation and prolonged overnutrition.

The MBH consists of multiple nuclei, including the arcuate nucleus (ARC), the PVN, dorsomedial hypothalamic nucleus (DMH), ventromedial hypothalamic nucleus (VMH) and the lateral hypothalamic nuclei (LH). The ARC is a master regulator of whole-body metabolism, as it is located adjacent to the median eminence at the base of the hypothalamus. It integrates peripheral hormones (e.g., leptin and insulin) and nutrients (e.g., glucose and free fatty acids) to orchestrate a coordinated feedback response to changes in peripheral energy stores ¹⁰⁵. The most researched and best-characterized neuronal subpopulations within the ARC are AGRP (agouti-related protein) and POMC expressing neurons, which act in an opposing manner on second-order neurons located in brain regions outside the ARC (e.g., PVN, VMH, DMH and LH,) to modulate food intake and systemic energy metabolism ⁸⁰ (depicted in Figure 5). This microcircuit is often referred to as the melanocortin system and has emerged as a crucial element of the energy homeostasis system. In addition, multiple other neuronal populations (e.g., tyrosine hydroxylase expressing neurons ¹⁰⁶ or prepronocopetin-expressing neurons ¹⁰⁷) and non-neuronal cells, such as astrocytes, were also shown to regulate whole-body metabolism ¹⁰⁸.

POMC neurons (co-expressing cocaine- and amphetamine-regulated transcript [CART]) are activated after nutrient ingestion and synthesize α -MSH (α – melanocyte stimulating hormone), by the cleavage

of POMC, to activate MC3R (melanocortin receptor 3) and MC4R (melanocortin receptor 4) on second order neurons in the PVN to inhibit food intake ⁹⁴. MC4R activation by POMC neurons also increases the activity of the SNS, leading to heightened brown adipose tissue (BAT) activity and an increase in energy expenditure ¹⁰⁹. The PVN itself, is considered a major nuclei in the control of energy homeostasis, as it was shown that deletion of the MC4R in the PVN resulted in hyperphagia and severe obesity in mice and humans ^{110,111}.

AgRP neurons (co-expressing neuropeptide Y [NPY]) lie adjacent to POMC neurons and are activated by fasting to stimulate feeding by releasing the neuropeptide AgRP, which acts as an antagonist to MC4R signaling in the PVN and thereby reduces its anorexigenic function ¹¹². NPY directly stimulates food intake via the activation of NPY receptors (Y1 and Y5) and reduces sympathetic output to BAT via a Y1 receptor-mediated reduction in tyrosine hydroxylase expression in the PVN, resulting in decreased energy expenditure ¹⁰⁵. In addition, AgRP/NPY neurons can directly inhibit the activity of POMC neurons by GABAergic inputs, which further facilitates positive energy balance ¹¹³.

Both neuronal subpopulations are highly sensitive to insulin and leptin. While AGRP neurons are inhibited by leptin ¹¹³ and insulin ¹¹⁴, leptin increases the activity of POMC neurons and the expression of POMC ⁹³ and consequently reduces food intake. However, the physiological response of POMC neurons to peripheral hormones is still not fully understood, because recent data suggest that POMC neurons form distinct molecular clusters with opposing responses to hormones and neurotransmitters. Interestingly, a subset of POMC neurons also co-express AGRP, indicating a shared developmental origin ^{108,115-117}.

The first evidence of the involvement of the VMH in the control of glucose and energy homeostasis was obtained by lesion studies, which resulted in hyperphagia and obesity ¹¹⁸. Neurons within the VMH are highly responsive to leptin, and selective deletion of the LepR in neurons that express steroid factor-1 (SF-1 neurons) in the VMH results in obese and hyperphagic mice ^{119,120}. Interestingly, this ablation provoked only little change at standard diet but rapidly induced severe adiposity on a HFD owing to a failure to increase energy expenditure with weight gain ¹¹⁹. The VMH is highly connected to neurons in the ARC by microcircuits. On the one hand, the VMH increases the activity of POMC neurons ¹²¹, and

these inputs decrease during fasting. On the other hand, the VMH contains both MC4R and NPY receptors, suggesting a regulatory role of ARC neurons on neuronal subpopulations in the VMH.

The DMH is a crucial player in the control of BAT thermogenesis in rodents ^{122,123}, and DMH lesions result in hypophagia and reduced body weight ¹²⁴. The DMH has a diverse population of different LepR expressing neurons, which regulate energy expenditure but not food intake ¹²⁵. NPY is also highly expressed in the DMH ^{126,127} and has a leptin-independent function regulating energy homeostasis ¹²⁶. The knockdown of NPY in the DMH promotes BAT activity and increases energy expenditure ¹²⁸. DMH neurons also project to the ARC and inhibit AgRP and POMC neurons to fine-tune feeding behavior ¹⁰⁸.

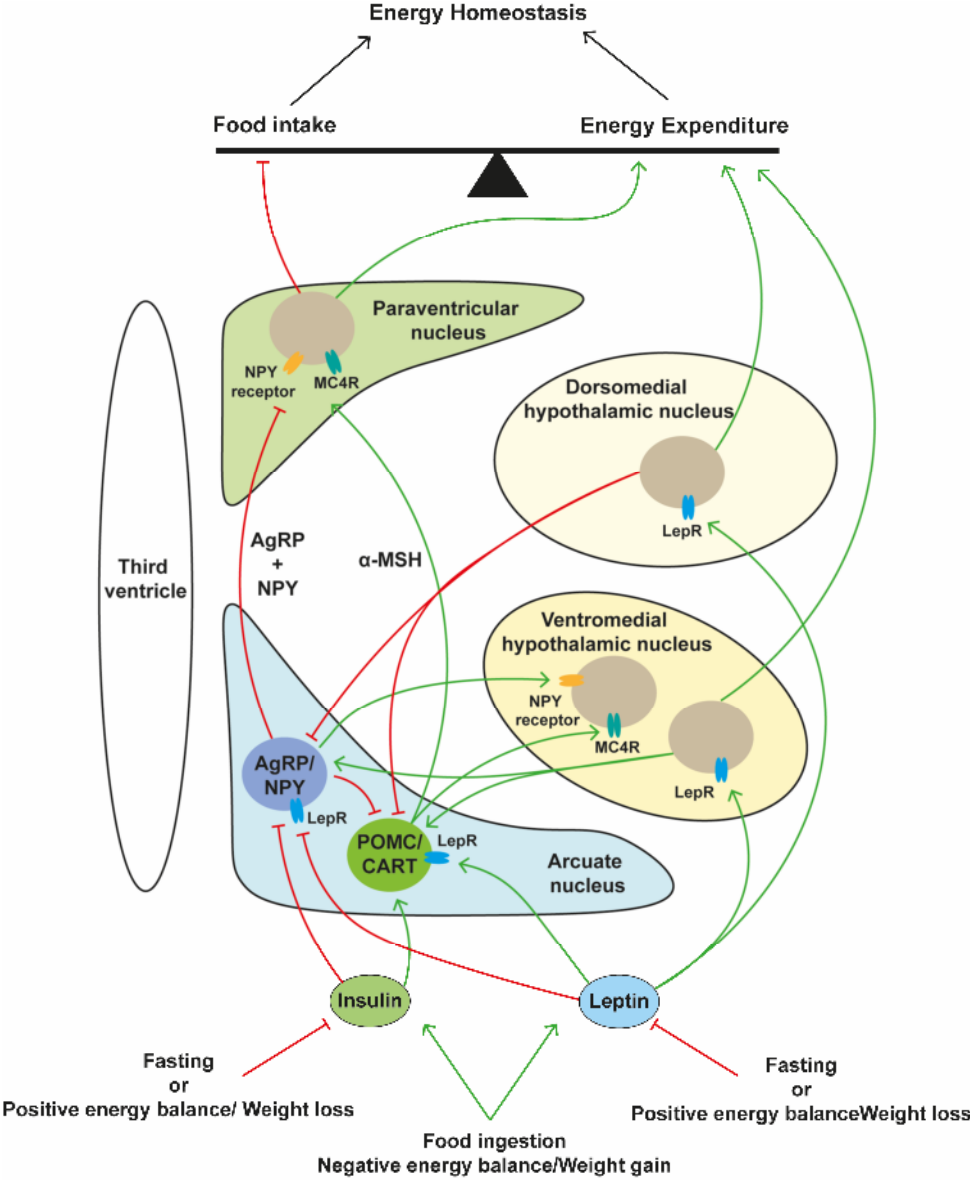


Figure 5: Schematic overview of the mediobasal hypothalamic neurocircuit in the control of food intake and energy expenditure. The arcuate nucleus, ventromedial hypothalamic nucleus, dorsomedial hypothalamic

nucleus, and paraventricular nucleus are highly sensitive to the peripheral signal's leptin and insulin. Both increase upon food ingestion or weight gain and act on receptors in the mediobasal hypothalamus to stimulate changes in food intake and energy expenditure. See main text for detailed description. Abbreviations: α -MSH, α -melanocyte stimulating hormone; AgRP, agouti-related protein; CART, co-expressing cocaine- and amphetamine-regulated transcript; MC4R, melanocortin receptor 4; NPY, neuropeptide Y; POMC, proopiomelanocortin. Red arrows: inhibitory; green arrows, activating.

Taken together, the central control of energy homeostasis is a multilayered system containing various nuclei and cell populations, in which the different nuclei and neurons are deeply connected and regulate each other's activity. Interestingly, FKBP51 is highly upregulated in several nuclei of the MBH, such as the PVN, ARC, and VMH, after metabolic challenges, such as food deprivation⁶⁰ and high-fat diet regimens¹²⁹. These findings might imply a more prominent role of hypothalamic FKBP51 in regulating metabolic stress responses.

1.4. Autophagy

Cellular and nutritional stress leads to the accumulation of damaged organelles or proteins and constantly threatens cellular balance¹³⁰. To dampen adverse effects on cell metabolism, organisms from yeast to mammals have developed an evolutionarily conserved process that removes toxic organelles, aggregated proteins, and invading microorganisms from the cell and recycles its components to reinstate cellular energy homeostasis. Therefore, the cargo is transported by double-membrane vesicles (autophagosomes) to lysosomes for degradation. The newly generated metabolites are then reutilized as a source of energy or building blocks to synthesize needed molecules and proteins¹³¹. This degradation process is called autophagy (from the ancient Greek meaning “self-eating”) and was first identified in yeast¹³².

Autophagy substrates can be endogenous (damaged mitochondria and nuclear fragments) or exogenous (viruses, bacteria escaping phagosomes) and divide autophagy into several forms that differ in their physiological function and their way of degradation. A detailed description of all different types of autophagy is beyond the scope of this thesis and is reviewed in-depth elsewhere^{133,134}. The three most studied degradation systems, however, are chaperone-mediated autophagy (CMA), microautophagy, and macroautophagy (depicted in Figure 6).

Macroautophagy (hereafter referred to as autophagy) is tightly controlled by an array of multiple proteins, commonly known as autophagy-related (ATG) proteins¹³⁵. Over the last decades, autophagy has emerged as a central biological pathway that promotes cellular homeostasis, typically induced during times of environmental and metabolic stress conditions, such as starvation. Moreover, alterations in autophagy signaling have been detected in human diseases, such as cancer, neurodegeneration, infectious diseases, and metabolic disorders, shedding light on possible new therapeutic avenues to cure one of those diseases^{134,136,137}.

Initial steps of autophagy include the formation (vesicle nucleation) and expansion (vesicle elongation) of an isolation membrane (also termed phagophore) on the surface of the endoplasmic reticulum. The mature autophagosome then fuses with a lysosome, forming an autolysosome, to degrade captured material (Figure 6c).

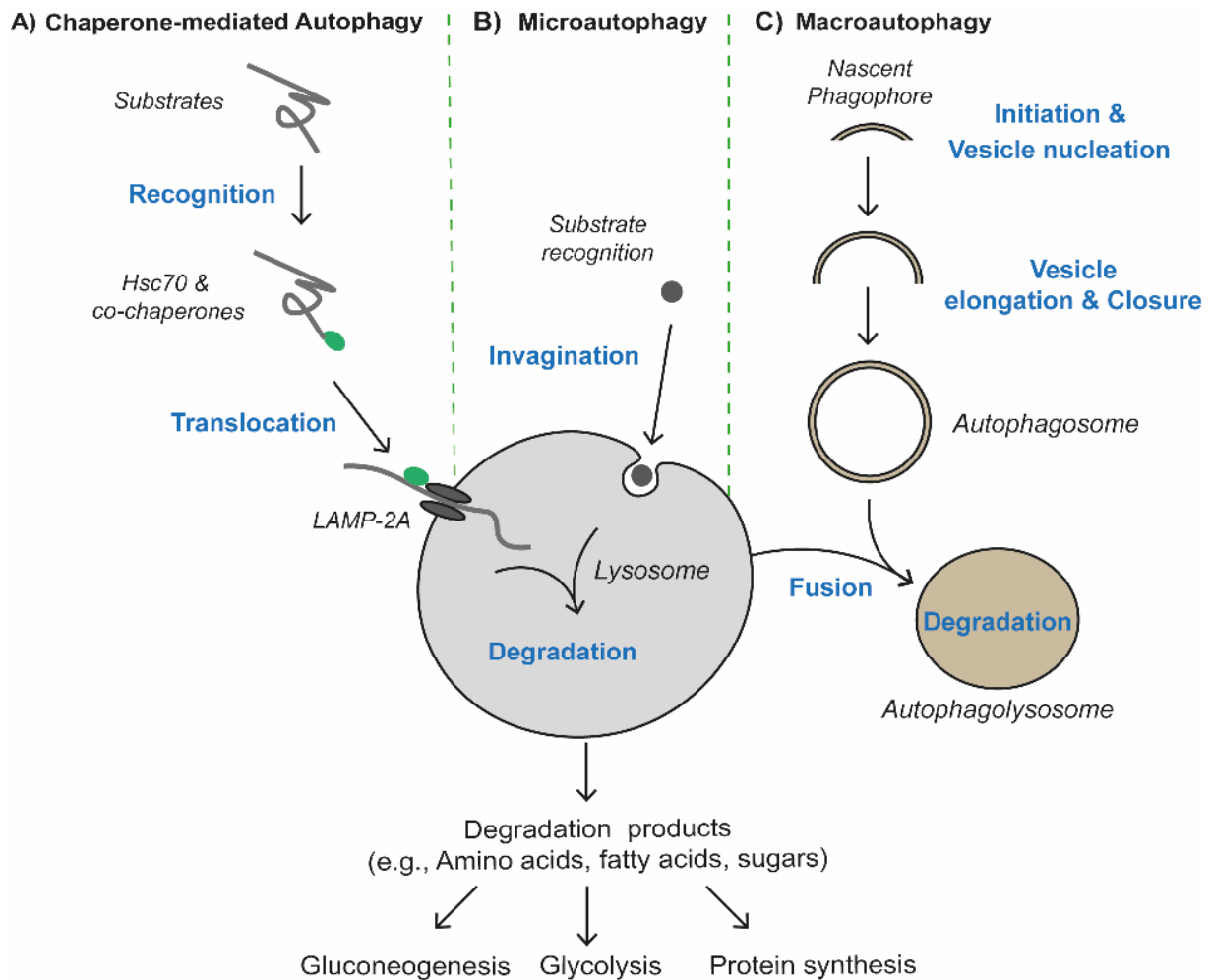


Figure 6: Three main degradation pathways. **A)** Chaperone-mediated autophagy is characterized by the direct recognition of substrates, which carry the pentapeptide KFERQ-like sequence, by the Hsc70 chaperone. The unfolded protein is then translocated into the lysosome via LAMP-2A receptors for degradation. **B)** During microautophagy, the targeted components are directly engulfed by the lysosomal membrane. **C)** Macroautophagy is characterized by the formation (vesicle nucleation) and expansion (vesicle elongation) of an isolation membrane (also termed phagophore). During phagophore expansion, autophagic cargo is targeted and enclosed in an autophagosome. Finally, the mature autophagosome fuses with a lysosome to form an autolysosome to degrade the captured material. Abbreviations: Hsc70, heat shock cognate 70; LAMP-2A, lysosome-associated membrane protein 2A.

1.4.1. Importance of autophagy in metabolism

As mentioned in the preview's sections, the development of obesity is controlled by multiple tissues, including muscle, adipose tissue and the MBH, and is accompanied with a massive expansion of fat depots¹³⁸. Interestingly, several research studies suggest that autophagy is involved in the cellular remodeling of adipose tissue by mediating adipocyte mass development and differentiation^{139,140}. In

fact, autophagic dysfunction is associated with decreased adipocyte differentiation and increased conversion of white adipocytes to brown adipocytes, which are associated with increased heat production and enhanced β -oxidation favoring a lean phenotype in mice ¹³⁹. Consequently, adipocyte-specific inhibition of autophagy in mice results in a lean and obesity-resistant phenotype without any differences in food intake ¹⁴¹. In line with these findings, autophagy is upregulated in adipocytes of obese individuals and therapeutic impairment of autophagy signaling might be beneficial to counterbalance the fat expansion during the development of obesity ¹⁴².

In the pancreas, studies showed that autophagy is essential for the maintenance and function of β -cells. Cell-specific deletion of autophagy in mice reduced insulin secretion under basal conditions. These rodents developed hyperglycemia and impaired glucose tolerance under a HFD challenge, indicating a severe diabetic phenotype. Also, evidence from additional studies demonstrated a crucial role of hepatic autophagy in the regulation of lipid metabolism by promoting the storage of triglycerides in lipid droplets and thus whole-body energy balance ¹³⁷.

Autophagy deletion, specifically in muscle tissue, is associated with the accumulation of toxic protein aggregates and muscle atrophy. Furthermore, autophagy signaling is highly upregulated during exercise in cardiac and skeletal muscle, and exercise-induced autophagy provides protection against glucose intolerance associated with a high-fat diet ¹⁴³. Together, these data indicate the importance of autophagy in skeletal muscle biology.

The role of autophagy in the MBH is not yet fully understood, but several research groups have already shown that obesity affects central autophagy signaling and that autophagy manipulation impacts whole-body metabolism. For instance, autophagy signaling is impaired in the arcuate nucleus after a chronic high-fat diet regimen. In line with this finding, Atg7 knockdown and thus autophagy inhibition in the MBH causes hyperphagia, decreased energy expenditure and massive obesity ¹⁴². A study by Kaushik and colleagues revealed that autophagy regulates AgRP expression in the ARC after starvation, which in turn increases food intake ¹⁴⁴. This study further showed that deletion of Atg7, specifically in AgRP neurons, reduces body weight and adiposity, which results in a lean phenotype ¹⁴⁴. In a follow-up study, Singh and colleagues investigated the role of autophagy in anorexigenic POMC neurons by deleting

Atg7, which resulted in increased food intake and obesity due to reduced secretion of α -MSH and impaired leptin signaling in POMC neurons of Atg7 mutant mice ¹⁴⁵.

Together, these data demonstrate that autophagy has an essential role in regulating metabolic processes, such as food intake, adipose tissue development, liver complications, and insulin resistance ^{139,146-148}.

1.4.2. Autophagy regulation and core molecular mechanism

The most potent and best-characterized stimuli to autophagy are changes in nutritional status, such as starvation. The two highly conserved energy sensors, AMPK (adenosine monophosphate protein kinase) and mTOR, detect these nutritional changes and act in synergy to modify autophagy signaling to induce catabolic or anabolic pathways, ensuring sufficient cellular energy supply.

In the presence of abundant nutrients, the mTOR complex 1 (mTORC1) is activated at the lysosomal surface and directly binds to the autophagy initiator protein kinase ULK1, thereby inhibiting autophagosome formation. ULK1 itself is a constantly assembled multiprotein complex, consisting of ULK1, ATG13, ATG101, and FIP200 (FAK family-interacting protein of 200 kDa, also known as RB1CC1). Under nutrient depletion, mTORC1 is inhibited by the TSC1/TSC2 complex, which contributes to the displacement of mTORC1 from the surface of the lysosome. The TSC1/TSC2 complex is activated by LKB1-mediated AMPK phosphorylation of TSC2 and triggers the dissociation of mTORC1 from ULK1, which initiates dephosphorylation and subsequently activation of ULK1. Furthermore, recent studies have shown that AMPK mediates ULK1 activation by direct phosphorylation independent of TSC1/TSC2 and mTORC1 ¹⁴⁹.

The ULK1 complex then translocates to the phagophore assembly site (PAS) to initiate membrane nucleation by the activation of the PI3K (or Beclin 1 complex), consisting of Beclin 1, the class III phosphatidylinositol 3-kinase (VSP34), the general vesicular transport factor p115, ATG14L, and the activation molecule in Beclin-1 regulated autophagy protein 1 (AMBRA1). Activation of the Beclin 1 complex generates a pool of phosphatidylinositol-3-phosphates (PI3P) on the site of phagophore formation, which promotes the recruitment of the PI3P effector proteins DFCP1 (zinc-finger FYVE domain-containing protein 1) and WD repeat domain phosphoinositide-interacting proteins (WIPIs) to initiate membrane elongation ¹³⁵.

The extension of the isolation membrane is mediated by several ATG proteins, which are organized in two ubiquitin-like conjugation systems. The first conjugation system forms a ubiquitin E3-ligase, the ATG12-ATG5-ATG16L multiprotein complex, which is assembled by the concerted action of the E1-like enzyme ATG7 and the E2-like conjugating enzyme ATG10. The ATG12-ATG5-ATG16L heterocomplex is then recruited to nascent autophagosomes by WIPI proteins and participates in the final lipidation step of the second conjugation system. For this system, the cytosolic and soluble form of LC3 (microtubule-associated protein 1 light chain 3) is transformed to its phosphatidylethanolamine (PE) conjugated form LC3-II. This process is mediated by the sequential action of the proteases ATG4, ATG7, and the E2-like enzyme ATG3 (Figure 7, step 5). LC3-II binds to the autophagosomal membrane and is vital for successful autophagosome closure. The selection and transportation of the autophagic cargo is also mediated by LC3-II and other receptors, such as p62 (SQSTM1). After degradation, LC3-II is recycled by ATG4 from the surface of autophagosomes for the next cycle of conjugation ¹³⁵. Because of the stable association of LC3-II to the autophagosome membrane, it is a commonly used marker to assess autophagy signaling ¹⁵⁰.

The final closure of the phagophore initiates the fusion of the autophagosome with the lysosome, thereby forming an autolysosome. Whereas the outer autophagosome membrane is incorporated into the lysosomal membrane, the inner membrane of the autophagosome and the autophagic cargo is degraded by acidic lysosomal hydrolases (Figure 7) ¹³⁶. The resulting metabolites (e.g., amino acids, fatty acids, nucleotides, and sugars) are used for several anabolic processes such as protein synthesis, gluconeogenesis, and ATP production ¹³¹. The increase in intracellular amino acids reactivates mTORC1 and thus initiates a negative feedback mechanism to inhibit excess autophagy signaling during starvation¹⁵¹.

Interestingly, as already discussed (see chapter 1.3.1 and 2), FKBP51 directly regulates AKT in cancer cells. In addition, recent evidence suggests that FKBP51 might regulate autophagy signaling via AKT. Gassen and colleagues could demonstrate that FKBP51 recruits the inactivated AKT and PHLPP to Beclin 1, thereby triggering autophagy signaling ²⁹. In a follow-up study, they further indicated that FKBP51 regulates the protein level of Beclin 1 by inactivating SKP2 (S-phase kinase-associated protein

2), which governs Beclin 1 level via direct ubiquitination¹⁵². Given the converging roles of FKBP51 and autophagy in several metabolic pathways, it might be promising to investigate, if FKBP51 has a more prominent role in autophagy signaling, especially after metabolic challenges.

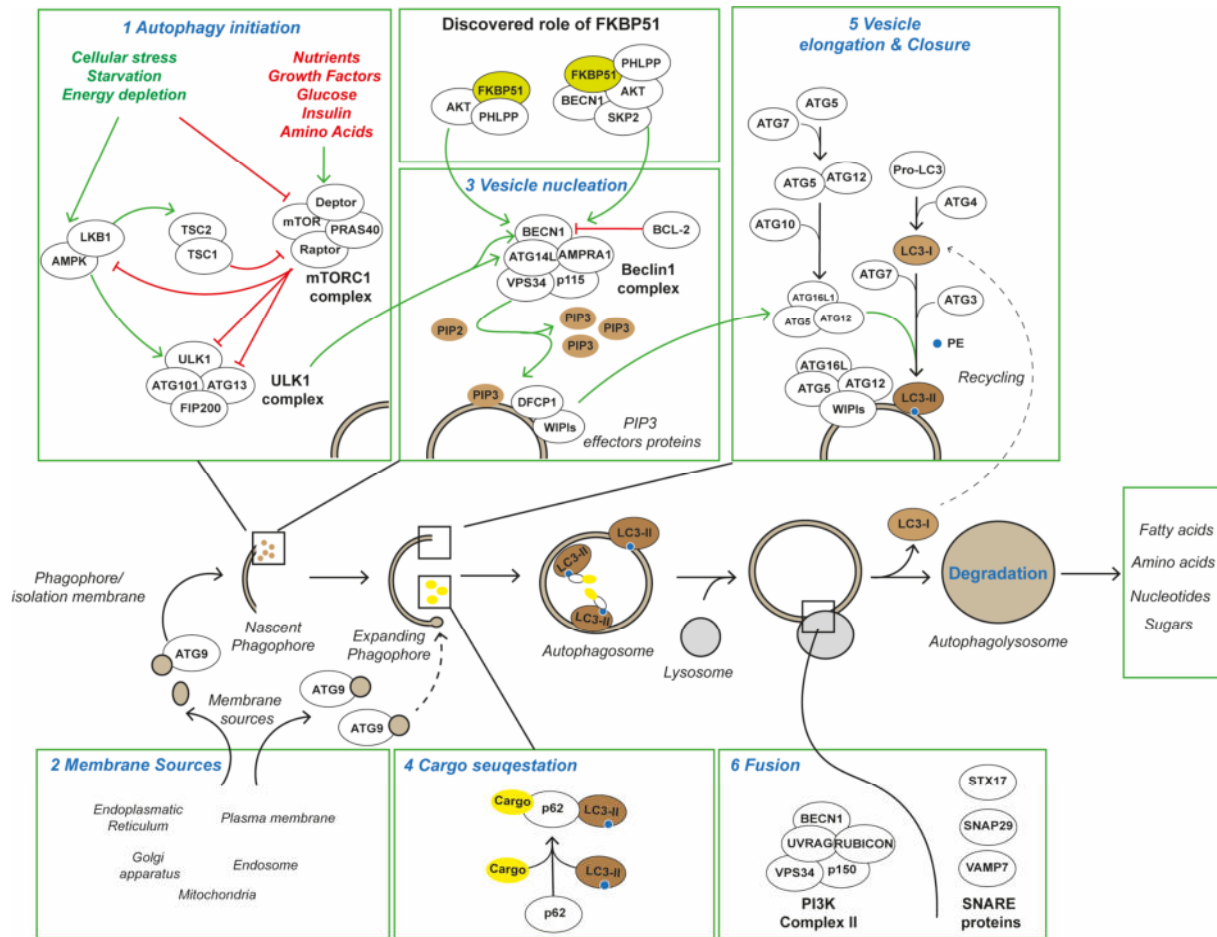


Figure 7: Molecular regulation of macroautophagy. Nutritional signals modulate autophagy dependent on mTORC1 activity, which is enhanced by glucose, amino acids, and insulin. mTORC1 acts as a negative regulator of autophagy by inhibiting the ULK1 complex. Upon cellular stress or nutrient depletion, AMPK is activated and triggers the activation of the ULK1 complex. The ULK1 complex activates the lipid kinase complex, class III PI3K that serves to recruit components of the two conjugation systems to the isolation membrane. Autophagic cargo is sequestered by direct recognition of LC3-interacting regions (LIRs) through LC3-II or indirectly through LIR-containing adaptor proteins, such as p62/SQSTM1. Fusion of the autophagosome and lysosome involves the PI3K complex II as well as multiple SNARE proteins. Abbreviations: AMBRA1, autophagy/Beclin 1 regulator 1; AMPK, AMP-activated protein kinase; mTOR, mammalian target of rapamycin; LC3, microtubule-associated protein 1 light chain 3; PE, phosphatidylethanolamine; PI3P, phosphatidylinositol-3-phosphate; ULK1, UNC-51-like kinase.

1.5. Aim of the thesis

Research on the co-chaperone FKBP51 made a tremendous step forward during the last decades and positioned FKBP51 as a crucial regulator in a wide range of signaling pathways. Furthermore, FKBP51 is considered a promising drug target for stress-related psychiatric and metabolic disorders. Since stress affects a highly balanced system of multiple central and peripheral signaling pathways, the changes in one system might impact the other.

To fully establish FKBP51 as a possible candidate for therapeutic interventions, it is essential to unravel the detailed mechanistic role of FKBP51 in the underlying signaling pathways, such as the PI3K-AKT and autophagy pathway, controlling energy homeostasis and the stress response on a cellular level.

In particular, the more profound understanding of FKBP51 in peripheral organs, such as muscle, or single brain regions, like the hypothalamus, is still a significant knowledge gap. Therefore, the current thesis addresses the tissue-specific action of FKBP51 in the regulation of the stress response and the control of body metabolism by tackling the following research questions:

1. Reviewing the existing knowledge about FKBP51 in the regulation of metabolism (Chapter 2)
2. The effect of total FKBP51 deletion on whole-body metabolism (Chapter 3.1)
3. The effect of hypothalamic FKBP51 manipulation on whole-body metabolism and the effects on autophagy signaling (Chapter 3.2)
4. The distinct role of FKBP51 in the PVN in response to an acute stressor (Chapter 3.3)

2. Focus on FKBP51: A molecular link between stress and metabolic disorders

Authors:

Alexander S. Häusl¹, Georgia Balsevich², Nils C. Gassen^{3,4} and Mathias V. Schmidt¹

Affiliations:

¹Research group Neurobiology of Stress Resilience, Max-Planck Institute of Psychiatry, 80804 Munich, Germany.

²Hotchkiss Brain Institute, University of Calgary, 3330 Hospital Drive NW, Calgary, Ab T2N 4N1, Canada

³Department of Psychiatry and Psychotherapy, Bonn Clinical Center, University of Bonn, 53127, Bonn, Germany

⁴Department of Translational Research in Psychiatry, Max Planck Institute of Psychiatry, 80804 Munich, Germany.

Originally published in:

Molecular Metabolism 29 (2019), 170-181

Focus on FKBP51: A molecular link between stress and metabolic disorders



Alexander S. Häusl^{1,*}, Georgia Balsevich², Nils C. Gassen^{3,4}, Mathias V. Schmidt^{1,**}

ABSTRACT

Background: Obesity, Type 2 diabetes (T2D) as well as stress-related disorders are rising public health threats and major burdens for modern society. Chronic stress and depression are highly associated with symptoms of the metabolic syndrome, but the molecular link is still not fully understood. Furthermore, therapies tackling these biological disorders are still lacking. The identification of shared molecular targets underlying both pathophysiologies may lead to the development of new treatments. The FK506 binding protein 51 (FKBP51) has recently been identified as a promising therapeutic target for stress-related psychiatric disorders and obesity-related metabolic outcomes.

Scope of the review: The aim of this review is to summarize current evidence of *in vitro*, preclinical, and human studies on the stress responsive protein FKBP51, focusing on its newly discovered role in metabolism. Also, we highlight the therapeutic potential of FKBP51 as a new treatment target for symptoms of the metabolic syndrome.

Major conclusions: We conclude the review by emphasizing missing knowledge gaps that remain and future research opportunities needed to implement FKBP51 as a drug target for stress-related obesity or T2D.

© 2019 The Authors. Published by Elsevier GmbH. This is an open access article under the CC BY-NC-ND license (<http://creativecommons.org/licenses/by-nc-nd/4.0/>).

Keywords FKBP51; SAFit2; Adipogenesis; Glucose uptake; Obesity; Stress; Type 2 diabetes

1. INTRODUCTION

Homeostatic mechanisms govern the stress response, energy balance, and glucose homeostasis in order to maintain a dynamic equilibrium following internal or external challenges [1]. This requires a complex physiological response (involving multiple organ systems) to sense, integrate, and respond to changes in the environment. Interestingly, regulation of these homeostatic systems relies on many shared environmental and genetic factors, whereby manipulation of one factor can simultaneously influence stress-coping behaviors, body weight, and blood glucose. Identification of such shared factors may prove beneficial in treating stress-related comorbidities such as psychiatric disorders, obesity, and T2D. In this context, FKBP51 has recently been identified as a promising therapeutic target for the treatment of stress-related psychiatric disorders [2,3] and obesity-related metabolic outcomes [4]. In this review, we first summarize key physiological mechanisms orchestrating the interplay of the body's stress response, energy balance, and glucose homeostasis, without giving an exhaustive overview (the reader is referred to in-depth reviews at each section). In the main part, we summarize and discuss the newly discovered role of FKBP51 in metabolism and highlighting its therapeutic potential for metabolic diseases.

1.1. The stress response

The stress response refers to the repertoire of physiological and behavioral reactions that arise in response to a stressor [5]. By definition, a stressor is any threat, real or perceived, to homeostasis. Therefore, stressors can either be physical in nature, such as metabolic stressors (fasting, physical activity) or psychogenic in nature, such as social stress or predator exposure. Although different types of stressors activate different brain networks, they all converge to stimulate the sympathoadrenomedullary (SAM) system and the hypothalamic-pituitary-adrenal (HPA) axis. The sympathetic nervous system comprises the most immediate physiological response involving direct catecholaminergic innervation of peripheral organs, including the adrenal medulla, which releases catecholamines into systemic circulation. Activation of the SAM system represents the “fight or flight” response, characterized by increased heart rate and respiration, redirection of blood flow away from digestive and reproductive organs, and mobilization of energy stores. Indeed, activation of the sympathetic nervous system has important metabolic effects. For example, increased sympathetic drive to white adipose tissue (WAT) and brown adipose tissue (BAT) recruits brown adipocytes and furthermore mobilizes free fatty acids [6–9]. Similarly, increased sympathetic drive enhances glycogenolysis and glucose output in the liver [10].

¹Research Group Neurobiology of Stress Resilience, Max Planck Institute of Psychiatry, 80804, Munich, Germany ²Hotchkiss Brain Institute, University of Calgary, 3330 Hospital Drive NW, Calgary, Ab T2N 4N1, Canada ³Department of Psychiatry and Psychotherapy, Bonn Clinical Center, University of Bonn, 53127, Bonn, Germany ⁴Department of Translational Research in Psychiatry, Max Planck Institute of Psychiatry, 80804, Munich, Germany

*Corresponding author. Kraepelinstr. 2-10, 80804 Munich, Germany. E-mail: alexander.haeusl@biophyll.com (A.S. Häusl).

**Corresponding author. Kraepelinstr. 2-10 80804 Munich, Germany. E-mail: mschmidt@psych.mpg.de (M.V. Schmidt).

Received July 4, 2019 • Revision received September 3, 2019 • Accepted September 5, 2019 • Available online 11 September 2019

<https://doi.org/10.1016/j.molmet.2019.09.003>

The HPA axis mediates the slower, sustained response to a certain stressor. Activation of the HPA axis involves the release of corticotropin-releasing hormone (CRH) and arginine-vasopressin (AVP) from parvocellular neurons within the hypothalamic paraventricular nucleus (PVN) into the hypophyseal portal blood system, which bridges the hypothalamus and anterior part of the pituitary gland. At the pituitary gland, CRH and AVP stimulate the release of adrenocorticotropic hormone (ACTH) into systemic circulation (reviewed by [5]). In turn, ACTH stimulates the secretion of glucocorticoids (GCs) from the adrenal cortex. GCs (cortisol in humans or corticosterone in rodents) are recognized as the major end products of the HPA axis, which subsequently act on multiple organs to modulate the effects of a wide range of physiological processes. GCs exert their effects through type I mineralocorticoid receptors (MRs) and type II glucocorticoid receptors (GRs), which present distinct binding affinities for GCs and distinct distribution profiles [11]. MRs have a higher affinity for GCs than GRs, and as a consequence GRs are only activated in response to stress or at the GC circadian peak [12]. Through GRs, GCs are involved in a negative feedback circuit whereby they operate at different levels of the HPA axis and at higher brain centers to terminate the stress response [5]. Furthermore, in terms of metabolic regulation, GR signaling is known to favor food intake, promote gluconeogenesis in the liver, protein degradation and amino acid mobilization in muscle, and lipolysis in fat [13–16]. Taken together, SAM activation coupled to GC actions favors processes that increase the availability of circulating energy stores.

1.2. Energy balance

Energy balance refers to the dynamic equilibrium between energy input and output. Body weight maintenance is a tightly regulated homeostatic system balancing energy input and output. This balance is subject to multiple levels of regulation involving complex, redundant mechanisms comprising thousands of genes and multiple organs and involving both hormonal and neuronal signaling networks. Especially, the proper communication between the brain, adipose tissue, and muscle tissue via hormones, like insulin and leptin, is essential for a healthy energy status. Further, interactions between environmental cues (diet, physical activity, stress exposure) and genetic factors determine individual susceptibility to gain weight as a result of diverging changes to components of energy intake or expenditure.

1.2.1. Energy intake

Energy intake refers to the caloric gain through ingestion of carbohydrates, fat, and protein. Two complementary drives regulate energy input: homeostatic and non-homeostatic pathways [17]. Whereas homeostatic pathways increase the motivation to eat in response to energy deficits, non-homeostatic pathways are able to override homeostatic pathways to favor consumption beyond metabolic needs. Non-homeostatic feeding relates to the rewarding properties of food. As a natural reward, palatable foods activate the brain's reward system, notably the mesocorticolimbic circuit, in which dopaminergic neurons originating in the ventral tegmental area (VTA) send projections to various regions including the nucleus accumbens (NAc). Activation of mesolimbic dopamine neurons is associated with increased motivation to obtain not only food rewards but also drugs of abuse. For homeostatic control of feeding, primary central pathways interact with peripheral pathways via metabolic signaling molecules. Several nuclei in the brain, primarily situated in the hypothalamus and the brainstem integrate information from circulating hormones about peripheral energy levels [18]. Leptin and insulin are two major hormones which inform the brain about recent changes in the metabolic

status [19]. Leptin is secreted proportional to body fat mass from adipocytes and reduces food intake and increases energy expenditure [20]. Insulin, secreted from the pancreas, also correlates with body weight and adiposity and acts as a negative feedback control for adiposity [21–23]. Both hormones reflect the energy status within the periphery, subsequently signaling to the brain to mount an appropriate response. In particular, the arcuate nucleus of the hypothalamus (ARC) is a key region to translate the hormonal signals into behavioral responses (i.e., eating). The ARC contains two main neuronal populations regulating feeding, the neuropeptide Y (NPY)/agouti related peptide (AGRP) expressing neurons and the proopiomelanocortin (POMC)/cocaine and amphetamine related transcript (CART) neurons. These neurons are able to sense a broad range of nutrient and hormonal signals (nutrients, insulin, and leptin), and their responses change according to the energy state [24,25].

1.2.2. Energy expenditure

Energy expenditure comprises the energy needed to maintain normal body functions and consists of obligatory energy expenditure, physical activity, and adaptive thermogenesis [26]. While obligatory energy expenditure (referring to the energy required for core body functions) is relatively fixed, adaptive thermogenesis (processes that dissipate energy as heat to maintain body temperature) is highly variable and is sensitive to environmental (e.g. cold temperature exposure and persistent organic pollutants [27]) and genetic factors, like mutations in gene sequences (e.g. leptin or the leptin receptor [28]). In mammals, there are two major types of adipose tissue, BAT and WAT, which are both structurally and functionally distinct [29]. Whereas WAT primarily acts as a storage site for lipids, BAT functions as a thermogenic tissue, dissipating energy as heat to mediate non-shivering thermogenesis. Although traditionally viewed as a function of BAT, adaptive thermogenesis is additionally governed by white adipocyte transdifferentiation into beige adipocytes, in a process referred to as 'browning.' The expression of UCP1 (uncoupling protein 1) in BAT mediates non-shivering thermogenesis through its ability to separate fatty acid oxidation from ATP synthesis [30]. Consequently, adipocytes in BAT have a relatively high metabolic rate. Inducible 'brown-like' adipocytes (beige cells) can be formed in WAT in response to various stimuli. Since there is a negative correlation between body mass index (BMI) and the activities of brown and beige cells, recruitment and/or activation of BAT holds promise for the treatment of metabolic diseases.

1.3. Glucose homeostasis

Glucose homeostasis refers to the hormonal and neural regulatory mechanisms that maintain blood glucose levels within a very narrow range. In healthy individuals, the body regulates glucose release and production in order to ensure sufficient glucose flux to meet the demands of the body [23]. The proper control of glucose homeostasis requires the synchronized actions of several organ systems, including but not limited to, the brain, liver, skeletal muscle, and adipose tissue [23,31]. The multiple mechanism regulating glucose metabolism are complex and tightly regulated by hormones, like insulin and leptin, and their impact on glucose homeostasis are in detail reviewed elsewhere [31]. Interestingly, blood glucose levels are highly influenced by GCs the main hormones released after a stressful event. For instance, GCs increase glucose production in the liver by stimulating hepatic gluconeogenesis [14]. Additionally, GCs decrease glucose utilization and uptake in skeletal muscle and WAT [32]. Indeed, energy and glucose homeostasis are intimately connected since both systems respond to changes in energy stores and availability. Accordingly, they share many common regulatory pathways.

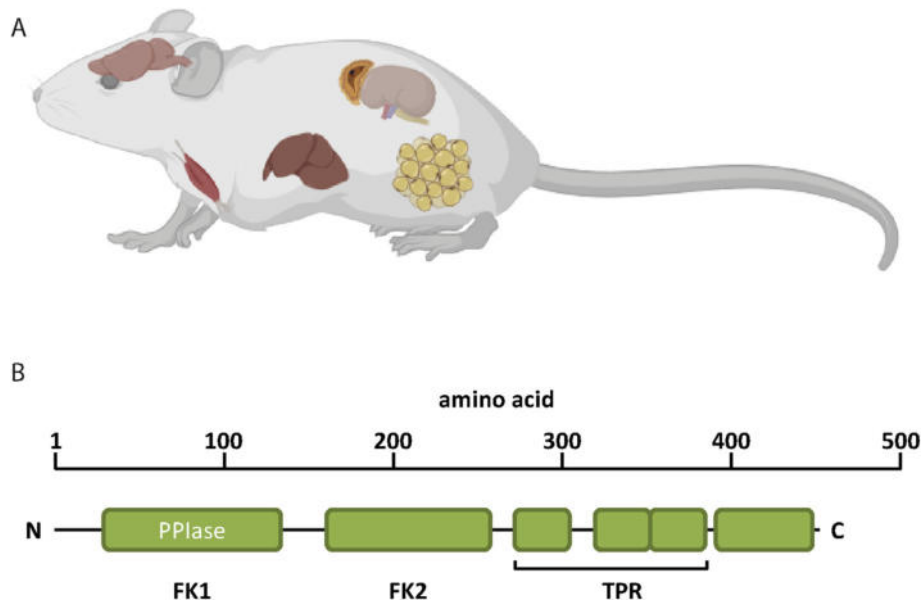


Figure 1: (A) Overview of important sites of metabolism related FKBP51 expression, including brain, adrenals, muscle, and fat tissue. (B) Schematic representation of the protein domain structure of the large immunophilins FKBP51 and FKBP52. FK1 and FK2 = FK506 binding domain. TPR = tetratricopeptide repeat domain.

1.4. Interplay between stress and metabolic regulation

Chronic stress is a major risk factor for obesity and metabolic-related diseases, highlighting the complementary biology between stress and metabolic regulation [33]. Yet the relationship between stress and energy metabolism is highly complex, exemplified by diverging metabolic outcomes in response to stress. For example, in response to stress, some individuals increase feeding and body weight whereas others decrease feeding and lose weight. Moreover, stress-induced hyperphagia is not necessarily followed by an increase in body weight, suggesting that mechanisms regulating energy expenditure are activated simultaneously. Such conflicting responses to stress indicate that opposing metabolic drives respond to stress. Specifically, GCs, the end products of the HPA axis, affect energy intake and expenditure to favor a positive energy balance [34]. In contrast, sympathetically-activated β -adrenergic receptors increase energy expenditure via activation of thermogenesis in BAT in order to favor a negative energy balance [26,35], a process that is suppressed by GCs [36,37]. Therefore, stress promotes body weight gain when hyperphagia prevails. However, in the presence of stress-induced hypophagia or when BAT recruitment dominates, weight loss results (reviewed by [38]). Despite clear effects of stress on metabolic outcomes, only a few molecular mediators at the interface between stress and metabolic regulation are yet discovered [39,40]. However, the complex interactions remain poorly defined. Here, we suggest that FKBP51 may also represent a molecular link between stress and metabolic pathways.

2. THE FK506 BINDING PROTEIN 51 IS A CO-CHAPERONE WITH MULTIPLE INTERACTION SITES

FKBP51 (encoded by the *FKBP5* gene) is a 51-kDa protein and a member of the immunophilin family, which is able to bind the immunosuppressants rapamycin and FK506 [41]. Unlike the lower molecular weight members, FKBP51 does not initiate the immunosuppression activity of FK506 [42,43]. Rather, FKBP51 is well established as a heatshock protein 90 kDa (HSP90)-associated co-

chaperone, regulating steroid hormone receptor signaling. FKBP51 negatively regulates the GR by reducing GC-binding, delaying nuclear translocation, and thereby decreasing GR-dependent transcriptional activity [44–47]. Its effects on GR signaling have important implications for the regulation of the stress response since GRs mediate the termination of the stress response. In fact, higher levels of *FKBP5* mRNA are associated with higher levels of circulating cortisol and reduced negative feedback inhibition of the stress response [44,46,48–50]. Through its regulation of GR sensitivity for hormone binding, FKBP51 is perfectly positioned to modulate stress-related metabolic outcomes that are mediated through GCs. Equally important, however, is that FKBP51 expression in turn is induced by GR activation itself, representing an ultra-short, negative feedback loop regulating GR sensitivity [51].

FKBP51 shares high protein domain structure homology to FKBP52 [43]. Both proteins contain two domains located N-terminally (FK1, FK2) with homology to FKBP12 (Figure 1). Only the FK1-domain (FK506 binding domain) interacts with the immunosuppressant drug tacrolimus (FK506). The FK1-domain of FKBP51 and FKBP52 is enzymatically active in catalyzing the isomerization of peptidyl-prolyl bonds of model peptides [52]. This domain has been shown to be the main determinant for the divergent impact of FKBP51 and FKBP52 on GR function [47,53]. While the FK1 domain is important for GR regulation, its biochemical activity is not [54]. To modulate GR function, the FK1-domain as well as the HSP90-binding TPR (tetratricopeptide repeat) domain are essential. The C-terminal TPR-domain is conserved in both FKBP51 and FKBP52 and enables binding to the EEVD motif at the C-terminus of HSP90 [55]. Moreover, through its scaffolding function, FKBP51 is known to regulate NF- κ B, Akt1&2, GSK3 β , calcineurin/NFAT, DNMT1, and autophagic signaling pathways [4,56–61]. FKBP51 and FKBP52 have distinct expression profiles and may therefore exert tissue- and cell type-specific effects [62, www.proteinatlas.org]. Importantly, when both proteins are expressed in the same cells they may have opposite functions, as already shown in the context of GR signalling [63,64]. It is therefore of high importance to differentiate between FKBP51- and FKBP52-mediated effects, an

issue that is most crucial when it comes to pharmacological manipulations (see section 4).

Given the significant interplay between diverse signaling pathways involved in the regulation of homeostatic systems, FKBP51 may be well positioned to mediate the crosstalk between stress and metabolic systems. As a stress-responsive gene, *FKBP5* is able to sense changes in the environment and respond accordingly, which is a defining feature of any metabolic regulatory pathway. In the following sections, we provide accumulated evidence that FKBP51 is an important regulator of whole-body energy and glucose homeostasis through its regulation of diverse signaling modalities. Further, we discuss the possible relevance of targeting FKBP51 for the treatment of stress-mediated pathophysiology.

2.1. FKBP51 shows its highest expression in muscle and adipose tissue

FKBP51 is broadly expressed in the mammalian body (Figure 1). Nevertheless, there are tremendous differences in FKBP51 expression across various tissues, with a high expression in metabolically relevant tissues in the periphery [65]. According to online gene banks and recent publications, FKBP51 shows its strongest expression in human adipocytes, skeletal muscle and lymphocytes [66]. The hippocampus and the amygdala, two central regions controlling the stress response and anxiety-related behaviors, show the highest expression of FKBP51 in the brain, especially after acute stress exposure [67]. Interestingly, FKBP51 is also highly expressed and regulated in control centers of whole-body metabolism, namely the ventromedial hypothalamic nuclei, ARC, PVN, and the nucleus of the solitary tract. Although the importance of tissue and nuclei specific actions of FKBP51 is increasingly recognized, to-date only limited data are available.

2.2. Human FKBP51 is associated with T2D and markers of insulin resistance

In humans, the *FKBP5* gene is mostly associated with gene x early life interactions [68] that are described to predict the adult risk to develop psychiatric disorders, such as depression and posttraumatic stress disorders [69,70]. Currently, there are only a few studies focusing on the link between FKBP51 and metabolic disorders. However, recent studies revealed new data on the co-chaperone's function in metabolism. The first study investigating the effects of FKBP51 expression in adipose tissue on metabolism was led by Eriksson and colleagues in 2014 [66]. The authors nicely showed that dexamethasone, a potent GR agonist, acts as a direct regulator of FKBP51 in subcutaneous and omental adipose tissue. Furthermore, they identified SNPs within the human *FKBP5* gene that were associated with T2D. They further proposed that the endogenous expression of *FKBP5* in adipose tissue correlates positively with markers of insulin resistance. Finally, the authors suggest that SNPs within the *FKBP5* gene may be linked to the susceptibility to develop insulin resistance and dyslipidemia. In a follow-up study with a larger and more diverse cohort, Sidibeh and colleagues provided further evidence that *FKBP5* gene expression is linked to insulin resistance [71]. They revealed that *FKBP5* negatively correlates with genes regulating adipogenesis, suggesting that human FKBP51 might be involved in adipocyte differentiation. These results are in line with preclinical results underpinning a regulatory role of FKBP51 in adipogenesis [72]. However, in humans it is not yet known whether this link is caused by changes in FKBP51 protein levels. Hence, it would be very interesting to include the changes in FKBP51 protein level as a parameter in future studies. In fact, results from animal studies suggest that loss of FKBP51 function leads to a better health status under high-fat diet conditions [4,73].

Also, a study by Ortiz and colleagues reported an association between *FKBP5* intronic methylation and a risk of cardiovascular disease in T2D patients [68]. In this study, the authors investigated the methylation of *FKBP5* at intron 2 in T2D patients only. Despite the limitations of a small cohort size and the lack of a control group, the results suggest that *FKBP5* methylation at intron 2 is a marker for increased cardiovascular risk in T2D [68]. Another study demonstrated that intronic DNA methylation of *FKBP5* at intron 2 and 7 is significantly lower in patients suffering from Cushing's Syndrome compared to the controls, which in turn leads to a higher gene expression and subsequently results in GC resistance [74].

Whereas the above mentioned studies could not find any correlation of *FKBP5* and body weight, a study by Hartmann and colleagues showed that the SNP rs1360780 within the *FKBP5* gene is associated with reduced weight loss following bariatric surgery [75]. Taken together, the few existing studies in human cohorts suggest a role of *FKBP5* in the development of metabolic disorders. However, additional clinical studies, with greater sample sizes, are required to solidify the current findings. Moreover, it is necessary to study broader population groups in order to characterize the association between stress and metabolic disorders.

2.3. Preclinical studies show a beneficial effect of FKBP51 loss in mice

In parallel to human studies of SNPs within the *FKBP5* gene, FKBP51 has been heavily researched in preclinical studies. Until now, the main focus of FKBP51 research *in vivo* has primarily examined the stress response, stress-related disorders, and cancer. Yet as early as 2012 two papers had reported that FKBP51 knockout (KO) mice are leaner than their littermates under normal chow diet [76,77]. These findings initiated the first studies examining FKBP51 within the context of metabolism. In 2014, a study from the Schmidt lab examined the interaction between chronic stress and obesity [78]. Despite the findings that chronic stress induces hyperphagia and weight loss, the results showed a positive correlation between *FKBP5* mRNA and body weight gain as well as food intake. Thus, the study was the first to suggest FKBP51 as a link between stress-related disorders and the metabolic syndrome. A few years later, two independent research groups showed that FKBP51 null mice are resistant against high fat diet-induced weight gain and adiposity and showed improved glucose tolerance and increased energy expenditure [4,73]. In both cases, genetic deletion of FKBP51 had no effect on food intake. Interestingly, while both studies observed the same body weight phenotype, they discovered independent pathways through which FKBP51 influences body weight. Stechschulte and colleagues identified FKBP51 as a regulator of adipocyte differentiation, in which loss of FKBP51 triggers browning in white adipose tissue. They showed that FKBP51 KO animals have a reduced PPAR γ activity and increased expression of markers of browning, (i.e. UCP-1 and PRDM16) in WAT [73]. Alternately, our own study demonstrated that FKBP51 acts through AKT2-AS160 signaling to regulate glucose uptake specifically in muscle tissue. Furthermore, our study was the first to present that treatment with a selective FKBP51 antagonist, SAFit2, improves the metabolic health of obese mice. Interestingly, while FKBP51 is also expressed and regulated in metabolic brain centers, its role in those centers is so far unexplored, leaving many directions for researchers to pursue.

3. MOLECULAR REGULATION OF METABOLIC PATHWAYS BY FKBP51

As introduced above, FKBP51 is mainly characterized as a co-chaperone of the HSP90 complex in order to regulate the ultra-short

negative feedback loop involved in terminating the stress response. However, FKBP51 has many more interaction partners like AKT, Beclin1 and NF- κ B. In the following paragraphs, we will show that many of FKBP51's interacting partners are involved in essential metabolic pathways, underpinning FKBP51 as a potential new therapeutic target for metabolic diseases (Figure 2).

3.1. FKBP51 regulates glucose uptake in muscle tissue

The AKT protein family consists of three related isoforms, AKT1, AKT2, and AKT3. All members share a high degree of homology, each containing a N-terminal pleckstrin homology (PH) domain, a kinase domain, and a hydrophobic motif at the C-terminus [79]. However, each isoform differs in its tissue expression levels. Whereas AKT1 is widely distributed across tissues and recognized for its role in cell growth and survival [80,81], AKT2 is largely restricted to insulin sensitive tissues, fat and muscle, where it contributes to the regulation of glucose homeostasis [82,83]. AKT3 expression is mainly limited to the testis and brain [84].

As a key downstream target of phosphoinositide-3 kinase (PI3K), many cytokines and growth factors, including insulin, activate AKT signaling. Briefly, PI3K converts phosphatidylinositol-4,5-bisphosphate (PIP2) into phosphatidylinositol-3,4,5-trisphosphate (PIP3), which subsequently acts as a binding site for PH domain proteins, including AKT and PDK1 (3-phosphoinositide-dependent protein kinase 1). At the plasma-membrane, PDK1 phosphorylates the activation loop of Akt at Thr308 [85]. For maximal activation, AKT is also phosphorylated at Ser473 (AKT2 Ser474) in the hydrophobic motif [86] by mTORC2 [87]. Once activated, AKT phosphorylates a plethora of downstream targets to regulate metabolism, cell proliferation, and cell survival [79]. To inactivate AKT signaling, protein phosphatase 2 (PP2) and PH domain leucine-rich repeat phosphatase (PHLPP) dephosphorylate Thr308 and Ser473, respectively [88,89]. Two isoforms of PHLPP (PHLPP1 and PHLPP2) exist, and while both dephosphorylate Ser473 (or Ser474 at

AKT2), PHLPP1 specifically acts on AKT2 and AKT3 whereas PHLPP2 acts on AKT1 and AKT3 providing specificity for the termination of AKT signaling [90].

FKBP51 has been shown to regulate AKT signaling through its role as a scaffolding protein. The first study to establish a link between FKBP51 and AKT demonstrated that overexpression of FKBP51 reduces phosphorylation of AKT1 at Ser473, but has no effect on the phosphorylation of Thr308 in a pancreatic cancer cell line [59]. Accordingly, siRNA downregulation or genetic deletion of FKBP51 increased Ser473 phosphorylation, with no effect on Thr308 phosphorylation. The authors demonstrated that FKBP51 regulates AKT1-Ser473 phosphorylation through its ability to interact with both PHLPP and AKT. Specifically, PHLPP and AKT co-immunoprecipitated with FKBP51, and in turn FKBP51 overexpression led to an increased interaction between PHLPP and AKT across all AKT isoforms and corresponding PHLPP isoforms. Importantly, decreased Ser473 phosphorylation resulted from FKBP51 overexpression was prevented by knockdown of PHLPP. At a functional level, FKBP51 expression is downregulated or lost in pancreatic cancer and breast cancer cell lines [59], which agrees with the observed AKT hyperactivation in many cancers. Reconstitution of FKBP51 in cancer cells decreased Akt phosphorylation at Ser473 and sensitized the cells to chemotherapeutic agents, supporting the earlier findings that loss of FKBP51 expression is associated with chemotherapy resistance [91].

Very recently, we demonstrated that FKBP51 is involved in the regulation of glucose homeostasis through its regulation of AKT2 signaling. We found that AKT2 signaling, as determined through the phosphorylation of AKT2 and downstream effectors (AKT substrate 160 (AS160) and p70S6K), is increased in skeletal muscle (soleus and extensor digitorum longus muscles) of FKBP51 KO mice and of mice treated with the FKBP51 antagonist SAFit2. This agrees with the relatively high expression level of FKBP51 and low expression level of its functional counterpart, FKBP52, detected in skeletal muscle. Given the

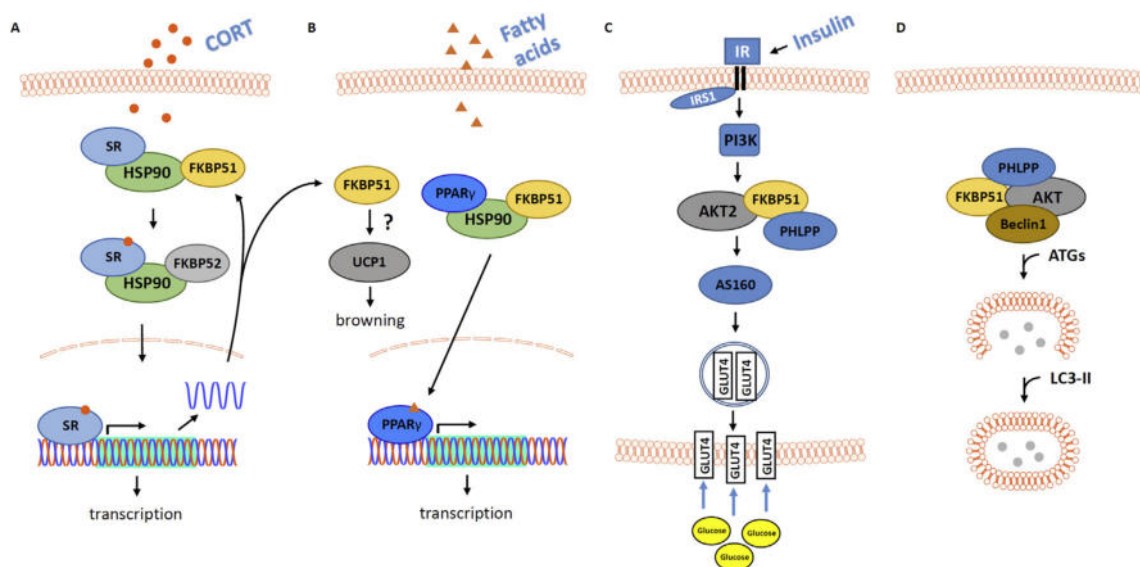


Figure 2: Schematic representation of important metabolism-related cellular signaling cascades where FKBP51 was shown to play a decisive role (see main text for further details). (A) FKBP51 interacts with HSP90 and several steroid receptors (SR), including the mineralocorticoid receptor (MR) and the glucocorticoid receptor (GR) and thereby modulates SR ligand sensitivity, translocation and function. Among the genes that are regulated by glucocorticoids (GCs) via MR/GR activation is Fkbp5, thereby forming an ultra-short feedback loop. At the same time, FKBP5 has been shown to interact with other signaling pathways, thereby affecting cellular function in a cell-type specific manner [132–134]. (B) In fat tissue, FKBP51 was shown to affect PPAR γ signaling and adipogenesis (not depicted) [73,105]. In addition, an effect of UCP1 and consequently browning of white adipose tissue (WAT) has been postulated [4,73]. (C) In muscle cells, FKBP51 interacts with AKT2 in the insulin signaling pathway, ultimately modulating cellular glucose uptake [4]. (D) In the brain, FKBP51 was shown to regulate autophagy via interaction with Beclin1 [56].

importance of skeletal muscle AKT signaling in the maintenance of glucose homeostasis [92,93], we examined molecular markers and functional readouts of glucose uptake. Briefly, the glucose transporter protein 4 (GLUT4) is responsible for insulin-stimulated glucose uptake in skeletal muscle. In an unstimulated state, GLUT4 is localized to specialized intracellular structures that consist of GLUT4 storage vesicles [94]. Upon insulin stimulation, AKT signaling is activated leading to the phosphorylation of AS160 and the translocation of GLUT4 to the plasma membrane, which facilitates increased glucose uptake [95]. Both pharmacological antagonism and genetic deletion of FKBP51 increase the expression of GLUT4 at the plasma membrane and increase 2-deoxyglucose uptake in primary myotubes. Meanwhile, simultaneous overexpression of AKT2 and FKBP51 prevented AKT2-induced increases in glucose uptake. Co-immunoprecipitation experiments revealed that FKBP51 not only interacts with AKT2 and PHLPP but interacts with the downstream effector AS160. Taken together, AKT2 signaling is an important regulator of cellular survival and metabolism. Through its function as regulator of AKT signaling, FKBP51 has been implicated in cellular survival in cancer and glucose uptake in obesity and diabetes. Whether FKBP51-AKT signaling is involved in additional metabolic functions beyond its regulation of glucose uptake is an open area of research.

3.2. FKBP51 regulates adipocyte differentiation in fat tissue

The pathophysiology of obesity is associated with the massive expansion of visceral and subcutaneous fat depots. Adipose tissue is a remarkable organ with fundamental effects on whole body metabolism. With its function as an energy storage site, a source of circulating free fatty acids, and a hormone secretion site, adipose tissue plays a major role in regulation and dysregulation of nutrient homeostasis [96,97]. Adipocytes are the major cell type of fat tissue. The accurate transformation of mesenchymal stem cells to mature adipocytes, so called adipogenesis, is crucial for proper functionality. Adipogenesis consists of 2 main phases, the determination of mesenchymal stem cells to pre-adipocytes and the final differentiation of pre-adipocytes to mature adipocytes. It is activated by multiple signaling cascades within the mitogen-activated protein (MAPK) family in response to a plethora of stimuli [98]. The so called 'master' regulator of adipogenesis is peroxisome-activated receptor γ (PPAR γ). PPAR γ acts as a pro-adipogenic factor, regulating the terminal differentiation phase [96]. The activation of PPAR γ by the AKT-p38/MAPK pathway was initially reported by Aoudi and colleagues [99,100]. Phosphorylation of AKT leads to an activation of p38 kinase, which phosphorylates the transcription factors GR α (at serine 220 and 234) [101] and PPAR γ (at serine 112) [102] to stimulate lipolysis and to reduce adipogenesis, respectively. Interestingly, recent data suggests that FKBP51 is one of the most highly induced proteins during WAT adipocyte differentiation [72,103]. *In vitro* studies in 3T3-L1 pre-adipocytes have shown that FKBP51 is an important regulator of adipocyte maturation [104]. In fact, loss of FKBP51 in pre-adipocytes prevents adipocyte differentiation and accumulation of lipid droplets [101]. Furthermore, FKBP51 KO cells tend to have an increased resistance to lipid accumulation and a decrease in the expression of lipogenic genes, such as CD36, in mature adipocytes [105]. The authors discovered that FKBP51 scaffolds PHLPP to inhibit AKT activity, through dephosphorylation, and thereby negatively regulates p38 kinase, which in turn reduces GR α activity to repress lipolysis and induces PPAR γ to increase adipogenesis [101,105]. These studies indicate that FKBP51 is an important regulator of the balance between lipolysis and lipogenesis in adipocytes.

A few years later, Stechschulte and colleagues confirmed their reduced PPAR γ and increased GR α activity in FKBP51 deficient mice *in vivo* [73]. Interestingly, they showed that FKBP51 null mice were resistant to the PPAR γ agonist rosiglitazone in WAT. These findings replicate the *in vitro* data and further support the notion that the FKBP51-Akt/p38 MAPK cascade is, in part, responsible for the reduced WAT mass in FKBP51 KO mice [73]. Surprisingly, the resistance to rosiglitazone was only observed in WAT. BAT of FKBP51 KO mice stayed responsive to the PPAR γ agonist.

The diverse effects of rosiglitazone in FKBP51 KO mice could be due to differences in FKBP51 expression in white and brown adipocytes, which derive from different adipocyte precursor lineages [106]. In fact, FKBP51 shows a lower expression in BAT compared to WAT [73]. Despite the expression differences of FKBP51, the levels of FKBP52 might be as important. FKBP52 competes for binding partners with FKBP51, thereby affecting downstream signaling pathways differently [43,63]. For instance, FKBP52 is minimally expressed in skeletal muscle and highly expressed in WAT. Consequently, FKBP52 does not compete with FKBP51 for the binding site with AKT2 in muscle, but interferes with its binding in WAT, thereby altering functional implications [4].

Next to its regulatory function on PPAR γ activity, FKBP51 also interacts in complex with Hsp90 with steroid receptors, like the GR, MR, AR, and PR [55]. So far, there are no conclusive data on a function of FKBP51 in modulating MR, AR, or PR function in adipocytes. Interestingly, especially adipocyte GRs are activated by glucocorticoids and are associated with adipogenesis [107] (the interplay between FKBP51, Hsp90 and GR are reviewed in detail elsewhere [64,104]). Within the first hours of adipocyte differentiation, FKBP51 rapidly translocates from the mitochondria to the nucleus. This shuttling of FKBP51 results in an increased interaction with GR and thereby a decrease of transcriptional activity of GR [72]. Whether or not the activation of PPAR γ and GR lead to nuclear shuttling of FKBP51 via differential mechanisms is so far not clear.

Mounting evidence suggests that FKBP51 is also important in the browning of WAT. Elevated levels of various thermogenic genes, such as PGC-1 α , UCP-1 and PRDM16 has been observed in WAT of FKBP51 KO mice. An upregulation of thermogenic genes is associated with increased energy expenditure and heat production, explaining the lean phenotype of FKBP51 KO mice [4,73]. However, the detailed molecular mechanism for the elevated energy expenditure and increased expression of browning markers in FKBP51 KO mice is still unclear. It is worth speculating that the observed effect of the UCP-1 upregulation in WAT of FKBP51 KO mice might not be mediated directly by FKBP51 but rather indirectly via sympathetic or parasympathetic innervation. Considering the distinct molecular and physiological properties of various fat depots within the body, specific manipulations of different adipose depots would be necessary to fully unravel the direct or indirect role of FKBP51 in the regulation of adipogenesis and browning *in vivo*.

3.3. Role of FKBP51 in modulating autophagy

Autophagy is an important catabolic process to maintain cellular homeostasis and cellular function. It is tightly regulated and crucial for targeting damaged cytosolic macromolecules such as organelles, proteins, glycogens, and lipids to lysosomes for degradation [108]. Recent data demonstrated an important role of autophagy in the regulation of metabolic processes such as, food intake, adipose tissue development, liver complications, and insulin resistance [109–111]. For instance, defects in autophagy signaling have been implicated in

the development of obesity and T2D [112]. Moreover, it has been shown that hypothalamic autophagy is increased during starvation to supply cells with sufficient nutrients [113]. Additionally, a regulatory role of autophagy in adipocyte mass development and differentiation has been reported [110,114]. Intriguingly, FKBP51 acts as a regulatory molecule of both processes as well [67,72], which indicates converging pathways of FKBP51 and autophagy. Indeed, in 2010, Romano et al. initially described a decisive role for FKBP51 in the cellular response to irradiation resulting in a shift from apoptosis to autophagy [115]. More recent studies have highlighted the mechanistic impact of FKBP51 on the regulation of autophagy and related processes. Furthermore, autophagy can be induced through GCs, and Hsp90 and its co-chaperone FKBP51 are key modulators of autophagy function [59,116–118]. The initiation and regulation of autophagy involves complex signaling pathways, which are not focus of this review, but are reviewed in depth elsewhere [119–121]. However, one key molecule, Beclin1, is of particular interest. Beclin1 interacts with several other proteins to induce the initiation of autophagy signaling. Interestingly, it was demonstrated that FKBP51 promotes the induction of autophagic signaling by phosphorylating Beclin1 at serine 234 and serine 295. In parallel, the Beclin1-phosphorylating kinase, AKT, is dephosphorylated at serine 473 by the FKBP51-mediated recruitment of PHLPP, which promotes the induction of autophagy. Furthermore, synthetic GCs (i.e. dexamethasone) and antidepressants act synergistically with FKBP51 in the induction of autophagy [56,122]. Despite the emerging roles of autophagy and FKBP51 in energy metabolism, no study has systemically investigated the FKBP51-Beclin1-Autophagy-axis in metabolic control. Indeed, in future studies, it will be important to delineate the regulatory action of FKBP51 on Beclin1 in the context of whole-body metabolism.

4. FKBP51 AS A THERAPEUTIC TARGET

FKBPs bind the immunosuppressive compounds FK506 and rapamycin [123,124]. These natural compounds, which were first isolated from bacterial *Streptomyces* strains, have been shown to bind to the peptidyl-prolyl-isomerase pocket of the FK1 domain, thereby inducing a complex with calcineurin (in the case of FK506) or mTOR (in the case of rapamycin) [125,126]. As FKBPs are also implicated in a wide range of intracellular signaling pathways that are independent of immune suppression [127,128], non-immunosuppressant FK506-derived ligands were developed (e.g. FK1706), which had neuroprotective properties [125]. However, none of these ligands could discriminate the different FKBPs, especially not between FKBP12 (with immunosuppressant properties) and the larger molecular weight FKBPs FKBP51 and FKBP52 (with non-immunosuppressant properties). Given the different and often opposing functions of the different FKBPs, selectivity of novel ligands is of utmost importance. As mentioned previously, while FKBP51 and FKBP52 share 70% sequence homology, they have diverging effects on many signaling pathways, including steroid hormone receptor signaling and AKT signaling pathways. Therefore, for the therapeutic potential of FKBP51 to be realized, agents must be able to select between FKBP51 and its often functional opposing homolog FKBP52. It soon became clear that the specific chemical targeting of FKBP51 is challenging, as large-scale screening assays for novel FKBP51 ligands did not reveal any new hits, other than the already known FK506 and rapamycin. The eventual breakthrough was achieved by Hausch and colleagues, using structure-based rational design [129]. In a stepwise approach guided by co-crystal structures a ligand-induced conformational change was observed that favored FKBP51 over FKBP52. Further development of the

prototype compounds eventually resulted in the first selective FKBP51 inhibitors termed SAFit1 (abbreviated for selective antagonists of the FK506-binding protein 51 by induced fit) and SAFit2 [2]. Both ligands have K_i values of less than 10 nM and show more than 10,000-fold selectivity of FKBP51 over FKBP52. These new compounds are non-immunosuppressive, and they selectively stimulate neurite outgrowth *in vitro*. For *in vivo* applications SAFit2 shows the better pharmacokinetic properties and crosses the blood brain barrier. As expected from the well-described function of FKBP51 in reducing the sensitivity of the GR to its ligand, treatment with SAFit2 enhanced GR-mediated GC feedback, as indicated by lower circadian peak corticosterone levels and an enhanced dexamethasone-mediated suppression of the HPA axis [2].

Since their first description, the selective FKBP51 ligands SAFit1 and SAFit2 have been tested in a number of *in vivo* disease models, underlining the versatile applicability of a selective pharmacological FKBP51 inhibition. As psychiatric disorders are closely linked to FKBP51 function, the brain-permeable SAFit2 was tested for effects on anxiety and depression-like behavior. Intriguingly, FKBP51 inhibition was shown to reduce passive stress coping behavior in the forced swim test and exploration anxiety in the elevated plus maze and the dark-light box after only a few hours post-administration [2,3]. The effect of FKBP51 antagonism on anxiety was specific to the amygdala, as the anxiolytic effect could be mimicked by injecting SAFit2 directly into this brain region. Similarly, FKBP51 inhibition was shown to reduce chronic pain [130,131]. When applied as treatment of metabolic disorders, we could recently show that prolonged SAFit2 treatment reduces body weight gain and reverses high-fat diet-induced glucose intolerance [4]. The effect mimicked the metabolic phenotype of FKBP51 KO mice, and no SAFit2 effect was observed when FKBP51 KO mice were treated, highlighting the specificity of the antagonist. Importantly, the improvement of glucose tolerance was already observed just 48 h after beginning treatment and preceded the body weight phenotype. This suggests that the effects of FKBP51 inhibition on glucose uptake are the most proximal beneficial treatment effects and independent of the improved body weight phenotype. Notably, pharmacological antagonism via SAFit2 disrupts the scaffolding function of FKBP51 by weakening the interaction between FKBP51 and AS160 while strengthening the interaction between AKT2 and AS160 to ultimately promote a steric arrangement that favors glucose uptake. Indeed, the first results of selective FKBP51 inhibition in relation to metabolism and metabolic disorders are highly promising and are a starting point for further investigations. Further improvement of the current inhibitors SAFit1 and SAFit2 to enhance their drug-like properties, including a lower molecular weight, will be important. Likewise, further improvement of the pharmacokinetic properties of SAFit1 would enable the pharmacological blockade of FKBP51 only in the periphery, as SAFit1 does not cross the blood brain barrier. Yet much work is still needed to disentangle the mechanism of action by which FKBP51 ligands work on the molecular level in the different tissues expressing FKBP51 in order to optimize the therapeutic effects of FKBP51 antagonists.

5. CONCLUSION AND FUTURE DIRECTIONS

This review's intent was to highlight the accumulating evidence that FKBP51 plays an important role in the regulation of whole-body energy and glucose metabolism, presenting FKBP51 as a complex co-chaperone beyond the well-established function as a negative GR regulator. The recent insights highlight FKBP51 as a potential drug target for obesity and its associated comorbidities. However, a lot of

research is needed to advance the field. Below, we list a few future directions, which we believe are crucial to advance the knowledge about FKBP51's metabolic action:

1. Tissue-specific manipulation of FKBP51 in muscle, adipose and brain tissue will be important to disentangle the differential functions of FKBP51 in specific cells-types.
2. Better insight into the specific actions of FKBP51 inhibitors at the molecular level will be necessary.
3. Development of pathway specific FKBP51 antagonists will be key for symptom tailored treatment.
4. Clinical studies examining FKBP51 in human cohorts in the context of metabolism will further the therapeutic development of FKBP51 antagonists

We hope that future preclinical and clinical studies will fill the knowledge gap to fully disentangle the molecular mechanism of FKBP51 in metabolism and help to implement FKBP51 as drug target for the treatment of metabolic disorders.

ACKNOWLEDGEMENTS

The current work was supported by the BioM M4 award "PROCERA" of the Bavarian State Ministry (Schmidt), the "OptiMD" grant of the Federal Ministry of Education and Research (01EE1401D; Schmidt) and the "GUTMOM" grant of the Federal Ministry of Education and Research (01EA1805; Schmidt).

CONFLICT OF INTERESTS

The authors declare conflict of interest.

REFERENCES

- [1] Chrousos, G.P., 2009. Stress and disorders of the stress system. *Nature Reviews Endocrinology* 5(7):374–381. <https://doi.org/10.1038/nrendo.2009.106>.
- [2] Gaali, S., Kirschner, A., Cuboni, S., Hartmann, J., Kozany, C., Balsevich, G., et al., 2015. Selective inhibitors of the FK506-binding protein 51 by induced fit. *Nature Chemical Biology* 11(1):33–37. <https://doi.org/10.1038/nchembio.1699>.
- [3] Hartmann, J., Wagner, K.V., Gaali, S., Kirschner, A., Kozany, C., Ruhter, G., et al., 2015. Pharmacological inhibition of the psychiatric risk factor FKBP51 has anxiolytic properties. *Journal of Neuroscience* 35:1529–2401. <https://doi.org/10.1523/JNEUROSCI.4024-14.2015> (Electronic): 9007–16.
- [4] Balsevich, G., Häusel, A.S., Meyer, C.W., Karamihalev, S., Feng, X., Pöhlmann, M.L., et al., 2017. Stress-responsive FKBP51 regulates AKT2-AS160 signaling and metabolic function. *Nature Communications* 8(1): 1725. <https://doi.org/10.1038/s41467-017-01783-y>.
- [5] Ulrich-Lai, Y.M., Herman, J.P., 2009. Neural regulation of endocrine and autonomic stress responses. *Nature Reviews Neuroscience* 10(6):397–409. <https://doi.org/10.1038/nrn2647>.
- [6] Cousin, B., Cinti, S., Morroni, M., Raimbault, S., Ricquier, D., Penicaud, L., et al., 1992. Occurrence of brown adipocytes in rat white adipose tissue: molecular and morphological characterization. *Journal of Cell Science* 103: 931–942 (Pt 4(0021-9533 (Print))).
- [7] Gilgen, A., Maickel, R.P., Nikodijevic, O., Brodie, B.B., 1962. Essential role of catecholamines in the mobilization of free fatty acids and glucose after exposure to cold. *Life Sciences* 1(1962):709–715.
- [8] Giordano, A., Morroni, M., Santone, G., Marchesi, G.F., Cinti, S., 1996. Tyrosine hydroxylase, neuropeptide Y, substance P, calcitonin gene-related peptide and vasoactive intestinal peptide in nerves of rat periovarian adipose tissue: an immunohistochemical and ultrastructural investigation. *Journal of Neurocytology* 25(2):125–136.
- [9] Young, P., Arch, J.R., Ashwell, M., 1984. Brown adipose tissue in the parametrial fat pad of the mouse. *FEBS Letters* 167(1):10–14.
- [10] Halter, J.B., Beard, J.C., Porte, D., 1984. Islet function and stress hyperglycemia: plasma glucose and epinephrine interaction. *American Journal of Physiology* 247(1 Pt 1):E47–E52. <https://doi.org/10.1152/ajpendo.1984.247.1.E47>.
- [11] de Kloet, E.R., 2013. Functional profile of the binary brain corticosteroid receptor system: mediating, multitasking, coordinating, integrating. *European Journal of Pharmacology* 719(1–3):53–62. <https://doi.org/10.1016/j.ejphar.2013.04.053>.
- [12] De Kloet, E.R., Joëls, M., Holsboer, F., 2005. Stress and the brain: from adaptation to disease. *Nature Reviews Neuroscience* 6(6):463–475. <https://doi.org/10.1038/nrn1683>.
- [13] Coderre, L., Srivastava, A.K., Chiasson, J.L., 1991. Role of glucocorticoid in the regulation of glycogen metabolism in skeletal muscle. *American Journal of Physiology* 260(6 Pt 1):E927–E932. <https://doi.org/10.1152/ajpendo.1991.260.6.E927>.
- [14] Exton, J.H., 1979. Regulation of gluconeogenesis by glucocorticoids. *Monographs on Endocrinology* 12:535–546.
- [15] Munck, A., Guyre, P.M., Holbrook, N.J., 1984. Physiological functions of glucocorticoids in stress and their relation to pharmacological actions. *Endocrine Reviews* 5(1):25–44. <https://doi.org/10.1210/edrv-5-1-25>.
- [16] Schweiger, M., Schreiber, R., Haemmerle, G., Lass, A., Fledelius, C., Jacobsen, P., et al., 2006. Adipose triglyceride lipase and hormone-sensitive lipase are the major enzymes in adipose tissue triacylglycerol catabolism. *Journal of Biological Chemistry* 281(52):40236–40241. <https://doi.org/10.1074/jbc.M608048200>.
- [17] Lutter, M., Nestler, E.J., 2009. Homeostatic and hedonic signals interact in the regulation of food intake. *Journal of Nutrition* 139(3):629–632. <https://doi.org/10.3945/jn.108.097618>.
- [18] Morton, G.J., Cummings, D.E., Baskin, D.G., Barsh, G.S., Schwartz, M.W., 2006. Central nervous system control of food intake and body weight. *Nature* 443(7109):289–295. <https://doi.org/10.1038/nature05026>.
- [19] Benoit, S.C., Clegg, D.J., Seeley, R.J., Woods, S.C., 2004. Insulin and leptin as adiposity signals. *Recent Progress in Hormone Research* 59:267–285. <https://doi.org/10.1210/rp.59.1.267>.
- [20] Cota, D., Marsicano, G., Tschöp, M., Grübler, Y., Flachskamm, C., Schubert, M., et al., 2003. The endogenous cannabinoid. *Journal of Clinical Investigation* 112(3):423–431. <https://doi.org/10.1172/JCI200317725>. Received.
- [21] Kahn, S.E., Hull, R.L., Utzschneider, K.M., 2006. Mechanisms linking obesity to insulin resistance and type 2 diabetes. *Nature* 444(7121):840–846. <https://doi.org/10.1038/nature05482>.
- [22] White, M.F., Kahn, C.R., 1994. The insulin signaling system. *Journal of Biological Chemistry* 269:1–4 (0021-9258 (Print)).
- [23] Saltiel, A.R., Kahn, C.R., 2001. Glucose and Lipid Metabolism 414(December):799–806.
- [24] Morton, G.J., Meek, T.H., Schwartz, M.W., 2014. Neurobiology of food intake in health and disease. *Nature Reviews Neuroscience* 15(6):367–378. <https://doi.org/10.1038/nrn3745>.
- [25] Cone, R.D., 2005. Anatomy and regulation of the central melanocortin system. *Nature Neuroscience* 8(5):571–578. <https://doi.org/10.1038/nn1455>.
- [26] Lowell, B.B., Spiegelman, B.M., 2000. Towards a molecular understanding of adaptive thermogenesis. *Nature* 404:652–660. <https://doi.org/10.1038/35007527>, 0028-0836 (Print).
- [27] Tremblay, A., Royer, M.-M., Chaput, J.-P., Doucet, E.É., 2012. Adaptive thermogenesis can make a difference in the ability of obese individuals to lose body weight. *International Journal of Obesity* 37:759–764. <https://doi.org/10.1038/ijo.2012.124>.

- [28] Mcpherson, R., 2007. Genetic contributors to obesity, vol. 23.
- [29] Saely, C.H., Geiger, K., Drexel, H., 2012. Brown versus white adipose tissue: a mini-review. *Gerontology* 58:15–23. <https://doi.org/10.1159/000321319>, 1423-0003 (Electronic).
- [30] Nicholls, D.G., 2006. The physiological regulation of uncoupling proteins. *Biochimica et Biophysica Acta* 1757:459–466. <https://doi.org/10.1016/j.bbabi.2006.02.005>, 0006-3002 (Print).
- [31] Morton, G., Schwartz, M., 2011. Leptin and the central nervous system control of glucose metabolism. *Physiological Reviews*(8):389–411. <https://doi.org/10.1152/physrev.00007.2010>.
- [32] Romero, L.M., Butler, L.K., 2007. *Endocrinology of stress*, vol. 20.
- [33] Ulrich-Lai, Y.M., Ryan, K.K., 2014. Neuroendocrine circuits governing energy balance and stress regulation: functional overlap and therapeutic implications. *Cell Metabolism* 19(6):910–925. <https://doi.org/10.1016/j.cmet.2014.01.020>.
- [34] Dallman, M.F., 2010. Stress-induced obesity and the emotional nervous system. *Trends in Endocrinology and Metabolism* 21:159–165. <https://doi.org/10.1016/j.tem.2009.10.004>, 1879-3061 (Electronic).
- [35] Cannon, B., Nedergaard, J., 2004. Brown adipose tissue: function and physiological significance. *Physiological Reviews* 84:277–359. <https://doi.org/10.1152/physrev.00015.2003>, 0031-9333 (Print).
- [36] Soumano, K., Desbiens, S., Rabelo, R., Bakopanos, E., Camirand, A., Silva, J.E., 2000. Glucocorticoids inhibit the transcriptional response of the uncoupling protein-1 gene to adrenergic stimulation in a brown adipose cell line. *Molecular and Cellular Endocrinology* 165(1–2):7–15. [https://doi.org/10.1016/S0303-7207\(00\)00276-8](https://doi.org/10.1016/S0303-7207(00)00276-8).
- [37] Van Den Beukel, J.C., Grefhorst, A., Quarta, C., Steenbergen, J., Mastroberardino, P.G., Lombés, M., et al., 2014. Direct activating effects of adrenocorticotropic hormone (ACTH) on brown adipose tissue are attenuated by corticosterone. *Federation of American Societies for Experimental Biology Journal* 28(11):4857–4867. <https://doi.org/10.1096/fj.14-254839>.
- [38] Razzoli, M., Bartolomucci, A., 2016. The dichotomous effect of chronic stress on obesity. *Trends in Endocrinology and Metabolism* 27(7):504–515. <https://doi.org/10.1016/j.tem.2016.04.007>.
- [39] Kuperman, Y., Issler, O., Regev, L., Musseri, I., Navon, I., Neufeld-Cohen, A., et al., 2010. Perifornical Urocortin-3 mediates the link between stress-induced anxiety and energy homeostasis. *Proceedings of the National Academy of Sciences of the United States of America* 107(18):8393–8398. <https://doi.org/10.1073/pnas.1003969107>.
- [40] Kuperman, Y., Weiss, M., Dine, J., Staikin, K., Golani, O., Ramot, A., et al., 2016. CRFR1 in AgRP neurons modulates sympathetic nervous system Activity to adapt to cold stress and fasting. *Cell Metabolism* 23(6):1185–1199. <https://doi.org/10.1016/J.CMET.2016.04.017>.
- [41] Sinars, C.R., Cheung-Flynn, J., Rimerman, R.A., Scammell, J.G., Smith, D.F., Clardy, J., 2003. Structure of the large FK506-binding protein FKBP51, an Hsp90-binding protein and a component of steroid receptor complexes. *Proceedings of the National Academy of Sciences of the United States of America* 100:868–873. <https://doi.org/10.1073/pnas.0231020100>, 0027-8424 (Print).
- [42] Galigniana, N.M., Ballmer, L.T., Toneatto, J., Erlejman, A.G., Lagadari, M., Galigniana, M.D., 2012. Regulation of the glucocorticoid response to stress-related disorders by the Hsp90-binding immunophilin FKBP51. *Journal of Neurochemistry* 122(1):4–18. <https://doi.org/10.1111/j.1471-4159.2012.07775.x>.
- [43] Storer, C.L., Dickey, C.A., Galigniana, M.D., Rein, T., Cox, M.B., 2011. FKBP51 and FKBP52 in signaling and disease. *Trends in Endocrinology and Metabolism* 22(12):481–490. <https://doi.org/10.1016/j.tem.2011.08.001>.
- [44] Denny, W.B., Valentine, D.L., Reynolds, P.D., Smith, D.F., Scammell, J.G., 2000. Squirrel monkey immunophilin {FKBP}51 is a potent inhibitor of glucocorticoid receptor binding. *Endocrinology* 141 (0013-7227 (Print)): 4107–13.
- [45] Scammell, J.G., Denny, W.B., Valentine, D.L., Smith, D.F., 2001. Overexpression of the FK506-binding immunophilin FKBP51 is the common cause of glucocorticoid resistance in three new world primates. *General and Comparative Endocrinology* 124(2):152–165. <https://doi.org/10.1006/GCEN.2001.7696>.
- [46] Westberry, J.M., Sadosky, P.W., Hubler, T.R., Gross, K.L., Scammell, J.G., 2006. Glucocorticoid resistance in squirrel monkeys results from a combination of a transcriptionally incompetent glucocorticoid receptor and overexpression of the glucocorticoid receptor co-chaperone {FKBP}51. *The Journal of Steroid Biochemistry and Molecular Biology* 100:34–41. <https://doi.org/10.1016/j.jsmb.2006.03.004>, 0960-0760 (Print).
- [47] Wochnik, G.M., Rüegg, J., Abel, G.A., Schmidt, U., Holsboer, F., Rein, T., 2005. FK506-binding proteins 51 and 52 differentially regulate dynein interaction and nuclear translocation of the glucocorticoid receptor in mammalian cells. *Journal of Biological Chemistry* 280(6):4609–4616. <https://doi.org/10.1074/jbc.M407498200>.
- [48] Binder, E.B., Bradley, R.G., Liu, W., Epstein, M.P., Deveau, T.C., Mercer, K.B., et al., 2008. Association of FKBP5 polymorphisms and childhood abuse with risk of posttraumatic stress disorder symptoms in adults. *Journal of the American Medical Association* 299. <https://doi.org/10.1001/jama.299.11.1291> (1538-3598 (Electronic)): 1291–305.
- [49] Touma, C., Gassen, N.C., Herrmann, L., Cheung-Flynn, J., Blü, D.R., Ionescu, I.A., et al., 2011. FK506 binding protein 5 shapes stress responsiveness: modulation of neuroendocrine reactivity and coping behavior. *Biological Psychiatry* 70(10):928–936. <https://doi.org/10.1016/j.biopsych.2011.07.023>.
- [50] Ising, M., Depping, A.M., Siebertz, A., Lucae, S., Unschuld, P.G., Kloiber, S., et al., 2008. Polymorphisms in the {FKBP}5 gene region modulate recovery from psychosocial stress in healthy controls. *European Journal of Neuroscience* 28:389–398. <https://doi.org/10.1111/j.1460-9568.2008.06332.x>, 1460-9568 (Electronic).
- [51] Vermeer, H., Hendriks-Stegeman, B.I., van der Burg, B., van Buul-Offers, S.C., Jansen, M., 2003. Glucocorticoid-induced increase in lymphocytic {FKBP}51 messenger ribonucleic acid expression: a potential marker for glucocorticoid sensitivity, potency, and bioavailability. *Journal of Clinical Endocrinology & Metabolism* 88 (0021-972X (Print)): 277–84.
- [52] Pirkil, F., Buchner, J., 2001. Functional analysis of the hsp90-associated human peptidyl prolyl Cis/Trans isomerases FKBP51, FKBP52 and cyp40. *Journal of Molecular Biology* 308(4):795–806. <https://doi.org/10.1006/JMBI.2001.4595>.
- [53] Riggs, D.L., Roberts, P.J., Chirillo, S.C., Cheung-Flynn, J., Prapapanich, V., Ratajczak, T., et al., 2003. The Hsp90-binding peptidylprolyl isomerase FKBP52 potentiates glucocorticoid signaling in vivo. *The EMBO Journal* 22(5): 1158–1167. <https://doi.org/10.1093/emboj/cdg108>.
- [54] Riggs, D.L., Cox, M.B., Tardif, H.L., Hessling, M., Buchner, J., Smith, D.F., 2007. Noncatalytic role of the FKBP52 peptidyl-prolyl isomerase domain in the regulation of steroid hormone signaling. *Molecular and Cellular Biology* 27(24):8658–8669. <https://doi.org/10.1128/MCB.00985-07>.
- [55] Schülke, J.-P., Wochnik, G.M., Lang-Rollin, I., Gassen, N.C., Knapp, R.T., Berning, B., et al., 2010. Differential impact of tetratricopeptide repeat proteins on the steroid hormone receptors. *PLoS One* 5(7):e11717. <https://doi.org/10.1371/journal.pone.0011717>.
- [56] Gassen, N.C., Hartmann, J., Zschocke, J., Stepan, J., Hafner, K., Zellner, A., et al., 2014. Association of FKBP51 with priming of autophagy pathways and mediation of antidepressant treatment response: evidence in cells, mice, and humans. *PLoS Medicine* 11(11):e1001755. <https://doi.org/10.1371/journal.pmed.1001755>.
- [57] Gassen, N.C., Hartmann, J., Zannas, a. S., Kretzschmar, A., Zschocke, J., Maccarrone, G., et al., 2016. FKBP51 inhibits GSK3 β and augments the effects of distinct psychotropic medications. *Molecular Psychiatry* 21(2): 277–289. <https://doi.org/10.1038/mp.2015.38>.

- [58] Jiang, W., Cazacu, S., Xiang, C., Zenklusen, J.C., Fine, H.A., Berens, M., et al., 2008. FK506 binding protein mediates glioma cell growth and sensitivity to rapamycin treatment by regulating NF-kappaB signaling pathway. *Neoplasia* 10:235–243, 1476–5586 (Electronic).
- [59] Pei, H., Li, L., Fridley, B.L., Jenkins, G.D., Kalari, K.R., Lingle, W., et al., 2009. FKBP51 affects cancer cell response to chemotherapy by negatively regulating Akt. *Cancer Cell* 16(3):259–266. <https://doi.org/10.1016/j.ccr.2009.07.016>.
- [60] Romano, S., Xiao, Y., Nakaya, M., D'Angelillo, A., Chang, M., Jin, J., et al., 2015. FKBP51 employs both scaffold and isomerase functions to promote NF-kappaB activation in melanoma. *Nucleic Acids Research* 43(14):6983–6993. <https://doi.org/10.1093/nar/gkv615>.
- [61] Zannas, A.S., Jia, M., Hafner, K., Baumert, J., Wiechmann, T., Pape, J.C., et al., 2019. Epigenetic upregulation of FKBP5 by aging and stress contributes to NF-κB-driven inflammation and cardiovascular risk. *Proceedings of the National Academy of Sciences of the United States of America* 116(23):11370–11379. <https://doi.org/10.1073/pnas.1816847116>.
- [62] Uhlen, M., Fagerberg, L., Hallstrom, B.M., Lindskog, C., Oksvold, P., Mardinoglu, A., et al., 2015. Tissue-based map of the human proteome. *Science* 347(6220). <https://doi.org/10.1126/science.1260419>, 1260419–1260419.
- [63] Schmidt, M.V., Paez-Pereda, M., Holsboer, F., Hausch, F., 2012. The prospect of FKBP51 as a drug target. *ChemMedChem* 7(8):1351–1359. <https://doi.org/10.1002/cmdc.201200137>.
- [64] Zgajnar, N.R., Leo, S.A. De., Lotufo, C.M., Erleijman, A.G., Pwien-Pilipuk, G., Galgiana, M.D., 2019. Biological actions of the hsp90-binding immunophilins FKBP51 and FKBP52. *Biomolecules* 9(2). <https://doi.org/10.3390/Biom9020052>.
- [65] Baughman, G., Widerrecht, G.J., Chang, F., Martin, M.M., Bourgeois, S., 1997. Tissue distribution and abundance of human FKBP51, and FK506-binding protein that can mediate calcineruin inhibition. *Biochemical and Biophysical Research Communications* 232(2):437–443.
- [66] Pereira, M.J., Palming, J., Svensson, M.K., Rizell, M., Dalenbäck, J., Hammar, M., et al., 2014. FKBP5 expression in human adipose tissue increases following dexamethasone exposure and is associated with insulin resistance. *Metabolism* 63:1198–1208. <https://doi.org/10.1016/j.metabol.2014.05.015>.
- [67] Scharf, S.H., Liebl, C., Binder, E.B., Schmidt, M.V., Müller, M.B., 2011. Expression and regulation of the Fkbp5 gene in the adult mouse brain. *PLoS One* 6(2):1–10. <https://doi.org/10.1371/journal.pone.0016883>.
- [68] Ortiz, R., Joseph, J.J., Lee, R., Wand, G.S., Golden, S.H., 2018. Type 2 diabetes and cardiometabolic risk may be associated with increase in DNA methylation of FKBP5. *Clinical Epigenetics* 10(1):82. <https://doi.org/10.1186/s13148-018-0513-0>.
- [69] Klengel, T., Mehta, D., Anacker, C., Rex-Haffner, M., Pruessner, J.C., Pariante, C.M., et al., 2013. Allele-specific FKBP5 DNA demethylation mediates gene-childhood trauma interactions. *Nature Neuroscience* 16(1):33–41. <https://doi.org/10.1038/nn.3275>.
- [70] Zannas, A.S., Binder, E.B., 2014. Gene-environment interactions at the FKBP5 locus: sensitive periods, mechanisms and pleiotropism. *Genes, Brain and Behavior* 13(1):25–37. <https://doi.org/10.1111/gbb.12104>.
- [71] Sidibeh, C.O., Pereira, M.J., Abalo, X.M., J Boersma, G., Skrtic, S., Lundkvist, P., et al., 2018. FKBP5 expression in human adipose tissue: potential role in glucose and lipid metabolism, adipogenesis and type 2 diabetes. *Endocrine* 62(1):116–128. <https://doi.org/10.1007/s12020-018-1674-5>.
- [72] Toneatto, J., Guber, S., Charo, N.L., Susperreguy, S., Schwartz, J., Galgiana, M.D., et al., 2013. Dynamic mitochondrial-nuclear redistribution of the immunophilin FKBP51 is regulated by the PKA signaling pathway to control gene expression during adipocyte differentiation. *Journal of Cell Science* 126(23):5357–5368. <https://doi.org/10.1242/jcs.125799>.
- [73] Stechschulte, L.A., Qiu, B., Warriar, M., Hinds, T.D., Zhang, M., Gu, H., et al., 2016. FKBP51 null mice are resistant to diet-induced obesity and the PPARγ agonist rosiglitazone. *Endocrinology* 157(10):3888–3900. <https://doi.org/10.1210/en.2015-1996>.
- [74] Resmini, E., Santos, A., Aulinas, A., Webb, S.M., Vives-Gilabert, Y., Cox, O., et al., 2016. Reduced DNA methylation of FKBP5 in Cushing's syndrome. *Endocrine* 54(3):768–777. <https://doi.org/10.1007/s12020-016-1083-6>.
- [75] Hartmann, I.B., Fries, G.R., Bucker, J., Scotton, E., von Diemen, L., Kauer-Sant'Anna, M., 2016. The FKBP5 polymorphism rs1360780 is associated with lower weight loss after bariatric surgery: 26 months of follow-up. *Surgery for Obesity and Related Diseases* 12(8):1554–1560. <https://doi.org/10.1016/j.soard.2016.04.016>.
- [76] Hartmann, J., Wagner, K.V., Liebl, C., Scharf, S.H., Wang, X.D., Wolf, M., et al., 2012. The involvement of FK506-binding protein 51 (FKBP5) in the behavioral and neuroendocrine effects of chronic social defeat stress. *Neuropharmacology* 62(1):332–339. <https://doi.org/10.1016/j.neuropharm.2011.07.041>.
- [77] Sanchez, E.R., 2012. Chaperoning steroidal physiology: lessons from mouse genetic models of Hsp90 and its cochaperones. *Biochimica et Biophysica Acta (BBA) - Molecular Cell Research* 1823(3):722–729. <https://doi.org/10.1016/j.bbamcr.2011.11.006>.
- [78] Balsevich, G., Uribe, A., Wagner, K.V., Hartmann, J., Santarelli, S., Labermaier, C., et al., 2014. Interplay between diet-induced obesity and chronic stress in mice: potential role of FKBP51. *Journal of Endocrinology* 222(1):15–26. <https://doi.org/10.1530/JOE-14-0129>.
- [79] Hers, I., Vincent, E.E., Tavaré, J.M., 2011. Akt signalling in health and disease. *Cellular Signalling* 23(10):1515–1527. <https://doi.org/10.1016/j.cellsig.2011.05.004>.
- [80] Chen, W.S., Xu, P.Z., Gottlob, K., Chen, M.L., Sokol, K., Shiyanova, T., et al., 2001. Growth retardation and increased apoptosis in mice with homozygous disruption of the Akt1 gene. *Genes & Development* 15(17):2203–2208. <https://doi.org/10.1101/gad.913901>.
- [81] Cho, H., Thorvaldsen, J.L., Chu, Q., Feng, F., Birnbaum, M.J., 2001. Akt1/PKBalpha is required for normal growth but dispensable for maintenance of glucose homeostasis in mice. *Journal of Biological Chemistry* 276(42):38349–38352. <https://doi.org/10.1074/jbc.C100462200>.
- [82] Garofalo, R.S., Orena, S.J., Rafidi, K., Torchia, A.J., Stock, J.L., Hildebrandt, A.L., et al., 2003. Sever diabetes, age-dependent loss of adipose tissue, and ild growth deficiency in mice lacking Akt2/PKBb. *Journal of Clinical Investigation* 112(2):197–208. <https://doi.org/10.1172/JCI16885> \ <https://doi.org/10.1172/JCI200316885> [pii].
- [83] Cho, H., Mu, J., Kim, J.K., Thorvaldsen, J.L., Chu, Q., Crenshaw, E.B., et al., 2001. Insulin resistance and a diabetes mellitus-like syndrome in mice lacking the protein kinase Akt2 (PKBβ). *Science* 292(5522):1728–1731. <https://doi.org/10.1126/science.292.5522.1728>.
- [84] Yang, Z.-Z., Tschopp, O., Hemmings-Mieszcak, M., Feng, J., Brodbeck, D., Perentes, E., et al., 2003. Protein kinase B alpha/Akt1 regulates placental development and fetal growth. *Journal of Biological Chemistry* 278(34):32124–32131. <https://doi.org/10.1074/jbc.M302847200>.
- [85] Alessi, D.R., James, S.R., Downes, C.P., Holmes, A.B., Gaffney, P.R., Reese, C.B., et al., 1997. Characterization of a 3-phosphoinositide-dependent protein kinase which phosphorylates and activates protein kinase Balpha. *Current Biology: CB* 7(4):261–269.
- [86] Alessi, D.R., Andjelkovic, M., Caudwell, B., Cron, P., Morrice, N., Cohen, P., et al., 1996. Mechanism of activation of protein kinase B by insulin and IGF-1. *The EMBO Journal* 15(23):6541–6551.
- [87] Sarbassov, D.D., Guertin, D.A., Ali, S.M., Sabatini, D.M., 2005. Phosphorylation and regulation of Akt/PKB by the rictor-mTOR complex. *Science (New York, N.Y.)* 307(5712):1098–1101. <https://doi.org/10.1126/science.1106148>.

- [88] Andjelković, M., Jakubowicz, T., Cron, P., Ming, X.F., Han, J.W., Hemmings, B.A., 1996. Activation and phosphorylation of a pleckstrin homology domain containing protein kinase (RAC-PK/PKB) promoted by serum and protein phosphatase inhibitors. *Proceedings of the National Academy of Sciences of the United States of America* 93(12):5699–5704.
- [89] Gao, T., Furnari, F., Newton, A.C., 2005. PHLPP: a phosphatase that directly dephosphorylates Akt, promotes apoptosis, and suppresses tumor growth. *Molecular Cell* 18(1):13–24. <https://doi.org/10.1016/j.molcel.2005.03.008>.
- [90] Brognard, J., Sierceki, E., Gao, T., Newton, A.C., 2007. PHLPP and a second isoform, PHLPP2, differentially attenuate the amplitude of Akt signaling by regulating distinct Akt isoforms. *Molecular Cell* 25(6):917–931. <https://doi.org/10.1016/j.molcel.2007.02.017>.
- [91] Li, L., Fridley, B., Kalari, K., Jenkins, G., Batzler, A., Safgren, S., et al., 2008. Gemcitabine and cytosine arabinoside cytotoxicity: association with lymphoblastoid cell expression. *Cancer Research* 68(17):7050–7058. <https://doi.org/10.1158/0008-5472.CAN-08-0405>.
- [92] DeFronzo, R.A., Tripathy, D., 2009. Skeletal muscle insulin resistance is the primary defect in type 2 diabetes. *Diabetes Care* 32(Suppl. 2):S157–S163. <https://doi.org/10.2337/dc09-S302> (1935-5548 (Electronic)).
- [93] Zierath, J.R., Wallberg-Henriksson, H., 2002. From receptor to effector: insulin signal transduction in skeletal muscle from type II diabetic patients. *Annals of the New York Academy of Sciences* 967 (0077-8923 (Print)): 120–34.
- [94] Leto, D., Saltiel, A.R., 2012. Regulation of glucose transport by insulin: traffic control of GLUT4. *Nature Reviews Molecular Cell Biology* 13. <https://doi.org/10.1038/nrm3351> (1471-0080 (Electronic)): 383–96.
- [95] Sano, H., Kane, S., Sano, E., Miinea, C.P., Asara, J.M., Lane, W.S., et al., 2003. Insulin-stimulated phosphorylation of a Rab GTPase-activating protein regulates GLUT4 translocation. *Journal of Biological Chemistry* 278. <https://doi.org/10.1074/jbc.C300063200> (0021-9258 (Print)): 14599–602.
- [96] Rosen, E.D., Spiegelman, B.M., 2014. What we talk about when we talk about fat. *Cell* 156(1–2):20–44. <https://doi.org/10.1016/j.cell.2013.12.012>.
- [97] MacDougald, O.A., Mandrup, S., 2002. Adipogenesis: forces that tip the scales. *Trends in Endocrinology and Metabolism* 13(1):5–11. [https://doi.org/10.1016/S1043-2760\(01\)00517-3](https://doi.org/10.1016/S1043-2760(01)00517-3).
- [98] Pearson, S.G., Robinson, F., Gibson, T.B., Xu, B.E., Karandikar, M., Berman, K., et al., 2001. Mitogen-activated protein (MAP) kinase pathways: regulation and physiological functions. *Endocrine Reviews*. <https://doi.org/10.1210/er.22.2.153>.
- [99] Aouadi, M., Laurent, K., Prot, M., Le Marchand-Brustel, Y., Binétruy, B., Bost, F., 2006. Inhibition of p38MAPK increases adipogenesis from embryonic to adult stages. *Diabetes*. <https://doi.org/10.2337/diabetes.55.02.06.db05-0963>.
- [100] Aouadi, M., Jager, J., Laurent, K., Gonzalez, T., Cormont, M., Binétruy, B., et al., 2007. p38MAP Kinase activity is required for human primary adipocyte differentiation. *FEBS Letters*. <https://doi.org/10.1016/j.febslet.2007.10.064>.
- [101] Stechschulte, L.A., Hinds, T.D., Khuder, S.S., Shou, W., Najjar, S.M., Sanchez, E.R., 2014. FKBP51 controls cellular adipogenesis through p38 kinase-mediated phosphorylation of GR α and PPAR γ . *Molecular Endocrinology* <https://doi.org/10.1210/me.2014-1022>.
- [102] Hu, E., Kim, J.B., Sarraf, P., Spiegelman, B.M., 1996. Inhibition of adipogenesis through MAP kinase-mediated phosphorylation of PPAR γ . *Science* <https://doi.org/10.1126/science.274.5295.2100>.
- [103] Yeh, W.C., Li, T.K., Bierer, B.E., McKnight, S.L., Smith, D.F., Clardy, J., 1995. Identification and characterization of an immunophilin expressed during the clonal expansion phase of adipocyte differentiation. *Proceedings of the National Academy of Sciences* 92(24):11081–11085. <https://doi.org/10.1073/pnas.92.24.11081>.
- [104] Toneatto, J., Charó, N.L., Galigniana, N.M., Piwien-Pilipuk, G., 2015. Adipogenesis is under surveillance of Hsp90 and the high molecular weight immunophilin FKBP51. *Adipocyte*. <https://doi.org/10.1080/21623945.2015.1049401>.
- [105] Stechschulte, L.A., Hinds, T.D., Ghanem, S.S., Shou, W., Najjar, S.M., Sanchez, E.R., 2014. FKBP51 reciprocally regulates GR α and PPAR γ activation via the Akt-p38 pathway. *Molecular Endocrinology*. <https://doi.org/10.1210/me.2014-1023>.
- [106] Inagaki, T., Sakai, J., Kajimura, S., 2016. Transcriptional and epigenetic control of brown and beige adipose cell fate and function. *Nature Reviews Molecular Cell Biology* 17(8):480–495. <https://doi.org/10.1038/nrm.2016.62>.
- [107] Marzolla, V., Armani, A., Zennaro, M.C., Cinti, F., Mammi, C., Fabbri, A., et al., 2012. The role of the mineralocorticoid receptor in adipocyte biology and fat metabolism. *Molecular and Cellular Endocrinology* 350(2):281–288. <https://doi.org/10.1016/j.mce.2011.09.011>.
- [108] Levine, B., Kroemer, G., 2008. Autophagy in the pathogenesis of disease. *Cell*. <https://doi.org/10.1016/j.cell.2007.12.018>.
- [109] Singh, R., 2012. Autophagy in the control of food intake. *Adipocyte* 1(2):75–79. <https://doi.org/10.4161/adip.18966>.
- [110] Singh, R., Kaushik, S., Wang, Y., Xiang, Y., Novak, I., Komatsu, M., et al., 2009. Autophagy regulates lipid metabolism. *Nature* 458(7242):1131–1135. <https://doi.org/10.1038/nature07976>.
- [111] Yamamoto, S., Kuramoto, K., Wang, N., Situ, X., Priyadarshini, M., Zhang, W., et al., 2018. Autophagy differentially regulates insulin production and insulin sensitivity. *Cell Reports* 23(11):3286–3299. <https://doi.org/10.1016/j.celrep.2018.05.032>.
- [112] Zhang, Y., Sowers, J.R., Ren, J., 2018. Targeting autophagy in obesity: from pathophysiology to management. *Nature Reviews Endocrinology* 14(6):356–376. <https://doi.org/10.1038/s41574-018-0009-1>.
- [113] Kaushik, S., Rodriguez-Navarro, J.A., Arias, E., Kiffin, R., Sahu, S., Schwartz, G.J., et al., 2011. Autophagy in hypothalamic AgRP neurons regulates food intake and energy balance. *Cell Metabolism* 14(2):173–183. <https://doi.org/10.1016/j.cmet.2011.06.008>.
- [114] An, L., Zhang, Y.Z., Yu, N.J., Liu, X.M., Zhao, N., Yuan, L., et al., 2008. Role for serotonin in the antidepressant-like effect of a flavonoid extract of Xiaobuxin-Tang. *Pharmacology Biochemistry and Behavior* 89(4):572–580. <https://doi.org/10.1016/j.pbb.2008.02.014>.
- [115] Romano, S., D'Angelillo, A., Pacelli, R., Staibano, S., De Luna, E., Bisogni, R., et al., 2010. Role of FK506-binding protein 51 in the control of apoptosis of irradiated melanoma cells. *Cell Death & Differentiation* 17(1):145–157. <https://doi.org/10.1038/cdd.2009.115>.
- [116] Marz, A.M., Fabian, A.-K., Kozany, C., Bracher, A., Hausch, F., 2013. Large FK506-binding proteins shape the pharmacology of rapamycin. *Molecular and Cellular Biology* 33(7):1357–1367. <https://doi.org/10.1128/MCB.00678-12>.
- [117] Wang, R.C., Wei, Y., An, Z., Zou, Z., Xiao, G., Bhagat, G., et al., 2012. Akt-mediated regulation of autophagy and tumorigenesis through Beclin 1 phosphorylation. *Science (New York, N.Y.)* 338(6109):956–959. <https://doi.org/10.1126/science.1225967>.
- [118] Laane, E., Tamm, K.P., Buentke, E., Ito, K., Khahariza, P., Oscarsson, J., et al., 2009. Cell death induced by dexamethasone in lymphoid leukemia is mediated through initiation of autophagy. *Cell Death & Differentiation* 16(7):1018–1029. <https://doi.org/10.1038/cdd.2009.46>.
- [119] Mizushima, N., Levine, B., Cuervo, A.M., Klionsky, D.J., 2008. Autophagy fights disease through cellular self-digestion. *Nature* 451(7182):1069–1075. <https://doi.org/10.1038/nature06639>.
- [120] Levine, B., Kroemer, G., 2019. Biological functions of autophagy genes: a disease perspective. *Cell* 176(1–2):11–42. <https://doi.org/10.1016/j.cell.2018.09.048>.
- [121] Maiuri, M.C., Zalckvar, E., Kimchi, A., Kroemer, G., 2007. Self-eating and self-killing: crosstalk between autophagy and apoptosis. *Nature Reviews Molecular Cell Biology*. <https://doi.org/10.1038/nrm2239>.

- [122] Gassen, N.C., Hartmann, J., Schmidt, M.V., Rein, T., 2015. FKBP5/FKBP51 enhances autophagy to synergize with antidepressant action. *Autophagy* 11(3):578–580. <https://doi.org/10.1080/15548627.2015.1017224>.
- [123] Bierer, B.E., Mattila, P.S., Standaert, R.F., Herzenberg, L.A., Burakoff, S.J., Crabtree, G., et al., 1990. Two distinct signal transmission pathways in T lymphocytes are inhibited by complexes formed between an immunophilin and either FK506 or rapamycin. *Proceedings of the National Academy of Sciences of the United States of America* 87(23):9231–9235.
- [124] Blackburn, E.A., Walkinshaw, M.D., 2011. Targeting FKBP isoforms with small-molecule ligands. *Current Opinion in Pharmacology* 11(4):365–371. <https://doi.org/10.1016/j.coph.2011.04.007>.
- [125] Duniak, B.M., Gestwicki, J.E., 2016. Peptidyl-proline isomerases (PPIases): targets for natural products and natural product-inspired compounds. *Journal of Medicinal Chemistry* 59(21):9622–9644. <https://doi.org/10.1021/acs.jmedchem.6b00411>.
- [126] Schreiber, S.L., 1991. Chemistry and biology of the immunophilins and their immunosuppressive ligands. *Science (New York, N.Y.)* 251(4991):283–287.
- [127] Bonner, J.M., Boulianne, G.L., 2017. Diverse structures, functions and uses of FK506 binding proteins. *Cellular Signalling* 38:97–105. <https://doi.org/10.1016/j.cellsig.2017.06.013>.
- [128] Ratajczak, T., Cluning, C., Ward, B.K., 2015. Steroid receptor-associated immunophilins: a gateway to steroid signalling. *Clinical Biochemist Reviews* 36(2):31–52.
- [129] Feng, X., Pomplun, S., Hausch, F., 2015. Recent progress in FKBP ligand development. *Current Molecular Pharmacology* 9(1):27–36.
- [130] Maiarù, M., Morgan, O.B., Mao, T., Breitsamer, M., Bamber, H., Pöhlmann, M., et al., 2018. The stress regulator Fkbp51: a novel and promising druggable target for the treatment of persistent pain states across sexes. *Pain*. <https://doi.org/10.1097/j.pain.0000000000001204>.
- [131] Maiarù, M., Tochiki, K.K., Cox, M.B., Annan, L.V., Bell, C.G., Feng, X., et al., 2016. The stress regulator FKBP51 drives chronic pain by modulating spinal glucocorticoid signaling. *Science Translational Medicine* 8(325):325ra19. <https://doi.org/10.1126/scitranslmed.aab3376>.
- [132] Criado-Marrero, M., Rein, T., Binder, E.B., Porter, J.T., Koren, J., Blair, L.J., 2018. Hsp90 and FKBP51: complex regulators of psychiatric diseases. *Philosophical Transactions of the Royal Society B: Biological Sciences*. <https://doi.org/10.1098/rstb.2016.0532>.
- [133] Davies, T.H., Ning, Y.M., Sánchez, E.R., 2002. A new first step in activation of steroid receptors. Hormone-induced switching of FKBP51 and FKBP52 immunophilins. *Journal of Biological Chemistry*. <https://doi.org/10.1074/jbc.C100531200>.
- [134] Hinds, T.D., Stechschulte, L.A., Elkhairi, F., Sanchez, E.R., 2014. Analysis of FK506, timcodar (VX-853) and FKBP51 and FKBP52 chaperones in control of glucocorticoid receptor activity and phosphorylation. *Pharmacology Research and Perspectives*. <https://doi.org/10.1002/prp2.76>.

3. Research articles

Chapter 1 **Stress-responsive FKBP51 regulates AKT2-AS160 signaling and metabolic function**

Originally published in Nature Communications, November 2017

Chapter 2 **Mediobasal hypothalamic FKBP51 acts as a molecular switch linking autophagy to whole-body metabolism.**

Originally published in Science Advances, March 2022

Chapter 3 **The co-chaperone Fkbp5 shapes the acute stress response in the paraventricular nucleus of the hypothalamus in male mice.**

Originally published in Molecular Psychiatry, March 2021

3.1. Stress-responsive FKBP51 regulates AKT2-AS160 signaling and metabolic function

Authors:

Georgia Balsevich¹, Alexander S. Häusl¹, Carola W. Meyer², Stoyo Karamihalev¹, Xixi Feng³, Max L. Pöhlmann¹, Carine Dournes¹, Andres Uribe-Marino¹, Sara Santarelli¹, Christiana Labermaier¹, Kathrin Hafner³, Tianqi Mao³, Michaela Breitsamer⁴, Marily Theodoropoulou³, Christian Namendorf³, Manfred Uhr³, Marcelo Paez-Pereda³, Gerhard Winter⁴, Felix Hausch⁵, Alon Chen¹, Mathias H. Tschöp², Theo Rhein³, Nils C. Gassen³ and Mathias V. Schmidt¹

Affiliations:

¹ *Department of Stress Neurobiology and Neurogenetics, Max Planck Institute of Psychiatry, Kraepelinstraße 2-10, 80804 Munich, Germany*

² *Institute of Diabetes and Obesity, Helmholtz Zentrum München, Parkring 13, 85748 Garching, Germany*

³ *Department of Translational Research in Psychiatry, Max Planck Institute of Psychiatry, Kraepelinstraße 2-10, 80804 Munich, Germany*

⁴ *Ludwig Maximilians University, Butenandtstr. 5-13, 81377 Munich, Germany*

⁵ *Technical University Darmstadt, Institute of Organic Chemistry and Biochemistry, Alrich-Weiss-Str. 4, 64287 Darmstadt, Germany*

Originally published in:



Nature Communications 8, 1725 (2017)

ARTICLE

DOI: 10.1038/s41467-017-01783-y

OPEN

Stress-responsive FKBP51 regulates AKT2-AS160 signaling and metabolic function

Georgia Balsevich¹, Alexander S. Häusl¹, Carola W. Meyer², Stoyo Karamihalev¹, Xixi Feng³, Max L. Pöhlmann¹, Carine Dournes¹, Andres Uribe-Marino¹, Sara Santarelli¹, Christiana Labermaier¹, Kathrin Hafner³, Tianqi Mao³, Michaela Breitsamer⁴, Marily Theodoropoulou³, Christian Namendorf³, Manfred Uhr³, Marcelo Paez-Pereda³, Gerhard Winter⁴, Felix Hausch⁵, Alon Chen¹, Matthias H. Tschöp², Theo Rein ³, Nils C. Gassen³ & Mathias V. Schmidt ¹

The co-chaperone FKBP5 is a stress-responsive protein-regulating stress reactivity, and its genetic variants are associated with T2D related traits and other stress-related disorders. Here we show that FKBP51 plays a role in energy and glucose homeostasis. Fkbp5 knockout (51KO) mice are protected from high-fat diet-induced weight gain, show improved glucose tolerance and increased insulin signaling in skeletal muscle. Chronic treatment with a novel FKBP51 antagonist, SAFit2, recapitulates the effects of FKBP51 deletion on both body weight regulation and glucose tolerance. Using shorter SAFit2 treatment, we show that glucose tolerance improvement precedes the reduction in body weight. Mechanistically, we identify a novel association between FKBP51 and AS160, a substrate of AKT2 that is involved in glucose uptake. FKBP51 antagonism increases the phosphorylation of AS160, increases glucose transporter 4 expression at the plasma membrane, and ultimately enhances glucose uptake in skeletal myotubes. We propose FKBP51 as a mediator between stress and T2D development, and potential target for therapeutic approaches.

¹ Department of Stress Neurobiology and Neurogenetics, Max Planck Institute of Psychiatry, Kraepelinstraße 2-10, 80804 Munich, Germany. ² Institute of Diabetes and Obesity, Helmholtz Zentrum München, Parkring 13, 85748 Garching, Germany. ³ Department of Translational Research in Psychiatry, Max Planck Institute of Psychiatry, Kraepelinstraße 2-10, 80804 Munich, Germany. ⁴ Ludwig Maximilians University, Butenandtstr. 5-13, 81377 Munich, Germany. ⁵ Technical University Darmstadt, Institute of Organic Chemistry and Biochemistry, Alarich-Weiss-Str. 4, 64287 Darmstadt, Germany. Georgia Balsevich and Alexander S. Häusl contributed equally to this work. Theo Rein, Nils C. Gassen and Mathias V. Schmidt jointly supervised this work. Correspondence and requests for materials should be addressed to G.B. (email: georgia.balsevich@ucalgary.ca) or to M.V.S. (email: mschmidt@psych.mpg.de)

FK506-binding protein 51 (FKBP51) is an immunophilin protein best known as a negative regulator of the glucocorticoid receptor (GR) and consequently the physiological stress response¹. Specifically, in complex with FKBP51 (*FKBP5* gene), the GR displays reduced ligand affinity, reduced nuclear translocation, and ultimately decreased GR sensitivity^{1–5}. By contrast, in complex with its functional counter-player FKBP52 (*FKBP4* gene), GR activity is enhanced⁶. Single-nucleotide polymorphisms (SNPs) in the *FKBP5* gene, which are associated with increased expression of *FKBP5* (high-induction allele), have been fundamentally linked to stress-related disorders, and most notably in psychiatric disorders⁷. In this context, it is possible that stress-induced *FKBP5* may similarly be implicated in additional stress-related pathophysiology, such as type 2 diabetes (T2D).

Exposure to nutrient overload, including exposure to a high-fat diet (HFD), is considered a metabolic stressor⁸. Interestingly, it was reported that 8 weeks of HFD exposure in mice led to enhanced *Fkbp5* expression in the hypothalamus⁹, suggesting that *Fkbp5* is responsive to metabolic stressors and is able to sense the nutrient environment. Accordingly, a study examining food restricted-responsive genes reported an induction of *Fkbp5* in the hypothalamus and ventral tegmental area¹⁰. This is in agreement with an earlier study, which used a 24-h food restriction paradigm as a stressor to investigate stress-induced *Fkbp5* expression across multiple brain regions¹¹.

There are several additional lines of evidence to support the possibility that FKBP51 links stress to metabolic function. Human adipocytes and skeletal muscle are among the tissues presenting the strongest expression of *FKBP5*¹². Recently, the high-induction *FKBP5* risk allele was associated with reduced weight loss following bariatric surgery¹³. A genome-wide association study furthermore demonstrated that SNPs within the *FKBP5* gene loci are associated with T2D and markers of insulin resistance¹⁴. Preclinical studies in animal models have similarly demonstrated that complete loss of FKBP51 protects against HFD-induced body weight gain and hepatic steatosis, which is, in part, explained by an increased expression of uncoupling protein 1 (UCP1), a specific marker of browning, in white adipose tissue (WAT) and increased thermogenesis¹⁵. Additionally, FKBP51 is a negative regulator of all 3 isoforms of the serine/threonine protein kinase AKT (AKT1, AKT2, and AKT3), and through this action, regulates the response to chemotherapy¹⁶. AKT is also a central node within the insulin signaling pathway, and deregulation of AKT activation, most notably AKT2 activation, has been linked to the pathogenesis of diabetes and obesity^{17, 18}. In this context, FKBP51 may be an important regulator of insulin signaling and consequently energy and glucose homeostasis¹⁹. Nevertheless, whether FKBP51 plays a critical role in whole body glucose metabolism remains to be elucidated. For this purpose, we aimed to characterize the role of FKBP51 in energy and glucose homeostasis using a combination of *Fkbp5* knockout (51KO) mice,

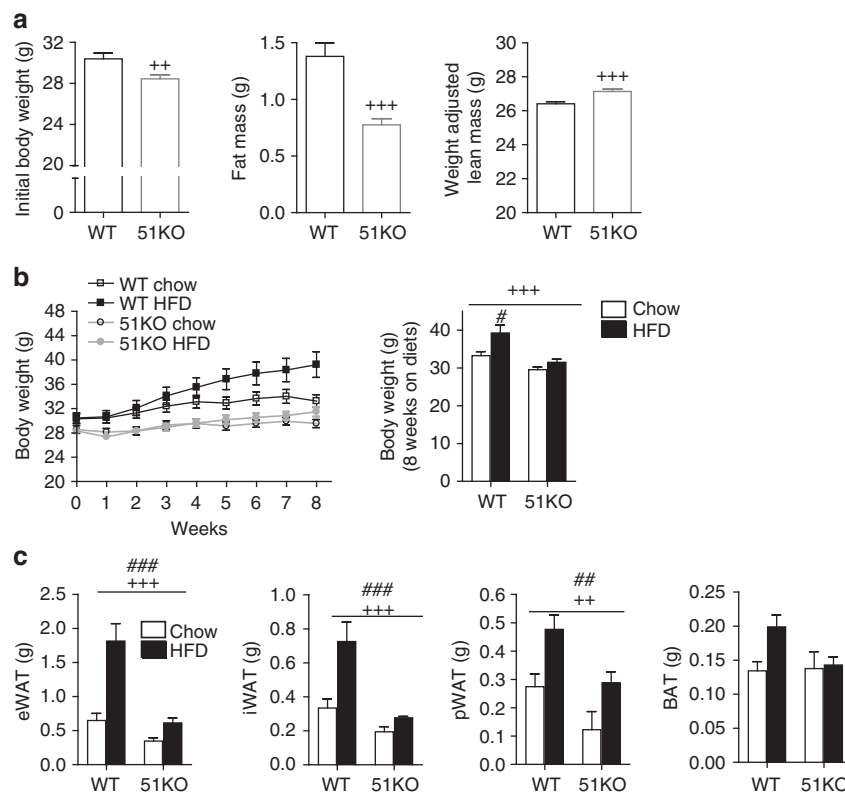


Fig. 1 Genetic ablation of FKBP51 prevents HFD-induced weight gain. **a** 51KO mice ($n = 16$) presented lowered body weight, decreased fat mass, and increased lean mass compared to WT littermates ($n = 18$) at the onset of the dietary feeding period. **b** 51KO mice weighed significantly less than WT mice throughout the 8-week dietary treatment and at the experimental end ($n = 9$ WT-Chow, $n = 9$ WT-HFD, $n = 9$ 51KO-Chow, $n = 7$ 51KO-HFD). Whereas WT mice were susceptible to HFD-induced weight gain, 51KO mice were not as interpreted from weight progression and final body weight (following 8 weeks on respective diets). **c** After 8 weeks on the dietary treatment, 51KO mice presented decreased fat pad weights for epididymal (e), inguinal (i), and perirenal (p) white adipose tissues (WAT) compared to WT counterparts whereas presented no change in brown adipose tissue (BAT) mass. HFD exposure significantly increased fat pad mass, regardless of genotype. Lean mass was adjusted for body weight and is expressed for a 30-g mouse. Data are represented as mean \pm SEM. $^*P < 0.05$, $^{**}P < 0.01$, $^{***}P < 0.001$; $^{\#}P < 0.05$, $^{\#\#}P < 0.01$, $^{\#\#\#}P < 0.001$, two-tailed t test for **a**, Repeated measures ANOVA and two-way ANOVA for **b**, two-way ANOVA for **c**; + significant genotype effect; # significant diet effect

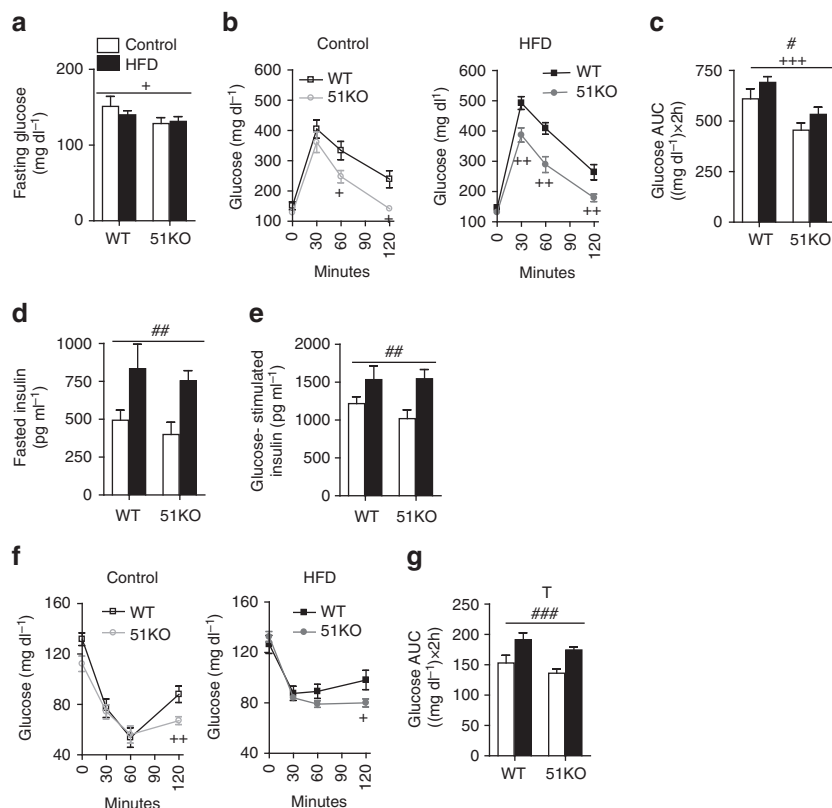


Fig. 2 Genetic ablation of FKBP51 improves glucose tolerance. **a** Blood glucose following a 14 h fast was significantly lower in 51KO mice compared to WT mice. **b** In the GTT, a HFD impaired glucose tolerance in WT mice but not in 51KO mice. **c** The glucose area under curve (AUC) illustrates the effect of genotype and diet on glucose tolerance. **d, e** Fasted insulin and glucose-stimulated insulin were significantly elevated from HFD exposure independent of genotype. **f** In HFD-fed mice, loss of FKBP51 significantly reduced insulin tolerance. Importantly blood glucose remained significantly lower 120 min following insulin administration on account of FKBP51 deletion under both chow conditions and HFD conditions. **g** The glucose AUC for ITT demonstrates the strong diet effect and a trend for genotype. $n = 8$ WT-Control, $n = 10$ WT-HFD, $n = 12$ 51KO-Control, $n = 13$ 51KO-HFD. Data are represented as mean \pm SEM. $^*P < 0.05$, $^{**}P < 0.01$, $^{***}P < 0.001$; $^{\#}P < 0.05$, $^{\#\#}P < 0.01$, $^{\#\#\#}P < 0.001$, $^T P < 0.1$, two-way ANOVA for **a**, Repeated measures ANOVA for **b, f**, two-way ANOVA for **c-e** and **g**; + significant genotype effect; # significant diet effect; T significant trend for genotype

pharmacological manipulations, and mechanistic studies. We found in this study that FKBP51 regulates glucose metabolism in mice, through its regulation of AKT2-AS160 signaling, glucose transporter expression, and glucose uptake in myotubes. Pharmacological antagonism of FKBP51 improves glucose tolerance, irrespective of body weight changes, which suggests an opportunity to target FKBP51 for the treatment of T2D.

Results

FKBP51 loss opposes obesity and improves glucose tolerance.

In order to examine the role of FKBP51 in energy and glucose homeostasis, we initially characterized the metabolic outcomes arising in 51KO mice. We found that 51KO mice fed with a standard chow diet showed a modest body weight reduction, reduced adiposity, and increased lean mass compared to WT littermates (Fig. 1a). When challenged with HFD exposure for 8 weeks, the 51KO mice were protected from both HFD-induced weight gain and increased adiposity (Fig. 1b, c). Loss of FKBP51 likewise counteracted diet-induced obesity under thermoneutral conditions (30 °C), arguing against a thermoregulatory basis of the phenotype (Supplementary Fig. 1). Indirect calorimetry revealed that the body weight phenotype observed in 51KO mice under standard chow conditions was accompanied by a modest increase in total energy expenditure, as a result of an increased resting metabolic rate (RMR) (Supplementary Fig. 2A). In

addition, 51KO mice presented a modest decrease in their respiratory exchange ratio (RER) and a slight increase in their home-cage activity (Supplementary Fig. 2B, C). By contrast, neither water nor food intakes were affected by loss of FKBP51 (Supplementary Fig. 2D, E). To confirm a lack of FKBP51 effect on feeding behavior, a separate pair-feeding experiment was performed, in which a cohort of WT mice was pair-fed to 51KO mice. This experiment again revealed no genotype effect on energy intake (Supplementary Fig. 2G). Cold-induced body temperature regulation was unaffected by FKBP51 genotype (Supplementary Fig. 2H).

To determine the effects of FKBP51 on glucose metabolism and insulin sensitivity, we performed glucose tolerance tests (GTTs) and insulin tolerance tests (ITTs) in a separate cohort of 51KO and WT mice. The body weight data were consistent with our previous experiments (Supplementary Fig. 3). FKBP51 deletion lowered fasting glucose (Fig. 2a) and remarkably improved glucose tolerance (Fig. 2b, c). Although the effect of FKBP51 deletion was present under the control condition, a metabolic challenge using HFD exposure heightened the genotype effect. Interestingly, the levels of fasted insulin and glucose-stimulated insulin were not different between 51KO and WT mice (Fig. 2d, e), indicating that differences in insulin secretion do not contribute to the improved glucose tolerance phenotype. In the ITT, 51KO mice presented a prolonged response to insulin under control and HFD conditions, despite

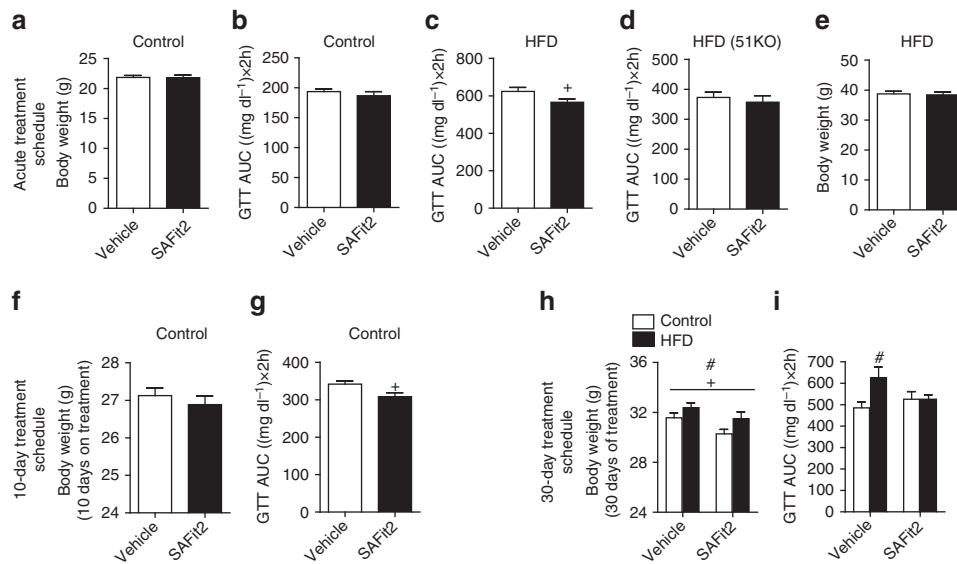


Fig. 3 FKBP51 antagonism parallels the metabolic effects resulting from genetic ablation of FKBP51. **a** A single application of a slow-release-formulated SAFit2 gel had no effect on glucose tolerance or **(b)** Body weight under control diet conditions. **c** Under HFD conditions, acute administration of SAFit2 gel significantly improved glucose tolerance. **d** The effects of SAFit2 on glucose tolerance under HFD conditions were not present in 51KO. **e** Despite the effects of acute SAFit2 on glucose tolerance under HFD conditions, there was no effect on body weight **(f)** 10-day SAFit2 treatment had no significant effect on body weight. **g** Despite no effect on body weight, SAFit2 treatment significantly improved glucose tolerance as reflected in the glucose area under the curve (AUC) for the GTT measured on treatment day 8. **h** At the experimental end point (following 30 days of treatment), mice treated with SAFit2 weighed significantly less than their diet counterparts. Nevertheless, mice fed with the HFD remained significantly heavier independent of treatment. **i** The extended SAFit2 treatment schedule furthermore protected against HFD-induced impaired glucose tolerance as reflected in the glucose AUC measured on day 25. For acute treatment schedule in C57BL6 $n = 12$ per treatment group; for acute treatment in 51KO $n = 8$ per treatment group. For the 10-day treatment schedule, $n = 8$ per treatment group. For 30-day treatment schedule $n = 12$ Vehicle-Control, $n = 13$ SAFit2-Control, $n = 12$ Vehicle-HFD, $n = 13$ SAFit2-HFD. The data are represented as mean \pm SEM. * $P < 0.05$; # $P < 0.05$, two-tailed t test for **a-g**, two-way ANOVA for **h**, two-way ANOVA plus Bonferroni testing for **i**; + significant treatment effect; # significant diet effect

the fact that both 51KO and WT mice remained vulnerable to HFD-induced insulin intolerance (Fig. 2f, g).

FKBP51 antagonism rapidly improves glucose tolerance. Due to the improved metabolic phenotype presented in 51KO mice, we subsequently assessed the effects of pharmacological blockade of FKBP51. Importantly, the first highly selective antagonist for FKBP51, SAFit2, has recently been developed²⁰. In the current study, we determined the efficacy of FKBP51 antagonism in mice on metabolic parameters. We examined the efficacy of a single application of SAFit2 gel (a slow release formulation, Supplementary Fig. 4A), to improve glucose tolerance. Although SAFit2 gel had no effect in chow-fed mice measured at 48 h following application (Fig. 3a, b), it significantly improved glucose tolerance in HFD-fed mice (Fig. 3c), supporting the literature demonstrating that FKBP51-mediated outcomes are more robust under challenging conditions^{21–25}. The effect of SAFit2 treatment on glucose tolerance is specific to FKBP51 inhibition, as no effect was observed in 51KO mice under HFD conditions (Fig. 3d). Importantly, body weight was not affected (Fig. 3e), arguing for a body weight-independent effect of FKBP51 inhibition on glucose tolerance. Acute SAFit2 treatment furthermore had no effect on energy expenditure, respiratory exchange ratio, or activity counts (Supplementary Fig. 4B–D). We also examined the expression of UCP1 in brown adipose tissue (BAT) of mice treated for 48 h with SAFit2 and found no effect of acute treatment (Supplementary Fig. 4E). We then examined the effects of a sub-chronic SAFit2 (20 mg kg⁻¹) regimen administered twice daily for 10 days to adult C57BL/6 mice by intraperitoneal injections under chow-fed conditions. The dose was selected based on the effective dose used in acute studies²⁶. Using a 10-day treatment schedule, we observed an effect of SAFit2 under chow diet conditions.

Specifically, although 10 days of FKBP51 antagonism again yielded no body weight phenotype, there was a marked improvement of glucose tolerance assessed on treatment day 8 (Fig. 3e, f). The lack of body weight change from either the acute or 10-day SAFit2 treatment schedule indicates that the FKBP51-dependent glucose tolerance phenotype is not secondary to the body weight phenotype. To determine whether a longer treatment period would replicate the body weight phenotype of 51KO mice, a new cohort of C57BL/6 mice was treated with SAFit2 for 30 days under both control and HFD conditions (for SAFit2 plasma levels see Supplementary Fig. 5A). At the onset of treatment, following 4 weeks of dietary exposure, there was no difference in body weight between the treatment groups (Supplementary Fig. 5B, C). However, we found that 30 days of SAFit2 administration led to a reduction in body weight under both control and HFD conditions (Fig. 3g). FKBP51 antagonism furthermore protected against HFD-mediated glucose intolerance (Fig. 3h). There was, however, no effect of SAFit2 on insulin tolerance or on locomotor activity tested in the open-field test (Supplementary Fig. 5D, E). We observed no unwanted side-effects of FKBP51 antagonism on behavioral readouts tested in the dark–light transition and elevated plus-maze tests (Supplementary Fig. 5F, G). Taken together, these results clearly demonstrate that (i) a body weight phenotype is secondary and not necessary for the effects of FKBP51 antagonism on glucose tolerance, and (ii) pharmacological blockade of FKBP51 parallels the effects of FKBP51 genetic ablation.

FKBP51 loss sensitizes insulin signaling in skeletal muscle. As the effect of FKBP51 on glucose tolerance was primary and independent to the body weight phenotype, we addressed this mechanism in the subsequent experiments. To unravel the FKBP51-dependent regulation of glucose metabolism, we first

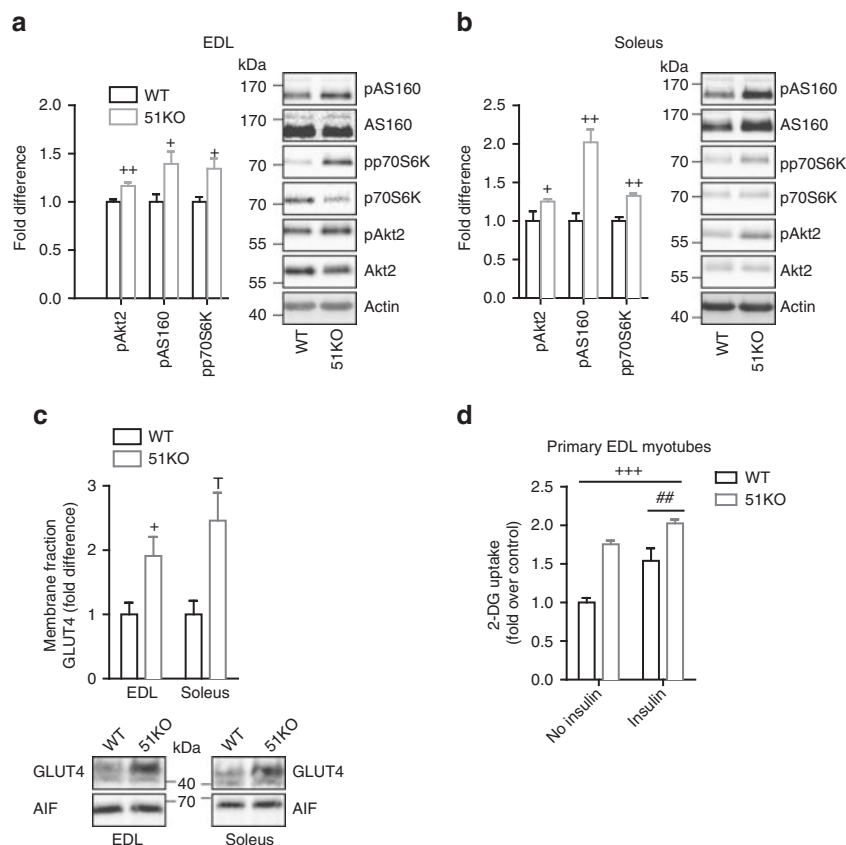


Fig. 4 FKBP51 affects insulin signaling and consequently glucose uptake. **a, b** Insulin signaling was enhanced in EDL (**a**) and soleus (**b**) skeletal muscles of 51KO mice compared to WT mice as assessed by pAkt2, pAS160, and pp70S6K protein expression. **c** Following subcellular fractionation to isolate the plasma membrane compartment, we observed increased GLUT4 expression in skeletal muscle membrane fractions of 51KO mice. **d** In primary EDL myotubes, loss of FKBP51 heightened glucose uptake under both no insulin and insulin-stimulated states. For quantification of phosphorylated protein, $n = 6$ per group. For GLUT4 membrane localization, $n = 3$ per group. For glucose uptake experiments, 3 wells for each condition were measured. The data are expressed as relative fold change compared to wild-type condition \pm SEM. $^*P < 0.05$, $^{**}P < 0.01$, $^{***}P < 0.001$, $^{##}P < 0.01$, two-tailed t tests for **a–d**, two-way ANOVA for **e**; + significant genotype effect, # significant insulin effect, T trend for genotype. Supplementary Fig. 12 shows uncropped gel images

examined FKBP51 protein expression across multiple peripheral tissues. Interestingly, FKBP51 was not ubiquitously expressed across all tissues examined, but rather showed a defined expression profile. FKBP51 was detected within skeletal muscle (soleus muscle and EDL) eWAT and iWAT (Supplementary Fig. 6A). By contrast, FKBP51 was not detected in the liver, kidney, spleen, pancreas, gut, or BAT. In addition, HFD exposure (for 8 weeks) significantly increased levels of FKBP51 in EDL skeletal muscle (Supplementary Fig. 6B), and supports the notion that a high-fat dietary environment acts as a metabolic stressor^{8, 27}.

As a next step, we examined the phosphorylation status of critical nodes along the insulin signaling cascade as a marker of insulin signaling activation. As we found a strong effect of FKBP51 loss on glucose tolerance without any change in circulating insulin levels, we hypothesized that intracellular insulin signaling is enhanced following loss of FKBP51. Indeed, 5 min following insulin stimulation (0.70 IU kg^{-1}), we found that insulin sensitivity (as reflected through the phosphorylation status of AKT2, AS160, and p70S6K) was markedly increased in skeletal muscle (soleus muscle and EDL) of 51KO mice (Fig. 4a, b), whereas insulin activation in WAT (iWAT and eWAT) and liver remained unchanged (Supplementary Fig. 7A, C). The skeletal muscle-specific effect of FKBP51 deletion on insulin signaling is in line with the high expression level of FKBP51 across skeletal muscle tissues (reported above).

We subsequently assessed whether events downstream of AKT2-AS160 signaling are likewise regulated by FKBP51.

Therefore, we first examined glucose transporter GLUT4 translocation to the plasma membrane, which is triggered by activated AKT2-AS160 signaling²⁸. We isolated the plasma membrane fraction from skeletal muscle extracted from WT and 51KO mice. 51KO mice display increased GLUT4 expression compared to WT mice (Fig. 4c). There was no difference in GLUT1 expression in the plasma membrane fraction between WT and 51KO mice. Importantly, there was no effect of FKBP51 deletion either on total GLUT1 or GLUT4 expression (Supplementary Fig. 7D). To assess the functional implications of these FKBP51-dependent events, we examined radiolabeled-2-deoxyglucose uptake in primary EDL myotubes collected either from WT or 51KO mice. Glucose uptake was significantly increased by both insulin and FKBP51 deletion (Fig. 4d). Moreover, the effect of FKBP51 ablation on glucose uptake was observed under both non-insulin and insulin-stimulated states, indicating that FKBP51 deletion enhances glucose uptake independent of the insulin state. In support of these findings, overexpression of AKT2 enhanced glucose uptake in C2C12 myotubes (a mouse skeletal muscle cell line), whereas simultaneous overexpression with FKBP51 prevented the AKT2-mediated enhanced uptake (Supplementary Fig. 8). Thus, FKBP51 acts along the AKT2-AS160 signaling pathway to dampen glucose uptake.

Given the effects of the FKBP51 antagonist, SAFit2, on glucose tolerance in mice, we sought to further investigate whether SAFit2 modulates AKT2 activation and downstream events based on the

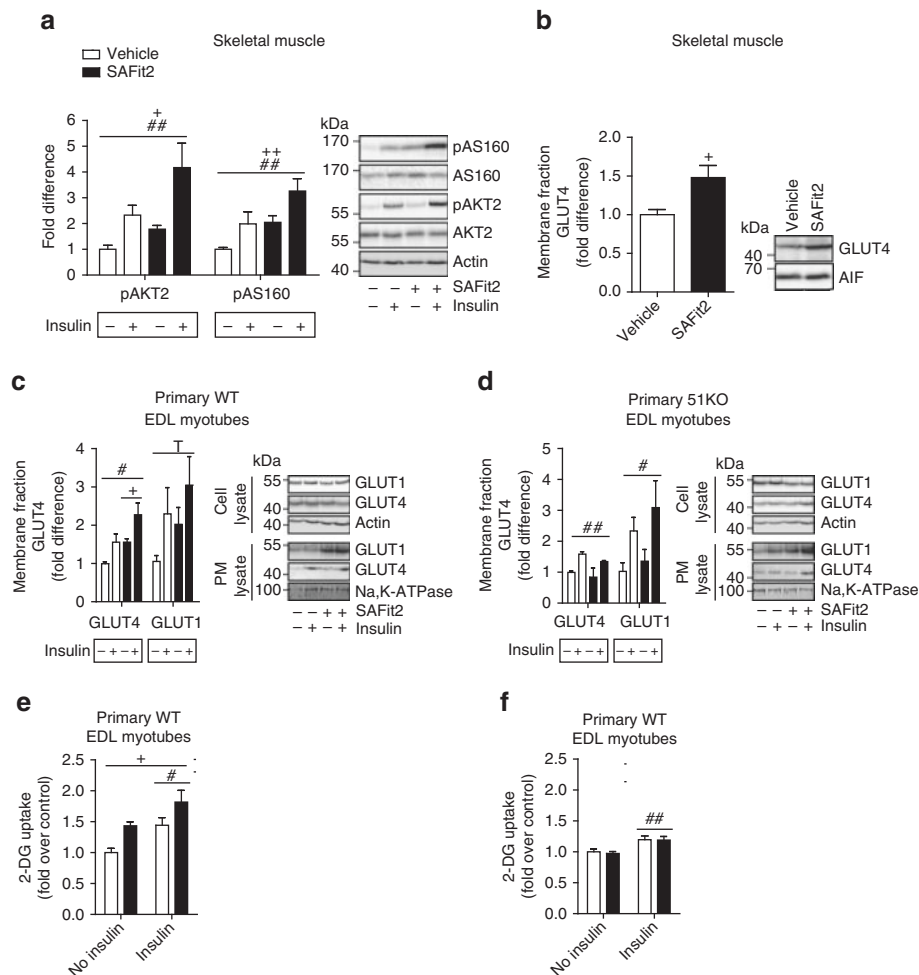


Fig. 5 FKBP51 antagonism affects insulin signaling and consequently glucose uptake. **a** The insulin signaling pathway was enhanced in EDL skeletal muscle of mice treated with SAFit2 compared to vehicle-treated mice, independent of insulin, as assessed by pAKT2, and pAS160 protein expression. **b** GLUT4 expression at the membrane was increased 6 h following SAFit2 treatment in soleus skeletal muscle. **c** GLUT4 expression at the membrane was increased from SAFit2 treatment in primary EDL myotubes from WT mice, whereas GLUT1 expression was unchanged by SAFit2 treatment. **d** SAFit2 had no effect on GLUT4 plasma membrane expression in primary EDL muscle cells collected from 51KO mice. **e** FKBP51 antagonism with SAFit2 increased 2-deoxyglucose uptake in primary EDL muscle cells collected from WT mice independent of insulin condition. **f** SAFit2 had no effect on 2-deoxyglucose uptake in primary 51KO muscle cells. For quantification of phosphorylated protein expression in mice, $n = 6$ per group. For quantification of GLUT4 expression in mice, $n = 7$ per treatment. For GLUT1/4 expression in primary EDL myotubes, $n = 3$ per group. For glucose uptake experiments, 3 wells for each condition were measured. Data are expressed as relative fold change compared to vehicle condition \pm SEM. * $P < 0.05$, ** $P < 0.01$, # $P < 0.05$, ## $P < 0.01$, two-way ANOVA for **a-f**; + significant treatment effect, # significant insulin effect, T trend ($p < 0.1$) for insulin effect. Supplementary Figs. 13 and 14 show uncropped gel images

known regulation of AKT2 by FKBP51¹⁶. We assessed pAKT2 and pAS160 in tissue collected from mice that had been pre-treated with vehicle or SAFit2 6 h prior to tissue collection in either an insulin-stimulated (0.70 IU kg^{-1} 5 min before tissue collection) or non-insulin (saline) condition. Although a single intraperitoneal injection of SAFit2 applied 6 h before testing had no effect on glucose tolerance (Supplementary Fig. 9), there was already a significant effect of SAFit2 treatment at a molecular level. SAFit2 significantly increased phosphorylated AKT2 and AS160 in EDL muscle and likewise increased expression of GLUT4 at the membrane in soleus muscle (Fig. 5a, b). Once again, the effect of FKBP51 antagonism on pAKT2-pAS160 was independent of the insulin-stimulated state. The same directional change on phosphorylation states was observed in soleus muscle, whereas this was not seen in eWAT (where FKBP51 expression is relatively low) (Supplementary Fig. 10A, B). To ensure that the effects of SAFit2 were selective for FKBP51, we additionally examined the effects of SAFit2 treatment on pAKT2 and pAS160

in primary EDL and soleus myotubes from WT and 51KO mice. While SAFit2 treatment increased the expression of pAKT2 (soleus and EDL muscle) and pAS160 (EDL muscle) in WT cells, there was no effect of FKBP51 antagonism in 51KO cells, confirming the specificity of SAFit2 action (Supplementary Fig. 10C, F). Moreover, following SAFit2 treatment, GLUT4 expression increased in the membrane fraction of primary EDL myotubes from WT mice, but not from 51KO mice (Fig. 5c, d). Finally, we applied SAFit2 to primary EDL myotubes and measured radiolabeled-2-deoxyglucose uptake. FKBP51 antagonism-increased glucose uptake in EDL cells collected from WT mice, but not 51KO mice, again demonstrating the specificity of SAFit2 (Fig. 5e, f). Taken together, FKBP51 antagonism increases AKT2-AS160 signaling, GLUT4 expression at the plasma membrane, and glucose uptake into primary myotubes.

From these results, and based on previous literature highlighting a role of FKBP51 as a scaffolding protein^{16, 21, 29}, we assessed whether FKBP51 forms a complex with AS160 and

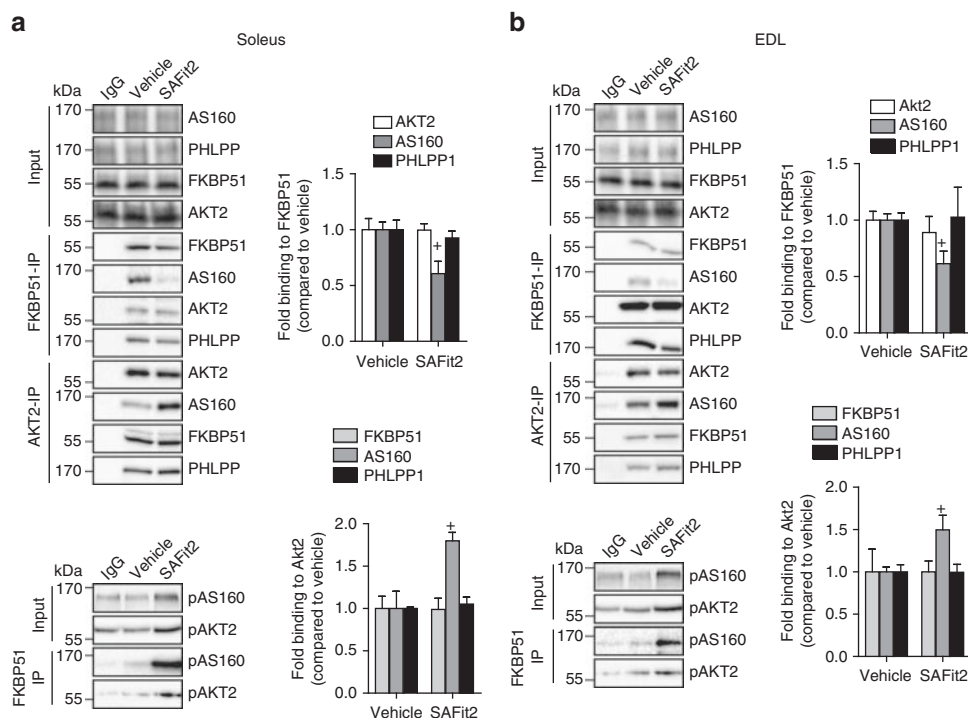


Fig. 6 FKBP51 antagonism affects AKT2-AS160 signaling complex. Tissue lysates from 30-day vehicle-treated or SAFit2-treated mice exposed to HFD were immunoprecipitated with anti-AKT2 and anti-FKBP51 and then analyzed by Western blot using FKBP51, (p)AKT2, (p)AS160, and PHLPP1. **a, b** Immunoprecipitation reactions revealed that SAFit2 treatment increased binding between (p)AKT2 and (p)AS160 in soleus (**a**) and EDL (**b**) muscles, while simultaneously decreased binding between FKBP51 and AS160 in both muscle types. For co-immunoprecipitation experiments $n = 3$ per group. Data are expressed as relative fold change compared to vehicle condition \pm SEM. $^*P < 0.05$, two-tailed t tests for **a, b**; + significant SAFit2 treatment effect. Supplementary Fig. 15 shows uncropped gel images

furthermore assessed whether SAFit2 modulates this interaction. Immunoprecipitation reactions, using protein extracts from 30-day vehicle-treated and SAFit2-treated mice, revealed that SAFit2 treatment strengthened the binding between AKT2 and AS160 (Fig. 6a, b, bottom). This is in line with increased glucose uptake given that AKT2 inactivates AS160, which in turn stimulates the translocation of GLUT4 to the plasma membrane²⁸. We furthermore observed a novel interaction between FKBP51 and AS160, and confirmed that SAFit2 disrupts this interaction (Fig. 6a, b, top). SAFit2, by contrast, had no effect on the binding strength between AKT2 and PHLPP1 (the negative regulator of AKT2). We confirmed that the phosphorylation state of AKT2 and AS160 does not interfere with the interaction between FKBP51 and either AKT2 or AS160 by also examining pAKT2 and pAS160. Co-immunoprecipitation does not discriminate between direct and indirect protein interactions, and it is possible that intermediate proteins are also involved in the interaction between FKBP51 and AS160. Regardless, these findings suggest that FKBP51 associates (directly or indirectly) with AS160 to reduce glucose uptake. By contrast, SAFit2 antagonizes FKBP51 and reduces the binding between FKBP51 and AS160 to promote a steric arrangement that favors glucose uptake.

We have shown that FKBP51 regulates insulin signaling selectively in skeletal muscle. Yet FKBP51 is nonetheless expressed in select WAT depots, albeit at lower levels. In order to account for the tissue-specific effects of FKBP51, we furthermore investigated the expression profile of FKBP52, a structural homolog of FKBP51 that competes as a scaffolding protein, resulting in opposite functional effects³⁰. Interestingly, the expression profile between FKBP51 and FKBP52 across WATs and skeletal muscle are very distinct and provide an explanation for the FKBP51 skeletal muscle-selective effects.

Specifically, FKBP51 expression is relatively high in skeletal muscle compared to WATs (Supplementary Fig. 6A). In stark contrast, levels of FKBP52 are high in WAT depots relative to skeletal muscle. (Supplementary Fig. 11A). We additionally performed co-immunoprecipitation reactions with FKBP52 to investigate whether FKBP51 and FKBP52 compete for binding to AKT2. We demonstrate that similar to FKBP51, FKBP52 is in complex with AKT2 and AS160 (Supplementary Fig. 11B). However, FKBP52 does not likewise interact with PHLPP1 (Supplementary Fig. 11B), the negative regulator of AKT2 signaling. Specifically, where ectopic overexpression of FKBP51 significantly decreased pAKT2 and pAS160 expression in C2C12 myotubes, simultaneous overexpression of FKBP52 abolished the effects of ectopic FKBP51 (Supplementary Fig. 10C). Taken together, FKBP51 and FKBP52 compete for binding with AKT2. The distinct expression profile and functional outcomes of FKBP51 and FKBP52 are responsible for the skeletal muscle-specific effects of SAFit2, which selectively antagonizes FKBP51.

Discussion

Here we describe that loss of FKBP51 in mice markedly improves metabolism and especially improves glucose tolerance under both control and HFD conditions. This is in line with earlier pre-clinical and human studies, which identified an association between FKBP51 ablation and *FKBP5* SNPs on traits related to body weight regulation and T2D, respectively^{14, 15}. Although the effects of FKBP51 loss are witnessed under dietary control conditions, the effects are significantly accentuated when mice are challenged to an HFD, which acts as a metabolic stressor⁸. This supports a large body of literature, demonstrating that an

environmental challenge is a prerequisite for FKBP51-mediated outcomes. For example, early life trauma (i.e., environmental challenge) increases the risk of various psychiatric disorders selectively in *FKBP5* risk allele carriers, which are associated with increased FKBP51 protein levels^{7, 24, 25, 31–33}. In rodent studies, 51KO mice present no overt phenotype under basal conditions, yet show improved stress resilience following either acute stress²³ or chronic stress²². Indeed, stressors induce *FKBP5* expression, and this may underlie the more pronounced effects of FKBP51 deletion on metabolic phenotypes seen in the current study. We certainly found that an HFD increases levels of FKBP51 in fat and skeletal muscle. Taken together, previous findings have found that higher levels of FKBP51 are associated with poorer outcomes in stress-related psychiatric disorders. The present study shows that higher levels of FKBP51 are likewise detrimental to metabolic health, especially when confronted with environmental challenges (i.e., an obesogenic environment).

Selective pharmacological antagonism of FKBP51 has only recently been realized²⁰. Selectivity for FKBP51 is especially important since its structural homolog, FKBP52, acts as a functional opponent. In fact, it was this structural similarity that initially hampered drug discovery for FKBP51. The current ability to antagonize FKBP51 offers new opportunities for drug development. To date, only three studies have investigated the effects of FKBP51 antagonism on functions related to FKBP51, and no study has yet been investigated for long-term (i.e., 30 day) applicability. These previous studies independently found that FKBP51 antagonism induces anxiolytic effects²⁶, reduces the severity of pain symptoms³⁴, and opposes the known ability of FKBP51 to promote NF κ B signaling³⁵. Nevertheless, FKBP51 is a multi-domain protein³⁶, and it remains unknown whether the FKBP51 antagonist, SAFit2, blocks all functions of FKBP51. Therefore, in order to address whether pharmacological antagonism affects metabolic function, mice were treated with SAFit2 once (slow release formula) or repeatedly for either 10 or 30 days. Administration of SAFit2 paralleled the metabolic phenotype arising from total genetic loss of FKBP51. Acute SAFit2 treatment improved glucose tolerance under metabolically challenging conditions (i.e., HFD conditions). Under metabolic control conditions (i.e., regular diet), FKBP51 blockade improved glucose tolerance as early as 8 days following treatment onset. Importantly, the effects of FKBP51 modulation on glucose tolerance were not secondary to changes in body weight since neither a single nor a 10-day SAFit2 exposure had an effect on body weight. It is possible that our study was underpowered to detect the modest effects of SAFit2 treatment on body weight, since the 10-day SAFit2-treated group showed a lower (non-significant) body weight phenotype compared to the vehicle-treated counterparts. Regardless, these data support our studies in 51KO mice, which collectively indicate that FKBP51 is an integral component of glucose homeostatic regulation, particularly in response to nutritional changes. In the context of body weight regulation, our findings that 30 days of SAFit2 treatment protects against HFD-induced weight gain supports the findings of a recently published paper demonstrating that 51KO mice resist HFD-induced weight gain and present increased UCP1 in WAT¹⁵. One limitation of our study is that we do not know the minimal effective dose of SAFit2 required to improve glucose tolerance. Nevertheless, the improved metabolic outcomes following systemic administration of the selective FKBP51 antagonist clearly demonstrate the applicability in a clinical setting.

It is well established that FKBP51 is able to regulate many signaling pathways through direct protein–protein interactions^{16, 21, 37, 38}. Through these interactions, FKBP51 has been implicated in various disease states (i.e., cancers, psychiatric disorders) and in the response to medications (i.e., chemotherapies,

antidepressants). For example, through the FKBP51-dependent regulation of AKT, Pei et al. (2009) reported that FKBP51 reduces tumor growth¹⁶. FKBP51 binds to both AKT1 and AKT2 isoforms and their corresponding negative regulators PHLPP2 and PHLPP1, to ultimately favor Akt inactivation. Interestingly, while Akt1 is best known for its regulation of cell growth^{39, 40}, AKT2 is best known for its regulation of glucose homeostasis^{17, 41}. Accordingly, in the present study, we determined that FKBP51 is also important for glucose disposal through the regulation of AKT2 and downstream AS160 (AKT substrate of 160 kDa), an important signaling protein involved in insulin-stimulated glucose transport in skeletal muscle^{28, 42}. 51KO mice exhibit enhanced insulin signaling, as interpreted from the increased phosphorylation of AKT2, AS160, and p70S6K. Interestingly, the FKBP51-dependent effects on insulin signaling observed in mice were highly tissue-specific, in which FKBP51-dependent increases in insulin signaling was limited to skeletal muscle. Indeed, skeletal muscle accounts for an estimated 80% of postprandial glucose disposal and is regarded as a principal site responsible for the maintenance of glucose homeostasis^{43, 44}. In this context, we also found that primary EDL myotubes from 51KO mice exhibited heightened glucose uptake compared to WT EDL myotubes. Ectopic FKBP51 overexpression furthermore completely reversed the enhanced glucose uptake arising from AKT2 overexpression in cultured myotubes, demonstrating that FKBP51 regulation of insulin signaling is critical for glucose uptake.

The FKBP51-dependent effects on the phosphorylation of AKT2 and AS160 as well as on glucose uptake were evident under both non-insulin- and insulin-stimulated states, suggesting that FKBP51 acts independent of insulin to improve glucose uptake and whole body glucose homeostasis. Follow-up studies should address whether FKBP51 is involved in insulin-independent glucose uptake through the regulation of auxiliary pathways. For example, AMP-activated protein kinase (AMPK) is a well-known regulator of insulin-independent glucose uptake, leading to increased AS160 phosphorylation and GLUT4 translocation in the skeletal muscle^{45, 46}. Furthermore, glucocorticoids are potent regulators of glucose homeostasis, and they have been shown to reduce insulin-stimulated glucose transport in muscle by blocking the recruitment of GLUT4 to the cell surface⁴⁷. Indeed, FKBP51 is known to reduce glucocorticoid receptor sensitivity¹, and therefore glucocorticoid signaling is another strong candidate pathway by which FKBP51 may regulate whole body glucose homeostasis. The data herein nevertheless provide unequivocal evidence that FKBP51 is a novel regulator of AKT2-AS160 signaling and glucose uptake.

Not only did FKBP51 antagonism parallel the metabolic phenotype arising from FKBP51 deletion, but it furthermore paralleled the molecular events induced by FKBP51 loss. SAFit2 treatment strongly induced AKT2 and AS160 phosphorylation and led to increased GLUT4 expression at the plasma membrane. Although we suspect that enhanced plasma membrane GLUT4 expression arises from pAKT2-pAS160-mediated increased GLUT4 translocation to the membrane, it is possible that SAFit2 treatment also increases the total expression level of GLUT4. At a functional level, SAFit2 heightened glucose uptake assessed in primary muscle cells. Importantly, SAFit2 action on glucose tolerance and glucose uptake was highly specific for FKBP51 since neither 51KO mice nor primary muscle cells collected from 51KO mice responded to SAFit2 treatment. The robust effects of FKBP51 antagonist SAFit2 on whole body glucose homeostasis and skeletal muscle glucose uptake led us to examine whether SAFit2 disrupts the well-characterized interaction between FKBP51, AKT2, and PHLPP1¹⁶. To our surprise we found no effect of SAFit2. Rather, we discovered a novel interaction between FKBP51 and AS160, which can be disrupted by FKBP51

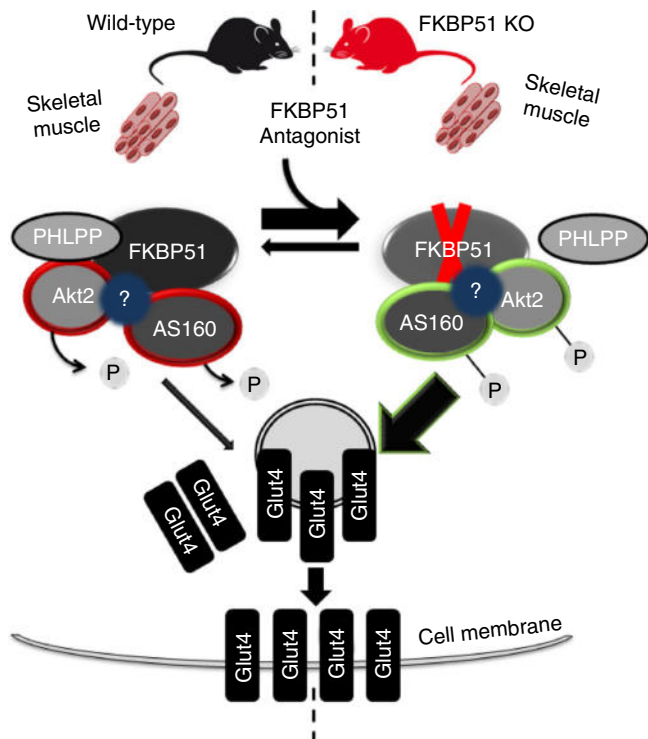


Fig. 7 Proposed model of FKBP51 as a regulator of glucose uptake. FKBP51 scaffolds Akt2, PHLPP1, and AS160. The associations between FKBP51, AKT2, PHLPP1, and AS160 may be either direct or indirect through additional intermediate proteins. In the presence of FKBP51, PHLPP1 phosphatase activity is directed towards AKT2 to favor inactive Akt2, decreased AS160 phosphorylation and reduced glucose uptake. By contrast, loss of FKBP51's scaffolding function leads to increased AKT2. In the presence of SAFit2, a conformational change within FKBP51 disrupts its ability to form a complex with AS160, while simultaneously enhancing AKT2-AS160 binding. Ultimately, loss of FKBP51 and FKBP51 antagonism with SAFit2 both promote glucose uptake. "?" refers to possible unidentified intermediate proteins within the FKBP51 signaling complex. Curved arrows indicate PHLPP1-mediated dephosphorylation of AKT2 at Ser473. The green double arrow indicates enhanced binding between AKT2 and AS160. The green outlines reflect enhanced phosphorylation; red outlines reflect decreased phosphorylation. The width of the arrows correspond to the magnitude of downstream activation

antagonism using SAFit2. This agrees nicely with our findings that SAFit2 treatment increases glucose uptake in primary myotubes and improves glucose tolerance in mice. Moreover this supports accumulating evidence that FKBP51 has important scaffolding properties to organize and concentrate various signaling complexes^{16, 21, 37}.

An important question raised by this study is how exactly FKBP51 acts within distinct cellular/tissue environments to affect whole body energy and glucose homeostasis. Previous studies have already alluded to the importance of tissue-specific actions of FKBP51^{26, 48}. Here we extend our current understanding of the tissue-specific actions of FKBP51 to include FKBP51-dependent regulation of insulin signaling exclusively within skeletal muscle. Despite microarray-based data demonstrating that skeletal muscle shows the second strongest expression profile of *FKBP5* across all tissues examined^{12, 14}, to our knowledge, the current study is the first to define a skeletal muscle-specific role for FKBP51. The distinct expression profiles of FKBP51 and FKBP52 provide an explanation as to why FKBP51 affects glucose uptake exclusively within skeletal muscle. Although FKBP52 shows strong

expression in WAT, it is expressed minimally in skeletal muscle. We found that FKBP52 competes with FKBP51 for binding to AKT2 in WAT, but this competition is minimal in skeletal muscle based on its expression profile. Importantly, although FKBP52 is found in complex with AKT2 and AS160, it is not found to interact with the negative regulator of AKT2, PHLPP1, and thus does not have the same functional implications on downstream AKT2 signaling compared to FKBP51.

Our study focused on the effects of FKBP51 modulation on glucose homeostasis and pAKT2-pAS160 signaling, effects which were independent of body weight. Nevertheless, we also reported that 51KO mice are resistant to diet-induced obesity, present a higher resting metabolic rate, and a slight increase in home-cage activity. In support of these findings, a recent report demonstrated that UCP1 expression is enhanced in select WAT depot in 51KO mice, which contributes to the improved body weight phenotype¹⁵. Our finding that 51KO mice also presented increased home-cage activity may furthermore underlie the improved body weight phenotype. Although we found no difference in activity-related energy expenditure, the increased activity in 51KO mice suggests that 51KO mice may have increased exercise efficacy. Follow-up studies are needed to address such effects of FKBP51 on exercise efficacy.

Our working model (Fig. 7) is that FKBP51 scaffolds AKT2, PHLPP1, and AS160 (both phosphorylated and unphosphorylated states), thereby enhancing PHLPP1 phosphatase activity towards AKT2 (at Ser473). Accordingly, higher levels of FKBP51, as is observed under HFD conditions, favors PHLPP1-mediated inactivation of AKT2, activation of AS160, and ultimately lower glucose uptake. Loss of FKBP51 results in AKT2 hyperactivation due to the loss of FKBP51's scaffolding function. Interestingly, in the presence of SAFit2, FKBP51 is no longer able to form a complex with AS160; meanwhile, the AKT2-AS160 binding is enhanced. Consequently, SAFit2 treatment favors a steric confirmation that promotes glucose uptake. In summary, we are the first study to describe a mode of action for SAFit2. Here, the ability of SAFit2 to oppose FKBP51-dependent glucose uptake relates to the disruption of the AS160-FKBP51 complex. Future studies are needed to delineate the full extent of SAFit2 action.

Together, this study defines a novel role for FKBP51 in the regulation of glucose uptake and whole body glucose homeostasis. Furthermore, we established a defined molecular target linking the stress system to the metabolic system, such that *FKBP5* induction in response to metabolic stress contributes to the metabolic fate of an individual. Our findings suggest that FKBP51-dependent regulation of AKT2-AS160 signaling contribute to improved glucose tolerance. In addition, we report the first long-term treatment study to employ the recently developed FKBP51 antagonist SAFit2. The positive effects of FKBP51 antagonism on glucose tolerance reported here suggest the opportunity to develop FKBP51 antagonists for the clinic, especially for the treatment of stress-related T2D.

Methods

Animals and animal housing. The *Fkbp5* knockout (51KO) mouse line, used in experiments 1, 2, and 3, had been previously generated⁴⁹. C57BL/6 mice were used in experiment 4 for the pharmacological blockade of FKBP51 (Charles River Laboratories, Maastricht, The Netherlands). For all experiments, male mice between 3 and 4 months old were used. During each experiment, the mice were singly housed. The mice were maintained on a 12:12 h light/dark cycle, with controlled temperature (22 ± 2 °C) and humidity (55 ± 5%) conditions. The mice received ad libitum access to water and standard lab chow, unless otherwise specified. The experiments were carried out in accordance with the European Communities' Council Directive 2010/63/EU. The protocols were approved to be carried out at the Max Planck Institute of Psychiatry (license holder) by the ethical committee for the Care and Use of Laboratory animals of the Government of Upper Bavaria, Germany.

Indirect calorimetry and body composition. The direct effects of FKBP51 deficiency on metabolic parameters were investigated using 51KO ($n = 16$) and wild-type (WT) ($n = 18$) mice. Body composition (fat and lean mass) was assessed using whole body magnetic resonance imaging (Echo-MRI, Houston, TX). Thereafter, the mice were surgically implanted with a telemetric transponder (Respironics, Murrysville, PA) for the measurement of core body temperature. The mice were allowed to recover for approximately 2 weeks before any metabolic recordings were performed. Indirect calorimetry and telemetry were performed on mice under chow conditions (TSE PhenoMaster, TSE Systems, Bad Homburg, Germany). For experimental details, see Supplemental Information. Each genotype group was subsequently divided into a chow diet and high-fat diet (HFD) (58% kcal from fat, D12331, Research Diets, New Brunswick, NJ, USA) group, matched for body weight. Body weight was measured throughout the experiment. After 8 weeks on the respective diets, 51KO and WT mice were killed. Epididymal (e), inguinal (i), and perirenal (p) WAT were collected and weighed; brown adipose tissue (BAT) was collected and weighed.

Thermoregulation. Body weight and body composition were examined in 51KO and WT mice ($n = 8$ per genotype) under HFD conditions at 30 °C to minimize the effects of thermal stress. A separate cohort of 51KO and WT mice were exposed to 6 h of cold exposure (4 °C) to assess cold-induced thermoregulation under both control and HFD conditions (see Supplemental Information).

Pair-feeding. To assess the contribution of food intake on body weight regulation in 51KO and WT mice, a pair-feeding experiment was performed. For experimental details, refer to Supplemental Information.

Glucose tolerance and insulin tolerance. Glucose tolerance and insulin tolerance were investigated in 51KO ($n = 25$) and WT mice ($n = 18$). Briefly, 51KO and WT mice were initially divided into a control diet group and an HFD group, matched for body weight. After 8 weeks on the dietary treatment, the mice were subjected to a glucose tolerance test (GTT). Additionally, blood was collected to assess fasting insulin and glucose-stimulated insulin levels. One week thereafter, an insulin tolerance test (ITT) was performed. See Supplemental Information for more details.

SAFit2 administration. To determine whether antagonizing FKBP51 may be an effective anti-obesity and/or diabetic therapeutic strategy, we treated mice with an antagonist of FKBP51, known as SAFit2²⁰. SAFit2 or vehicle was administered either acutely as a slow releasing vesicular phospholipid gel (VPG) (2 mg SAFit2 or vehicle) or repeatedly by intraperitoneal (i.p.) injections (20 mg kg⁻¹ SAFit2 or vehicle) twice daily. For i.p. injections, SAFit2 was solubilized in vehicle containing 4% ethanol, 5% Tween80, and 5% PEG400 in 0.9% saline. Body weight and food intake were measured daily throughout the treatment periods. VPGs were composed of 50% (m/m) egg-lecithin containing at least 80% phosphatidylcholine (Lipoid E80, Lipoid GmbH, Ludwigshafen, Germany) and 10 mM phosphate buffered saline (PBS), pH 7.4, and were prepared by a dual asymmetric centrifugation technique⁵⁰. SAFit2 was encapsulated in the formulation by a direct incorporation method. See Supplemental Information for more details.

Acute SAFit2 treatment. Male C57BL/6 mice were divided into vehicle-treated and SAFit2-treated groups matched for body weight ($n = 12$ per group). On treatment day 1, mice were administered (subcutaneous injection between the shoulders) a slow release-formulated gel containing either SAFit2 or vehicle. After 48 h, a GTT was performed following an overnight fast.

Sub-chronic SAFit2 treatment. One day before the treatment period, male C57BL/6 mice were divided into a vehicle-treated group and a SAFit2-treated group matched for body weight ($n = 8$ per group). On treatment day 7, locomotor activity was assessed in the open field test. On treatment day 8, a GTT was performed. SAFit2 levels were assessed in plasma from blood taken at the time of killing. The animals were killed on day 10 following the treatment onset.

Chronic SAFit2 treatment. Four weeks before treatment onset, male C57BL/6 mice were divided into a control diet group ($n = 25$) and an HFD group ($n = 25$) matched for body weight. One day before the treatment period, mice of each dietary group were further subdivided into a vehicle-treated group and a SAFit2-treated group matched for body weight. SAFit2 or vehicle were administered twice daily for 30 days. On treatment days 10 and 30, SAFit2 levels were assessed in plasma. The open field, dark-light transition, and elevated plus-maze behavioral tests were performed on treatment days 15, 16, and 17, respectively. The GTT was performed on treatment day 25 and the ITT on treatment day 29. The animals were killed on day 31 following treatment onset; tissues were collected and stored at -80 °C for further analyses.

Tissue collection. Mice were anesthetized with isoflurane and immediately killed by decapitation. Basal trunk blood was collected and subsequently processed (plasma was collected and stored at -20 °C). Skeletal muscle (extensor digitorum

longus (EDL) and soleus), WAT (iWAT, eWAT, and pWAT), and liver were collected and stored at -80 °C until used.

Cell lines. C2C12 myoblasts were maintained in Dulbecco's modified Eagle's medium (DMEM) supplemented with 10% fetal bovine serum and 1x penicillin streptomycin antibiotics at 37 °C in a humidified atmosphere with 5% CO₂. Once the cells reached ~90% confluency, C₂C₁₂ myoblasts were detached from the plate and 2 × 10⁶ cells were re-suspended in 100 μl of transfection buffer (50 mM HEPES [pH 7.3], 90 mM NaCl, 5 mM KCl, and 0.15 mM CaCl₂). A total of 2.5 μg of plasmid DNA was used per transfection. Plasmids expressing AKT2-HA and FKBP51-FLAG or GFP (control) have been described previously^{21, 51}. Ectopic overexpression of AKT2 and FKBP51 resulted in a 3.2-fold and 2.8-fold increase in their expression, respectively. Electroporation was performed using the Amaxa Nucleofector system (program #T-032). The cells were re-seeded onto 0.75% gelatin-coated 12-well plates at a density of ~10⁵ cells per cm². Transfected cells were induced to differentiate once they reached 90% confluency. Differentiation was induced by switching the growth medium to DMEM containing 2% horse serum for 3 days.

Primary EDL myotubes were prepared from satellite cells collected from soleus muscle and EDL myofibers of 4- to 8-week old WT and 51KO mice as described previously⁵². Briefly, dissected muscles were washed in warm 1 x PBS and subsequently were digested in Collagenase 1 at 37 °C for 1.5 h. Thereafter, single fibers were washed in DMEM with 1% P/S. After washing, the fibers were transferred to a 60mm plate (coated with 0.75% gelatin) and were allowed to incubate at 37 °C for 3 days in growth medium (DMEM + 20% FBS + 1%P/S). The satellite cells were detached from the plate and were re-plated onto 24-well multi-well dishes. The medium was exchanged every 2–3 days and cells were split at 90–100% confluency. Differentiation was induced by switching the growth medium to DMEM containing 5% horse serum for 5 days.

Glucose uptake. Primary EDL myotubes or transfected C2C12 myotubes were used for glucose uptake experiments. For SAFit2 experiments, a toxicity assay was initially performed to determine the appropriate SAFit2 concentration for subsequent experiments. Based on a lethal dose of 15 (LD 15), the cells were incubated with 0.6 μM SAFit2 or DMSO overnight before inducing glucose uptake.

Basal and insulin-stimulated glucose uptake in primary EDL muscle cells and differentiated C2C12 myotubes was examined. Briefly, the cells were serum-starved in low glucose (1000 mg L⁻¹) DMEM for 4 h, and then incubated in Krebs-Ringer-HEPES (KRH) buffer (136 mM NaCl, 4.7 mM KCl, 10 mM sodium phosphate buffer, 1 mM MgSO₄, 1 mM CaCl₂, and 10 mM HEPES, pH 7.4, 0.2% BSA) for 10 min. The cells were stimulated with insulin (100 nM) or left unstimulated for 1 h. Glucose uptake was induced by the addition of KRH buffer containing 100 μM 2-deoxy-D-[1,2-³H]glucose, 2 μCi ml⁻¹ (Perkin Elmer) to each well. After 4 min, the reactions were terminated by washing the cells with ice-cold PSB containing 10 μM cytochalasin B (inhibitor of membrane transporter-dependent glucose transport), and then 2 additional washes with ice-cold 1x PBS. Cells were lysed with 0.1 M NaOH for 30 min, and the incorporated radioactivity was determined by liquid scintillation counting. 2-deoxy-D-[1,2-³H]glucose uptake was furthermore normalized to total protein content assessed by the BCA assay (BCA Protein Assay Kit, Life Technologies, Darmstadt, Germany).

Antibodies. Detailed information on antibodies and dilutions is provided in Supplementary Information.

GLUT4 membrane localization. Primary EDL myotubes were exposed to 0.6 μM SAFit2 or DMSO (vehicle) overnight. The following day, cells were serum-starved in low glucose (1000 mg L⁻¹) DMEM for 4 h with SAFit2 or DMSO, and were subsequently collected for the rapid preparation of the plasma membrane fraction as described previously⁵³. The membrane fraction was used in subsequent Western blot assays for the detection of GLUT4. For quantification, GLUT4 was normalized to both Na,K-ATPase (plasma membrane marker) and normalized total GLUT4, as described previously⁵⁴.

For GLUT4 membrane localization in 51KO ($n = 6$) and WT ($n = 5$) mice, the mice were fasted for 6 h. Insulin was injected by i.p. administration (0.70 IU kg⁻¹) 5 min before mice were anesthetized with isoflurane, and were immediately killed by decapitation. Tissues were collected and stored at -80 °C until used. 2-way subcellular fractionation was performed as described previously⁵⁵.

Co-immunoprecipitation (coIP). Immunoprecipitations of endogenous proteins were performed using protein extracts ($n = 3$ per group) from soleus muscle, EDL, and eWAT of vehicle-treated and SAFit2-treated mice that were fed HFD. The CoIP experiments were performed with beads conjugated with rabbit IgG. Briefly, 500 μg of lysate was incubated overnight with 2 μg of the appropriate Ig-antibody (AKT2 (CST, #2964); FKBP5/FKBP51 (Bethyl, A301-430); and FKBP4/FKBP52 (Bethyl, A301-427A) (See Supplementary Table 1) at 4 °C. 20 μl of protein G dynabeads (Invitrogen, 100-03D) was blocked with bovine serum albumin and subsequently added to the lysate-antibody mix and allowed to incubate at 4 °C for 3 h in order to mediate binding between the dynabeads and the antibody-antigen complex of interest. The beads were washed three times with ice-cold PBS. The

protein-antibody complexes were eluted with 60 μ L Laemmli loading buffer. Thereafter, the eluate was boiled for 5 min at 95 $^{\circ}$ C. Then 2–5 μ L of each immunoprecipitate reaction product was separated by SDS-PAGE and electrotransferred onto nitrocellulose membranes. For assessing protein complexes, immunoblotting against AKT2, FKBP51, PHLPP1 (Millipore, #07-1341), and AS160 was performed. See Supplemental Information ‘Western blot analysis’ for details.

Statistical analysis. Data were analyzed using IBM SPSS Statistics 18 software (IBM SPSS Statistics, IBM, Chicago, IL, USA). The decomposition of total energy expenditure (TEE) into activity-related energy expenditure (AEE) and resting metabolic rate (RMR) was performed in MATLAB (The MathWorks, Natick, MA, USA) using a custom-designed toolbox graciously provided by JB van Klinken (Leiden University Medical Center, Leiden, The Netherlands). Body weight was included as a covariate in the analyses of energy expenditure⁵⁶. Statistical analyses for all energy expenditure outcome variables, respiratory exchange ratio (RER), home-cage activity, food intake, water intake, and body temperature were performed on 24-hour averages. Statistical significance was set at $p < 0.05$; a statistical tendency was set at $p < 0.1$. For interactions at $p < 0.1$, we also examined lower order main effects. Data are presented as the mean \pm SEM.

Data availability. The data herein are available from the corresponding authors upon reasonable request.

Received: 28 June 2016 Accepted: 12 October 2017

Published online: 23 November 2017

References

- Ratajczak, T., Cluning, C. & Ward, B. K. Steroid receptor-associated immunophilins: A gateway to steroid signalling. *Clin. Biochem. Rev.* **36**, 31–52 (2015).
- Denny, W. B., Valentine, D. L., Reynolds, P. D., Smith, D. F. & Scammell, J. G. Squirrel monkey immunophilin {FKBP}51 is a potent inhibitor of glucocorticoid receptor binding. *Endocrinology* **141**, 4107–4113 (2000).
- Wochnik, G. M. et al. {FK}506-binding proteins 51 and 52 differentially regulate dynein interaction and nuclear translocation of the glucocorticoid receptor in mammalian cells. *J. Biol. Chem.* **280**, 4609–4616 (2005).
- Vermeer, H., Hendriks-Stegeman, B. I., van der Burg, B., van Buul-Offers, S. C. & Jansen, M. Glucocorticoid-induced increase in lymphocytic {FKBP}51 messenger ribonucleic acid expression: a potential marker for glucocorticoid sensitivity, potency, and bioavailability. *J. Clin. Endocrinol. Metab.* **88**, 277–284 (2003).
- Jääskeläinen, T., Makkonen, H. & Palvimo, J. J. Steroid up-regulation of FKBP51 and its role in hormone signaling. *Curr. Opin. Pharmacol.* **11**, 326–331 (2011).
- Riggs, D. L. et al. The Hsp90-binding peptidylprolyl isomerase FKBP52 potentiates glucocorticoid signaling in vivo. *EMBO. J.* **22**, 1158–1167 (2003).
- Zannas, A. S., Wiechmann, T., Gassen, N. C. & Binder, E. B. Gene–stress–epigenetic regulation of FKBP5: clinical and translational implications. *Neuropsychopharmacology* **41**, 261–274 (2016).
- Karalis, K. P. et al. Mechanisms of obesity and related pathology: linking immune responses to metabolic stress. *FEBS. J.* **276**, 5747–5754 (2009).
- Balsevich, G. et al. Interplay between diet-induced obesity and chronic stress in mice: potential role of FKBP51. *J. Endocrinol.* **222**, 15–26 (2014).
- Guarnieri, D. J. et al. Gene profiling reveals a role for stress hormones in the molecular and behavioral response to food restriction. *Biol. Psychiatry* **71**, 358–365 (2012).
- Scharf, S. H., Liebl, C., Binder, E. B., Schmidt, M. V. & Müller, M. B. Expression and regulation of the Fkbp5 gene in the adult mouse brain. *PLoS ONE* **6**, e16883 (2011).
- Su, A. I. et al. A gene atlas of the mouse and human protein-encoding transcriptomes. *Proc. Natl Acad. Sci. USA* **101**, 6062–6067 (2004).
- Hartmann, I. B. et al. The FKBP5 polymorphism rs1360780 is associated with lower weight loss after bariatric surgery: 26 months of follow-up. *Surg. Obes. Relat. Dis.* **12**, 1554–1560 (2016).
- Pereira, M. J. et al. FKBP5 expression in human adipose tissue increases following dexamethasone exposure and is associated with insulin resistance. *Metabolism* **63**, 1198–1208 (2014).
- Stechschulte, L. A. et al. FKBP51 null mice are resistant to diet-induced obesity and the PPAR γ agonist rosiglitazone. *Endocrinology* **157**, 3888–3900 (2016).
- Pei, H. et al. FKBP51 affects cancer cell response to chemotherapy by negatively regulating Akt. *Cancer Cell* **16**, 259–266 (2009).
- Cho, H. et al. Insulin resistance and a diabetes mellitus-like syndrome in mice lacking the protein kinase Akt2 (PKB β). *Science* **292**, 1728–1731 (2001).
- Taniguchi, C. M., Emanuelli, B. & Kahn, C. R. Critical nodes in signalling pathways: insights into insulin action. *Nat. Rev. Mol. Cell Biol.* **7**, 85–96 (2006).
- Zannas, A. S., Balsevich, G. & Gassen, N. C. The emerging role of FKBP5 in the regulation of metabolism and body weight. *Surg. Obes. Relat. Dis.* **12**, 1560–1561 (2016).
- Gaali, S. et al. Selective inhibitors of the FK506-binding protein 51 by induced fit. *Nat. Chem. Biol.* **11**, 33–37 (2015).
- Gassen, N. C. et al. Association of FKBP51 with priming of autophagy pathways and mediation of antidepressant treatment response: evidence in cells, mice, and humans. *PLoS Med.* **11**, e1001755 (2014).
- Hartmann, J. et al. The involvement of FK506-binding protein 51 (FKBP5) in the behavioral and neuroendocrine effects of chronic social defeat stress. *Neuropharmacology* **62**, 332–339 (2012).
- Touma, C. et al. FK506 binding protein 5 shapes stress responsiveness: modulation of neuroendocrine reactivity and coping behavior. *Biol. Psychiatry* **70**, 928–936 (2011).
- Zimmermann, P. et al. Interaction of FKBP5 gene variants and adverse life events in predicting depression onset: results from a 10-year prospective community study. *Am. J. Psychiatry* **168**, 1107–1116 (2011).
- Klengel, T. et al. Allele-specific FKBP5 DNA demethylation mediates gene-childhood trauma interactions. *Nat. Neurosci.* **16**, 33–41 (2013).
- Hartmann, J. et al. Pharmacological inhibition of the psychiatric risk factor FKBP51 Has anxiolytic properties. *J. Neurosci.* **35**, 9007–9016 (2015).
- Tamashiro, K. L., Sakai, R. R., Shively, C. A., Karatsoreos, I. N. & Reagan, L. P. Chronic stress, metabolism, and metabolic syndrome. *Stress* **14**, 468–474 (2011).
- Sano, H. et al. Insulin-stimulated phosphorylation of a Rab GTPase-activating protein regulates GLUT4 translocation. *J. Biol. Chem.* **278**, 14599–14602 (2003).
- Fabian, A. K. et al. InterAKTions with FKBP5-mutational and pharmacological exploration. *PLoS ONE* **8**, e57508 (2013).
- Storer, C. L., Dickey, C. A., Galigiana, M. D., Rein, T. & Cox, M. B. FKBP51 and FKBP52 in signaling and disease. *Trends Endocrinol. Metab.* **22**, 481–490 (2011).
- Roy, A., Gorodetsky, E., Yuan, Q., Goldman, D. & Enoch, M. A. Interaction of FKBP5, a stress-related gene, with childhood trauma increases the risk for attempting suicide. *Neuropsychopharmacology* **35**, 1674–1683 (2010).
- Mehta, D. et al. Using polymorphisms in {FKBP}5 to define biologically distinct subtypes of posttraumatic stress disorder: evidence from endocrine and gene expression studies. *Arch. Gen. Psychiatry* **68**, 901–910 (2011).
- Binder, E. B. et al. Association of FKBP5 polymorphisms and childhood abuse with risk of posttraumatic stress disorder symptoms in adults. *JAMA* **299**, 1291–1305 (2008).
- Maiaur, M. et al. The stress regulator FKBP51 drives chronic pain by modulating spinal glucocorticoid signaling. *Sci. Transl. Med.* **8**, 1–11 (2016).
- Romano, S. et al. FKBP51 employs both scaffold and isomerase functions to promote NF- κ B activation in melanoma. *Nucleic Acids Res.* **43**, 6983–6993 (2015).
- Sinars, C. R. et al. Structure of the large FK506-binding protein FKBP51, an Hsp90-binding protein and a component of steroid receptor complexes. *Proc. Natl Acad. Sci. USA* **100**, 868–873 (2003).
- Gassen, N. C. et al. FKBP51 inhibits GSK3 β and augments the effects of distinct psychotropic medications. *Mol. Psychiatry* **21**, 277–289 (2016).
- Jiang, W. et al. FK506 binding protein mediates glioma cell growth and sensitivity to rapamycin treatment by regulating NF- κ B signaling pathway. *Neoplasia* **10**, 235–243 (2008).
- Chen, W. S. et al. Growth retardation and increased apoptosis in mice with homozygous disruption of the Akt1 gene. *Genes Dev.* **15**, 2203–2208 (2001).
- Cho, H., Thorvaldsen, J. L., Chu, Q., Feng, F. & Birnbaum, M. J. Akt1/PKB α is required for normal growth but dispensable for maintenance of glucose homeostasis in mice. *J. Biol. Chem.* **276**, 38349–38352 (2001).
- Garofalo, R. S. et al. Severe diabetes, age-dependent loss of adipose tissue, and mild growth deficiency in mice lacking Akt2/PKB β . *J. Clin. Invest.* **112**, 197–208 (2003).
- Kramer, H. F. et al. AS160 regulates insulin- and contraction-stimulated glucose uptake in mouse skeletal muscle. *J. Biol. Chem.* **281**, 31478–31485 (2006).
- DeFronzo, R. A., Gunnarsson, R., Bjorkman, O., Olsson, M. & Wahren, J. Effects of insulin on peripheral and splanchnic glucose metabolism in noninsulin-dependent (type {II}) diabetes mellitus. *J. Clin. Invest* **76**, 149–155 (1985).
- Zierath, J. R. & Wallberg-Henriksson, H. From receptor to effector: insulin signal transduction in skeletal muscle from type {III} diabetic patients. *Ann. N. Y. Acad. Sci.* **967**, 120–134 (2002).
- Kurth-Kraczek, E. J., Hirshman, M. F., Goodyear, L. J. & Winder, W. W. 5' AMP-activated protein kinase activation causes GLUT4 translocation in skeletal muscle. *Diabetes* **48**, 1667–1671 (1999).

46. Treebak, J. T. et al. AMPK-mediated AS160 phosphorylation in skeletal muscle is dependent on AMPK catalytic and regulatory subunits. *Diabetes* **55**, 2051–2058 (2006).
47. Weinstein, S. P., Wilson, C. M., Pritsker, A. & Cushman, S. W. Dexamethasone inhibits insulin-stimulated recruitment of {GLUT}4 to the cell surface in rat skeletal muscle. *Metabolism* **47**, 3–6 (1998).
48. Toneatto, J. et al. Dynamic mitochondrial-nuclear redistribution of the immunophilin FKBP51 is regulated by the PKA signaling pathway to control gene expression during adipocyte differentiation. *J. Cell Sci.* **126**, 5357–5368 (2013).
49. Tranguch, S. et al. Cochaperone immunophilin FKBP52 is critical to uterine receptivity for embryo implantation. *Proc. Natl Acad. Sci. USA* **102**, 14326–14331 (2005).
50. Brandl, M., Drechsler, M., Bachmann, D. & Bauer, K. H. Morphology of semisolid aqueous phosphatidylcholine dispersions, a freeze fracture electron microscopy study. *Chem. Phys. Lipids*. **87**, 65–72 (1997).
51. Kim, D. et al. A small molecule inhibits Akt through direct binding to Akt and preventing Akt membrane translocation. *J. Biol. Chem.* **291**, 22856 (2016).
52. Shefer, G. & Yablonka-Reuveni, Z. Isolation and culture of skeletal muscle myofibers as a means to analyze satellite cells. *Methods Mol. Biol.* **290**, 281–304 (2005).
53. Nishiumi, S. & Ashida, H. Rapid preparation of a plasma membrane fraction from adipocytes and muscle cells: application to detection of translocated glucose transporter 4 on the plasma membrane. *Biosci. Biotechnol. Biochem.* **71**, 2343–2346 (2007).
54. Kong, D. et al. Overexpression of mitofusin 2 improves translocation of glucose transporter 4 in skeletal muscle of high-fat diet-fed rats through AMP-activated protein kinase signaling. *Mol. Med. Rep.* **8**, 205–210 (2013).
55. Hwang, S.-I. & Han, D. K. Subcellular fractionation for identification of biomarkers: serial detergent extraction by subcellular accessibility and solubility. *Methods Mol. Biol.* **1002**, 25–35 (2013).
56. Arch, J. R., Hislop, D., Wang, S. J. & Speakman, J. R. Some mathematical and technical issues in the measurement and interpretation of open-circuit indirect calorimetry in small animals. *Int. J. Obes.* **30**, 1322–1331 (2006).

Acknowledgements

The authors thank Marc Cox and Dave Smith (University of Texas at El Paso, El Paso, Texas, US) for originally sharing 51KO mice and MEFs and Lisa Tietze and Jose Monteserin (Max Planck Institute of Psychiatry, Munich, Germany) for their excellent technical assistance. N.C.G. was supported by a European Research Council starting grant (grant# 281338, GxE molmech) within the FP7 framework.

Author contributions

G.B., A.S.H., N.C.G., M.V.S. and T.R.: Conceived the project and designed the experiments. G.B. and M.L.P.: Managed the colony/genotyping. G.B. and A.S.H.: Performed animal experiments and glucose uptake experiments in cell culture. N.C.G. and K.H.: Performed CoIP experiments, western blot, and subcellular fractionation experiments. C.W.M.: Performed calorimetry experiments and analyses. S.K.: Helped with the calorimetry experiment analyses. M.L.P., C.D., S.S., C.L., A.U. and M.T.: Helped perform animal experiments. X.F. and F.H.: Synthesized SAFit2. M.B. and G.W.: Designed and provided the SAFit2 slow release formulation. C.N. and M.U.: Performed LC/MS/MS. G.B.: Wrote initial version of the manuscript. M.-P.P., A.C., M.H.T., T.R., N.C.G. and M.V.S.: Supervised the research and all authors revised the manuscript.

Additional information

Supplementary Information accompanies this paper at [doi:10.1038/s41467-017-01783-y](https://doi.org/10.1038/s41467-017-01783-y).

Competing interests: The authors declare no competing financial interests.

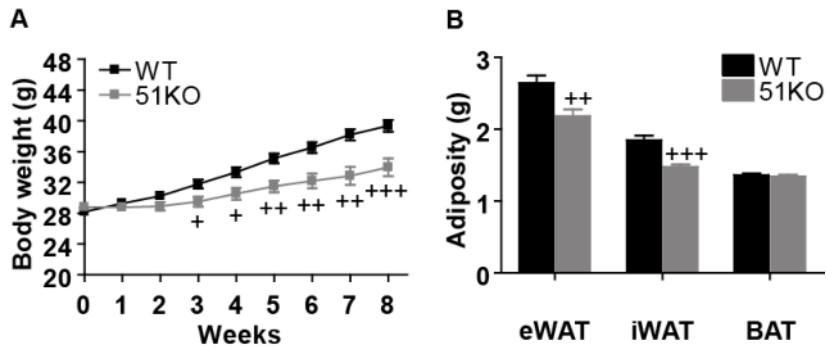
Reprints and permission information is available online at <http://npg.nature.com/reprintsandpermissions/>

Publisher's note: Springer Nature remains neutral with regard to jurisdictional claims in published maps and institutional affiliations.



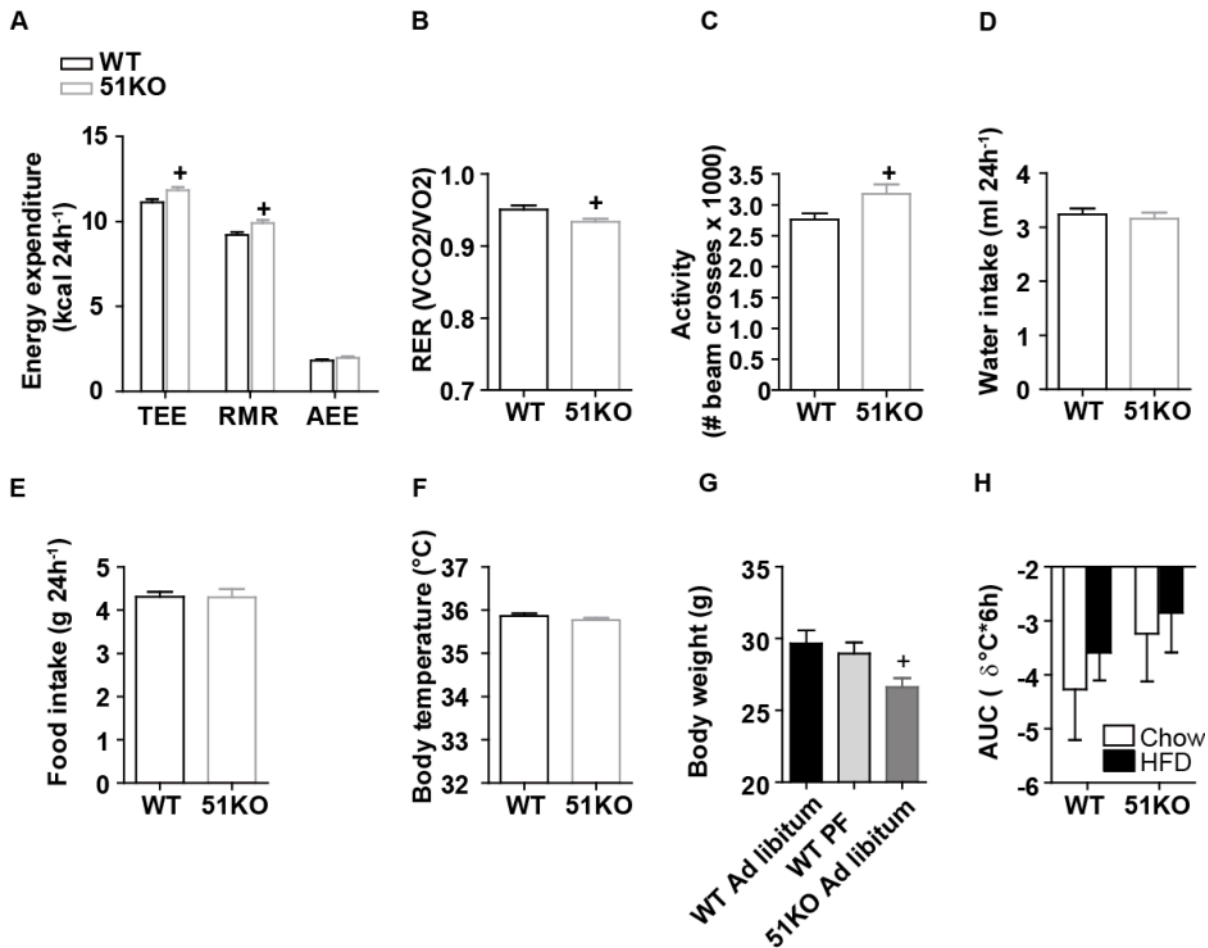
Open Access This article is licensed under a Creative Commons Attribution 4.0 International License, which permits use, sharing, adaptation, distribution and reproduction in any medium or format, as long as you give appropriate credit to the original author(s) and the source, provide a link to the Creative Commons license, and indicate if changes were made. The images or other third party material in this article are included in the article's Creative Commons license, unless indicated otherwise in a credit line to the material. If material is not included in the article's Creative Commons license and your intended use is not permitted by statutory regulation or exceeds the permitted use, you will need to obtain permission directly from the copyright holder. To view a copy of this license, visit <http://creativecommons.org/licenses/by/4.0/>.

© The Author(s) 2017



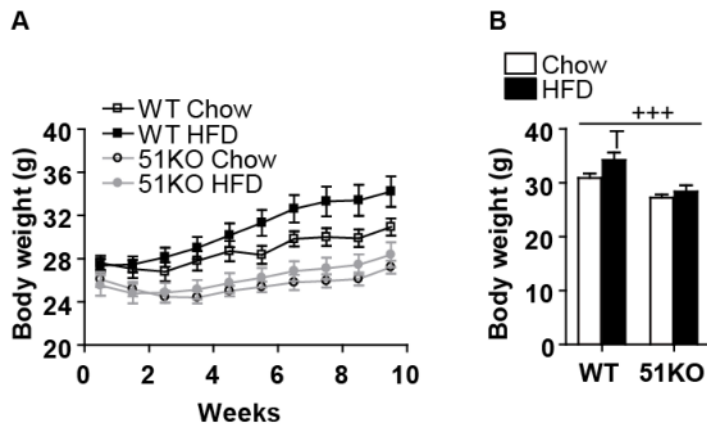
Supplementary Figure 1. Genetic ablation of FKBP51 protects against diet-induced obesity under thermoneutral conditions.

(A) Over 8 weeks of HFD exposure at 30 °C, 51KO mice resisted HFD-induced weight gain and (B) adiposity, indicating that genetic ablation of FKBP51 protects against diet-induced obesity under thermoneutral conditions. n = 8 per genotype group. Repeated measures ANOVA for panel A, 2-tailed t tests for panel B. Data are expressed as means ± SEM. ⁺P < 0.05, ⁺⁺P < 0.01, ⁺⁺⁺P < 0.001; + significant genotype effect.



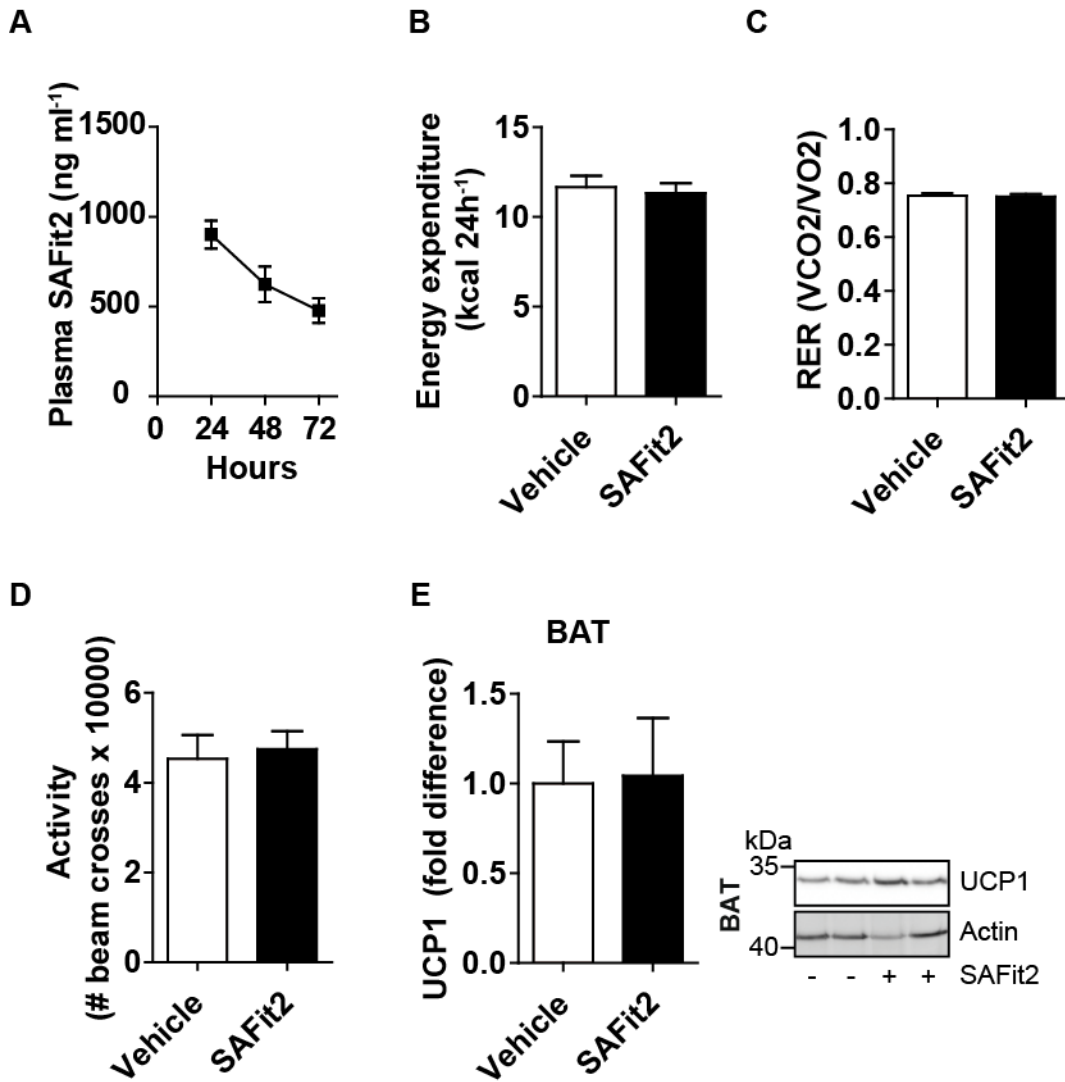
Supplementary Figure 2. Metabolic phenotype in 51KO transgenic mice. Metabolic readouts were assessed in WT mice (n = 18) and 51KO mice (n = 16) under chow conditions in TSE PhenoMaster Systems. (A) Total energy expenditure (TEE), adjusted for body weight, was higher in the chow-fed 51KO animals measured across 24 h. Decomposition of TEE into its resting (RMR) and activity-related (AEE) components revealed that the observed TEE difference was due to increased RMR in the 51KO animals measured over 24 h. AEE did not differ between genotypes as assessed across 24 h. (B) Loss of FKBP51 furthermore decreased the average respiratory exchange ratio (RER) and (C) increased the average home-cage activity assessed across 24 h. There was however no effect of genotype on either (D) water consumption, (E) food intake or (F) body temperature assessed across 24 h. (G) In a separate cohort of animals, a pair-feeding experiment was performed to assess genotype-dependent effects on food intake. 51KO (n = 9) and WT (n = 11) mice in the ad libitum groups had free access to food, whereas WT PF (n = 9) mice were pair-fed to the 51KO mice. After 6 weeks on the pair-feeding paradigm, 51KO mice weighed significantly less compared to WT ad libitum mice. (H) A separate

cohort of mice was examined for cold-induced rectal temperature changes following exposure to 4 °C under control and HFD conditions (n = 11 per group). Neither genotype nor diet had an effect on body temperature following short-term (6 h) cold exposure. Data are expressed as means \pm SEM. [†]P < 0.05, ANCOVA adjusted body weight for panels A – C, 2-tailed t tests for panels D – F & H, 1-way ANOVA plus Bonferroni testing for panel G; + significant genotype effect.

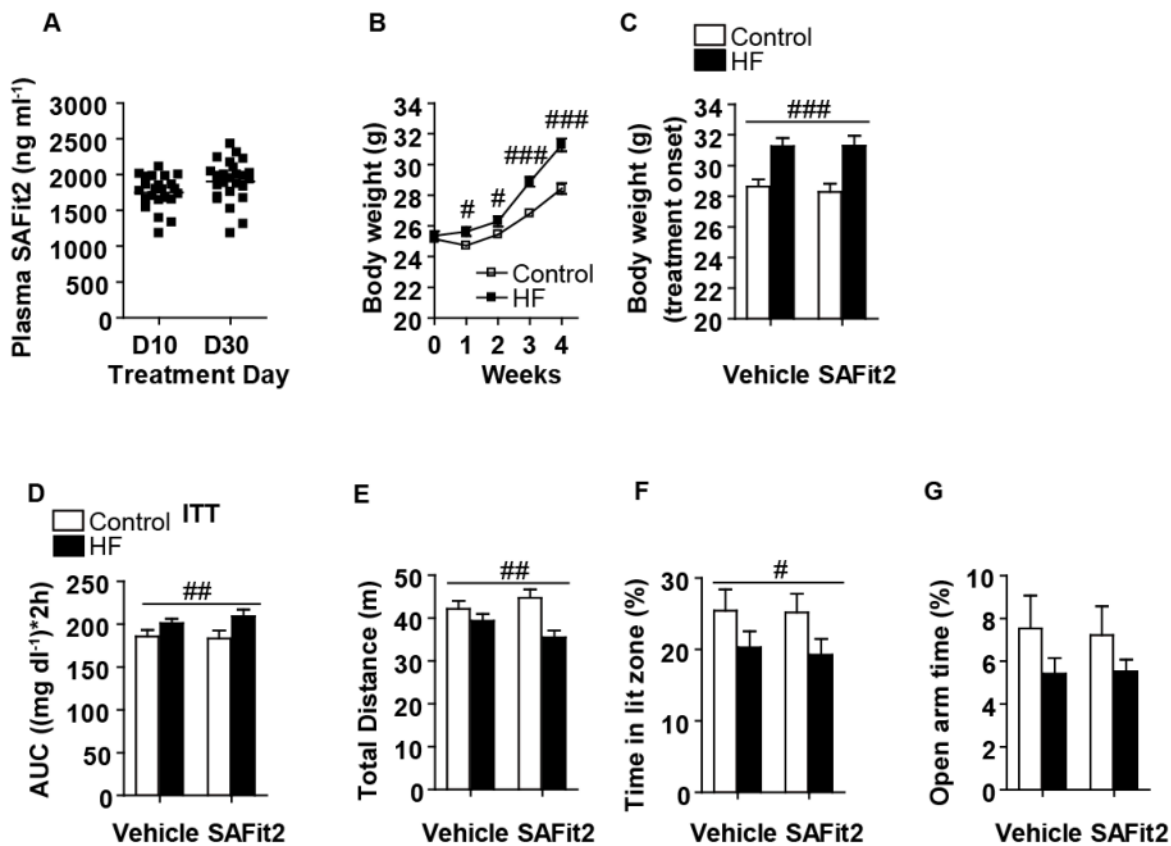


Supplementary Figure 3. Genetic ablation of FKBP51 prevents HFD-induced weight gain observed across 2 independent experiments. In an independent experiment used to assess glucose and insulin tolerance, 51KO mice presented the same body weight phenotype compared to WT mice as reported in Experiment 1. (A) 51KO mice weighed significantly less than WT mice throughout the 8 week dietary treatment and (B) at the experimental end. Furthermore, a tendency was observed indicating that WT mice were susceptible to HFD-induced weight gain compared to 51KO mice as interpreted from body weight progression. Data are expressed as means \pm SEM.

^TP < 0.1, ⁺⁺⁺P < 0.001; + significant genotype effect; T trend for diet, Repeated measure ANOVA for panel A, 2-way ANOVA plus Bonferroni testing for panel B.

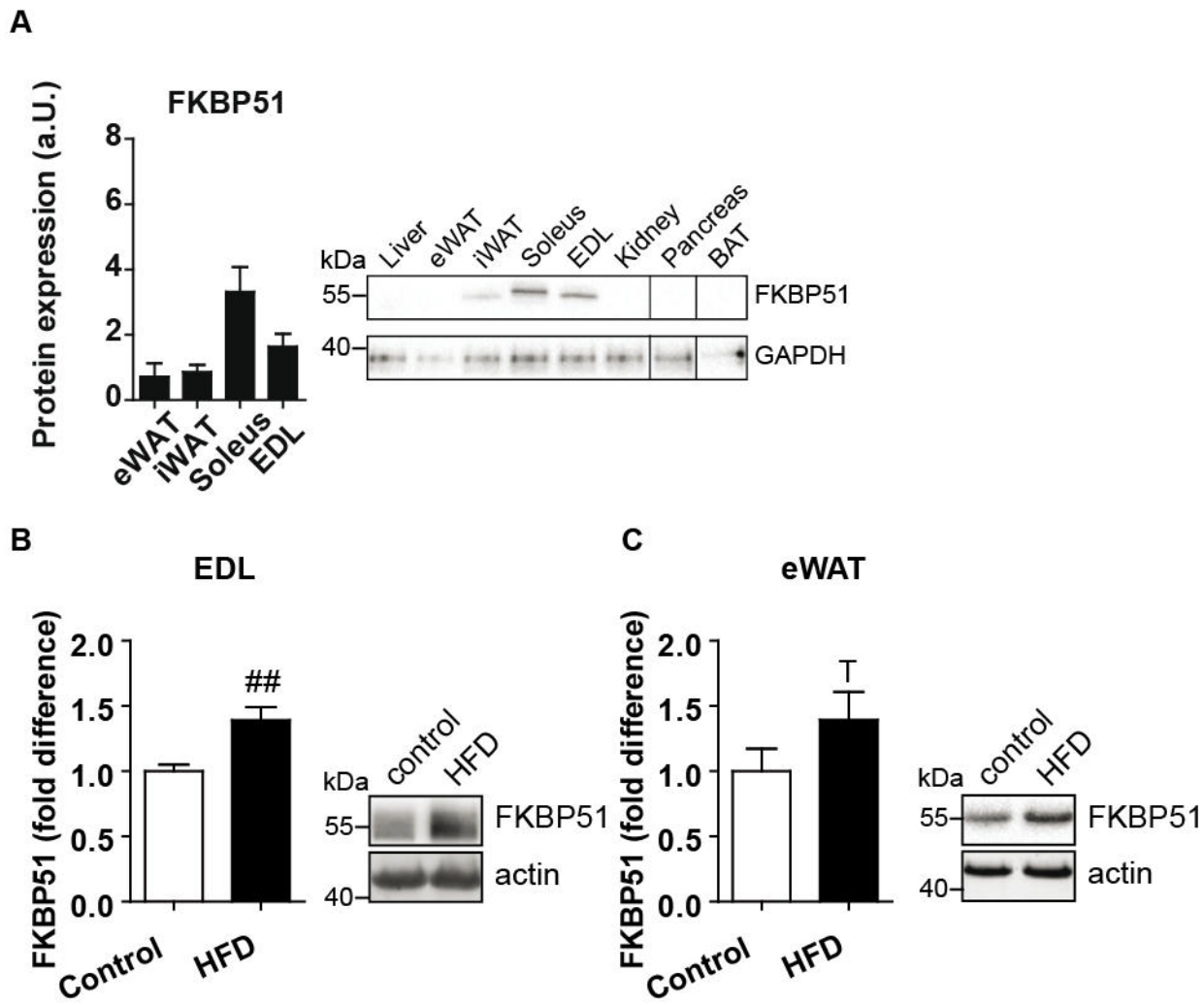


Supplementary Figure 4. Acute administration of the FKBP51 antagonist SAFit2. (A) A single application of slow-release formulated SAFit2 gel (2 mg, s.c.) resulted in high SAFit2 plasma levels measured at 24h, 48h, and 72h post-injection. (B) (B – D) Total energy expenditure (TEE) adjusted for body weight (B), respiratory exchange ratio (RER) (C), and home-cage activity (D) were unaffected by FKBP51 antagonism. (F) Acute SAFit2 had no effect on UCP1 expression in BAT measured 48 h after SAFit2 administration. Panel A: n = 6; panel B – E: n = 8 per treatment group. Data are expressed as means ± SEM. 2-tailed T-tests for panels B – E.

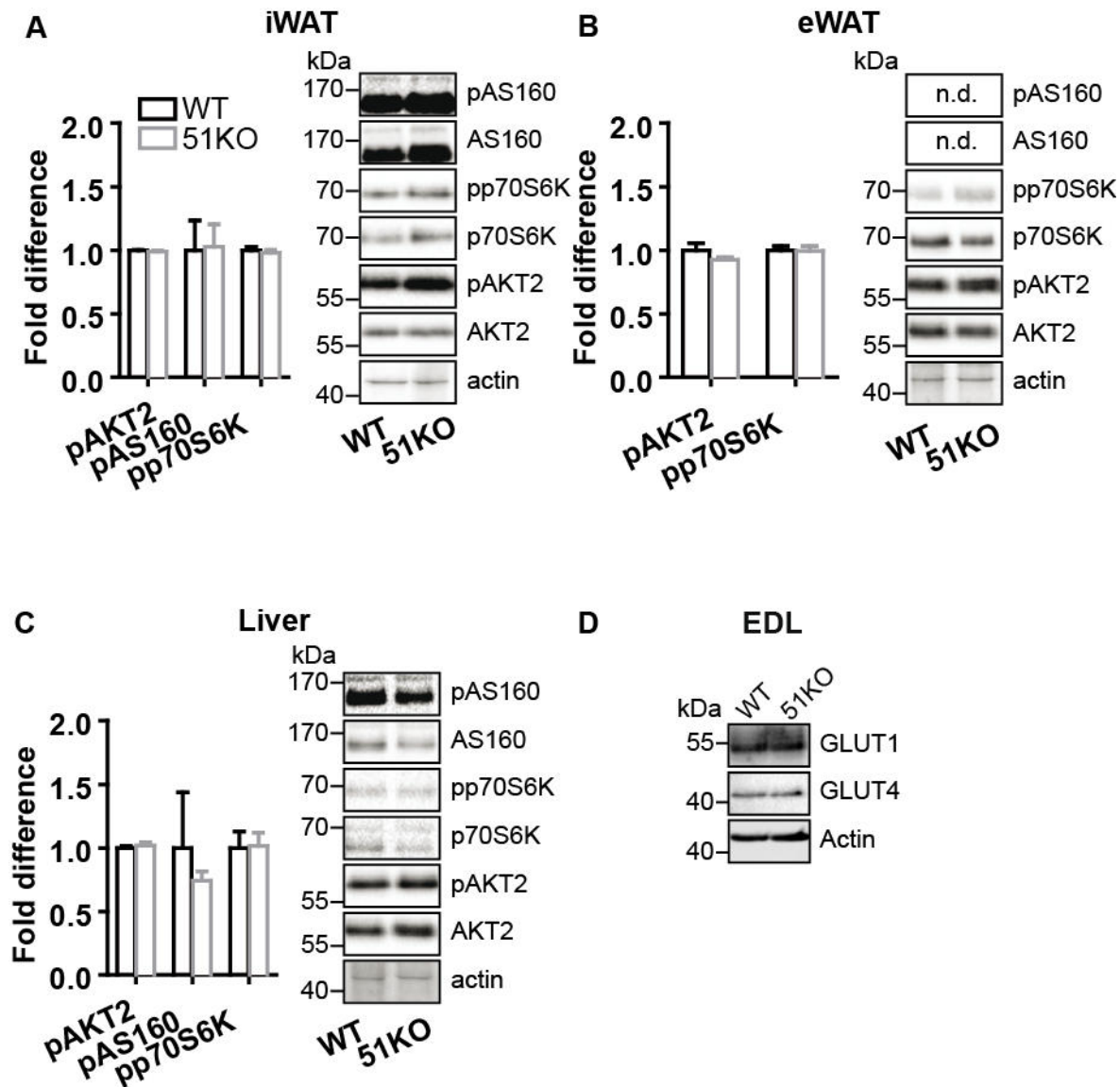


Supplementary Figure 5. Repeated administration of the FKBP51 antagonist SAFit2. (A) Administration of SAFit2 (twice daily at 20 mg per kg) by intraperitoneal injections resulted in high SAFit2 plasma levels and minimal inter-animal variability on day 10 and day 30 of treatment schedule (n = 24 plasma samples for each time point). (B) 4 weeks before SAFit2 treatment onset, mice were randomly assigned to either the control diet or HFD group. Exposure to the HFD resulted in a significant increase in body weight progression (n = 25 per diet group) (C) At treatment onset, mice were subdivided into treatment groups counterbalanced by body weight, and therefore within each dietary group there was no difference in body weight. (D) Although insulin tolerance was significantly impaired by HFD exposure, there was no improvement on account of SAFit2 treatment, demonstrated by the glucose AUC. (E) SAFit2 treatment had no effect on locomotor activity assessed as total distance traveled in an open field, although HFD exposure significantly reduced locomotor activity. (F – G) 30-day administration of SAFit2 had no undesirable behavioral side effects on anxiety-like behavior examined in both the dark-light transition test and the elevated plus maze test. By contrast, exposure to a HFD decreased the time spent in the lit compartment of the dark-light test. Panels A – E: n = 12 Vehicle-Control, n = 13 SAFit2-

Control, n = 12 Vehicle-HFD, n = 13 SAFit2-HFD). Data are expressed as means \pm SEM. #P < 0.05, ##P < 0.01, ###P < 0.001, Repeated measures ANOVA for panel B, 2-way ANOVA for panels C – G; # significant diet effect.



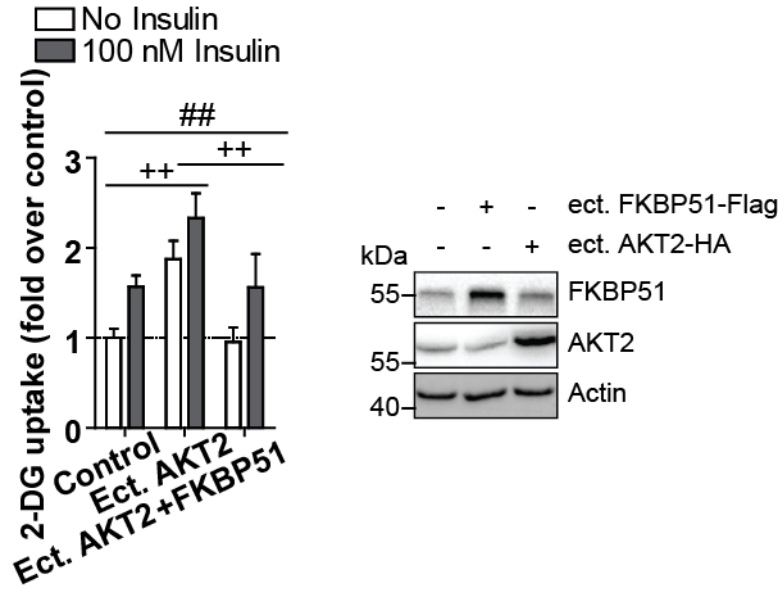
Supplementary Figure 6. Molecular characterization of FKBP51. (A) FKBP51 protein expression was detectable in eWAT, iWAT, soleus muscle, and EDL muscle, whereas was not detected in liver, kidney, spleen, pancreas, gut, or BAT. For FKBP51 tissue expression, n = 6 per tissue. (B) 8 weeks of HFD exposure significantly increased FKBP51 protein expression in EDL skeletal muscle, n = 6 per group. (C) A tendency for HFD-induced FKBP51 expression was furthermore detected in eWAT, n = 6 per group. Data are expressed as relative fold change compared to control diet condition ± SEM. ^{##}P < 0.01, 2-tailed t tests for panels B – C; # significant diet effect, T trend for diet.



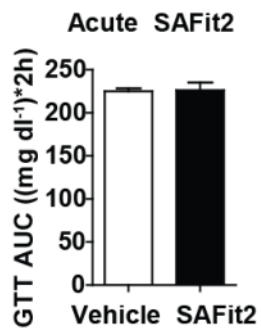
Supplementary Figure 7. FKBP51 selectively effects the insulin signaling pathway and glucose uptake.

Insulin signalling assessed by pAKT2, pAS160, and pp70S6K protein expression was not affected by FKBP51 genetic ablation in iWAT (A), eWAT (B), or liver (C). (D) Total GLUT1 and GLUT4 expression EDL muscle was unaffected by FKBP51 deletion. For quantification of phosphorylated protein, n = 4 per genotype. For GLUT1/4 expression in EDL muscle n = 3 per group. Data are expressed as relative fold change compared to wild-type condition \pm SEM. 2-tailed t tests for panels A – C. ‘n.d.’ denotes ‘not detectable’.

C2C12 myotubes

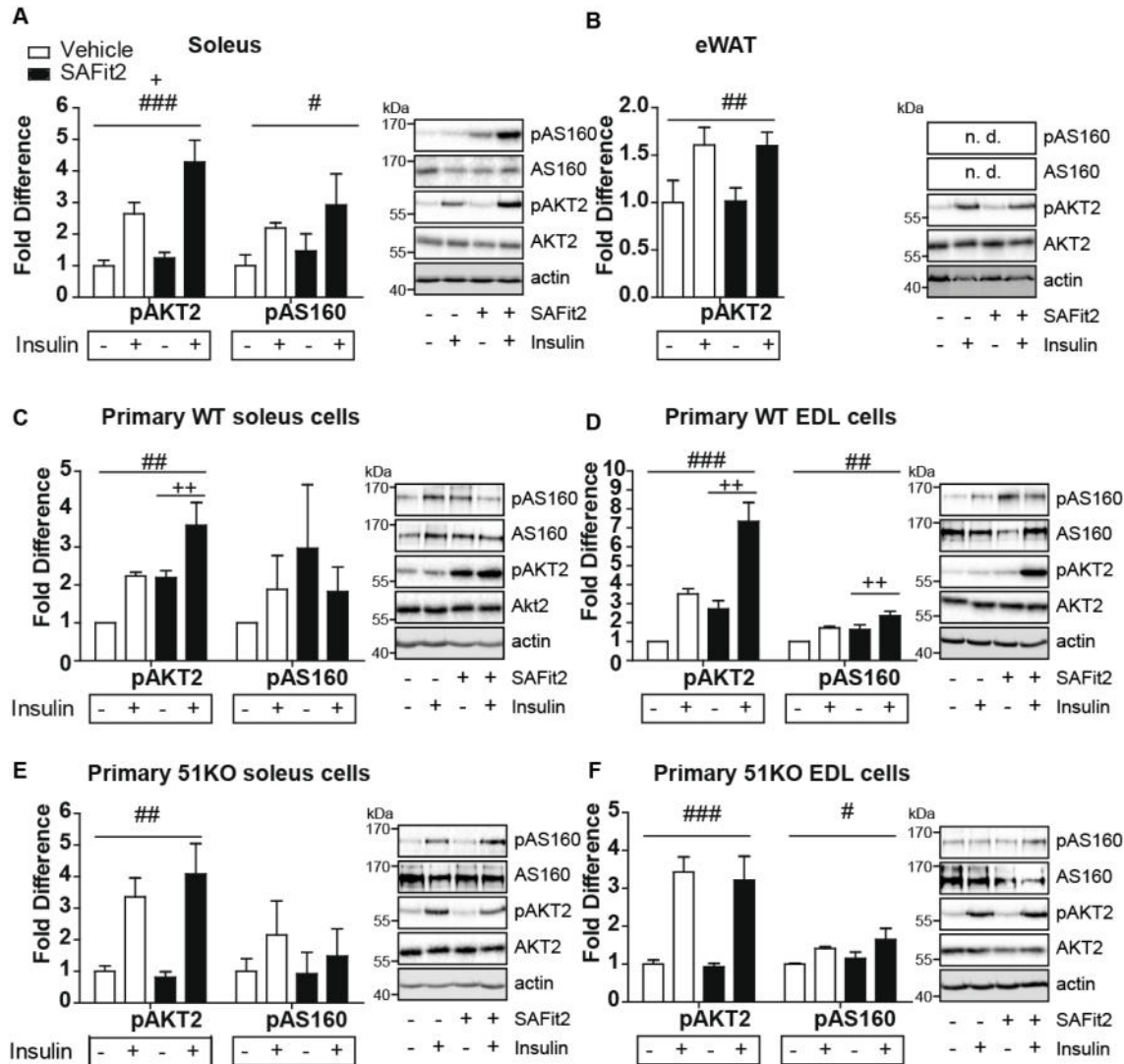


Supplementary Figure 8. Effects of ectopic overexpression of FKBP51 and AKT2 on glucose uptake. In C2C12 myotubes, enhanced glucose uptake from AKT2 overexpression was lost by simultaneous FKBP51 overexpression. Confirmation of ectopic overexpression in differentiated C2C12 cells harvested 4 days post-transfection assessed by FLAG-tagged FKBP51 and HA-tagged AKT2 antibodies. Data are expressed as relative fold change compared to control condition \pm SEM. $^{++}P < 0.01$, $^{##}P < 0.01$, 2-way ANOVA plus Bonferroni testing; + significant genotype effect, # significant insulin effect.



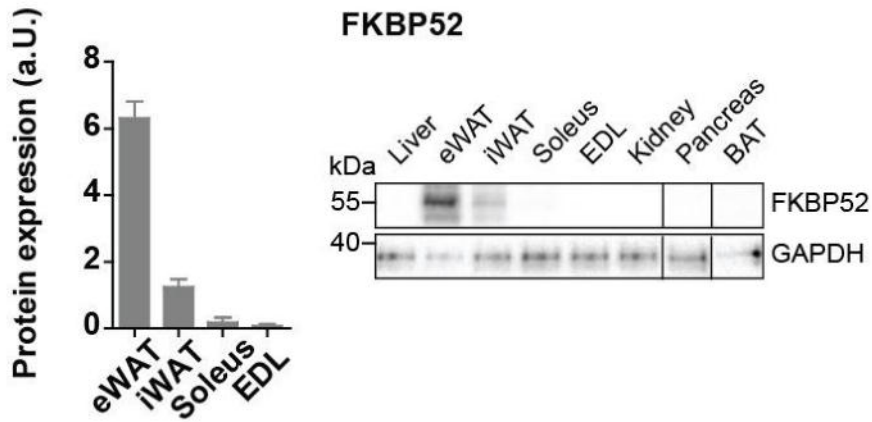
Supplementary Figure 9. Effects of FKBP51 antagonism on 6h glucose tolerance

Acute administration of SAFit2 (20mg per kg, i.p.) had no effect on glucose tolerance measured 6h following SAFit2 delivery. n = 12/treatment. Data are expressed as means \pm SEM. 2-tailed T-tests.

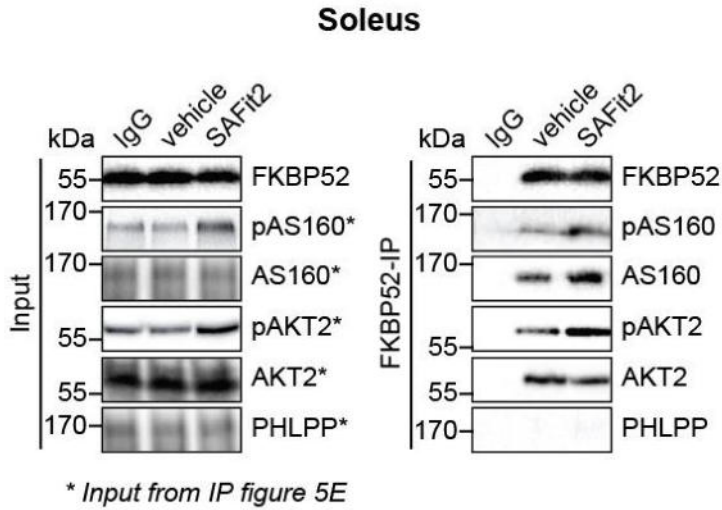


Supplementary Figure 10. Effects of FKBP51 antagonism on insulin signaling pathway and glucose uptake. (A) SAFit2 treatment increases pAKT2 in soleus muscle and insulin increases both pAKT2 and pAS160 in soleus muscle. (B) SAFit2 has no effect on pAKT2 in eWAT, whereas insulin increased pAKT2 expression. (C – D) SAFit2 increased pAKT2 in primary EDL and soleus myotubes from WT mice, and also increased pAS160 in EDL myotubes. (E – F) By contrast, there was no effect of SAFit2 treatment in cells harvested from 51KO skeletal muscle (EDL or soleus). Data are expressed as relative fold change compared to control condition \pm SEM. For quantification of phosphorylated protein expression in mice, $n = 6$ per group and in primary myotubes, $n = 3$ per group. $^+P < 0.05$, $^{++}P < 0.01$, $^{\#}P < 0.05$, $^{\#\#}P < 0.01$, $^{\#\#\#}P < 0.001$. 2-way ANOVA for panels A – F; + significant treatment effect, # significant insulin effect.

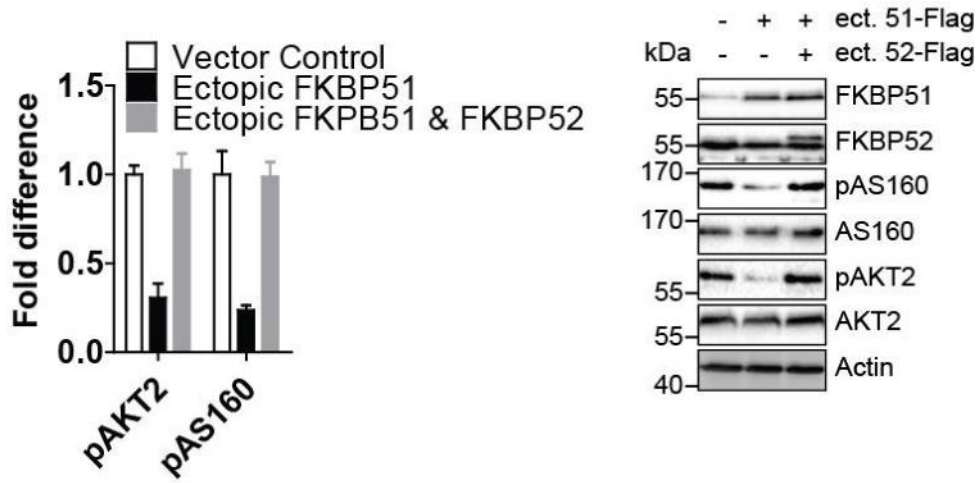
A



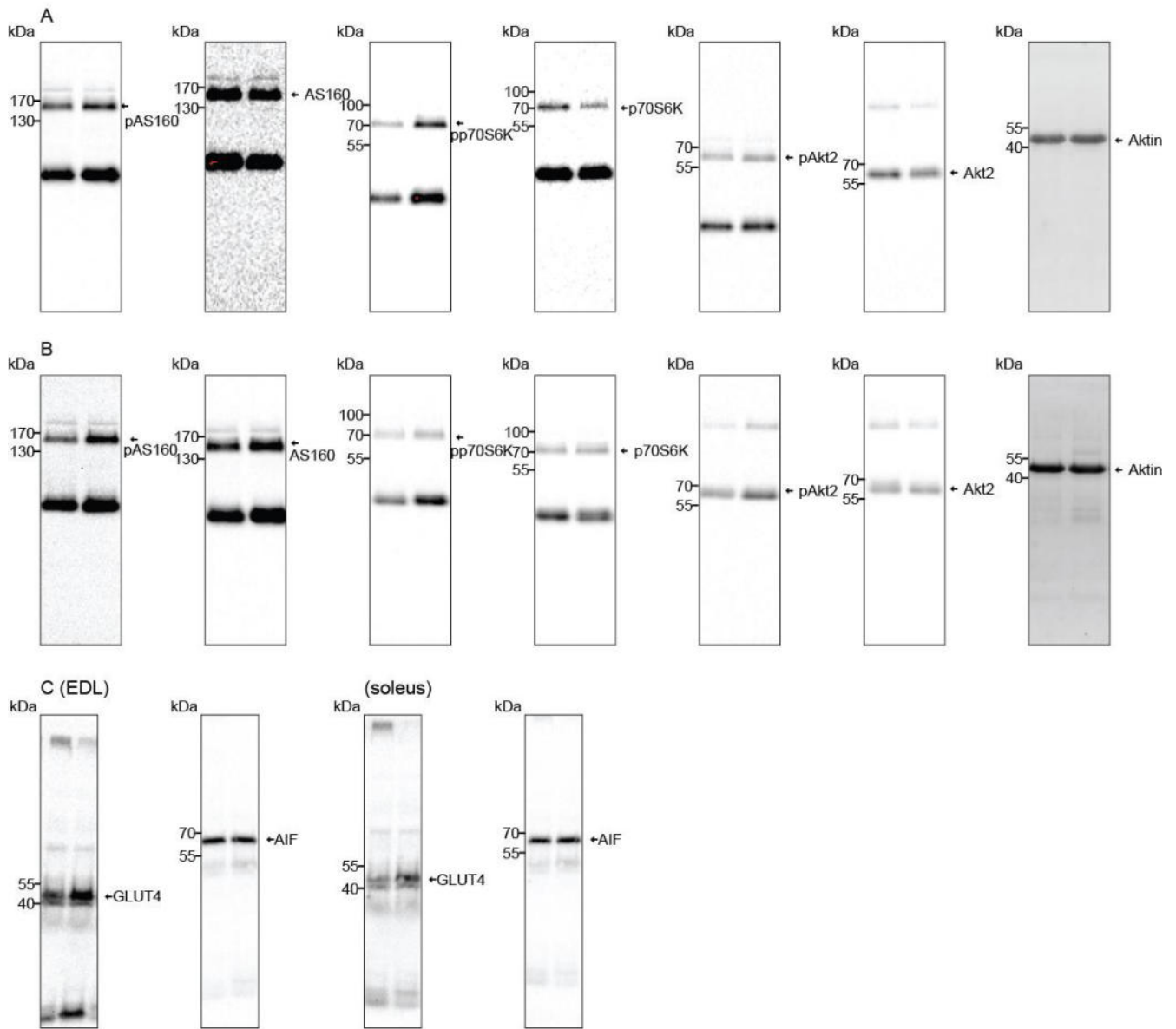
B



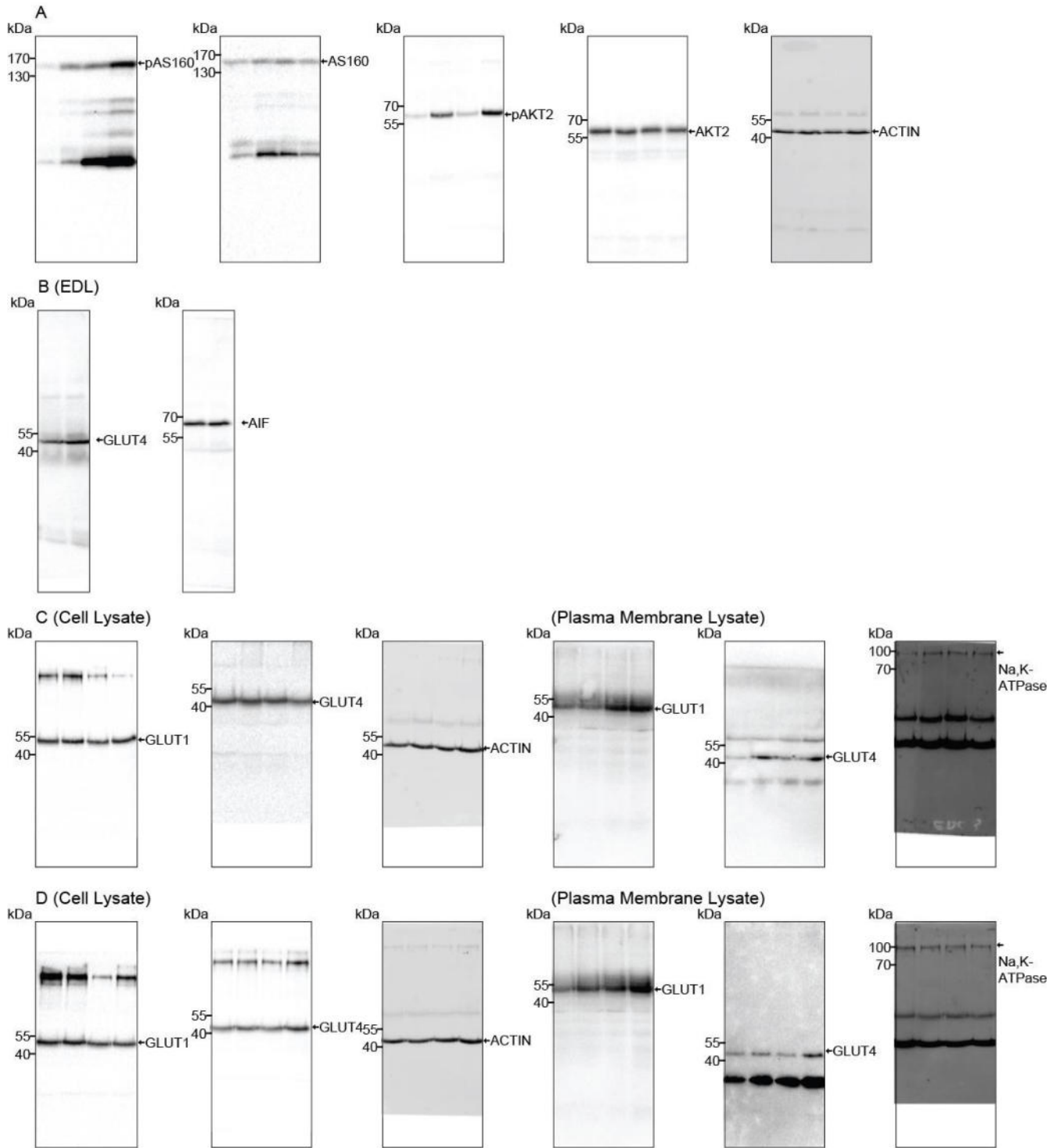
C2C12 myotubes



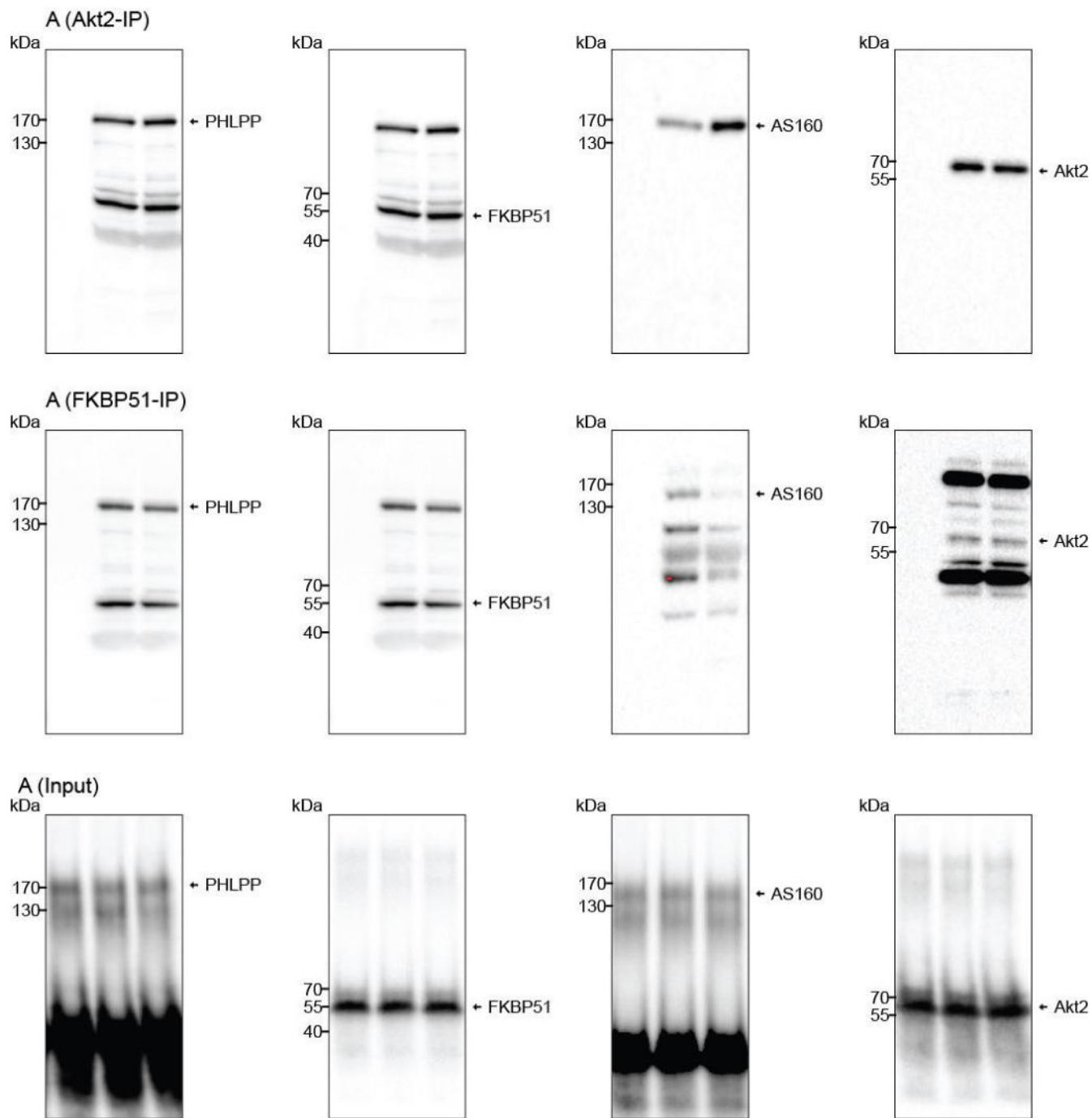
Supplementary Figure 11. FKBP52 expression and function account for muscle-specific effects of FKBP51 loss and antagonism. (A) Quantified FKBP52 protein expression in eWAT, iWAT, soleus muscle, and EDL muscle, n = 6 per tissue. (B) Tissue lysates from 30-day vehicle-treated or SAFit2-treated mice exposed to HFD were immunoprecipitated with anti-FKBP52 and then analyzed by Western blot using FKBP52, (p)AKT2, (p)AS160, and PHLPP. Immunoprecipitation reactions revealed that FKBP52 is in complex with AKT2 and AS160 but not PHLPP. (C) Ectopic overexpression of FKBP51 in C2C12 myotubes decreased pAKT2 and pAS160 expression. By contrast, simultaneous ectopic overexpression of FKBP51 and FKBP52 prevented the FKBP51-dependent decreases in expression of pAKT2 and pAS160. Panel A n = 6 per tissue; panel B n = 3 per group; panel C n = 4 per group. Data are expressed as relative fold change compared to control condition \pm SEM. 'a.U.' denotes arbitrary units.



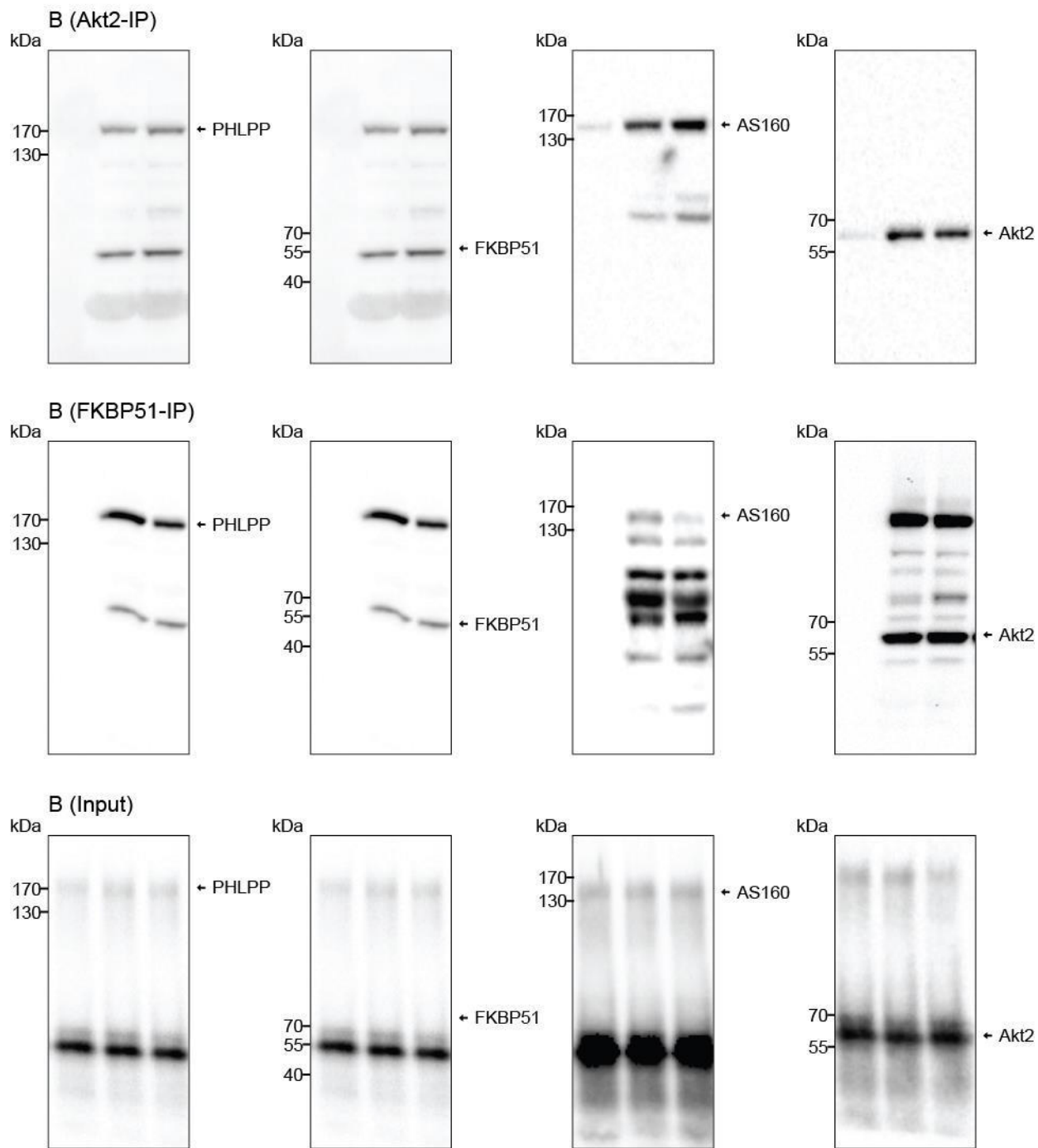
Supplementary Figure 12. Uncropped Images of Western blots from Figure 4. Uncropped Western Blots from Fig. 4A (A), Fig. 4B (B), Fig. 4C (C)



Supplementary Figure 13. Uncropped Images of Western blots from Figure 5. Uncropped Western Blots from Fig. 5A (A), Fig. 5B (B), Fig. 5C (C), Fig. 5(D)



Supplementary Figure 14. Uncropped Images of Western blots from Figure 6. Uncropped Western Blots from Fig. 6A (A)



Supplementary Figure 15. Uncropped Images of Western blots from Figure 6. Uncropped Western Blots from Fig. 6B (B)

Supplementary Methods

Indirect Calorimetry

Energy expenditure was assessed using indirect calorimetry (TSE PhenoMaster, TSE Systems, Bad Homburg, Germany). Briefly, animals were allowed to habituate to the indirect calorimetry cages for 48h before data were collected. Following 48 h of acclimatization, O₂ consumption and CO₂ production were measured every 5 min for a total of 68.5 h. Indirect calorimetry was performed at room temperature (experiment 1, cohort 1). Heat production (referred to as total energy expenditure (TEE), [kcal 24_h⁻¹]) was calculated from O₂ consumption (VO₂, [ml h⁻¹]) and CO₂ production (VCO₂, [ml h⁻¹]) using the Weir equations¹. The respiratory exchange ratio (RER) was calculated as the ratio of volumes of CO₂ produced to volumes of O₂ consumed (VCO₂/ VO₂). Home-cage locomotor activity was assessed by beam breaks using an ActiMot infrared light beam system within the calorimetry system.

Assessment of Energy Expenditure Components

The delay in acquisition between the indirect calorimetry measurements and the instantaneous locomotor activity measurements was corrected for by a deconvolution procedure, which was performed using a two-compartment gas diffusion model^{2,3}, taking into account chamber washout characteristics at a cage size of 8 L and a flow rate of 0.45 L min⁻¹. Following deconvolution, total energy expenditure (TEE, kcal 24h⁻¹) was decomposed into its activity-related energy expenditure (AEE) and resting metabolic rate (RMR). RMR was modelled in a time-dependent manner using a method based on penalized spline regression, allowing for the detection of up to four RMR frequency components per 24 h (8 knots 24h⁻¹)². Cases were excluded if the correlation between the convoluted activity and TEE did not reach an arbitrary cutoff of $r \geq 0.7$. Model fit was assessed by visual inspection of the component analysis residuals.

Pair-Feeding Paradigm

Mice were initially singly-housed one week prior to the experimental onset. On day one of the pair-feeding paradigm, 51KO mice (n = 9) and WT mice (n = 11) received ad libitum access to HFD (D12331, Research Diets, New Brunswick, NJ, USA). A second group of WT mice (WT-PF) were pair-fed to the 51KO mice. Each

day for 6 weeks, mice in the WT-PF group received restricted access to the HFD, defined as the amount consumed by the 51KO mice 2 days earlier. Food was weighed and replaced daily at 08:00. If residual food remained in the cages of WT-PF mice, it was removed and weighed prior to the delivery of the next daily food portion.

Cold-Induced Thermoregulation

51KO and WT males were divided into a control diet (10.5%kcal fromfat,D12329, ResearchDiets, Inc., New Brunswick, NJ, USA) and a HFD group (n = 11/group). After 5 weeks on their respective diets, cold-induced thermoregulation was monitored. Initially rectal body temperature was measured for 4 days prior to the cold exposure paradigm to habituate mice to the rectal thermocouple probe. On the 5th day, rectal temperatures were monitored at 0, 2, 4, and 6 h following exposure to 4 °C using an Oakton Acorn Temp JKT Thermocouple Thermometer (Oakton Instruments, IL, USA).

Intraperitoneal Glucose Tolerance Test (GTT)

An intraperitoneal injection of D- glucose (2 g per kg body weight) was delivered to fasted mice (14 h fast). Blood glucose levels were measured on blood collected by tail cut at 0, 30, 60, and 120 min intervals following the glucose load. Glucose levels were measured using a handheld Contour XT glucometer (Bayer Health Care, Basel, Switzerland). Plasma was also collected from blood at 0 and 30 min to assess fasting insulin and glucose-stimulated insulin levels, respectively.

Intraperitoneal Insulin Tolerance Test (ITT)

Mice were fasted for ~12 h and subsequently received intraperitoneal injections of 0.5 IU per kg body weight of insulin. Blood glucose levels were assessed from tail cuts at 0, 30, 60, and 120 min following the insulin load. Glucose levels were measured using a handheld Contour XT glucometer (Bayer Health Care, Basel, Switzerland).

Behavioral Analyses

All behavioral tests were performed between 08:00 and 12:00 (Experiment 4). General locomotor activity was examined in an empty open field arena over 15 min under 15 lux illumination. Anxiety-related behaviors were

assessed using the elevated plus maze and dark-light transition tests as previously described⁴. Each test was videotaped by an overhead camera and analyzed using the automated video-tracking software ANYmaze4.9 (Stoelting, Wood Dale, IL, USA).

Hormone Quantification

Plasma insulin levels were determined using a mouse metabolic magnetic bead panel (Millipore Corp. Billerica, MA, USA; sensitivity: insulin 14 pg ml⁻¹). For the assessment of fasting insulin levels, blood was collected 14 h following an overnight fast by tail cut. Similarly, glucose-stimulated insulin levels were measured from plasma taken from blood collected 30 min following glucose load during the glucose tolerance test.

Preparation of vesicular phospholipid gels

Vesicular phospholipid gels (VPGs) with a phospholipid content of 50% (m/m) were prepared as slow releasing formulation for SAFit2. Encapsulation of SAFit2 into the gel was done by a direct incorporation method of the poorly water-soluble substance. Therefore, accurately weighted phospholipid was solved in ethanol (100%) and a stock solution of SAFit2 (20.0mg ml⁻¹ in 100% ethanol) was added. Then the solvent was evaporated for two days under constant vacuum in a drying oven (25 °C, 10 mbar). The solid mixture was hydrated with buffer and homogenized by dual asymmetric centrifugation using a SpeedmixerTM DAC 150.1 FVZ (Hauschild GmbH & Co KG, Hamm, Germany) for 45 minutes at 3500 rpm.^{1,2} The final SAFit2 concentration in the gel was 10mg g⁻¹.

SAFit2 Quantification

The concentration of plasma SAFit2 was quantified following acute administration of the SAFit2 gel and following intraperitoneal administration on treatment days 10 and 30 by Liquid chromatography/mass spectrometry (LC/MS/MS). Briefly, plasma was analyzed using the combined high-performance liquid chromatography/mass spectrometry (HPLC/MS-MS) technique. Analysis was performed using an Agilent 1100 Series (Agilent, Waldbronn, Germany) liquid chromatograph which was interfaced to the ESI source of an Applied Biosystems API 4000 (ABSciex, Darmstadt, Germany) triple quadrupole mass spectrometer. All samples were added to Ostro protein precipitation and phospholipid removal plates (Waters, Eschborn,

Germany). Deuterated clomipramine (Clomi-D3) was used as internal standard. Chromatography was performed using a gradient elution in an Accucore RP-MS 2,6 μ m column (2.1 x 50 mm, Thermo Scientific, Dreieich, Germany) at a flow rate of 0.3 ml min⁻¹ and 30°C.

Toxicity Assays

LDH assay To assess membrane disruption and cell death, the release of lactate dehydrogenase (LDH) into the growth medium of C2C12 cells was measured. The assay (LDH cytotoxicity detection system) was carried out according to the manufacturer's protocol (Clontech, Mountain View, CA, USA). As a positive control, 0.02% Triton X-100 was added to the medium 1-2 h prior to performing the assay; wells containing only medium were used as a negative control.

MTT assay C2C12 cells were incubated in the presence of 0.5 mg mL⁻¹ tetrazole 3-(4,5-dimethylthiazol-2-yl)-2,5-diphenyltetrazolium bromide (MTT) for 4 h at 37°C and 5% CO₂. The plates were read as described previously⁸.

Western Blot Analysis

To analyze insulin signaling, tissues from 5 h-fasted WT and 51KO mice (n = 4/group) were harvested 5 min after insulin administration (0.75 IU per kg). To analyze FKBP51 expression, various tissues (brown adipose, EDL, eWAT, iWAT, kidney, liver, pancreas, and soleus muscle) were harvested from adult C57BL6/N male mice (n = 6). Tissues were homogenized in lysis buffer containing 62.5 mM Tris-HCl, 2% SDS, and 10% sucrose supplemented with protease (Sigma, P2714) and phosphatase (Roche, 04906837001) inhibitor cocktails, and subsequently centrifuged at 12,000 x g to remove cell debris. Lysates were sonicated three times, and protein concentrations were measured using the BCA assay (BCA Protein Assay Kit, Life Technologies, Darmstadt, Germany). After dilution, protein samples (40 μ g) were heated for 5 min at 95°C in loading buffer. Equal amounts of proteins were separated by SDS-PAGE and electro-transferred onto nitrocellulose membranes. Non-specific binding was blocked in Tris-buffered saline, supplemented with 0.05% Tween (P2287; Sigma-Aldrich, St. Louis, MO, USA) and 5% non-fat milk for 1 h at room temperature. Blots were subsequently incubated with primary antibody (diluted in TBS/0.05% Tween) overnight at 4 °C. A list of primary antibodies used in this study is provided below. The following day, blots were washed and probed with the respective horseradish

peroxidase secondary antibody for 1 h at room temperature. Immuno-reactive bands were visualized either using ECL detection reagent (Millipore, Billerica, MA, USA, WBKL0500) or directly by excitation of the respective fluorophore. Band intensities were evaluated with the ChemiDoc Imaging System (Bio-Rad, Laboratories Inc., Hercules, CA, USA).

List of all primary antibodies:

Primary Antibody	Dilution	Phosphorylation site	Company
actin	1:5000	/	SCBT, sc-1616
AKT2	1:2000	/	CST, #3063
AS160	1:1000	/	CST, #2670
p70S6K	1:1000	/	CST, #9202
pAKT2	1:1000	S473	CST, # 4058
pAS160	1:1000	T642	CST, #8881
pp70S6K	1:1000	T389	CST, #9234
AIF	1:1000	/	Chemicon, #AB16501
HA	1:7000	/	Roche, 11667475001
FLAG	1:10000	/	Rockland, 600-401-383
GLUT4	1:1000	/	CST, #2213
FKBP51	1:1000	/	Bethyl, A301-430A
PHLPP1	1:1000	/	Millipore, #07-1341
GLUT1	1:1000	/	Thermofisher, PA1-1063
FKBP52	1:1000	/	Bethyl, A301-427A
UCP1	1:1000		Abcam ab10983

Quantification of Protein Data

The level of each phosphorylated protein was normalized to its respective non-phosphorylated protein. For total protein content, actin or AIF were used as internal controls.

Supplementary References

1. WEIR, J. B. New methods for calculating metabolic rate with special reference to protein metabolism. *J.Physiol* **109**, 1–9 (1949).
2. van Klinken, J. B., van den Berg, S. A. A., Havekes, L. M. & Willems Van Dijk, K. Estimation of activity related energy expenditure and resting metabolic rate in freely moving mice from indirect calorimetry data. *PLoS One* **7**, (2012).
3. Arch, J. R., Hislop, D., Wang, S. J. & Speakman, J. R. Some mathematical and technical issues in the measurement and interpretation of open-circuit indirect calorimetry in small animals. *Int.J.Obes.(Lond)* **30**, 1322–1331 (2006).
4. Schmidt, M. V *et al.* Postnatal glucocorticoid excess due to pituitary glucocorticoid receptor deficiency: differential short- and long-term consequences. *Endocrinology* **150**, 2709–2716 (2009).
5. Shefer, G. & Yablonka-Reuveni, Z. Isolation and culture of skeletal muscle myofibers as a means to analyze satellite cells. *Methods Mol. Biol.* **290**, 281–304 (2005).
6. Kim, D. *et al.* A small molecule inhibits Akt through direct binding to Akt and preventing Akt membrane translocation. *J. Biol. Chem.* **291**, 22856(2016).
7. Gassen, N. C. *et al.* Association of FKBP51 with Priming of Autophagy Pathways and Mediation of Antidepressant Treatment Response: Evidence in Cells, Mice, and Humans. *PLoS Med.* **11**, (2014).
8. Zschocke, J. *et al.* Antidepressant drugs diversely affect autophagy pathways in astrocytes and neurons -- dissociation from cholesterol homeostasis. *Neuropsychopharmacology* **36**, 1754–68 (2011).

3.2. Mediobasal hypothalamic FKBP51 acts as a molecular switch linking autophagy to whole-body metabolism

Authors:

Alexander S. Häusl¹, Thomas Bajaj², Lea M. Brix^{1,3}, Max L. Pöhlmann¹, Kathrin Hafner⁴, Meri De Angelis⁵, Joachim Nagler⁵, Frederik Dethloff⁶, Georgia Balsevich¹, Karl-Werner Schramm⁵, Patrick Giavalisco⁶, Alon Chen^{7,8}, Mathias V. Schmidt¹ and Nils C. Gassen^{2,4}

Affiliations:

¹ *Research Group Neurobiology of Stress Resilience, Max Planck Institute of Psychiatry, 80804 Munich, Germany*

² *Neurohomeostasis Research Group, Department of Psychiatry and Psychotherapy, Bonn Clinical Center, University of Bonn, 53127 Bonn, Germany*

³ *International Max Planck Research School for Translational Psychiatry (IMPRS-TP), Kraepelinstr. 2-10, 80804 Munich, Germany*

⁴ *Department of Translational Research in Psychiatry, Max Planck Institute of Psychiatry, 80804 Munich, Germany*

⁵ *Helmholtz Center Munich Germany Research Center for Environmental Health, Molecular EXposomics, Neuherberg Germany*

⁶ *Max Planck Institute for Aging, 50931 Cologne, Germany,*

⁷ *Department of Stress Neurobiology and Neurogenetics, Max Planck Institute of Psychiatry, 80804 Munich, Germany*

⁸ *Department of Neurobiology, Weizmann Institute of Science, Rehovot, Israel*

Originally published in:

Science Advances, Vol 8 Issue 10, 09 March 2022

CELL BIOLOGY

Mediobasal hypothalamic FKBP51 acts as a molecular switch linking autophagy to whole-body metabolism

Alexander S. Häusl^{1†}, Thomas Bajaj^{2†}, Lea M. Brix^{1,3}, Max L. Pöhlmann¹, Kathrin Hafner⁴, Meri De Angelis⁵, Joachim Nagler⁵, Frederik Dethloff⁶, Georgia Balsevich¹, Karl-Werner Schramm⁵, Patrick Gialvalisco⁶, Alon Chen^{7,8}, Mathias V. Schmidt^{1*‡}, Nils C. Gassen^{2,4*‡}

The mediobasal hypothalamus (MBH) is the central region in the physiological response to metabolic stress. The FK506-binding protein 51 (FKBP51) is a major modulator of the stress response and has recently emerged as a scaffold regulating metabolic and autophagy pathways. However, the detailed protein-protein interactions linking FKBP51 to autophagy upon metabolic challenges remain elusive. We performed mass spectrometry-based metabolomics of FKBP51 knockout (KO) cells revealing an increased amino acid and polyamine metabolism. We identified FKBP51 as a central nexus for the recruitment of the LKB1/AMPK complex to WIPI4 and TSC2 to WIPI3, thereby regulating the balance between autophagy and mTOR signaling in response to metabolic challenges. Furthermore, we demonstrated that MBH FKBP51 deletion strongly induces obesity, while its overexpression protects against high-fat diet (HFD)-induced obesity. Our study provides an important novel regulatory function of MBH FKBP51 within the stress-adapted autophagy response to metabolic challenges.

INTRODUCTION

An adequate response to nutritional changes requires a well-coordinated interplay between the central nervous system and multiple peripheral organs and tissues to maintain energy homeostasis. High-caloric food intake and chronic overnutrition strongly challenge this system on a cellular and organismic level and are main drivers in the development of obesity, a hallmark of the metabolic syndrome (1).

Autophagy is an evolutionarily conserved process that efficiently degrades cellular components, like unfolded proteins or organelles, to provide internal nutrients and building blocks for cellular fitness (2). Dysfunctional autophagy is associated with many diseases, such as neurodegeneration, liver disease, cancer, and metabolic syndrome (3–5). In obesity, however, the alterations of autophagy are not fully explored yet. Autophagic signaling in obese individuals is suppressed in pancreatic B cells, liver, and muscle, whereas other studies demonstrated enhanced autophagy signaling in adipose tissue (3, 6, 7). Autophagy initiation is tightly controlled by a series of proteins encoded by autophagy-related genes (ATGs) and regulatory heteroprotein complexes, including the systemic energy sensor adenosine 5'-monophosphate (AMP)-activated protein kinase (AMPK) that is in balance with the mechanistic target of rapamycin (mTOR) (8). Amino acid surplus activates mTOR signaling, which further suppresses autophagy by inhibiting the UNC51-like kinase 1 (ULK1) complex [composed of ULK1, ATG13, FIP200 (FAK family

kinase-interacting protein of 200 kDa), and ATG101]. In the course of nutrient deprivation, elevated AMP activates AMPK to initiate autophagy via the ULK1 complex and in turn diminishes mTOR signaling (9, 10). It has recently been shown that the tryptophan-aspartic acid (WD)-repeat proteins that interact with the phosphoinositide protein family (WIPI proteins) act as subordinate scaffolders of the liver kinase B1 (LKB1)/AMPK/TSC2 (tuberous sclerosis complex 2)/FIP200 network linking AMPK and mTOR signaling to the control of autophagy upon metabolic stress (11).

In the mediobasal hypothalamus (MBH), the brain's central region for metabolic control, the deletion of ATG7 (a ubiquitin E1-like ligase, downstream of the ULK1 complex) in proopiomelanocortin (POMC)-expressing neurons resulted in obesity and dampened sympathetic outflow to white adipose tissue (WAT) (12), while ATG7 deficiency exclusively in agouti-related protein (AgRP)-expressing neurons resulted in decreased body weight (13). Together, these data indicate a role of MBH autophagy in the development of obesity, but key regulatory proteins remain largely elusive.

The FK506-binding protein 51 (FKBP51, encoded by *Fkbp5*) is the main modulator of the stress response and is best characterized as a co-chaperone to HSP90, thereby orchestrating diverse pathways important to maintain homeostatic control (14–17). We and others have provided evidence that FKBP51 is associated with type 2 diabetes and have shed light on its role as a fundamental regulator of obesity and glucose metabolism (18–22). Following the identification of FKBP51 as a negative regulator of the serine/threonine kinase AKT in cancer cells (23), we showed that FKBP51 acts as a modulator of glucose uptake by mediating the AKT2/PHLPP (PH domain leucine-rich repeat-containing protein phosphatase)/AS160 (AKT substrate of 160 kDa) complex specifically in muscle (18). Furthermore, we demonstrated that FKBP51 induces autophagy through autophagy-promoting beclin-1 (BECN1) in two ways: (i) FKBP51 limits AKT-directed inhibitory phosphorylation of BECN1 at S234 and S295 (24, 25), and (ii) it reduces AKT-mediated phosphorylation of S-phase kinase-associated protein 2 (SKP2) at S72 and thereby lowering its E3-ligase activity, preventing BECN1 from proteasomal degradation (26). Autophagy and FKBP51 are involved in the regulatory role of

¹Research Group Neurobiology of Stress Resilience, Max Planck Institute of Psychiatry, 80804 Munich, Germany. ²Neurohomeostasis Research Group, Department of Psychiatry and Psychotherapy, Bonn Clinical Center, University of Bonn, 53127 Bonn, Germany. ³International Max Planck Research School for Translational Psychiatry (IMPRS-TP), Kraepelinstr. 2-10, 80804 Munich, Germany. ⁴Department of Translational Research in Psychiatry, Max Planck Institute of Psychiatry, 80804 Munich, Germany. ⁵Helmholtz Center Munich Germany Research Center for Environmental Health, Molecular Exposomics, Neuherberg, Germany. ⁶Max Planck Institute for Biology of Ageing, 50931 Cologne, Germany. ⁷Department of Stress Neurobiology and Neurogenetics, Max Planck Institute of Psychiatry, 80804 Munich, Germany. ⁸Department of Neurobiology, Weizmann Institute of Science, Rehovot, Israel.

*Corresponding author. Email: mschmidt@psych.mpg.de (M.V.S.); nils.gassen@ukbonn.de (N.C.G.)

†These authors contributed equally to this work as first authors.

‡These authors contributed equally to this work as senior authors.

adipocyte differentiation and mass development (19, 27–29) and are up-regulated in the MBH following starvation (13, 30, 31). The data indicate converging mechanisms of FKBP51-directed protein scaffolding and autophagy, and therefore, we hypothesized a subordinate role of FKBP51 in concert with members of the autophagy signaling network in shaping central and peripheral autophagy signaling. In the current study, we set out to identify the molecular interplay of FKBP51 with cellular autophagic signaling and tested whether FKBP51 shapes the *in vivo* whole-body response to an obesogenic challenge. Our study unravels the tissue specificity of autophagy signaling in response to obesity and reveals FKBP51 as a previously unknown regulatory link between the stress-induced LKB1/AMPK-mediated autophagy induction and WIPI protein scaffolds.

RESULTS

FKBP51 deletion increases AMPK and mTOR-associated amino acid and polyamine biosynthesis

As a first approach to broaden our insights into the contribution of FKBP51 under basal (1× glucose) and metabolically challenging (2× glucose) conditions, we performed a multilevel mass spectrometry (MS)-based metabolomics profiling analysis of human neuroblastoma SH-SY5Y cells lacking FKBP51 [(FKBP51 knockout (KO)) and wild-type (WT) controls. FKBP51 KO cells showed an increase in multiple metabolites compared to WT cells to different extents under basal and high glucose conditions (fig. S1, A to D). Most frequent and pronounced alterations could be attributed to biosynthetic and metabolic pathways of various amino acids, including but not limited to arginine, valine, leucine, and isoleucine biosynthesis and histidine, cysteine, and methionine metabolism (Fig. 1A and fig. S1E). It is well known that amino acids signal to mTOR and that mTOR itself actively participates in the sensing of amino acids in the lysosomal lumen. Particularly, the branched-chain amino acids (BCAAs) leucine, valine, and isoleucine, all elevated in FKBP51 KO cells (Fig. 1B, top right), can activate mTOR and thereby block the autophagy pathway (32–34). On the other hand, the pathway analysis showed increased AMP/adenosine 5'-triphosphate (ATP) ratio and strongly increased levels of polyamines and their metabolites in FKBP51 KO cells (Fig. 1B, left and bottom right). AMP/ATP ratio was strongly reduced in FKBP51 KO cells under metabolically challenging conditions (fig. S2E).

The overall increase in amino acids most likely results from ubiquitous protein degradation, in line with enhanced cellular catabolic processes. We performed isotope tracing with ¹³C-labeled glucose to determine the intracellular flux in FKBP51 KO cells. Here, we observed no substantial differences between both cell types (fig. S1F), corroborating the fact that cellular catabolic processes rather dominate over anabolic processes. To exclude that the observed effects are specific to a human cell line, we performed the metabolomics profiling also in mouse Neuro2a (N2a) cells (fig. S2, A to E). While the effects of amino acid biosynthesis are more pronounced in the human cell line following FKBP51 deletion, the data nonetheless point in the same direction and support our hypothesis that FKBP51 affects autophagy and mTOR signaling. We were therefore further encouraged to disentangle the underlining metabolic pathways.

FKBP51 is essential for homeostatic autophagy following nutrient deprivation

Because autophagy and FKBP51 expression levels are highly induced after starvation (4, 31), we tested whether deletion of FKBP51,

in turn, affects the induction of autophagy after nutrient deprivation. To do so, we exposed FKBP51 KO or WT cells to Hank's balanced salt solution (HBSS) for 4 hours to induce cellular starvation. FKBP51 KO cells showed less phosphorylated AMPK (pAMPK) at T172 and lower levels of LKB1 compared to WT cells already under nutrient-rich conditions (Fig. 2A and fig. S3A), while there was a significant increase in activating phosphorylation of SKP2 at S72 and AKT at S473 (fig. S3, B and C). These changes in upstream signaling resulted in the slight but not significant accumulation of the autophagy receptor and substrate p62 (Fig. 2B), which is an important measure to determine autophagic activity (35). On the other hand, we could observe increased levels of pp70S6K at T389 in FKBP51 KO cells (Fig. 2C). These data imply a reduction of autophagy signaling and increased mTOR signaling after FKBP51 deletion under basal conditions (36). The deletion of FKBP51 blocked the starvation-induced increase in LKB1 protein and the activation of AMPK at T172 (Fig. 2A and fig. S3A) and thereby reduced the level of autophagy signaling. These data underline the importance of FKBP51 in the autophagic stress response after starvation and suggest a tight regulation of FKBP51 on AMPK and LKB1.

Next, we investigated whether FKBP51 up-regulation can enhance autophagy by moderately overexpressing (OE) Flag-tagged FKBP51 in N2a cells (fig. S3D). In line with our hypothesis, FKBP51 OE resulted in highly increased phosphorylation of AMPK at T172 and enhanced levels of LKB1 (Fig. 2E and fig. S3E), which indicate an increase of upstream autophagy initiation, further evidenced by increased phosphorylation of ULK1 at S555 (fig. S3E). Consequently, there was an increase in proautophagic phosphorylation of BECN1 at S14 and S91/S94 (in humans at S93/S96) through kinases ULK1 and AMPK, respectively (fig. S3E) (37). Previous literature has shown that increased LKB1/AMPK signaling also activates the TSC1/TSC2 complex, which, in turn, inhibits mTOR activity (38). In line with that, phosphorylation of TSC2 at S1387 was significantly enhanced (fig. S3E), and the phosphorylation of AKT at S473, SKP2 at S72, and the mTOR substrate pp70S6K at T389 was significantly decreased (Fig. 2F and fig. S2F). In addition, we validated autophagy signaling by the increase in phosphorylation of ATG16L1 at S278, a recently described marker for autophagy induction (39), and the decrease in the autophagy substrate p62 (Fig. 2G and fig. S2G). Last, we assessed autophagic flux by the quantification of LC3B-II (lipidated microtubule-associated proteins 1A/1B light chain 3B) accumulation in response to starvation (HBSS) and the autophagy inhibitor bafilomycin A1 (BafA1) in FKBP51 OE, KO, and FKBP51 KO + OE N2a cells (Fig. 2, I and J, and fig. S3, H and I). BafA1 led to a significant increase in LC3B-II levels in FKBP51 WT and FKBP51 OE N2a cells, but not in FKBP51 KO and FKBP51 KO + OE N2a cells, as compared to FKBP51 WT N2a cells during baseline conditions. Under starvation conditions (HBSS treatment), BafA1 caused a significant accumulation of LC3B-II in all genotypes; however, this increase was attenuated in FKBP51 KO N2a cells.

The data from our metabolomic analysis indicated that alteration in FKBP51 levels might enhance hypusination of the translation factor eIF5A and thereby positively regulate autophagy via nuclear translocation of transcription factor EB (TFEB) (40). To test this hypothesis, we measured the translocation of TFEB into the nucleus using a TFEB-green fluorescent protein (GFP) reporter assay in N2a cells. Here, we observed reduced baseline levels of nuclear TFEB in FKBP51 KO N2a cells and diminished nuclear translocation of TFEB after starvation (HBSS) of FKBP51 KO cells compared

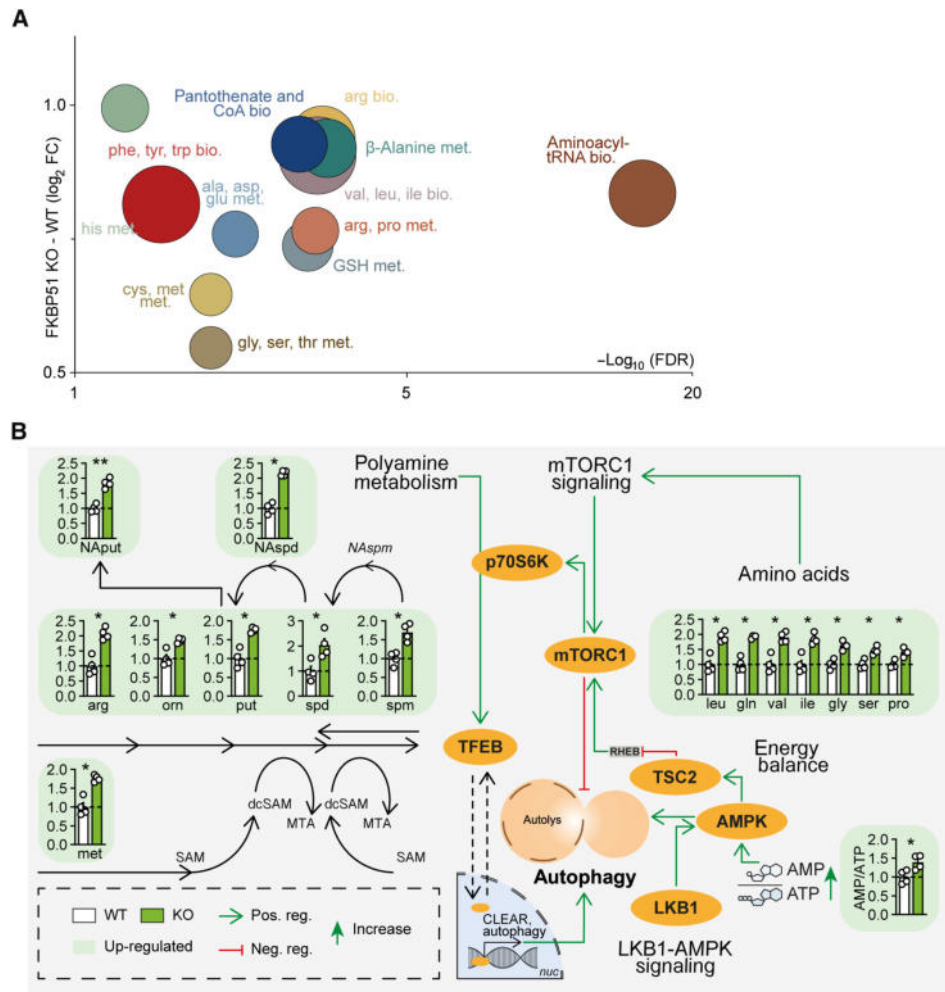


Fig. 1. FKBP51 associates with amino acids and polyamine biosynthesis pathways. (A) Analysis and regulation of significantly altered pathways of FKBP51 KO and WT cells. The $f(x)$ axis shows the (median) \log_2 fold change (FC) of all significantly altered metabolites of the indicated pathway, and the false discovery rate (FDR) (equals the $-\log_{10}$ -adjusted P value) is shown on the x axis. The size of the circles represents the amount of significantly changed metabolites in comparison to all metabolites of a particular pathway. tRNA, transfer RNA. (B) FKBP51 deletion increases metabolites of the polyamine pathway, the AMP/ATP ratio, and enhances levels of amino acids associated with mTOR signaling. Data in (B) are shown as means \pm SEM and were analyzed by a two-way analysis of variance (ANOVA) and a subsequent Bonferroni multiple comparison analysis. ala, alanine; AMPK, AMP-activated protein kinase; arg, arginine; asp, asparagine; bio., biosynthesis; CoA, coenzyme A; cys, cysteine; dcSAM, decarboxylated *S*-adenosylmethionine; gln, glutamine; glu, glutamic acid; gly, glycine; GSH, glutathione (reduced); his, histidine; ile, isoleucine; leu, leucine; LKB1, liver kinase B1; met, methionine; met., metabolism; MTA, 5'-methylthioadenosine; mTORC1, mechanistic target of rapamycin complex 1; NAPut, *N*-acetylputrescine; NASpd, *N*-acetylspermidine; NASpm, *N*-acetylspermine; orn, ornithine; pro, proline; phe, phenylalanine; put, putrescine; SAM, *S*-adenosylmethionine; ser, serine; spd, spermidine; spm, spermine; TFEB, transcription factor EB; TSC2, tuberous sclerosis complex 2; thr, threonine; trp, tryptophan; tyr, tyrosine; val, valine. * $P < 0.05$, ** $P < 0.01$.

to the control (Fig. 2, K and L). OE of FKBP51 in WT cells could further increase nuclear TFEB under basal conditions. The nuclear TFEB signal could not be further increased by OE under starvation compared to the WT control (Fig. 2, K and L). We could not detect any differences in the hypusination of eIF5A (fig. S4, A and B).

Together, these findings demonstrate that FKBP51 regulates autophagy induction, especially after a metabolic challenge. However, it is still unclear whether FKBP51 shapes the autophagic response via direct protein-protein interactions to AMPK and LKB1. Given the fact that FKBP51 was previously shown to interact with several signaling molecules within the autophagy pathway (Fig. 3A), we were encouraged to unravel the underlying molecular mechanism and identify potential novel interactions of FKBP51 with members of the autophagy signaling network.

FKBP51 associates with LKB1/AMPK/WIPI4 and TSC2/WIPI3 heteroprotein complexes to regulate autophagy and mTOR signaling

A recent study by Bakula and colleagues (11) investigated the role of the four WIPI proteins on autophagy, and the WIPI protein interactome revealed an association of WIPI4 with FKBP51, AMPK α 1, and AMPK γ 2 (11). WIPI proteins are essential scaffolding proteins that function as central molecular hubs to link key regulatory elements of autophagy with proteins that are sensitive to main metabolic cascades such as amino acid and glucose metabolism (41). On the basis of our FKBP51 starvation and OE experiments, we hypothesized that FKBP51 might scaffold WIPI4 and AMPK to induce autophagy initiation and therefore performed co-immunoprecipitation (co-IP) studies using N2a cells, with FKBP51-Flag OE.

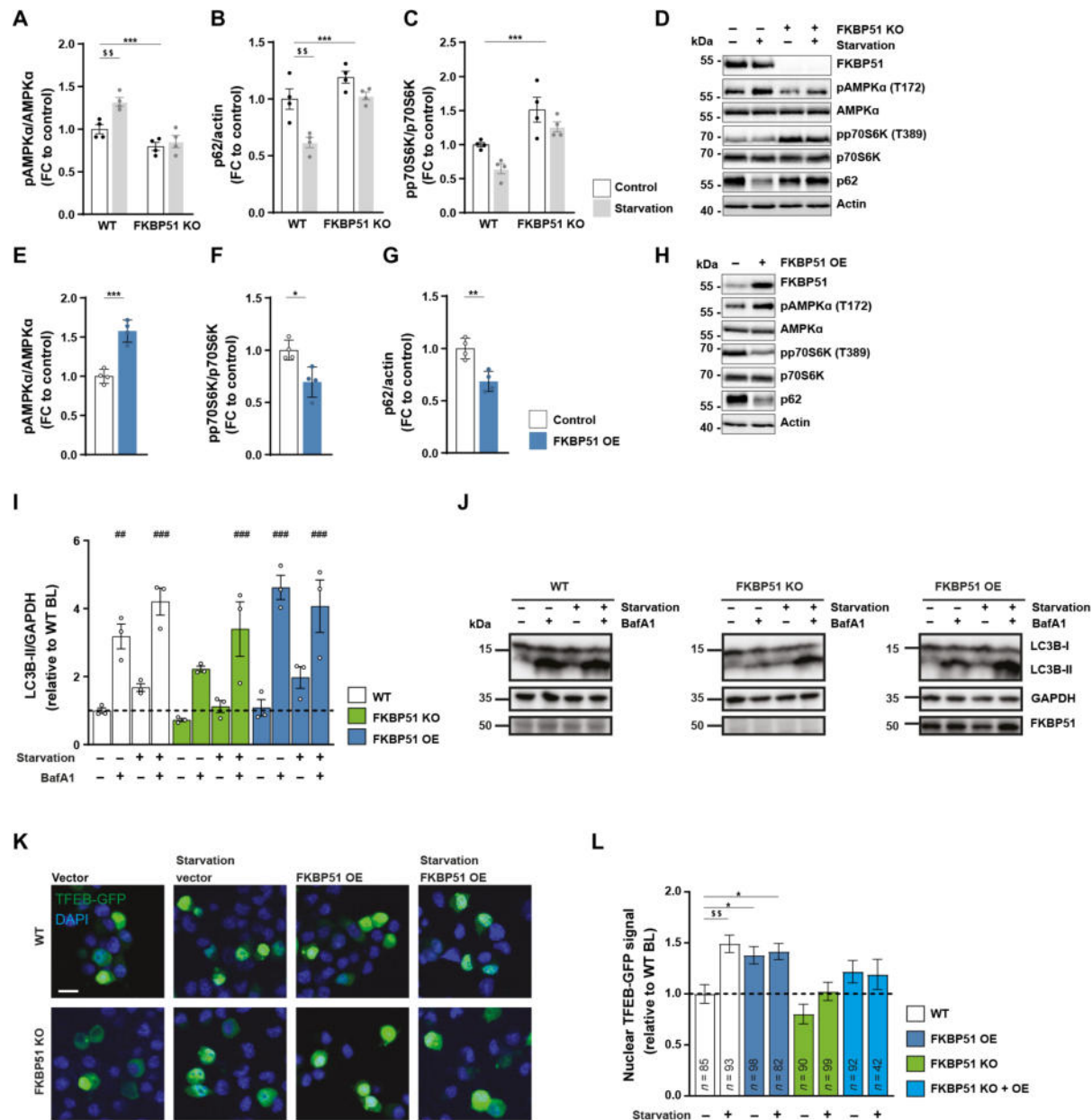


Fig. 2. FKBP51 regulates AMPK and mTOR activity following nutrient deprivation. (A) WT or FKBP51 KO cells were starved in HBSS medium for 4 hours to induce autophagy, followed by quantification of pAMPK α (T172), (B) p62, and (C) pp70S6K (T389). Representative blots are shown in (D). FKBP51 overexpression (FKBP51 OE) in N2a cells (see fig. S3D for validation) enhanced autophagy signaling. Quantification of (E) pAMPK α (T172), (F) pp70S6K (T389), (G) p62, and (H) representative blots. (I) Quantification of autophagic flux in FKBP51 KO and FKBP51 OE cells in response to starvation. GAPDH, glyceraldehyde-3-phosphate dehydrogenase. (J) Representative blots of autophagic flux measurements. (K) Representative pictures of TFEB nuclear localization/translocation. DAPI, 4',6-diamidino-2-phenylindole. Scale bar, 10 μ m. (L) Quantification of TFEB reporter assay. BL, baseline. All data (A to J) are shown as relative fold change compared to control condition; \pm SEM; * P < 0.05, ** P < 0.01, *** P < 0.001; ## P < 0.01, ### P < 0.001; \$\$\$ P < 0.01. Two-way ANOVA was performed in (A) to (C) and followed by a Tukey's multiple comparisons test. One-way ANOVA was performed for (I) and (L), followed by a Dunnett's multiple comparison test. The unpaired Student's t test was performed for (E) to (G). *, significant genotype effect; \$, significant starvation effect; #, significant treatment effect.

These experiments confirmed that FKBP51 associates with WIPI4 but not with WIPI1 and WIPI2 (Fig. 3B), as suggested by Bakula and colleagues (11). Intriguingly, our experiments revealed a previously unidentified association of FKBP51 with WIPI3 (Fig. 3B). Next, we assessed the association of FKBP51 with various isoforms of AMPK

and validated the expected interactions of FKBP51 with AMPK α 1 and AMPK γ 2 and further revealed a interaction with AMPK β 1 (Fig. 3C). We validated the previously unknown interactions of FKBP51 with WIPI3, WIPI4, AMPK α , and LKB1 in mouse WT N2a neuroblastoma cells performing IPs and co-IPs from endogenous proteins (fig. S5A).

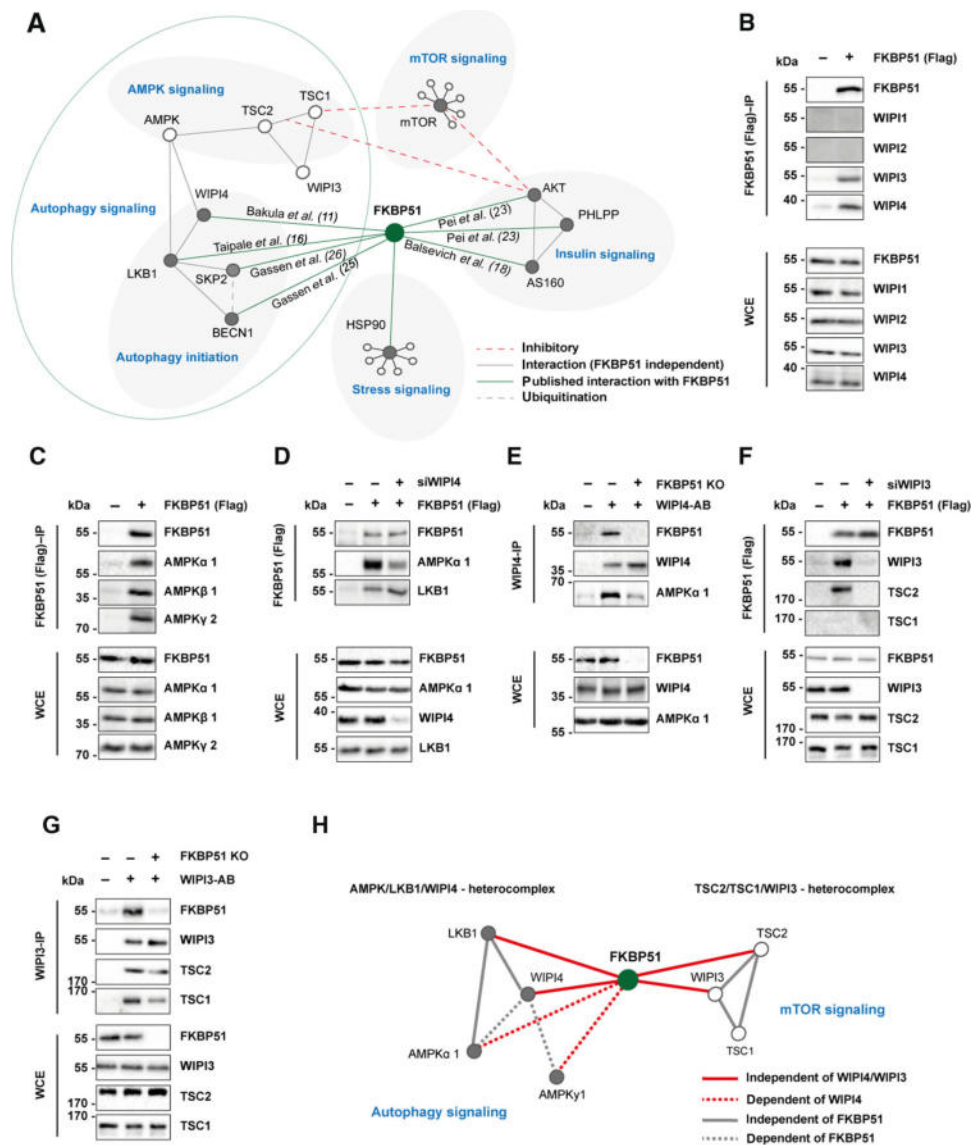


Fig. 3. FKBP51 associates with AMPK, TSC2, and WIPI3 and WIPI4 to regulate autophagy and mTOR signaling. (A) Published protein-protein interactions of FKBP51. (B) FKBP51 associates with WIPI3 and WIPI4, but not with WIPI1 and WIPI2. WCE, whole-cell extract; IP, immunoprecipitation. (C) Interaction of FKBP51 with AMPK subunits. (D) Interaction of FKBP51 with LKB1 and AMPK α in WIPI4 KD cells. (E) Interaction of WIPI4 with AMPK α in FKBP51-lacking cells. (F) FKBP51 interacts with TSC2 in dependency of WIPI3. (G) WIPI3 interacts with TSC2 and TSC1 in the presence or absence of FKBP51. (H) Identified associations of FKBP51 in the regulation of autophagy and mTOR signaling and the proposed model of interaction. FKBP51 recruits LKB1 to the AMPK-WIPI4 complex and thereby facilitates AMPK activation. Furthermore, FKBP51 scaffolds TSC2-WIPI3 binding to alter mTOR signaling. AB, antibody.

To investigate the functional relevance of WIPI4 in the association of FKBP51 with AMPK, we generated WIPI4 knockdown (KD) N2a cells using small interfering RNA (siRNA) cotransfected with FKBP51-Flag (fig. S5B). We observed that FKBP51 binding to AMPK was reduced in cells lacking WIPI4 (Fig. 3D and fig. S5C). Our precipitation studies further demonstrated that FKBP51 interacts with LKB1, which confirmed the finding of a previous interactomics-based screening experiment by Taipale and colleagues (16) and further revealed that this interaction is independent of WIPI4 (Fig. 3D and fig. S5, D and A). Furthermore, we could demonstrate that WIPI4 deletion blocked the phosphorylation effect of FKBP51 OE on pAMPK at T172 (fig. S5E), suggesting that FKBP51 binds to AMPK in dependency of WIPI4. In addition, studies in FKBP51 KO cells revealed that the WIPI4

interaction to AMPK depends on the presence of FKBP51 (Fig. 3E), indicating a subordinate role of FKBP51 as a molecular bridge that links the autophagy-relevant WIPI network to AMPK signaling.

Last, we assessed the functional relevance of WIPI3-FKBP51 binding. Performing co-IP studies in N2a cells in the presence or absence of WIPI3 (fig. S5F), we observed that FKBP51 interacts with TSC2 but not TSC1 (Fig. 3F), which are upstream master regulators of mTOR (42). Further, we confirmed the association of FKBP51 with TSC2, which depends on the presence of WIPI3 (Fig. 3F), whereas the interaction of WIPI3 to TSC2 and TSC1 is independent of FKBP51 (Fig. 3G).

Collectively, we demonstrate that FKBP51 regulates autophagy in concert with the WIPI protein family, specifically WIPI3 and

WIPI4 via interactions with the mTOR and AMPK cascades (Fig. 3H). The combined interpretation of our molecular and metabolomic analyses led us to hypothesize that FKBP51 regulates autophagy and consequently whole-body metabolism *in vivo*, especially after a metabolic challenge.

MBH FKBP51 is a regulator of body weight and food intake

We and others have previously shown that FKBP51 acts in a tissue-specific manner in soleus muscle (SM), epididymal WAT (eWAT), and the hypothalamus to regulate metabolism (18, 19, 22, 30). However, the interconnected response of autophagy and FKBP51 to a metabolic stressor, such as HFD, remains elusive and encouraged us to investigate the possible relationship between FKBP51 expression and autophagic flux (the protein turnover through catabolic autophagy).

Our analysis revealed that C57BL/6N mice showed significantly increased FKBP51 protein levels (Fig. 4A) and diminished accumulation of the autophagy substrate p62 in the MBH upon 10 weeks of HFD (58% kcal from fat) (Fig. 4B). HFD *per se* did not affect the lipidation of the autophagosome-spiking protein light chain 3 (LC3B-I) to LC3B-II (Fig. 4C), which binds the autophagosome and is a reliable marker to analyze autophagic flux (35). However, levels of LC3B-II were similarly increased in both conditions after treatment with chloroquine (50 mg/kg), an inhibitor of lysosomal acidification and autophagosome-lysosome fusion that, in turn, blocks degradation of autophagosome cargo (35). In line with the reduced levels of p62, these results indicate an active central autophagic flux after HFD.

In peripheral eWAT and SM, however, chloroquine treatment did increase LC3B-II levels only in chow-fed animals (fig. S6, A and B), implying reduced or even blocked autophagy signaling under HFD conditions. This hypothesis is supported by an increased accumulation of p62 in these peripheral tissues with a significant increase in SM (fig. S6C). FKBP51 protein levels were unaffected in eWAT and slightly but not significantly decreased in SM (fig. S6D). These data suggested a possible interconnected role of FKBP51 and autophagy flux, particularly in the MBH. We, therefore, decided to further test the effects of FKBP51 on autophagy signaling and its relevance for whole-body metabolism *in vivo* by manipulating FKBP51 in the MBH.

First, we injected a *Cre*-expressing virus into the MBH of FKBP51^{lox/lox} animals (Fig. 4D) to evaluate the effects of central FKBP51 deletion. FKBP51^{MBH-KO} animals showed a massive increase in body weight 6 weeks after surgery, despite their regular chow diet (Fig. 4E). The bodyweight increase was accompanied by increased food intake and decreased glucose tolerance (Fig. 4, F and G). These findings were unexpected, considering the lean phenotype of full-body FKBP51-deficient mice after prolonged exposure to an HFD (18, 19) and further highlight the tissue specificity of FKBP51.

Next, we injected an adeno-associated virus (AAV)-mediated FKBP51 OE virus into the MBH of C57/Bl6 mice (FKBP51^{MBH-OE}, Fig. 4H). FKBP51^{MBH-OE} animals showed no substantial differences in body weight gain within the first 4 weeks after surgery. Therefore, we challenged FKBP51^{MBH-OE} animals with a metabolic stressor by feeding them an HFD for 8 weeks. Animals overexpressing FKBP51 displayed significantly reduced body weight gain compared to the control group (Fig. 4I), paralleled by a reduction in food intake (Fig. 4J). In a second cohort of FKBP51^{MBH-OE} animals [with an identical body weight phenotype (fig. S6E)], we investigated whether glucose

metabolism was altered and observed improved glucose tolerance and insulin sensitivity compared to the control group under HFD but not under normal chow diet (Fig. 4K and fig. S6, F to H). Together, these experiments reveal an essential role of MBH FKBP51 in central coping mechanisms with an obesogenic stressor and position MBH FKBP51 as a key regulator of whole-body metabolism.

MBH FKBP51 fine-tunes autophagy signaling in an inverted U-shaped manner

Given the opposing phenotypes of FKBP51^{MBH-KO} and FKBP51^{MBH-OE} animals and the discovered regulatory function of FKBP51 in the metabolic control of autophagy, we were interested in the underlying regulation of autophagy signaling. In our KO experiment, viral injection resulted in a high-deletion rate within the MBH of FKBP51^{MBH-KO} animals (Fig. 5, A and B). According to our hypothesis, we observed a reduced binding of LKB1 and AMPK to WIPI4 (Fig. 5C and see fig. S7A for quantification), which was accompanied by a reduction in the phosphorylation of AMPK at T172, causing less active AMPK (Fig. 5D). Downstream of AMPK, we monitored diminished phosphorylation of ULK1 at S555, BECN1 at S91/S94, and TSC2 at S1387 (fig. S7, B to D). Parallel to the effects of AMPK downstream proteins, we detected reduced levels of TSC2 binding to WIPI3 (Fig. 5E and see fig. S7E for quantification). Furthermore, we observed increased levels of phosphorylated AKT at S473 and phosphorylated ULK1 at S757 (fig. S7, F and G), indicating increased AKT/mTOR signaling. The increased mTOR activity could be validated by increased levels of pp70S6K (Fig. 5F). Last, loss of FKBP51 resulted in decreased levels of LC3B-II and the accumulation of p62 (Fig. 5, G and H). Together, these data suggest that FKBP51 deletion reduced autophagy signaling in the MBH via the reduction of AMPK activity and an increased mTOR signaling, which is in line with our *in vitro* data.

Animals overexpressing FKBP51 in the MBH showed an excessive up-regulation of FKBP51 (Fig. 5, I and J). Co-IP studies indicated that following the excessive overexpression (OE) of FKBP51, AMPK binding to WIPI4 was decreased. Furthermore, LKB1 levels were strongly reduced and binding of LKB1 to WIPI4 vanished (Fig. 5K and fig. S7A). Consequently, phosphorylation of AMPK at T172 was significantly reduced (Fig. 5L). Downstream of AMPK, we observed a decrease in phosphorylation of ULK1 at S555 and no changes of phosphorylated BECN1 levels (fig. S7, B and C). Phosphorylation of TSC2 at S1387 and the binding of TSC2 to WIPI3 were significantly decreased (Fig. 5M and fig. S7, D and E). Phosphorylation of AKT at S473 was unchanged (fig. S7F). On the other hand, FKBP51^{MBH-OE} animals showed increased mTOR signaling, indicated by increased phosphorylation of ULK1 at S757 and elevated levels of pp70S6K (Fig. 5N and fig. S7G). Last, FKBP51 OE animals showed increased levels of LC3B-II. However, treatment with chloroquine (50 mg/kg) did not further increase the LC3B-II levels in FKBP51^{MBH-OE} animals (Fig. 5O), indicating that the fusion of autophagosomes with lysosomes is impaired and central autophagic flux is blocked. This hypothesis is supported by the fact that FKBP51 OE resulted in the accumulation of the autophagy substrate p62 (Fig. 5P). These data are in contrast to our previously observed findings and imply that FKBP51^{MBH-OE} animals, despite their highly elevated FKBP51 levels, have blocked autophagy signaling in the MBH.

The observation that viral overexpression of FKBP51 in the MBH resulted in a massive overexpressing of FKBP51 led us to hypothesize that the level of FKBP51 expression directly correlates with the degree

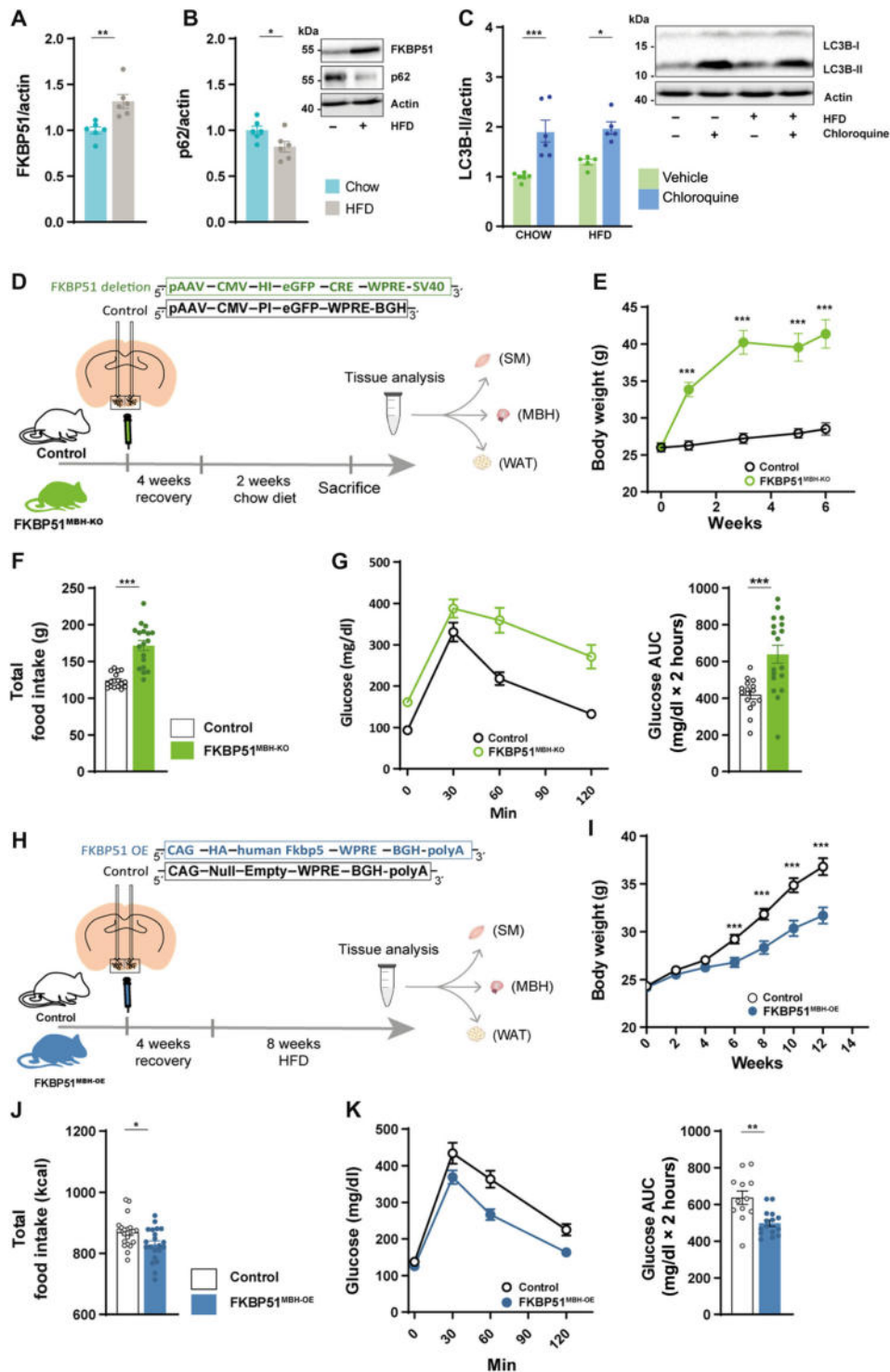


Fig. 4. MBH FKBP51 regulates body weight gain, food intake and glucose metabolism. (A) Ten weeks of HFD increased hypothalamic FKBP51 in the MBH [*n* (chow) = 6 versus *n* (HFD) = 6]. (B) Effects of HFD on the accumulation of p62. (C) Treatment with chloroquine (50 mg/kg) increased LC3B-II level under chow and HFD conditions. (D) FKBP51^{lox/lox} animals were injected with 200 nl of Cre-expressing virus and fed a chow diet for 6 weeks. (E) FKBP51^{MBH-KO} showed significant body weight increase after virus injection on a regular chow diet. (F) FKBP51^{MBH-KO} animals showed increased food intake and (G) enhanced glucose intolerance. AUC, area under the curve. (H) For FKBP51 overexpression, animals were injected with an AAV virus into the MBH. (I) FKBP51^{MBH-OE} animals showed reduced body weight gain on an HFD diet compared to their control animals (J) FKBP51^{MBH-OE} animals showed reduced food intake. (K) FKBP51^{MBH-OE} animals showed improve glucose tolerance under HFD conditions. For (A), (B), (F), (G), (J), and (K), an unpaired Student's *t* test was performed. For (C), a two-way ANOVA was performed, followed by a Tukey's multiple comparison test. For (E) and (I), a repeated measurements ANOVA was performed. ± SEM; **P* < 0.05, ***P* < 0.01, and ****P* < 0.001.

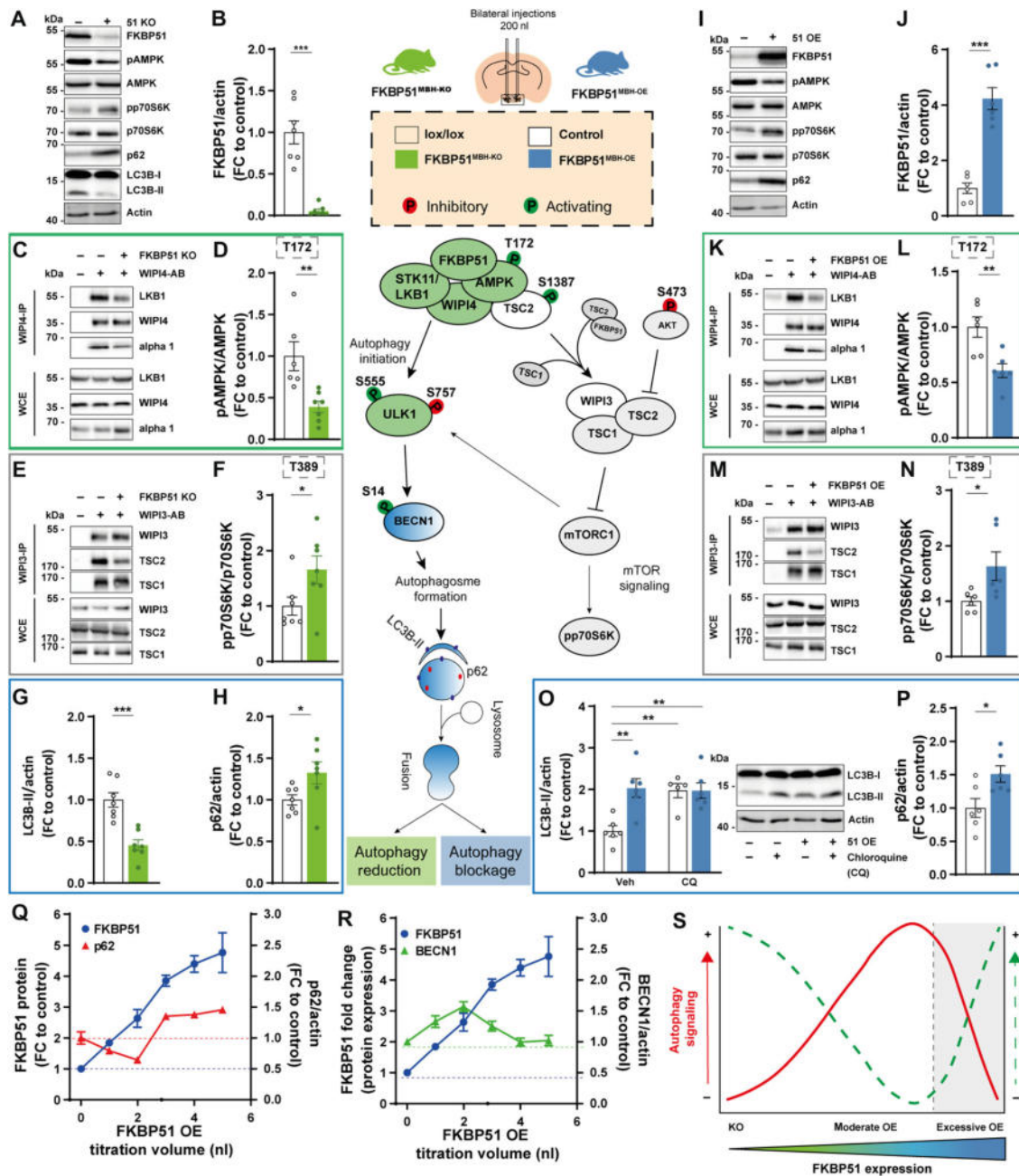


Fig. 5. MBH FKBP51 regulates autophagy in an inverted U-shaped manner. FKBP51 deletion is depicted in green, and FKBP51 overexpression is depicted in blue. (A) Representative blots of autophagy and mTOR markers in FKBP51^{MBH-KO} mice. (B) Quantification of FKBP51 deletion. (C) FKBP51 deletion reduced LKB1 and AMPK binding to WIPI4 as well as (D) AMPK phosphorylation at T172. (E) TSC2-WIPI3 binding was decreased in FKBP51^{MBH-KO} animals. (F) Quantification of mTOR substrate pp70S6K (T389). (G) LC3B-II and (H) p62 levels in the MBH. (I) Representative blots of autophagy and mTOR marker in FKBP51^{MBH-OE} mice. (J) Quantification of viral FKBP51 overexpression. (K) FKBP51 overexpression reduced LKB1 and AMPK binding to WIPI4. (L) Quantification of AMPK phosphorylation at T172. (M) TSC2-WIPI3 binding was decreased. (N) Quantification of pp70S6K phosphorylation at T389. (O) To assess autophagic flux FKBP51^{MBH-OE} animals were treated with chloroquine (50 mg/kg), and LC3B-II levels were analyzed 4 hours after treatment. (P) FKBP51 overexpression blocked autophagic flux and resulted in an accumulation of p62. (Q and R) Quantification of FKBP51, p62, and BECN1, while titrating AAV-HA-FKBP51 virus into mouse neuroblastoma cells. (S) MBH FKBP51 regulates autophagy and mTOR signaling in a dose-dependent manner. All data are shown as \pm SEM. Data are shown as the relative protein expression compared to control; for (A) to (N), an unpaired Student's *t* test was performed. **P* < 0.05, ***P* < 0.01, and ****P* < 0.001.

of autophagy signaling. Therefore, we gradually increased FKBP51 levels in N2a cells by the titration of AAV-hemagglutinin tag (HA)-FKBP51. Following a moderate increase of FKBP51, we observed a decrease in the accumulation of p62 and an increase in BECN1, supporting the activating role of FKBP51. In parallel, we could observe a slight

decrease in p70S6K phosphorylation. However, upon a stimulus threshold (at approximately three- to fourfold FKBP51), we observed an inhibitory effect on autophagy with decreased protein level of BECN1 and an increased phosphorylation of p70S6K and enhanced accumulation of p62 (Fig. 5, Q and R, and fig. S7H).

Our pathway analysis demonstrates that deletion of FKBP51 reduces autophagy signaling, and excessive levels of FKBP51 protein results in a total block of autophagy, causing a substantial shift from autophagy to mTOR signaling. In conclusion, we suggest that FKBP51 dose dependently regulates autophagy signaling in an inverted U-shaped manner (Fig. 5S).

MBH FKBP51 alters sympathetic outflow and thereby regulates autophagy signaling in the periphery

The MBH is an established regulatory center for sympathetic outflow to peripheral tissues (43). Consequently, we were interested whether the sympathetic tone of the brain into peripheral tissues was affected in FKBP51^{MBH-OE} animals. To do so, we treated FKBP51^{MBH-OE} mice with a single dose of the norepinephrine (NE) synthesis inhibitor α -methyl-*p*-tyrosine (α -MPT) to block NE synthesis in the periphery, thereby enabling the assessment of the catecholamine turnover rate (cTR) (44, 45). MBH FKBP51 OE led to a reduction in the cTR in muscle and eWAT (Fig. 6, A and B). Further, inguinal WAT (iWAT) of FKBP51^{MBH-OE} animals showed significant differences in initial NE levels, but not in cTR (fig. S8A). We also observed a mildly but not significantly decreased cTR in brown adipose tissue (BAT) (fig. S8B), whereas no effects were detected in the pancreas or heart tissue (fig. S8, C and D). Together, these data demonstrate that MBH FKBP51 OE dampens the sympathetic outflow especially to muscle and fat tissue and encouraged us to investigate changes in autophagy signaling in both tissues.

In FKBP51^{MBH-OE} animals, we observed increased levels of FKBP51 in SM and eWAT (fig. S8E), which resulted in increased AMPK activity (Fig. 6C) by enhanced binding of AMPK and LKB1 to WIPI4 (fig. S8, F and G). Downstream of AMPK, we observed increased phosphorylation of ULK1, BECN1, and TSC2, indicating enhanced autophagy initiation in the periphery (fig. S8, H to J). We again assessed mTOR signaling and observed increased binding of TSC2 to WIPI3 (fig. S8K) and a strong reduction in the phosphorylation of AKT at S473 and ULK1 at S757 (fig. S8, L and M), which resulted in reduced levels of pp70S6K (T389) (Fig. 6D). Furthermore, we monitored reduced levels of p62 (Fig. 6, E and F). To verify the increase in autophagy signaling, we analyzed LC3B-II levels before and after chloroquine treatment. Here, we detected a true increase in LC3B-II levels after chloroquine treatment (Fig. 6, G to I). These data imply an increase in autophagy flux in the periphery of FKBP51^{MBH-OE} animals. This is in line with our hypothesis that moderately elevated levels of FKBP51 increase autophagy signaling and suggest that the balance between active mTOR signaling in the MBH and active autophagy signaling in the periphery is one driving factor of the lean phenotype of the FKBP51^{MBH-OE} animals.

In FKBP51^{MBH-KO} mice, we observed an opposing phenotype with reduced autophagy signaling in SM, whereas autophagy signaling in eWAT was unaltered. In both tissues, we did not observe significant changes in FKBP51 protein level (fig. S8N). However, we could detect less phosphorylation of AMPK at T172 (Fig. 6J) and reduced binding of AMPK/LKB1 to WIPI4 (fig. S8, O and P). These findings were accompanied by reduced levels of ULK1, BECN1, and TSC2 (fig. S8, Q to S). Furthermore, we monitored increased levels of pp70S6K (T389), pULK1 (S757), and pAKT (S473), suggesting increased mTOR signaling (Fig. 6K and fig. S8, U and V). Last, LC3B-II levels were significantly reduced (Fig. 6L) in combination with elevated levels of p62 in SM (Fig. 6, M and N), which is indicative of reduced autophagy signaling solely in this peripheral tissue.

We could not detect any differences in autophagy signaling in other peripheral tissues, such as the liver (fig. S9, A and B). In summary, we suggest that the combined reduction of autophagy in the MBH and peripheral tissues, such as muscle and adipose tissue, is driving the observed body weight phenotype in FKBP51^{MBH-KO} mice.

DISCUSSION

In the current study, we examined the role of stress-activated chaperone FKBP51 as a molecular master switch linking autophagy and whole-body metabolism. We here present that FKBP51 actively modulates the response of the AMPK-mTOR network to an HFD by scaffolding autophagy-upstream AMPK/LKB1/WIPI4 and TSC2/WIPI3 heteroprotein complexes. We identify a tissue-specific function of FKBP51 by providing in vivo evidence that hypothalamic FKBP51 acts as a dose-specific mediator of whole-body metabolism.

Metabolomic profiling of neuronal-like cells lacking FKBP51 revealed a substantial increase for several metabolites and amino acids and suggests a role of FKBP51 in BCAA metabolism. BCAAs are important regulators of neurotransmitters and protein synthesis as well as food intake (46, 47). The increase of multiple BCAAs have been associated with obesity and insulin resistance (48, 49). In our in vitro metabolomic profiling analysis, isoleucine, leucine, valine, and tyrosine were strongly elevated in FKBP51 KO cells under normal and high glucose concentrations, which is indicative of constantly active mTOR signaling (50). Furthermore, it has been shown that excess leucine can reduce abdominal fat loss, whereas leucine deprivation promotes fat loss via cyclic AMP response element-binding protein signaling and increased expression of CRH (corticotropin-releasing hormone) in the hypothalamus. This effect is conveyed by the activation of the sympathetic nervous system (51). Leucine is an important regulator of mTOR and negatively affects the biogenesis of autophagosomes through its metabolite acetyl coenzyme A, which thereby enhances acetylation of the regulatory-associated protein of mTOR (RPTOR) via acetyltransferase EP300 in neurons and other cell types. This cascade of events ultimately leads to autophagy inhibition and mTOR activation (52, 53). At the same time, the increased levels of polyamines, observed in FKBP51 KO cells, are in contrast to autophagy inhibition. In particular, spermidine was shown to be capable of autophagy induction via inhibition of EP300 (54). Nevertheless, cell type-specific effects have to be taken into account as studies suggest an increased expression of EP300 in response to spermidine supplementation in aged and osteoarthritic chondrocytes (55).

To gain further insight into the underlying mechanisms, we built on already existing knowledge about FKBP51 regarding its regulatory role on single autophagy-related proteins [like BECN1, WIP1, and SKP2 (11, 16, 26)], which further positions FKBP51 as a major upstream regulator of autophagy. AMPK is activated by the phosphorylation of T172, which is regulated by LKB1 (56), and increased LKB1/AMPK signaling activates the TSC1/TSC2 complex, which, in turn, inhibits mTOR activity (38). Recently, Bakula and colleagues (11) showed that the WIPI protein family members WIPI3 and WIPI4 are essential scaffolders of the LKB1/AMPK/TSC1/2 signaling network thereby regulating autophagy and mTOR signaling. Here, we extended this knowledge by revealing that FKBP51 recruits LKB1 to the WIPI4-AMPK regulatory platform to induce AMPK phosphorylation at T172, which further increases autophagy initiation by direct phosphorylation of ULK1 at S555 (10). On the other hand, FKBP51 associates with the TSC2/WIPI3 heterocomplex to coregulate

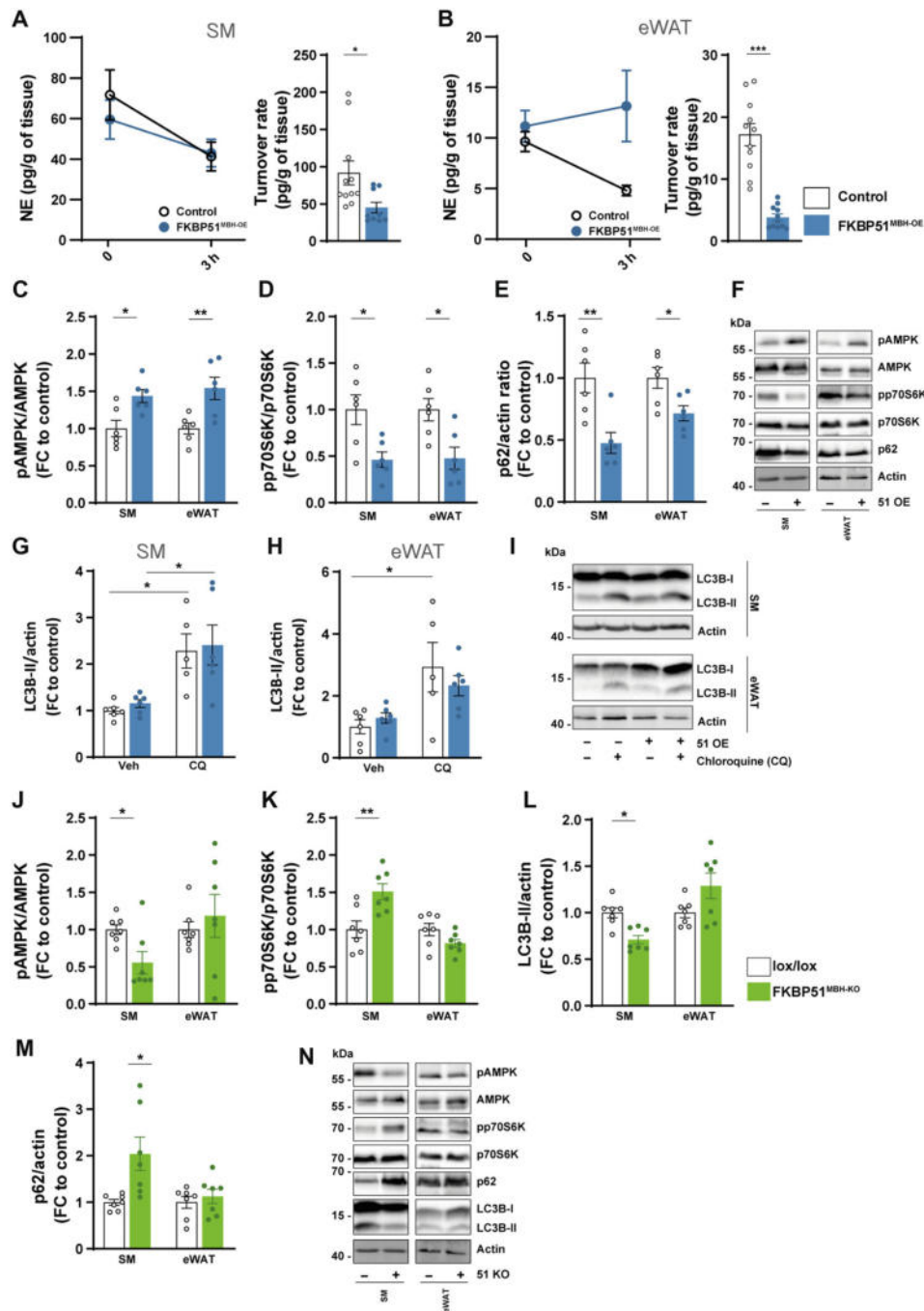


Fig. 6. MBH FKBP51 affects sympathetic outflow and peripheral autophagy signaling. FKBP51 overexpression is depicted in blue, and FKBP51 deletion is depicted in green. (A and B) Representative decrease in tissue NE content after α -MPT injection (left) and turnover rate (right) were determined on SM and eWAT (see fig. S8 for pancreas, heart, iWAT, and BAT tissues). Quantification of (C) pAMPK (T172) and (D) pp70S6K (T389), and (E) p62 level in the SM and eWAT. (F) Representative blots. (G to H) FKBP51 overexpression increased autophagic flux and in SM and eWAT. (I) Representative blots of chloroquine the experiment. Quantification of (J) pAMPK (T172), (K) pp70S6K (T389), (L) LC3B-II, and (M) p62 levels in SM and eWAT in animals lacking FKBP51 in the MBH. (N) Representative blots of FKBP51^{MBH-KO} protein analysis. All data are shown as \pm SEM. Protein data are shown as the relative protein expression compared to control. A two-way ANOVA was performed, followed by a Tukey's multiple comparison test in (F) and (G). For (A) to (E) and (I) to (L), an unpaired Student's *t* test was performed. **P* < 0.05, ***P* < 0.01, and ****P* < 0.001.

mTOR signaling and thus position FKBP51 as a main regulatory switch between autophagy initiation and mTOR signaling. Our experiments in vivo and in vitro led us to propose a model in which physiological levels of FKBP51 are essential for normal cellular autophagy-mediated homeostasis. Hereby, the absence of FKBP51 reduces autophagy

signaling and capacity in contrast to excessive, nonphysiological levels of FKBP51, which block autophagy in favor of mTOR signaling. The relative amounts of FKBP51 complexed with autophagy regulators within a cell govern the threshold for a transition from cell homeostasis to impaired autophagy in an inversed U-shaped manner.

FKBP51 has been shown to act tissue-specific to control adipocyte differentiation, browning (19, 57), and glucose metabolism (18). Most studies investigated global FKBP51 KO mice and observed a lean phenotype after an HFD regimen. These observations would imply that hypothalamic FKBP51 OE increases body weight gain, whereas deletion reduces body weight. We here observed that the acute FKBP51 manipulation in the MBH acts in an opposing manner with a central deletion leading to obesity and an overexpression to a lean phenotype, emphasizing its tissue specificity. These data suggest that hypothalamic FKBP51 regulates body weight and food intake in a U-shaped manner, which is supported by the fact that HFD increases FKBP51 expression and that a modest increase of hypothalamic FKBP51 induces body weight gain (30).

Several studies have already addressed the functional role of hypothalamic autophagy in the regulation of whole-body metabolism. Mice challenged with a chronic HFD showed impaired autophagy in the arcuate nucleus, and a deletion of ATG7 in the MBH resulted in hyperphagia and increased body weight (58). The MBH, however, is a complex brain region with multiple different nuclei, which have various opposing roles in the control of whole-body metabolism (1, 59). Here, we targeted FKBP51 nonselectively in various nuclei within the MBH, which is a limitation of the study. However, it also raises the question, which nuclei or neuronal subpopulations are the driving force behind our observed phenotypes. Previous studies have shown that specific deletion of autophagy in POMC neurons leads to hyperphagia and obesity (12). These findings are in line with our data of the FKBP51^{MBH-KO} animals, which develop obesity and hyperphagia on a regular chow diet in combination with decreased activity of central autophagy. Intriguingly, animals overexpressing FKBP51 in the MBH have a reduced body weight progression, increased glucose tolerance, and insulin sensitivity under an HFD regimen despite the hypothalamic autophagy blockage. The deletion of autophagy in AgRP neurons resulted in decreased body weight and food intake in response to fasting (13). The current study, however, cannot fully address whether the observed effects on obesity and the sympathetic effect output are purely driven by FKBP51 manipulation and whether autophagy is required for this effect. Future studies should emphasize the specific neuronal action of FKBP51 on autophagy to regulate body weight progression and food intake and investigate whether a blockade of autophagy can indeed counteract the effects of FKBP51 overexpression and vice versa.

Last, we suggest that the altered balance between hypothalamic and peripheral autophagy–mTOR signaling is a major contributor to the observed phenotype of FKBP51^{MBH-OE} and FKBP51^{MBH-KO} animals. FKBP51^{MBH-KO} animals showed decreased autophagy and increased mTOR signaling in the periphery (eWAT and SM), whereas peripheral autophagy signaling in FKBP51^{MBH-OE} animals displayed the opposite phenotype. The importance of central-peripheral mTOR and autophagy signaling has already been studied intensely. For instance, peripheral mTOR activity was shown to be involved in the pathogenesis of obesity and is enhanced in muscle and adipose tissue in obese animals (60, 61), whereas the activation of central mTOR can reduce food intake and body weight gain (62). In particular, the mTOR substrate p70S6K was shown to regulate body weight by mediating the sensitivity of leptin to AMPK via PI3K/AKT1/mTOR pathway (63, 64). Here, we extend this finding by the fact that the combination of peripheral and central p70S6K activity is an important contributor to the development of obesity. One has to keep in mind, although, that FKBP51 is highly dynamically

regulated by stressful situations and acts in concert with other chaperone proteins in a cell type- and tissue-specific manner. This may also explain apparent minor inconsistencies in our data and warrants further investigation.

In conclusion, this study provides a conceptual framework for the regulatory function of the stress-responsive co-chaperone FKBP51 on autophagy signaling and establishes a physiological role of MBH FKBP51 in the regulation of food intake and body weight regulation. We further suggest that FKBP51 is a crucial sensor linking signaling pathways controlling the stress response, autophagy, and metabolism. The ability of FKBP51 to regulate autophagy and energy homeostasis might therefore open new promising treatment avenues for metabolic disorders, such as obesity and type 2 diabetes.

MATERIALS AND METHODS

Antibodies

The following antibodies were used: goat polyclonal anti-actin (I-19) (sc-1616, Santa Cruz Biotechnology), rabbit polyclonal anti-FKBP51 (A301-430A, Bethyl Laboratories), rabbit monoclonal anti-FKBP5 (D5G2, #12210, Cell Signaling Technology), rabbit monoclonal anti-LKB1 (D60C5, #3047, Cell Signaling Technology), rabbit polyclonal anti-pAMPK α ^{T172} (#2531, Cell Signaling Technology), rabbit polyclonal anti-pAMPK α (#2532, Cell Signaling Technology), rabbit polyclonal anti-SKP2 (L70, #4313, Cell Signaling Technology), rabbit anti-pSKP2^{S72} (was a gift from Cell Signaling Technology), rabbit polyclonal anti-AKT (#9272, Cell Signaling Technology), rabbit monoclonal anti-pAKT^{S473} (D9E, #4060, Cell Signaling Technology), rabbit polyclonal anti-p62 (#5114, Cell Signaling Technology), rabbit monoclonal anti-LC3B (D11, #3868, Cell Signaling Technology), rabbit polyclonal anti-pULK1^{S757} (#6888, Cell Signaling Technology), rabbit monoclonal anti-pULK1^{S555} (D1H4, #5869, Cell Signaling Technology), rabbit monoclonal anti-ULK1 (D8H5, #8054, Cell Signaling Technology), anti-pBECN1^{S93/S96} (in mouse S91/S94) (#12476, Cell Signaling Technology), rabbit polyclonal anti-pBECN1^{S15} (#84966, Cell Signaling Technology), rabbit polyclonal anti-BECN1 (#3738, Cell Signaling Technology), rabbit polyclonal anti-TSC2 (#3612, Cell Signaling Technology), rabbit polyclonal anti-pTSC2^{S1387} (#5584, Cell Signaling Technology), rabbit monoclonal anti-pATG16L1^{S278} (EPR19016, ab195242, Abcam), rabbit polyclonal anti-WIPI4 (WDR45) (19194-1-AP, Proteintech), mouse monoclonal anti-WIPI4 (G12, sc-398272, Santa Cruz Biotechnology), rabbit polyclonal anti-WIPI3 (WDR45L) (SAB2102704, Sigma-Aldrich), mouse monoclonal anti-WIPI3 (B-7, sc-514194, Santa Cruz Biotechnology), rabbit polyclonal anti-WIPI2 (#8567, Cell Signaling Technology), rabbit polyclonal anti-WIPI1 (HPA007493, Sigma-Aldrich), rabbit polyclonal anti-AMPK α 1 (#2795, Cell Signaling Technology), rabbit polyclonal anti-AMPK γ 2 (#2536, Cell Signaling Technology), rabbit polyclonal anti-AMPK α 2 (#2757, Cell Signaling Technology), rabbit monoclonal anti-AMPK β 1 (71C10, #4178, Cell Signaling Technology), rabbit polyclonal anti-AMPK γ 1 (#4187, Cell Signaling Technology), rabbit polyclonal anti-AMPK β 2 (#4188, Cell Signaling Technology), rabbit polyclonal anti-AMPK γ 3 (#2550, Cell Signaling Technology), rabbit monoclonal anti-TSC1 (D43E2, #6935, Cell Signaling Technology), rabbit polyclonal anti-Flag (600-401-383, Rockland Inc.), rabbit polyclonal anti-hypusine (ABS1046, Merck Millipore), rabbit monoclonal anti-eIF5A (D8L8Q, #20765, Cell Signaling Technology), and rabbit polyclonal anti-TFEB (ab245350, Abcam).

Animals and animal housing

All experiments and protocols were approved by the committee for the Care and Use of Laboratory Animals of the Government of Upper Bavaria and were performed in accordance with the European Communities' Council Directive 2010/63/EU. All animals were kept singly housed in individually ventilated cages (IVCs) (30 cm by 16 cm by 16 cm; 501 cm²) with ad libitum access to water and food and constant environmental conditions (12-hour light/12-hour dark cycle, 23° ± 2°C, and humidity of 55%) during all times. All IVCs had sufficient bedding and nesting material as well as a wooden tunnel for environmental enrichment. All animals were fed with a standard research chow diet (Altromin 1318, Altromin GmbH, Germany) or an HFD (58% kcal from fat; D12331, Research Diets, New Brunswick, NJ, USA). For all experiments, male C57BL/6N or male *Fkbp5*^{lox/lox} mice [described in (65)] aged between 2 and 5 months were used.

Viral overexpression and knockdown of FKBP51

For overexpression of FKBP51, we injected an AAV vector containing a CAG-HA-tagged FKBP51-WPRE-BGH-polyA expression cassette (containing the coding sequence of human FKBP51 National Center for Biotechnology Information CCDS ID CCDS4808.1) in C57BL/6N mice. The same vector construct without expression of FKBP51 (CAG-Null/Empty-WPRE-BGH-polyA) was used as a control. Virus production, amplification, and purification were performed by GeneDetect. A viral vector containing a *Cre*-expressing cassette (pAAV-CMV-HI-eGFP-*Cre*-WPRE-SV40, #105545, Addgene) was used to induce FKBP51 deletion in *Fkbp5*^{lox/lox} mice. Control animals were injected with a control virus (pAAV-CMV-PI-eGFP-WPRE-bGH, #105530, Addgene). For both experiments, stereotactic injections were performed as described previously (66). Briefly, mice were anesthetized with isoflurane prior surgery, and 0.2 µl of the abovementioned viruses (titers: 1.6 × 10^{12–13} genomic particles/ml) was bilaterally injected in the MBH at 0.05 µl/min by glass capillaries with a tip resistance of 2 to 4 megohm in a stereotactic apparatus. The following coordinates were used: –1.5 mm anterior to bregma, 0.4 mm lateral from midline, and 5.6 mm below the surface of the skull, targeting the MBH. After surgery, mice were treated for 3 days with Metacam via intraperitoneal injections and were housed for 3 to 4 weeks for total recovery before the actual experiments. Successful overexpression and KD of FKBP51 were verified by Western blot.

Autophagic flux

We investigated the autophagic flux by the injection of chloroquine (50 mg/kg), an inhibitor of lysosomal acidification and autophagosome-lysosomal fusion that blocks degradation of autophagosome cargo (35). We injected C57BL/6N mice in the morning with chloroquine (50 mg/kg) or saline as control. Multiple tissues were removed and shock-frozen 4 hours after injection and stored at –80°C until protein analysis of LC3B-II normalized to glyceraldehyde-3-phosphate dehydrogenase or actin. Lipidation of LC3B in protein homogenates obtained from animals treated with chloroquine (fusion block) was compared to LC3B lipidation of animals treated with vehicle.

Sample collection

On the day of euthanization, animals were deeply anesthetized with isoflurane and euthanized by decapitation. Trunk blood was collected in labeled 1.5-ml EDTA-coated microcentrifuge tubes (Sarstedt) and kept on ice until centrifugation. After centrifugation (4°C, 8000 rpm

for 1 min), the plasma was removed and transferred to new, labeled tubes and stored at –20°C until hormone quantification. For protein analysis, the MBH, skeletal muscle (SM), and WAT (eWAT) were collected and immediately shock-frozen and stored at –80°C until protein analysis.

cTR determination

Catecholamine turnover was measured on the basis of the decline in tissue NE content after the inhibition of catecholamine biosynthesis with α -methyl-DL-tyrosine (α -MPT) (200 mg/kg i.p. injection; Sigma-Aldrich, ST, Quentin, France), as described previously (44).

In the morning, bedding was changed, and C57BL/6N mice were food-deprived for 3 hours to insure postprandial state and injected with α -methyl-DL-tyrosine (α -MPT; a tyrosine hydroxylase inhibitor) to block catecholamine synthesis. Before (time = 0) and 3 hours after the injection (time = 3 hours), animals were euthanized, and the tissues were removed, flash-frozen in liquid nitrogen, and stored at –80°C for monoamine and metabolite analysis.

Catecholamine content at time = 0 [NE (0)] was determined on a group of animals receiving a saline injection. Because the concentration of catecholamine in tissues declined exponentially, we could obtain the rate constant of NE efflux (expressed in h^{–1}). Comprehensive analysis of NE was carried out by reverse-phase liquid chromatography (LC) with electrochemical detection as described in (67). The values obtained were expressed as nanogram per milligram wet tissue and were logarithmically transformed for calculation of linearity of regression, SE of the regression coefficients, and significance of differences between regression coefficients.

Glucose tolerance and insulin tolerance

Alteration of glucose metabolism in *Fkbp5*^{MBH-OE} and *Fkbp5*^{MBH-KO} mice was investigated by a glucose (glucose tolerance test) and insulin tolerance (insulin tolerance test) test as described previously (18).

Hormone assessment

Corticosterone concentrations were determined by radioimmunoassay using a corticosterone double antibody ¹²⁵I radioimmunoassay kit (sensitivity: 12.5 ng/ml; MP Biomedicals Inc.) and were used following the manufacturers' instructions. Radioactivity of the pellet was measured with a gamma counter (Packard Cobra II Auto Gamma, PerkinElmer). Final corticosterone levels were derived from the standard curve.

Cell lines and transfection

N2a WT, N2a FKBP51 KO, SH-SY5Y WT, and FKBP51 KO (68) cells were maintained in Dulbecco's modified Eagle's medium supplemented with 10% fetal bovine serum and 1× penicillin-streptomycin antibiotics at 37°C in a humidified atmosphere with 5% CO₂. At 90% confluency, N2a cells were detached from the plate, and 2 × 10⁶ cells were resuspended in 100 µl of transfection buffer [50 nM Heps (pH 7.3), 90 mM NaCl, 5 mM KCl, and 0.15 mM CaCl₂]. A total of 2.5 µg of plasmid DNA or 80 ng of siRNA (siWIPI3, EMU081491 or siWIPI4, EMU007321 or siControl, and SIC001, all Sigma-Aldrich) was used per transfection. Electroporation was performed using the Amaxa Nucleofector System 2b (program T-020). For OE experiments, N2a cells were transfected with FKBP51-Flag expression or TFEB-GFP reporter plasmid using Lipofectamine 2000 (Thermo Fisher Scientific) according to the manufacturer's instructions.

Generation of FKBP51 KO N2a cells

N2a (Sigma-Aldrich) FKBP51 KO cell line was generated with the Alt-R CRISPR-Cas9 System from Integrated DNA Technologies (IDT) according to the manufacturer's instructions. Briefly, RNA oligos [Alt-R CRISPR-Cas9 crRNA against murine FKBP51 and Alt-R CRISPR-Cas9 trans-activating crRNA (tracrRNA)] were mixed in nuclease-free duplex buffer (IDT) in equimolar concentrations yielding a final duplex of 1 μ M and then heated at 95°C for 5 min and combined with 1 μ M Alt-R S.p. HiFi Cas9 Nuclease V3 diluted in Opti-MEM (Thermo Fisher Scientific). Ribonucleoprotein (RNP) complexes were assembled at room temperature (RT) for 5 min and mixed with Lipofectamine RNAiMAX reagent (Thermo Fisher Scientific) and Opti-MEM (Thermo Fisher Scientific) and incubated for 20 min at RT to form transfection complexes. Subsequently, 40,000 N2a cells per well were reverse-transfected using complete culture media without antibiotics in a 96-well tissue culture plate with a final RNP concentration of 10 nM. After 48 hours (37°C, 5% CO₂), single-cell clones were obtained by array dilution method, expanded, and analyzed by Western blotting. FKBP51 WT control cells were identified by immunoblotting after single-cell cloning procedures and, therefore, underwent the same transfection and isolation procedure as the FKBP51 KO cells. Predesigned Alt-R CRISPR Cas9 guide RNAs (IDT) were used for KO generation (protospacer adjacent motif sequence in italics). Mm.Cas9.FKBP51.AA: CGATCCCAATCGGAATGTCGTGG.

Treatment of N2a cells

Treatments of N2a cell cultures included glucocorticoid receptor (GR) stimulation with dexamethasone (Sigma-Aldrich) ranging from 1 to 100 nM for 24 hours, HBSS (Thermo Fisher Scientific)-induced starvation for 4 hours, and inhibition of autophagosome-lysosome fusion by BafA1 (100 nM, 4 hours; Alfa Aesar).

Co-immunoprecipitation

IPs of endogenous proteins were performed from protein extracts ($n = 3$ to 4 per group) derived from N2a cells, SH-SY5Y WT or FKBP51 KO cells, SM, eWAT, and MBH. For co-IPs, 500 μ g of lysate was incubated with 2 μ g of the appropriate IP antibody [anti-Flag (FKBP51), anti-FKBP51, anti-WIPI4, and anti-WIPI3] at 4°C overnight. A total of 20 μ l of rabbit immunoglobulin G-conjugated protein G Dynabeads (Invitrogen, 100-03D) were blocked with bovine serum albumin and subsequently added to the lysate-antibody mixture and allowed to incubate at 4°C for 3 hours to mediate binding between Dynabeads and the antibody-antigen complex of interest. Beads were then washed three times with ice-cold phosphate-buffered saline, and the protein antibody complexes were eluted with 60 μ l of Laemmli loading buffer. Thereafter, the eluate was boiled for 5 min at 95°C. Then, 2 to 5 μ l of each immunoprecipitate were separated by SDS-polyacrylamide gel electrophoresis (SDS-PAGE) and electro-transferred onto nitrocellulose membranes. For assessing protein complexes, immunoblotting against WIPI1-WIPI4, FKBP51, LKB1, AMPK, TSC1, and TSC2 was performed.

Western blot analysis

Protein extracts were obtained by lysing cells [in radioimmunoprecipitation assay buffer (150 mM NaCl, 1% IGEPAL CA-630, 0.5% sodium deoxycholate, 0.1% SDS, and 50 mM tris (pH 8.0)) freshly supplemented with protease inhibitor (Merck Millipore, Darmstadt, Germany), benzonase (Merck Millipore), 5 mM dithiothreitol

(Sigma-Aldrich, Munich, Germany), and phosphatase inhibitor cocktail (Roche, Penzberg, Germany). Proteins were separated by SDS-PAGE and electro-transferred onto nitrocellulose membranes. Blots were placed in tris-buffered saline supplemented with 0.05% Tween (Sigma-Aldrich) and 5% nonfat milk for 1 hour at RT and then incubated with primary antibody (diluted in tris-buffered saline/0.05% Tween) overnight at 4°C.

Subsequently, blots were washed and probed with the respective horseradish peroxidase or fluorophore-conjugated secondary antibody for 1 hour at RT. The immunoreactive bands were visualized either using an enhanced chemiluminescence detection reagent (Millipore, Billerica, MA, USA) or directly by excitation of the respective fluorophore. Determination of the band intensities was performed with Bio-Rad, ChemiDoc MP.

LC-MS analysis of amine-containing metabolites

The benzoyl chloride derivatization method was used for amino acid analysis (69). Briefly, the dried metabolite pellets were resuspended in 90 μ l of the LC-MS grade water (Milli-Q 7000 equipped with an LC-Pak and a Millipak filter, Millipore). Then, 20 μ l of the resuspended sample was mixed with 10 μ l of 100 mM sodium carbonate (Sigma-Aldrich), followed by the addition of 10 μ l of 2% benzoyl chloride (Sigma-Aldrich) in acetonitrile (Optima-Grade, Fisher Scientific). Samples were vortexed before centrifugation for 10 min at 21,300g at 20°C. Clear supernatants were diluted 1:10 with LC-MS grade water and transferred to fresh autosampler tubes with conical glass inserts (Chromatographie Zubehoer Trott) and analyzed using a Vanquish UHPLC (Thermo Fisher Scientific) connected to a Q-Exactive HF (Thermo Fisher Scientific).

For the analysis, 1 μ l of the derivatized sample were injected onto a 100 \times 2.1 mm HSS T3 UPLC column (Waters). The flow rate was set to 400 μ l/min using a buffer system consisting of buffer A [10 mM ammonium formate (Sigma-Aldrich) and 0.15% formic acid (Sigma-Aldrich) in LC-MS grade water] and buffer B (acetonitrile, Optima-grade, Fisher Scientific). The LC gradient was 0% buffer B at 0 min, 0 to 15% buffer B at 0 to 0.1 min, 15 to 17% buffer B at 0.1 to 0.5 min, 17 to 55% buffer B at 0.5 to 7 min, 55 to 70% buffer B at 7 to 7.5 min, 70 to 100% buffer B at 7.5 to 9 min, 100% buffer B at 9 to 10 min, 100 to 0% buffer B at 10 to 10.1 min, and 0% buffer B at 10.1 to 15 min. The mass spectrometer was operating in positive-ionization mode monitoring the mass range, mass/charge ratio of 50 to 750. The heated electrospray ionization (ESI) source settings of the mass spectrometer were as follows: spray voltage of 3.5 kV, capillary temperature of 250°C, sheath gas flow of 60 arbitrary units (AU), and auxiliary gas flow of 20 AU at a temperature of 250°C. The S-lens was set to a value of 60 AU.

Data analysis was performed using the TraceFinder software (version 4.2, Thermo Fisher Scientific). Identity of each compound was validated by authentic reference compounds, which were analyzed independently. Peak areas were analyzed using extracted ion chromatogram (XIC) of compound-specific $[M + nBz + H]^+$, where n corresponds to the number of amine moieties, which can be derivatized with a benzoyl chloride (Bz). XIC peaks were extracted with a mass accuracy (<5 parts per million) and a retention time tolerance of 0.2 min.

Anion-exchange chromatography MS of the analysis of tricarboxylic acid cycle and glycolysis metabolites

Anion-exchange chromatography was performed simultaneously to the LC-MS analysis. First, 50 μ l of the resuspended sample was diluted 1:5 with LC-MS grade water and analyzed using a Dionex

ion chromatography system (ICS-5000, Thermo Fisher Scientific). The applied protocol was adopted from (70). Briefly, 10 μ l of polar metabolite extract was injected in full-loop mode using an overflow factor of 3, onto a Dionex IonPac AS11-HC column (2 mm by 250 mm, 4- μ m particle size, Thermo Fisher Scientific) equipped with a Dionex IonPac AS11-HC guard column (2 mm by 50 mm, 4 μ m, Thermo Fisher Scientific). The column temperature was held at 30°C, while the autosampler was set to 6°C. A potassium hydroxide gradient was generated by the eluent generator using a potassium hydroxide cartridge that was supplied with deionized water. The metabolite separation was carried at a flow rate of 380 μ l/min, applying the following gradient: 0 to 5 min, 10 to 25 mM KOH; 5 to 21 min, 25 to 35 mM KOH; 21 to 25 min, 35 to 100 mM KOH, 25 to 28 min, 100 mM KOH; and 28 to 32 min, 100 to 10 mM KOH. The column was re-equilibrated at 10 mM for 6 min. The eluting metabolites were detected in negative ion mode using ESI MRM (multireaction monitoring) on a Xevo TQ (Waters) triple quadrupole mass spectrometer applying the following settings: capillary voltage of 1.5 kV, desolvation temperature of 550°C, desolvation gas flow of 800 liters/hour, and collision cell gas flow of 0.15 ml/min. All peaks were validated using two MRM transitions, one for quantification of the compound, while the second ion was used for qualification of the identity of the compound. Data analysis and peak integration were performed using the TargetLynx Software (Waters).

Analysis of nuclear translocation of TFEB

Images for assessment of nuclear translocation of TFEB-GFP in paraformaldehyde-fixed N2a cells were acquired using the VisiScope CSU-W1 spinning disk confocal microscope and the VisiView Software (Visitron Systems GmbH). Settings for laser and detector were maintained constant for the acquisition of each image. For analysis, at least three images were acquired using the 20 \times objective. For quantification of nuclear TFEB-GFP translocation, GFP intensity was determined in ImageJ by manually drawing a border around randomly selected, 4',6-diamidino-2-phenylindole-positive nuclei of N2a cells with a GFP signal.

Statistical analysis

The data presented are shown as means \pm SEM, and samples sizes are indicated in the figure legends. All data were analyzed by the commercially available software SPSS v17.0 and GraphPad v8.0. The unpaired Student's *t* test was used when two groups were compared. For four-group comparisons, two-way analysis of variance (ANOVA) was performed, followed by Tukey's or Dunnett's multiple comparisons test, as appropriate. *P* values of less than 0.05 were considered statistically significant.

SUPPLEMENTARY MATERIALS

Supplementary material for this article is available at <https://science.org/doi/10.1126/sciadv.abi4797>

[View/request a protocol for this paper from Bio-protocol.](#)

REFERENCES AND NOTES

- G. J. Morton, T. H. Meek, M. W. Schwartz, Neurobiology of food intake in health and disease. *Nat. Rev. Neurosci.* **15**, 367–378 (2014).
- L. Galluzzi, J. M. Bravo-San Pedro, B. Levine, D. R. Green, G. Kroemer, Pharmacological modulation of autophagy: Therapeutic potential and persisting obstacles. *Nat. Rev. Drug Discov.* **16**, 487–511 (2017).
- Y. Zhang, J. R. Sowers, J. Ren, Targeting autophagy in obesity: From pathophysiology to management. *Nat. Rev. Endocrinol.* **14**, 356–376 (2018).
- J. D. Rabinowitz, E. White, Autophagy and metabolism. *Science* **330**, 1344–1348 (2010).
- B. Levine, G. Kroemer, Biological functions of autophagy genes: A disease perspective. *Cell* **176**, 11–42 (2019).
- Y. Potes, B. de Luxán-Delgado, S. Rodríguez-González, M. R. M. Guimaraes, J. J. Solano, M. Fernández-Fernández, M. Bermúdez, J. A. Boga, I. Vega-Naredo, A. Coto-Montes, Overweight in elderly people induces impaired autophagy in skeletal muscle. *Free Radic. Biol. Med.* **110**, 31–41 (2017).
- Y. Mizunoe, Y. Sudo, N. Okita, H. Hiraoka, K. Mikami, T. Narahara, A. Negishi, M. Yoshida, R. Higashibata, S. Watanabe, H. Kaneko, D. Natori, T. Furuichi, H. Yasukawa, M. Kobayashi, Y. Higami, Involvement of lysosomal dysfunction in autophagosome accumulation and early pathologies in adipose tissue of obese mice. *Autophagy* **13**, 642–653 (2017).
- K. Inoki, J. Kim, K.-L. Guan, AMPK and mTOR in cellular energy homeostasis and drug targets. *Annu. Rev. Pharmacol. Toxicol.* **52**, 381–400 (2012).
- M. M. Mihaylova, R. J. Shaw, The AMPK signalling pathway coordinates cell growth, autophagy and metabolism. *Nat. Cell Biol.* **13**, 1016–1023 (2011).
- J. Kim, M. Kundu, B. Viollet, K. L. Guan, AMPK and mTOR regulate autophagy through direct phosphorylation of Ulk1. *Nat. Cell Biol.* **13**, 132–141 (2011).
- D. Bakula, A. J. Müller, T. Zuleger, Z. Takacs, M. Franz-Wachtel, A. K. Thost, D. Brigger, M. P. Tschan, T. Frickey, H. Robenek, B. Macek, T. Proikas-Cezanne, WIPI3 and WIPI4 β -propellers are scaffolds for LKB1-AMPK-TSC signalling circuits in the control of autophagy. *Nat. Commun.* **8**, 15637 (2017).
- S. Kaushik, E. Arias, H. Kwon, N. M. Lopez, D. Athonvarangkul, S. Sahu, G. J. Schwartz, J. E. Pessin, R. Singh, Loss of autophagy in hypothalamic POMC neurons impairs lipolysis. *EMBO Rep.* **13**, 258–265 (2012).
- S. Kaushik, J. A. Rodríguez-Navarro, E. Arias, R. Kiffin, S. Sahu, G. J. Schwartz, A. M. Cuervo, R. Singh, Autophagy in hypothalamic AgRP neurons regulates food intake and energy balance. *Cell Metab.* **14**, 173–183 (2011).
- D. L. Riggs, P. J. Roberts, S. C. Chirillo, J. Cheung-Flynn, V. Prapapanich, T. Ratajczak, R. Gaber, D. Picard, D. F. Smith, The Hsp90-binding peptidylprolyl isomerase FKBP52 potentiates glucocorticoid signaling in vivo. *EMBO J.* **22**, 1158–1167 (2003).
- G. M. Wochnik, J. Rüegg, G. A. Abel, U. Schmidt, F. Holsboer, T. Rein, FK506-binding proteins 51 and 52 differentially regulate dynein interaction and nuclear translocation of the glucocorticoid receptor in mammalian cells. *J. Biol. Chem.* **280**, 4609–4616 (2005).
- M. Taipale, G. Tucker, J. Peng, I. Krykbaeva, Z. Y. Lin, B. Larsen, H. Choi, B. Berger, A. C. Gingras, S. Lindquist, A quantitative chaperone interaction network reveals the architecture of cellular protein homeostasis pathways. *Cell* **158**, 434–448 (2014).
- M. V. Schmidt, M. Paez-Pereda, F. Holsboer, F. Hausch, The prospect of FKBP51 as a drug target. *ChemMedChem* **7**, 1351–1359 (2012).
- G. Balsevich, A. S. Häusl, C. W. Meyer, S. Karamihalev, X. Feng, M. L. Pöhlmann, C. Dournes, A. Uribe-Marino, S. Santarelli, C. Labermaier, K. Hafner, T. Mao, M. Breitsamer, M. Theodoropoulou, C. Namendorf, M. Uhr, M. Paez-Pereda, G. Winter, F. Hausch, A. Chen, M. H. Tschöp, T. Rein, N. C. Gassen, M. V. Schmidt, Stress-responsive FKBP51 regulates AKT2-AS160 signaling and metabolic function. *Nat. Commun.* **8**, 1725 (2017).
- L. A. Stechschulte, B. Qiu, M. Warrior, T. D. Hinds, M. Zhang, H. Gu, Y. Xu, S. S. Khuder, L. Russo, S. M. Najjar, B. Lecka-Czernik, W. Yong, E. R. Sanchez, FKBP51 null mice are resistant to diet-induced obesity and the PPAR γ agonist rosiglitazone. *Endocrinology* **157**, 3888–3900 (2016).
- M. J. Pereira, J. Palming, M. K. Svensson, M. Rizell, J. Dalenbäck, M. Hammar, T. Fall, C. O. Sidibeh, A. Svensson, J. W. Eriksson, FKBP5 expression in human adipose tissue increases following dexamethasone exposure and is associated with insulin resistance. *Metabolism* **63**, 1198–1208 (2014).
- C. O. Sidibeh, M. J. Pereira, X. M. Abalo, G. J. Boersma, S. Skrtic, P. Lundkvist, P. Katsogiannis, F. Hausch, C. Castillejo-López, J. W. Eriksson, FKBP5 expression in human adipose tissue: Potential role in glucose and lipid metabolism, adipogenesis and type 2 diabetes. *Endocrine* **62**, 116–128 (2018).
- A. S. Häusl, G. Balsevich, N. C. Gassen, M. V. Schmidt, Focus on FKBP51: A molecular link between stress and metabolic disorders. *Mol. Metab.* **29**, 170–181 (2019).
- H. Pei, L. Li, B. L. Fridley, G. D. Jenkins, K. R. Kalari, W. Lingle, G. Petersen, Z. Lou, L. Wang, FKBP51 affects cancer cell response to chemotherapy by negatively regulating Akt. *Cancer Cell* **16**, 259–266 (2009).
- R. C. Wang, Y. Wei, Z. An, Z. Zou, G. Xiao, G. Bhagat, M. White, J. Reichelt, B. Levine, Akt-mediated regulation of autophagy and tumorigenesis through Beclin 1 phosphorylation. *Science* **338**, 956–959 (2012).
- N. C. Gassen, J. Hartmann, M. V. Schmidt, T. Rein, FKBP5/FKBP51 enhances autophagy to synergize with antidepressant action. *Autophagy* **11**, 578–580 (2015).
- N. C. Gassen, D. Niemeyer, D. Muth, V. M. Corman, S. Martinelli, A. Gassen, K. Hafner, J. Papiés, K. Mösbauer, A. Zellner, A. S. Zannas, A. Herrmann, F. Holsboer, R. Brack-Werner, M. Boshart, B. Müller-Myhsok, C. Drosten, M. A. Müller, T. Rein, SKP2 attenuates autophagy through Beclin1-ubiquitination and its inhibition reduces MERS-Coronavirus infection. *Nat. Commun.* **10**, 5770 (2019).

27. R. Singh, S. Kaushik, Y. Wang, Y. Xiang, I. Novak, M. Komatsu, K. Tanaka, A. M. Cuervo, M. J. Czaja, Autophagy regulates lipid metabolism. *Nature* **458**, 1131–1135 (2009).
28. J. Tonzetta, S. Guber, N. L. Charo, S. Susperreguy, J. Schwartz, M. D. Galiginiana, G. Pwien-Pilipuk, Dynamic mitochondrial-nuclear redistribution of the immunophilin FKBP51 is regulated by the PKA signaling pathway to control gene expression during adipocyte differentiation. *J. Cell Sci.* **126**, 5357–5368 (2013).
29. Y. Zhang, S. Goldman, R. Baerga, Y. Zhao, M. Komatsu, S. Jin, Adipose-specific deletion of autophagy-related gene 7 (atg7) in mice reveals a role in adipogenesis. *Proc. Natl. Acad. Sci. U.S.A.* **106**, 19860–19865 (2009).
30. L. Yang, F. Isoda, K. Yen, S. P. Kleopoulos, W. Janssen, X. Fan, J. Mastaitis, A. Dunn-Meynell, B. Levin, R. McCrimmon, R. Sherwin, S. Musatov, C. V. Mobbs, Hypothalamic Fkbp51 is induced by fasting, and elevated hypothalamic expression promotes obese phenotypes. *AJP Endocrinol. Metab.* **302**, E987–E991 (2012).
31. S. H. Scharf, C. Liebl, E. B. Binder, M. V. Schmidt, M. B. Müller, Expression and regulation of the Fkbp5 gene in the adult mouse brain. *PLOS ONE* **6**, e16883 (2011).
32. R. L. Wolfson, D. M. Sabatini, The dawn of the age of amino acid sensors for the mTORC1 pathway. *Cell Metab.* **26**, 301–309 (2017).
33. S. M. Son, S. J. Park, H. Lee, F. Siddiqi, J. E. Lee, F. M. Menzies, D. C. Rubinsztein, Leucine signals to mTORC1 via its metabolite acetyl-coenzyme A. *Cell Metab.* **29**, 192–201.e7 (2019).
34. D. Meng, Q. Yang, H. Wang, C. H. Melick, R. Navlani, A. R. Frank, J. L. Jewell, Glutamine and asparagine activate mTORC1 independently of Rag GTPases. *J. Biol. Chem.* **295**, 2890–2899 (2020).
35. D. J. Klionsky, Guidelines for the use and interpretation of assays for monitoring autophagy (3rd edition). *Autophagy* **12**, 1–222 (2016).
36. A. Arif, J. Jia, B. Willard, X. Li, P. L. Fox, Multisite phosphorylation of S6K1 directs a kinase phospho-code that determines substrate selection. *Mol. Cell.* **73**, 446–457.e6 (2019).
37. J. Kim, Y. C. Kim, C. Fang, R. C. Russell, J. H. Kim, W. Fan, R. Liu, Q. Zhong, K. L. Guan, Differential regulation of distinct Vps34 complexes by AMPK in nutrient stress and autophagy. *Cell* **152**, 290–303 (2013).
38. D. B. Shackelford, R. J. Shaw, The LKB1-AMPK pathway: Metabolism and growth control in tumour suppression. *Nat. Rev. Cancer* **9**, 563–575 (2009).
39. W. Tian, R. Alsaadi, Z. Guo, A. Kalinina, M. Carrier, M. E. Tremblay, B. Lacoste, D. Lagace, R. C. Russell, An antibody for analysis of autophagy induction. *Nat. Methods* **17**, 232–239 (2020).
40. H. Zhang, G. Alsaleh, J. Feltham, Y. Sun, G. Napolitano, T. Riffelmacher, P. Charles, L. Frau, P. Hublitz, Z. Yu, S. Mohammed, A. Ballabio, S. Balabanov, J. Mellor, A. K. Simon, Polyamines control eIF5A hypusination, TFEF translation, and autophagy to reverse B cell senescence. *Mol. Cell.* **76**, 110–125.e9 (2019).
41. W. Wan, Z. You, L. Zhou, Y. Xu, C. Peng, T. Zhou, C. Yi, Y. Shi, W. Liu, mTORC1-regulated and HUWE1-mediated WIPI2 degradation controls autophagy flux. *Mol. Cell.* **72**, 303–315.e6 (2018).
42. G. Y. Liu, D. M. Sabatini, mTOR at the nexus of nutrition, growth, ageing and disease. *Nat. Rev. Mol. Cell Biol.* **21**, 183–203 (2020).
43. C. Broberger, Brain regulation of food intake and appetite: Molecules and networks. *J. Intern. Med.* **258**, 301–327 (2005).
44. B. B. Brodie, E. Costa, A. Dlabac, N. H. Neff, H. H. Smookler, Application of steady state kinetics to the estimation of synthesis rate and turnover time of tissue catecholamines. *J. Pharmacol. Exp. Ther.* **154**, 493–498 (1966).
45. A. Joly-Amado, R. G. P. Denis, J. Castel, A. Lacombe, C. Cansell, C. Rouch, N. Kassis, J. Dairou, P. D. Cani, R. Ventura-Clapier, A. Prola, M. Flamment, F. Fougelle, C. Magnan, S. Luquet, Hypothalamic AgRP-neurons control peripheral substrate utilization and nutrient partitioning. *EMBO J.* **31**, 4276–4288 (2012).
46. J. E. Spurringer, A. Addington, S. M. Hutson, Branched-chain amino acids and brain metabolism. *Neurochem. Res.* **42**, 1697–1709 (2017).
47. J. D. Fernstrom, *Journal of Nutrition* (American Institute of Nutrition, 2005; <https://academic.oup.com/jn/article/135/6/1539S/4663842>), vol. 135, pp. 1539S–1546S.
48. C. B. Newgard, J. An, J. R. Bain, M. J. Muehlbauer, R. D. Stevens, L. F. Lien, A. M. Haqq, S. H. Shah, M. Arlotto, C. A. Slentz, J. Rochon, D. Gallup, O. Ilkayeva, B. R. Wenner, W. S. Yancy, H. Eisensohn, G. Musante, R. S. Surwit, D. S. Millington, M. D. Butler, L. P. Svetkey, A branched-chain amino acid-related metabolic signature that differentiates obese and lean humans and contributes to insulin resistance. *Cell Metab.* **9**, 311–326 (2009).
49. T. J. Wang, M. G. Larson, R. S. Vasan, S. Cheng, E. P. Rhee, E. McCabe, G. D. Lewis, C. S. Fox, P. F. Jacques, C. Fernandez, C. J. O'Donnell, S. A. Carr, V. K. Mootha, J. C. Florez, A. Souza, O. Melander, C. B. Clish, R. E. Gerszten, Metabolite profiles and the risk of developing diabetes. *Nat. Med.* **17**, 448–453 (2011).
50. M. S. Yoon, The emerging role of branched-chain amino acids in insulin resistance and metabolism. *Nutrients* **8**, 405 (2016).
51. Y. Cheng, Q. Zhang, Q. Meng, T. Xia, Z. Huang, C. Wang, B. Liu, S. Chen, F. Xiao, Y. Du, F. Guo, Leucine deprivation stimulates fat loss via increasing CRH expression in the hypothalamus and activating the sympathetic nervous system. *Mol. Endocrinol.* **25**, 1624–1635 (2011).
52. G. Mariño, F. Pietrocola, T. Eisenberg, Y. Kong, S. A. Malik, A. Andryushkova, S. Schroeder, T. Pendl, A. Harger, M. Niso-Santano, N. Zamzami, M. Scoazec, S. Durand, D. P. Enot, Á. F. Fernández, I. Martins, O. Kepp, L. Senovilla, C. Bauvy, E. Morselli, E. Vacchelli, M. Bennetzen, C. Magnes, F. Sinner, T. Pieber, C. López-Otin, M. C. Maiuri, P. Codogno, J. S. Andersen, J. A. Hill, F. Madeo, G. Kroemer, Regulation of autophagy by cytosolic acetyl-coenzyme A. *Mol. Cell* **53**, 710–725 (2014).
53. S. M. Son, S. J. Park, E. Stamatakou, M. Vicinanza, F. M. Menzies, D. C. Rubinsztein, Leucine regulates autophagy via acetylation of the mTORC1 component raptor. *Nat. Commun.* **11**, 3148 (2020).
54. F. Pietrocola, S. Lachkar, D. P. Enot, M. Niso-Santano, J. M. Bravo-San Pedro, V. Sica, V. Izzo, M. C. Maiuri, F. Madeo, G. Mariño, G. Kroemer, Spermidine induces autophagy by inhibiting the acetyltransferase EP300. *Cell Death Differ.* **22**, 509–516 (2015).
55. P. K. Sacitharan, S. Lwin, G. B. Gharos, J. R. Edwards, Spermidine restores dysregulated autophagy and polyamine synthesis in aged and osteoarthritic chondrocytes via EP300. *Exp. Mol. Med.* **50**, 1–10 (2018).
56. D. G. Hardie, AMP-activated/SNF1 protein kinases: Conserved guardians of cellular energy. *Nat. Rev. Mol. Cell Biol.* **8**, 774–785 (2007).
57. L. A. Stechschulte, T. D. Hinds, S. S. Khuder, W. Shou, S. M. Najjar, E. R. Sanchez, FKBP51 controls cellular adipogenesis through p38 kinase-mediated phosphorylation of GR α and PPAR γ . *Mol. Endocrinol.* **28**, 1265–1275 (2014).
58. Q. Meng, D. Cai, Defective hypothalamic autophagy directs the central pathogenesis of obesity via the I κ B kinase β (IKK β)/NF- κ B pathway. *J. Biol. Chem.* **286**, 32324–32332 (2011).
59. M. G. Myers, D. P. Olson, Central nervous system control of metabolism. *Nature* **491**, 357–363 (2012).
60. S. H. Um, F. Frigerio, M. Watanabe, F. Picard, M. Joaquin, M. Sticker, S. Fumagalli, P. R. Allegrini, S. C. Kozma, J. Auwerx, G. Thomas, Absence of S6K1 protects against age- and diet-induced obesity while enhancing insulin sensitivity. *Nature* **431**, 200–205 (2004).
61. L. Khamzina, A. Veilleux, S. Bergeron, A. Marette, Increased activation of the mammalian target of rapamycin pathway in liver and skeletal muscle of obese rats: Possible involvement in obesity-linked insulin resistance. *Endocrinology* **146**, 1473–1481 (2005).
62. D. Cota, K. Proulx, K. A. B. Smith, S. C. Kozma, G. Thomas, S. C. Woods, R. J. Seeley, Hypothalamic mTOR signaling regulates food intake. *Science* **312**, 927–930 (2006).
63. C. Blouet, H. Ono, G. J. Schwartz, Mediobasal hypothalamic p70 S6 kinase 1 modulates the control of energy homeostasis. *Cell Metab.* **8**, 459–467 (2008).
64. Y. Dagon, E. Hur, B. Zheng, K. Wellenstein, L. C. Cantley, B. B. Kahn, P70S6 kinase phosphorylates AMPK on serine 491 to mediate leptin's effect on food intake. *Cell Metab.* **16**, 104–112 (2012).
65. A. Häusl, J. Hartmann, M. Pöhlmann, L. Brix, J.-P. Lopez, E. Brivio, C. Engelhardt, S. Roeh, L. Rudolph, R. Stoffel, K. Hafner, H. Goss, J. Reul, J. Deussing, K. Ressler, N. Gassen, A. Chen, M. Schmidt, The co-chaperone Fkbp5 shapes the acute stress response in the paraventricular nucleus of the hypothalamus. *bioRxiv*, 824664 (2019).
66. M. V. Schmidt, J.-P. Schulke, C. Liebl, M. Stiess, C. Avrabos, J. Bock, G. M. Wozniak, H. A. Davies, N. Zimmermann, S. H. Scharf, D. Trumbach, W. Wurst, W. Zieglsberger, C. Turck, F. Holsboer, M. G. Stewart, F. Bradke, M. Eder, M. B. Müller, T. Rein, Tumor suppressor down-regulated in renal cell carcinoma 1 (DRR1) is a stress-induced actin bundling factor that modulates synaptic efficacy and cognition. *Proc. Natl. Acad. Sci.* **108**, 17213–17218 (2011).
67. J. Nagler, S. C. Schriever, M. De Angelis, P. T. Pfluger, K. W. Schramm, Comprehensive analysis of nine monoamines and metabolites in small amounts of peripheral murine (C57Bl/6 J) tissues. *Biomed. Chromatogr.* **32**, e4151 (2018).
68. S. Martinelli, E. A. Anderzhanova, S. Wiechmann, F. Dethloff, K. Weckmann, T. Bajaj, J. Hartmann, K. Hafner, M. L. Pöhlmann, L. Jollans, G. Maccarrone, F. Hausch, C. W. Turck, A. Philipsen, M. V. Schmidt, B. Kuster, N. C. Gassen, Stress-primed secretory autophagy drives extracellular BDNF maturation. *bioRxiv* **2020**, 2020.05.13.090514 (2020).
69. J. M. T. Wong, P. A. Malec, O. S. Mabrouk, J. Ro, M. Dus, R. T. Kennedy, Benzoyl chloride derivatization with liquid chromatography-mass spectrometry for targeted metabolomics of neurochemicals in biological samples. *J. Chromatogr. A* **1446**, 78–90 (2016).
70. M. Schwaiger, E. Rampler, G. Hermann, W. Miklos, W. Berger, G. Koellensperger, Anion-exchange chromatography coupled to high-resolution mass spectrometry: A powerful tool for merging targeted and non-targeted metabolomics. *Anal. Chem.* **89**, 7667–7674 (2017).

Acknowledgments: We thank C. Kühne, D. Harbich and B. Schmid (Max Planck Institute of Psychiatry, Munich, Germany) for excellent technical assistance and support. We thank J. Deussing and the scientific core unit Genetically Engineered Mouse Models for providing technical support and guidance. We thank the Microscopy Core Facility of the Medical Faculty at the

University of Bonn for providing support and instrumentation funded by the Deutsche Forschungsgemeinschaft, project number: 388169927. **Funding:** This work was supported by the "OptiMD" grant of the Federal Ministry of Education and Research (01EE1401D to M.V.S.), the BioM M4 award "PROCERA" of the Bavarian State Ministry (to M.V.S.), the "GUTMOM" grant of the Federal Ministry of Education and Research (01EA1805, to M.V.S.), and the "Kids2Health" grant of the Federal Ministry of Education and Research (01GL1743C, to M.V.S.). **Author contributions:** A.S.H, G.B., M.V.S., and N.C.G. conceived the project and designed the experiments. A.S.H and L.M.B. managed the mouse lines and genotyping. A.S.H., M.L.P., and L.M.B. performed animal experiments and surgeries. K.H., T.B., and N.C.G. performed protein work. P.G. and T.B. performed and analyzed metabolomics experiments. M.D.A, J.N., and K.-W. S. performed catecholamine extraction. A.S.H. wrote the initial version of the manuscript. M.V.S., A.C., and N.C.G. supervised the research, and all authors revised the manuscript. **Competing interests:** The authors declare

that they have no competing interests. **Data and materials availability:** All data needed to evaluate the conclusions in the paper are present in the paper and/or the Supplementary Materials and in the source data table. All data needed to interpret the metabolomics analyses are included in the source data file. Raw files of MS measurements are deposited at Zenodo and can be accessed using the following DOIs: For Bz measurements, 10.5281/zenodo.5772429; and for IC measurements, 10.5281/zenodo.5775917. Sample IDs can be inferred from the source data file "MS_SAMPLE_IDS_metabolomics."

Submitted 13 March 2021

Accepted 6 January 2022

Published 9 March 2022

10.1126/sciadv.abi4797

Supplementary Materials for

Mediobasal hypothalamic FKBP51 acts as a molecular switch linking autophagy to whole-body metabolism

Alexander S. Häusl*, Thomas Bajaj*, Lea M. Brix, Max L. Pöhlmann, Kathrin Hafner, Meri De Angelis, Joachim Nagler, Frederik Dethloff, Georgia Balsevich, Karl-Werner Schramm, Patrick Giavalisco, Alon Chen, Mathias V. Schmidt, Nils C. Gassen

*Corresponding author. Email: mschmidt@psych.mpg.de (M.V.S.); nils.gassen@ukbonn.de (N.C.G.)

Published 9 March 2022, *Sci. Adv.* **8**, eabi4797 (2022)

DOI: 10.1126/sciadv.abi4797

The PDF file includes:

Figs. S1 to S10

Other Supplementary Material for this manuscript includes the following:

Data S1

Supplementary figure 1: FKBP51 deletion alters AMPK and mTOR-associated amino acid metabolic and biosynthetic pathways.

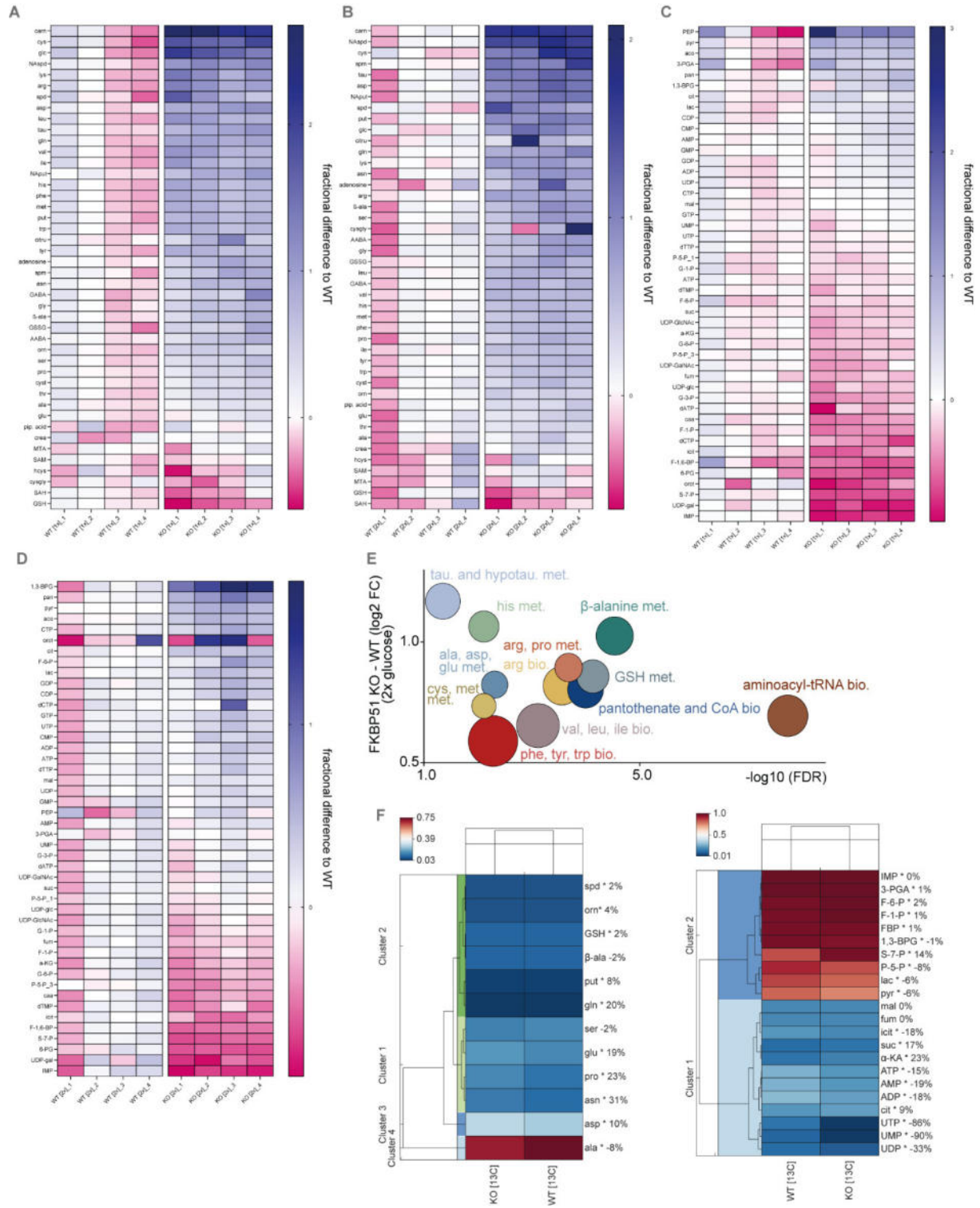


Fig. S1: FKBP51 deletion alters AMPK and mTOR-associated amino acid metabolic and biosynthetic pathways. **(A)** Heatmap of altered amine-containing (Bz) metabolites in SH-SY5Y cells lacking FKBP51 and WT control cells cultured under normal glucose condition (1x, 4.5 g/l) and **(B)** increased glucose condition (2x, 9 g/l). **(C)** Heatmaps of altered anionic (IC) metabolites in SH-SY5Y cells lacking FKBP51 compared to WT control cells under normal and **(D)** increased glucose culturing conditions. The fractional differences of each replicate are shown for all metabolites comparing the genotype and the different glucose conditions. **(E)** Analysis and regulation of significantly altered pathways of FKBP51 KO and WT cells under excessive glucose conditions. The f(x)-axis shows the (median) log₂ fold change (FC) of all significantly altered metabolites of the indicated pathway and the false discovery rate (FDR, equals the $-\log_{10}$ adjusted p-value) is shown on the x-axis. The size of the circles represents the amount of significantly changed metabolites in comparison to all metabolites of a particular pathway. **(F)** Analysis of the metabolic flux in FKBP51 KO cells compared to WT cells using C¹³ glucose as tracer. The enrichment of C¹³ is displayed for each metabolite investigated.

Fig. S2: FKBP51 deletion alters AMPK and mTOR-associated amino acid metabolic and biosynthetic pathways in murine neuroblastoma cells.

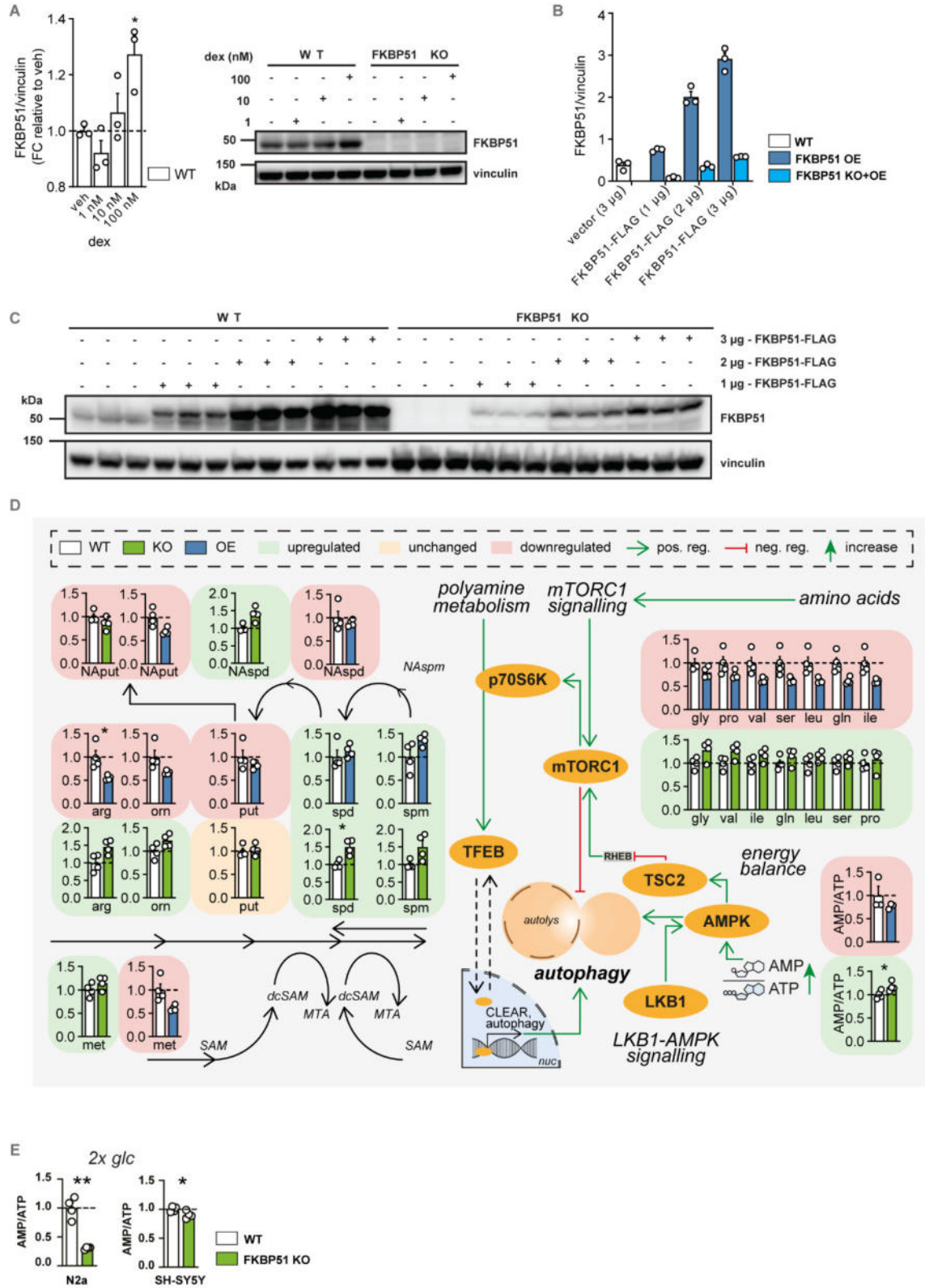


Fig. S2: FKBP51 deletion alters AMPK and mTOR- associated amino acid metabolic and biosynthetic pathways in murine neuroblastoma cells. (A, B) Validation of FKBP51 responsiveness in WT N2a cells to dexamethasone stimulation. (C) Titration of FKBP51-FLAG expression construct in FKBP51 WT and KO N2a cells (n=3). (D) FKBP51 deletion and overexpression (OE) in N2a cells alters metabolites of the polyamine pathway and levels of amino acids associated with mTOR signaling. (E) AMP/ATP ratio in N2a and SH-SY5Y FKBP51 KO cells under increased glucose conditions. All data are shown as relative fold change compared to control condition; \pm s.e.m.; One-way ANOVA followed by Dunnett's multiple comparison test for A, the paired student's t-test was performed in D and E. * $p < 0.05$, ** $p < 0.01$, * $p < 0.001$;**

Abbreviations: AMP, adenosine monophosphate; AMPK, AMP-activated protein kinase; arg, arginine; ATP, adenosine triphosphate; dex, dexamethasone; dcSAM, decarboxylated S-adenosylmethione; glc, glucose; gln, glutamine; gly, glycine; ile, isoleucine; leu, leucine; LKB1, liver kinase B 1; met, methionine; MTA, 5'-methylthioadenosine; mTORC1, mechanistic target of rapamycin complex 1; NAput, N-acetylputrescine; NAspd, N-acetylspermidine; NAspm, N-acetylspermine; orn, ornithine pro; proline; put, putrescine; SAM, S-adenosylmethionine; ser, serine; spd, spermidine; spm, spermine; TFEB, transcription factor EB; TSC2, tuberous sclerosis complex 2; val, valine; veh, vehicle.

Fig. S3: *In-vitro* manipulation of FKBP51 and its effects on autophagy signaling.

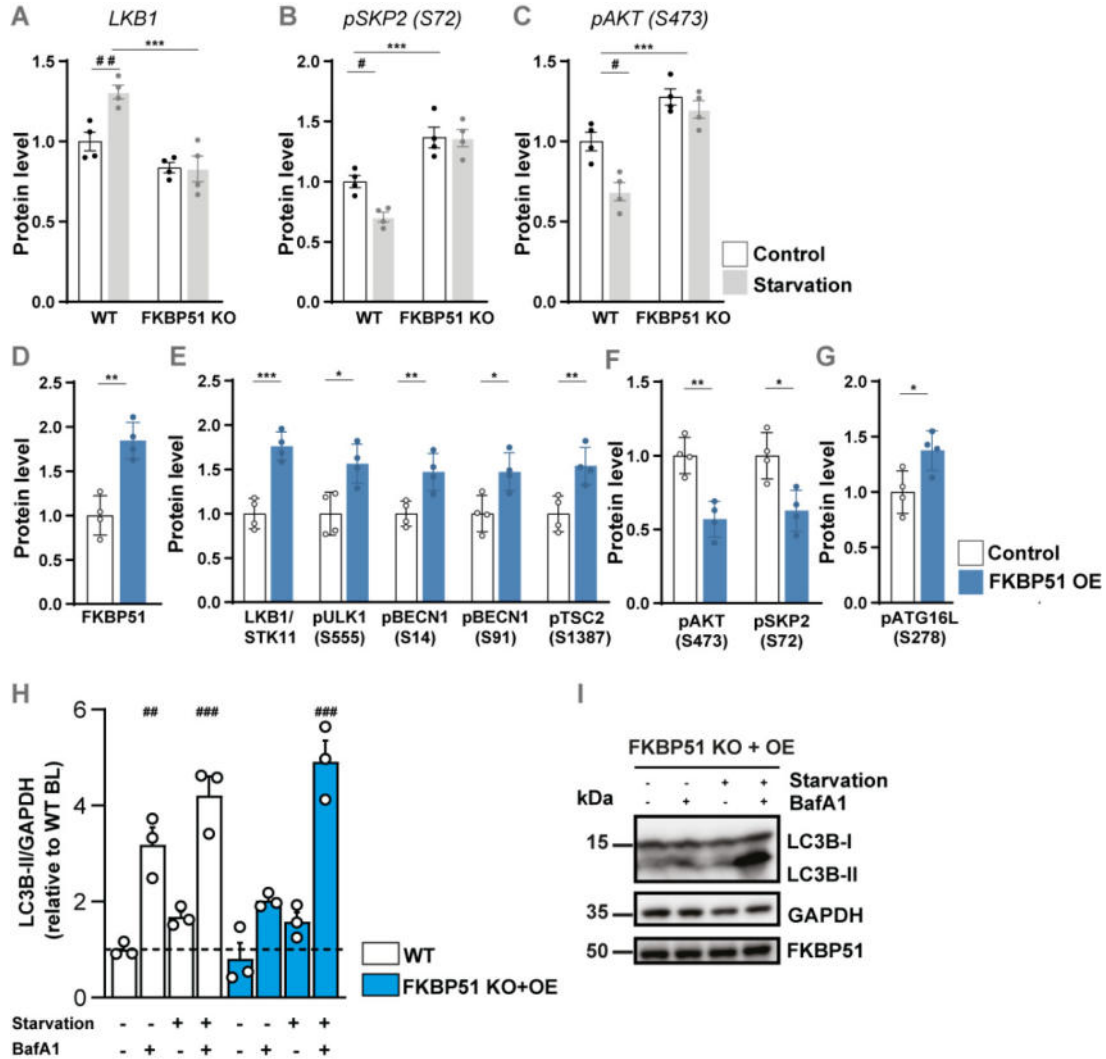


Fig. S3: *In-vitro* manipulation of FKBP51 and its effects on autophagy signaling. Wildtype (WT) or FKBP51 knockout (FKBP51 KO) cells were starved in HBSS medium for 4 h to induce autophagy. The levels of autophagy markers were determined by immunoblotting. **(A)** Quantification of LKB1, **(B)** pSKP2 (S72), and **(C)** pAKT (S473). **(D)** Validation of FKBP51 overexpression (FKBP51 OE) in mouse neuroblastoma cells. **(E)** FKBP51 OE in N2a cells enhanced phosphorylation of autophagy markers regulating autophagy initiation. **(F)** Quantification of pAKT (S473) and pSKP2 (S72). **(G)** Phosphorylation of ATGL16L1 at S278. **(H)** LC3B-II accumulation in FKBP51 KO+OE N2a cells in response to starvation and in the

presence or absence of BafA1 to assess autophagy flux (**I**). Representative blots of autophagy flux assay. All data are shown as relative fold change compared to control condition; \pm s.e.m.; a two-way ANOVA was performed in (**A-C**) and followed by a Tukey's multiple comparison test. One-way ANOVA followed by a Dunnett's multiple comparison test was performed for (**I**). The unpaired student's t-test was performed in (**D-L**). * $p < 0.05$, ** $p < 0.01$, *** $p < 0.001$; # $p < 0.05$, ## $p < 0.01$. * = significant genotype effect; # = significant treatment effect.

Fig. S4: FKBP51 does not alter hypusination of eIF5A.

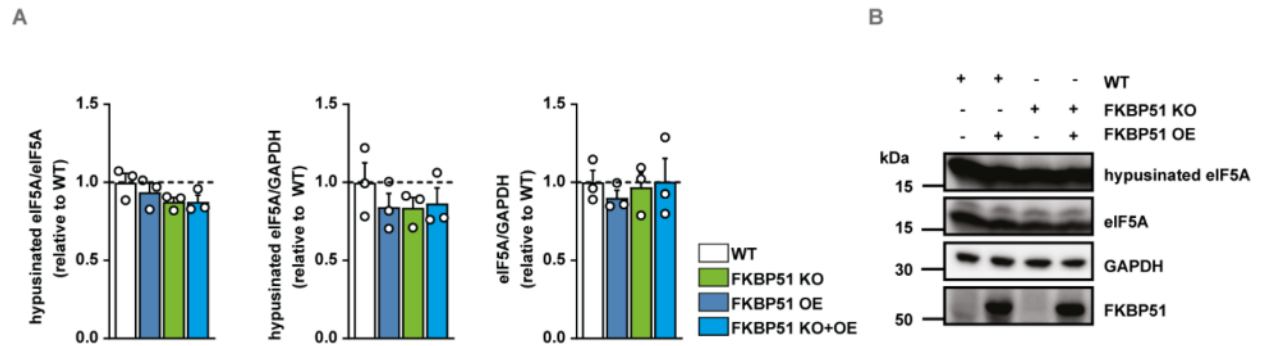


Fig. S4: FKBP51 does not alter hypusination of eIF5A.

(A) Hypusination of eIF5A is not affected by FKBP51 KO or expression level in N2a cells.

(B) Representative blots of hypusinated eIF5A, total eIF5A, GAPDH and FKBP51.

Fig. S5: *In-vitro* manipulation of FKBP51 and its effects on autophagy signaling.

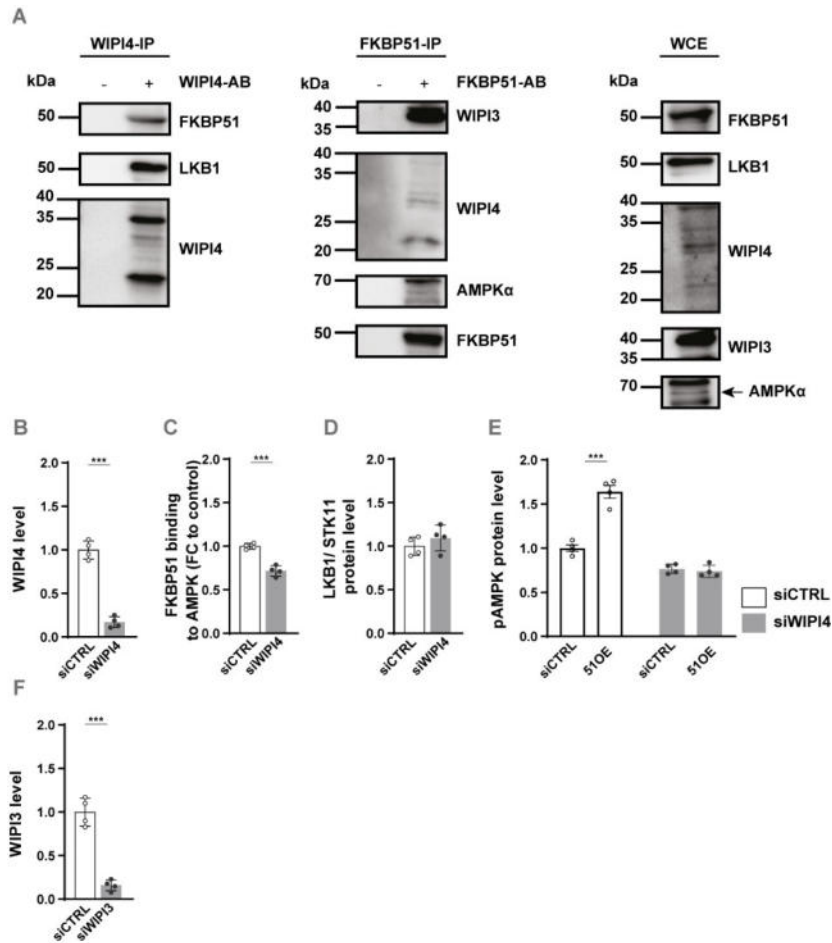


Fig. S5: FKBP51 associates with AMPK, TSC2, and WIPI3 & 4 to regulate autophagy and mTOR signaling. (A) Endogenously expressed FKBP51 associates with WIPI4, LKB1, WIPI3 and AMPK α in WT N2a cells. (B) Confirmation of WIPI4 KD in N2a cells. (C) FKBP51 binding to AMPK α 1 in WIPI4 KD cells. (D) LKB1 binding to FKBP51 was not affected in WIPI4-KD cells. (E) WIPI4 KD blocked the FKBP51 overexpressing (51OE) effect on pAMPK at T172 (F) WIPI3 KD in N2a cells. All data are shown as relative fold change compared to control condition and were analyzed with an unpaired t-test; \pm SEM; * $p < 0.05$, ** $p < 0.01$, *** $p < 0.001$.

Fig. S6: FKBP51 overexpression in the MBH affects sympathetic outflow to muscle and fat tissue.

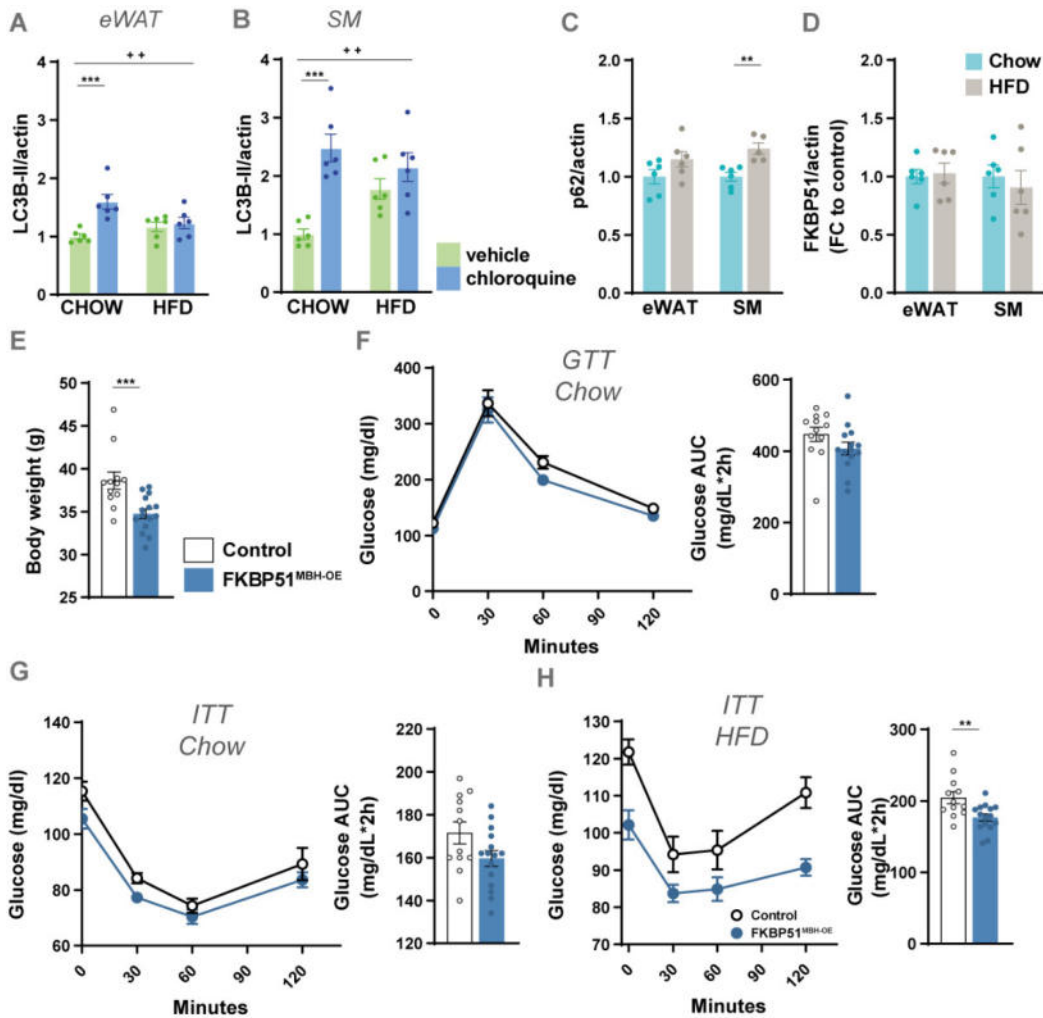


Fig. S6: FKBP51 overexpression in the MBH affects sympathetic outflow to muscle and fat tissue. (A) LC3B-II levels before and after chloroquine treatment (50 mg/kg) in eWAT and **(B)** soleus muscle under chow and HFD conditions **(C)** 10 weeks of HFD increased the accumulation of the autophagy receptor p62 in SM, but not in eWAT. **(D)** FKBP51 expression in soleus muscle (SM) and epididymal white adipose tissue (eWAT) after 10 weeks of HFD. **(E)** Overexpression of FKBP51 in a second cohort of C57/B16 animals resulted in a lean body weight phenotype after 10 weeks of HFD. **(F-H)** Differences in glucose metabolism were investigated by performing a

glucose tolerance test (GTT) and an insulin tolerance test (ITT) under chow and HFD conditions. For **(A, B)** a two-way ANOVA was performed followed by a Tukey's multiple comparisons test and data are shown as relative fold change compared to control condition. For **(C - H)** an unpaired student's t-test was performed. \pm SEM; * $p < 0.05$, ** $p < 0.01$, *** $p < 0.001$; + $p < 0.05$, ++ $p < 0.01$. * = significant treatment effect; + = significant treatment x diet interaction.

Fig. S7: FKBP51 regulates autophagy signaling in the MBH.

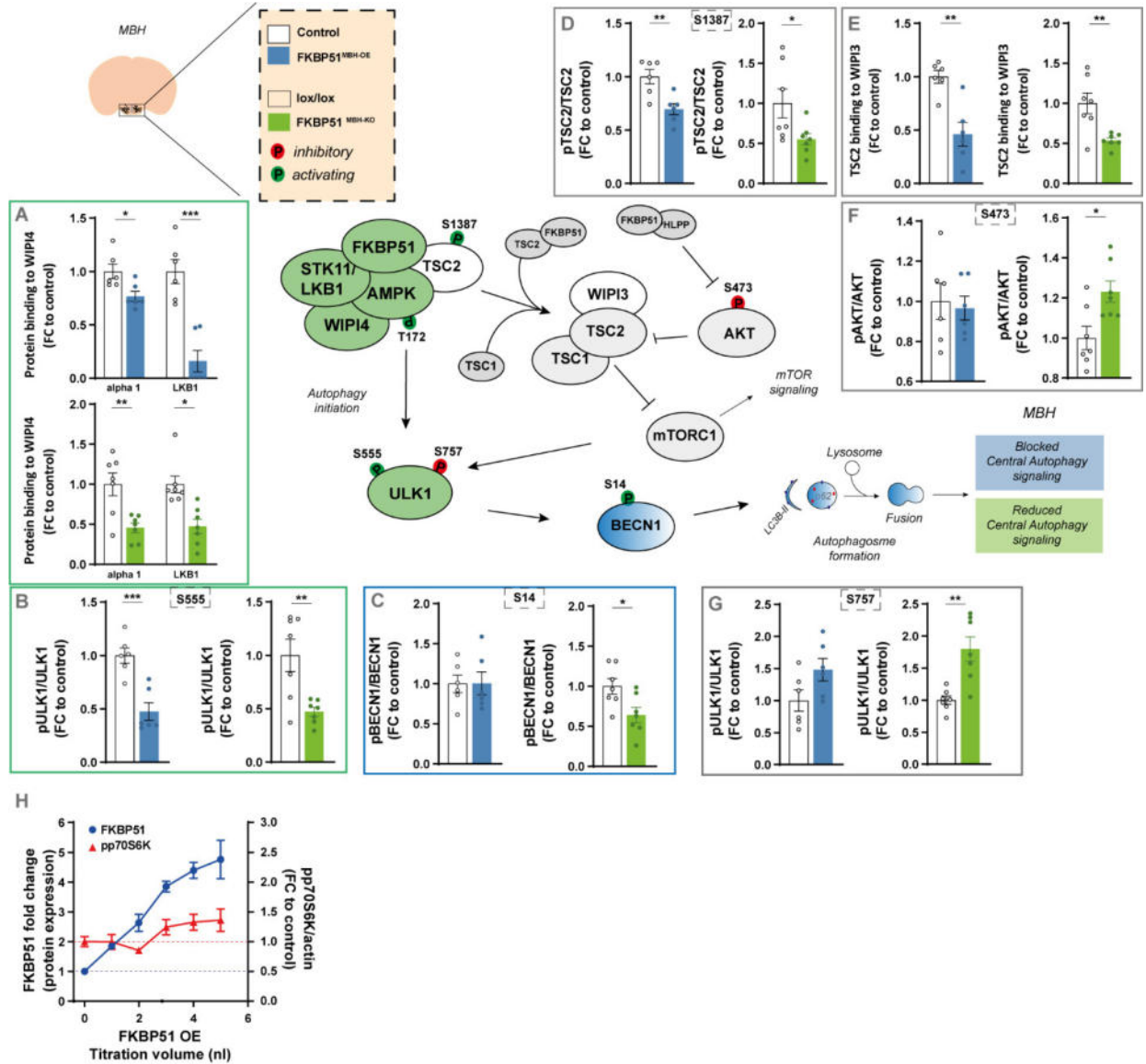


Fig. S7: FKBP51 regulates autophagy signaling in the MBH. Pathway analysis of main autophagy and mTOR regulators in the mediobasal hypothalamus (MBH). FKBP51 overexpression is depicted in blue and FKBP51 deletion is depicted in green. (A) Quantification of LKB1 and AMPK binding to WIPI4. (B) Phosphorylation of ULK1 at S555, (C) pBECN1 at S14, (D) pTSC2 at S1387. (E) Quantification of TSC2 binding to WIPI3. (F) Phosphorylation of AKT at S473, and (G) ULK1 at S757. (H) Quantification of pp70S6K while titrating AAV-HA-

FKBP51 virus into N2a cells. All data are shown as relative fold change compared to control condition and were analyzed with an unpaired t-test.; \pm SEM; * $p < 0.05$, ** $p < 0.01$, *** $p < 0.001$.

Fig. S8: Effects of hypothalamic FKBP51 overexpression on peripheral autophagy signaling.

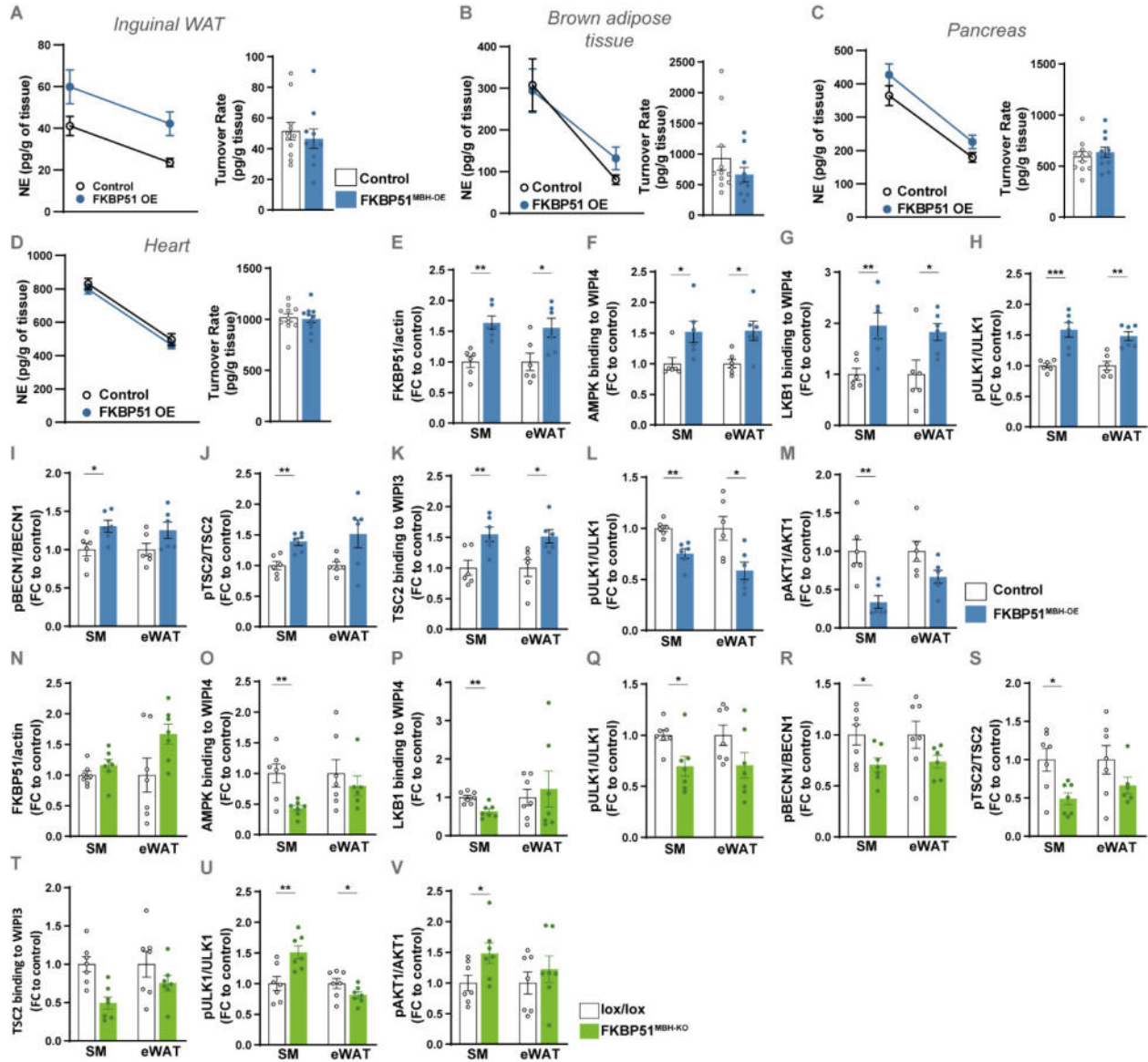


Fig. S8: Effects of hypothalamic FKBP51 overexpression on peripheral autophagy signaling.

(A-D) Representative decrease in tissue NE content after MPT injection (left panel) and turnover rate (right panel) were determined on inguinal WAT and brown adipose tissue (BAT), pancreas, and heart. (E-V) Pathway analysis of main autophagy and mTOR marker in the soleus muscle (SM) and epididymal white adipose tissue (eWAT). FKBP51 overexpression is depicted in blue and FKBP51 deletion is depicted in green. (E) Quantification of FKBP51 protein level. (F)

Quantification of AMPK and (G) LKB1 binding to WIPI4. (H) Phosphorylation of ULK1 at S555, (I) pBECN1 at S14, (J) TSC2 at S1387. (K) Quantification of TSC2 binding to WIPI3. (L) Phosphorylation of ULK1 at S757, and (M) AKT1 at S473. (N) FKBP51 level in SM and eWAT of FKBP51^{MBH-KO} mice. (O) Quantification of AMPK and (P) LKB1 binding to WIPI4. (Q) Phosphorylation of ULK1 at S555, (R) pBECN1 at S14, (S) TSC2 at S1387. (T) Quantification of TSC2 binding to WIPI3. (U) Phosphorylation of ULK1 at S757, and (V) AKT1 at S473. All data are shown as relative fold change compared to control condition and were analyzed with an unpaired t-test.; ± SEM; * p < 0.05, **p < 0.01, ***p < 0.001.

Fig. S9: AMPK and mTOR signaling was not affected in in liver tissue of FKBP51^{MBH-KO} mice.

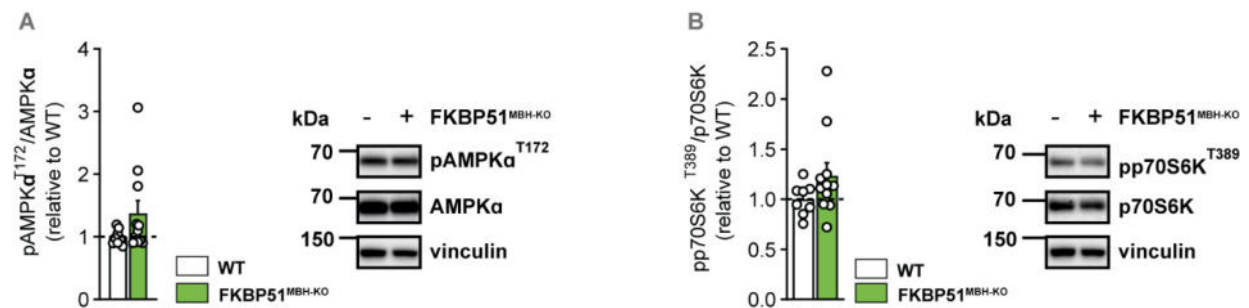


Fig. S9: AMPK and mTOR signaling was not affected in liver tissue of FKBP51^{MBH-KO} mice.

(A) Representative blots and quantification of AMPK phosphorylation at T172 and (B) p70S6K in liver tissue of FKBP51^{MBH-KO} mice (n = 8 for WT, n = 11 for KO). All data are shown as relative fold change compared to control condition and were analyzed with an unpaired t-test.; ± SEM; * p < 0.05, **p < 0.01, ***p < 0.001.

Fig. S10:

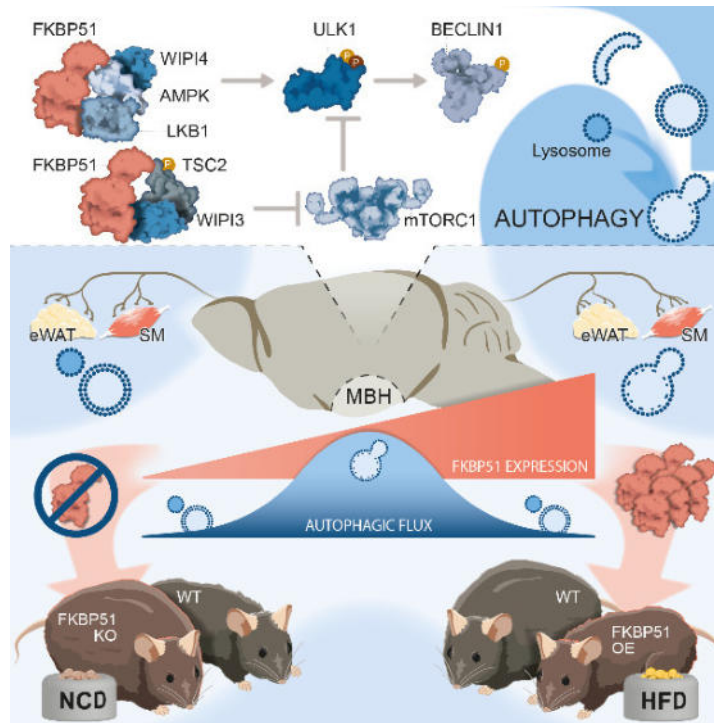


Fig. S10: The stress-responsive FKBP51 controls body weight gain by regulating the balance between autophagy and mTOR signaling. We identified FKBP51 as a central nexus for the recruitment of the LKB1/AMPK complex to WIPI4 and TSC2 to WIPI3, thereby regulating the balance between autophagy and mTOR signaling in response to metabolic challenges. MBH FKBP51 dose-dependently regulates autophagy both in the brain as well as in peripheral metabolic tissues. Consequently, deletion of MBH FKBP51 strongly induces obesity, while its overexpression protects against high-fat diet (HFD) induced obesity.

3.3. The co-chaperone Fkbp5 shapes the acute stress response in the paraventricular nucleus of the hypothalamus of male mice

Authors:

Alexander S. Häusl¹, Lea M. Brix^{1,2}, Jakob Hartmann³, Max L. Pöhlmann¹, Juan-Pablo Lopez⁴, Danusa Menegaz⁵, Elena Brivio^{2,4}, Clara Engelhardt¹, Simone Roeh⁶, Thomas Bajaj⁷, Lisa Rudolph⁴, Rainer Stoffel⁴, Kathrin Hafner⁶, Hannah M. Goss⁸, Johannes M.H.M. Reul⁸, Jan M. Deussing⁹, Matthias Eder⁵, Kerry J. Ressler³, Nils C. Gassen^{6,7}, Alon Chen^{4,10} and Mathias V. Schmidt¹.

Affiliations:

¹ *Research Group Neurobiology of Stress Resilience, Max Planck Institute of Psychiatry, 80804 Munich, Germany*

² *International Max Planck Research School for Translational Psychiatry (IMPRS-TP), Kraepelinstr. 2-10, 80804 Munich, Germany*

³ *Department of Psychiatry, Harvard Medical School, McLean Hospital, Belmont, MA, USA*

⁴ *Department of Stress Neurobiology and Neurogenetics, Max Planck Institute of Psychiatry, 80804 Munich, Germany*

⁵ *Electrophysiology Core Unit, Max Planck Institute of Psychiatry, 80804 Munich, Germany*

⁶ *Department of Translational Research in Psychiatry, Max Planck Institute of Psychiatry, 80804 Munich, Germany*

⁷ *Department of Psychiatry and Psychotherapy, Bonn Clinical Center, University of Bonn, 53127 Bonn, Germany*

⁸ *Neuro-Epigenetics Research Group, Bristol Medical School, University of Bristol, Bristol BS1 3NY, United Kingdom*

⁹ *Research Group Molecular Neurogenetics, Max Planck Institute of Psychiatry, 80804 Munich, Germany*

¹⁰ *Weizmann Institute of Science, Department of Neurobiology, Rehovot, Israel*

Originally published in:

Molecular Psychiatry 26, 3060-3076 (2021)



The co-chaperone Fkbp5 shapes the acute stress response in the paraventricular nucleus of the hypothalamus of male mice

Alexander S. Häusl¹ · Lea M. Brix^{1,2} · Jakob Hartmann³ · Max L. Pöhlmann¹ · Juan-Pablo Lopez⁴ · Danusa Menegaz⁵ · Elena Brivio^{2,4} · Clara Engelhardt¹ · Simone Roeh⁶ · Thomas Bajaj⁷ · Lisa Rudolph⁴ · Rainer Stoffel⁴ · Kathrin Hafner⁶ · Hannah M. Goss⁸ · Johannes M. H. M. Reul⁸ · Jan M. Deussing⁹ · Matthias Eder⁵ · Kerry J. Ressler³ · Nils C. Gassen^{6,7} · Alon Chen^{4,10} · Mathias V. Schmidt¹

Received: 21 November 2019 / Revised: 19 January 2021 / Accepted: 2 February 2021
© The Author(s) 2021. This article is published with open access

Abstract

Disturbed activation or regulation of the stress response through the hypothalamic-pituitary-adrenal (HPA) axis is a fundamental component of multiple stress-related diseases, including psychiatric, metabolic, and immune disorders. The FK506 binding protein 51 (FKBP5) is a negative regulator of the glucocorticoid receptor (GR), the main driver of HPA axis regulation, and *FKBP5* polymorphisms have been repeatedly linked to stress-related disorders in humans. However, the specific role of *Fkbp5* in the paraventricular nucleus of the hypothalamus (PVN) in shaping HPA axis (re)activity remains to be elucidated. We here demonstrate that the deletion of *Fkbp5* in *Sim1*⁺ neurons dampens the acute stress response and increases GR sensitivity. In contrast, *Fkbp5* overexpression in the PVN results in a chronic HPA axis over-activation, and a PVN-specific rescue of *Fkbp5* expression in full *Fkbp5* KO mice normalizes the HPA axis phenotype. Single-cell RNA sequencing revealed the cell-type-specific expression pattern of *Fkbp5* in the PVN and showed that *Fkbp5* expression is specifically upregulated in *Crh*⁺ neurons after stress. Finally, *Crh*-specific *Fkbp5* overexpression alters *Crh* neuron activity, but only partially recapitulates the PVN-specific *Fkbp5* overexpression phenotype. Together, the data establish the central and cell-type-specific importance of *Fkbp5* in the PVN in shaping HPA axis regulation and the acute stress response.

These authors contributed equally: Alexander S. Häusl, Lea M. Brix

Supplementary information The online version contains supplementary material available at <https://doi.org/10.1038/s41380-021-01044-x>.

✉ Mathias V. Schmidt
mschmidt@psych.mpg.de

¹ Research Group Neurobiology of Stress Resilience, Max Planck Institute of Psychiatry, Munich, Germany

² International Max Planck Research School for Translational Psychiatry (IMPRS-TP), Munich, Germany

³ Department of Psychiatry, Harvard Medical School, McLean Hospital, Belmont, MA, USA

⁴ Department of Stress Neurobiology and Neurogenetics, Max Planck Institute of Psychiatry, Munich, Germany

⁵ Electrophysiology Core Unit, Max Planck Institute of Psychiatry, Munich, Germany

Introduction

Life is full of challenges and appropriate coping with such events implies proper activation and termination of the stress response. The hypothalamic-pituitary-adrenal (HPA) axis is the central orchestrator of the stress response and its end product glucocorticoids (cortisol in humans, corticosterone (CORT) in rodents) mediates the adaptation to acute

⁶ Department of Translational Research in Psychiatry, Max Planck Institute of Psychiatry, Munich, Germany

⁷ Department of Psychiatry and Psychotherapy, Bonn Clinical Center, University of Bonn, Bonn, Germany

⁸ Neuro-Epigenetics Research Group, Bristol Medical School, University of Bristol, Bristol, United Kingdom

⁹ Research Group Molecular Neurogenetics, Max Planck Institute of Psychiatry, Munich, Germany

¹⁰ Department of Neurobiology, Weizmann Institute of Science, Rehovot, Israel

and chronic stressors in peripheral tissues as well as in the brain [1]. A hallmark of HPA axis regulation is the negative feedback on the secretion of stress hormones to terminate the stress response which is controlled by glucocorticoids via the glucocorticoid receptor (GR).

A critical regulator of GR and therefore key to a successful termination of the stress response is FKBP5 binding protein 51 (FKBP5), which is encoded by the *FKBP5* gene [2]. FKBP5 is an Hsp90-associated co-chaperone that restricts GR function by reducing ligand binding, delaying nuclear translocation, and decreasing GR-dependent transcriptional activity [3, 4]. Hence, higher levels of *FKBP5* mRNA are associated with higher levels of circulating cortisol and reduced negative feedback inhibition of the stress response [5–9]. Consequently, GR-induced *FKBP5* levels reflect the environmental stress condition, and as such, *FKBP5* expression has been used as a stress-responsive gene marker [10]. Importantly, *FKBP5* polymorphisms have been consistently associated with stress-related psychiatric disorders such as major depression and PTSD [11–13], where a demethylation-mediated increase in *FKBP5* expression was identified as causal in risk-allele carriers [14].

Despite the central importance of FKBP5 in stress system biology and stress-related disorders, detailed functional and mechanistic studies are still largely missing. Only a few human post-mortem studies focus on central tissue in order to dissect FKBP5 mechanisms [15, 16], while the majority of studies use peripheral blood mononuclear cells as a correlate of FKBP5 brain activity [17]. Most of the animal data were obtained from wild-type (WT) or conventional *Fkbp5* knockout mice, thereby lacking cell-type-specific insights of *Fkbp5* function [8, 18]. To tackle this paucity of information, we here investigate the specific role of *Fkbp5* in the paraventricular nucleus of the hypothalamus (PVN) the key brain region orchestrating the stress response [19]. Interestingly, previous data in rats suggested a potentially decisive role of *Fkbp5* expression in the PVN to drive HPA axis hyperactivity achieved by a selective breeding approach [20]. Using site-specific manipulations of *Fkbp5*, single-cell RNA expression profiling, and functional downstream pathway analyzes, our data unravel a key role of PVN *Fkbp5* in shaping the body's stress system (re) activity, with important implications for its contribution to stress-related disorders.

Material and methods

Animals and animal housing

All experiments were performed in accordance with the European Communities' Council Directive 2010/63/EU. The protocols were approved by the committee for the care

and use of laboratory animals of the Government of Upper Bavaria, Germany. The mouse lines *Fkbp5*^{lox/lox}, *Fkbp5*^{PVN-/-}, *Fkbp5*^{Frt/Frt}, and CRH-ires-CRE/Ai9 were generated in house. Experiments were performed on male mice aged between 3 and 5 months unless stated otherwise in the results section. During the experimental time, animals were kept singly housed in individually ventilated cages (IVC; 30 cm × 16 cm × 16 cm; 501 cm²), serviced by a central airflow system (Tecniplast, IVC Green Line—GM500). Animals were maintained on a 12:12 h light/dark cycle, with constant temperature (23 ± 2 °C) and humidity of 55% during all times. Experimental animals received *ad libitum* access to water and a standard research diet (Altromin 1318, Altromin GmbH, Germany) and IVCs had sufficient bedding and nesting material as well as a wooden tunnel for environmental enrichment. Animals were allocated to experimental groups in a semi-randomized fashion and data analysis was performed blinded to the group allocation.

Generation of *Fkbp5* mice

Conditional *Fkbp5* knockout mice are derived from embryonic stem cell clone EPD0741_3_H03 which was targeted by the knockout mouse project (KOMP). Frozen sperm obtained from the KOMP repository at UC Davis was used to generate knockout mice (*Fkbp5*^{tm1a(KOMP)Wtsi}) by in vitro fertilization. These mice designated as *Fkbp5*^{Frt/Frt} are capable to re-express functional *Fkbp5* upon Flp recombinase-mediated excision of an *frt*-flanked reporter-selection cassette integrated into the *Fkbp5* gene. Mice with a floxed *Fkbp5* gene designated as *Fkbp5*^{lox/lox} (*Fkbp5*^{tm1c(KOMP)Wtsi}) were obtained by breeding *Fkbp5*^{Frt/Frt} mice to Deleter-Flpe mice [21]. Finally, mice lacking *Fkbp5* in PVN neurons (*Fkbp5*^{PVN-/-}) were obtained by breeding *Fkbp5*^{lox/lox} mice to Sim1-Cre mice [22]. The CRH-ires-CRE/Ai9 mouse line was generated previously [23]. Genotyping details are available upon request.

Viral overexpression and rescue of *Fkbp5*

For overexpression and rescue experiments, stereotactic injections were performed as described previously [24]. In brief, mice aged between 10 and 12 weeks were anesthetized with isoflurane, and 0.2 µl of the below-mentioned viruses (titers: 1.6 × 10^{12–13} genomic particles/ml) were bilaterally injected in the PVN at 0.05 µl/min by glass capillaries with tip resistance of 2–4 MΩ in a stereotactic apparatus. The following coordinates were used: –0.45 mm anterior to bregma, 0.3 mm lateral from midline, and 4.8 mm below the surface of the skull, targeting the PVN. After surgery, mice were treated for 3 days with Metacam via i.p. injections and were allowed to recover for 3–4 weeks before

the start of the testing. Successful overexpression or reinstatement of *Fkbp5* was verified by ISH and RNAscope. For in vivo experiments, we used adeno-associated bicistronic AAV1/2 vectors. In the overexpression experiments, the vector contained a CAG-HA-tagged-FKBP51-WPRE-BGH-polyA expression cassette (containing the coding sequence of human Fkbp51 NCBI CCDS ID CCDS4808.1). The same vector constructs without expression of *Fkbp5* (CAG-Null/Empty-WPRE-BGH-polyA) was used as a control. For the *Crh* specific overexpression of *Fkbp5*, we used a viral vector containing an AAV1/2-Cre-dept-HA-FKBP51 (pAAV-Cre-dependent-CAG-HA-human wildtype FKBP51 WPRE-BGH-polyA) and a control virus containing AAV1/2-Cre-dept-GFP (pAAV-Cre-dependent-CAG-GFP-WPRGE-BGH-polyA). Virus production, amplification, and purification were performed by GeneDetect. For the rescue experiment, a viral vector containing a flippase expressing cassette (AAV2-eSYN-eGFP-T2A-FLPo, Vector Biolabs; VB1093) was used to induce endogenous *Fkbp5* expression in *Fkbp5*^{FRT/FRT} mice. Control animals were injected with a control virus (AAV2-eSYN-eGFP; Vector Biolabs; VB1107).

Acute stress paradigm

For acute stress exposure, the restraint stress paradigm was used, as it was shown to be a reliable and robust stressor in rodents [25]. One to 2 h after lights on each animal was placed in a restrainer (50 ml falcon tube with holes at the bottom and the lid to provide enough oxygen and space for tail movement) for 15 min in their individual home cage. After 15 min, animals were removed from the tube and the first blood sample was collected by tail cut. Until the following tail cuts at 30, 60, and 90 min after stress onset, the animals remained in their home cage to recover. Basal CORT levels (morning CORT) were collected one week prior to the acute stress paradigm at 8 a.m.

Combined Dex/CRH test

To investigate the HPA axis function we performed a combined Dex/CRH test as described previously [8]. On an experimental day, mice were injected with a low dose of dexamethasone (0.05 mg/kg, Dex-Ratiopharm, 7633932) via i.p injections at 9 a.m. in the morning. At this dose Dex does not cross the blood-brain barrier and acts predominantly in the periphery [26] Here, the most important site of action in relation to HPA axis function, especially when combined with a challenge with the neuropeptide CRH, is the pituitary. Thus, 6 h after Dex injection, a blood sample was collected via tail cut (after Dex value), followed by an injection of CRH (0.15 mg/kg, CRH Ferrin Amp). Thirty-minute after CRH injection, another blood sample

was obtained (after CRH value). All samples from the acute stress experiments and the Dex/CRH test were collected in 1.5 ml EDTA-coated microcentrifuge tubes (Sarstedt, Germany). All blood samples were kept on ice and were centrifuged for 15 min at 8000 rpm and 4 °C. Plasma was transferred to new, labeled microcentrifuge tubes and stored at −20 °C until further processing.

Sampling procedure

On the day of sacrifice, animals were deeply anesthetized with isoflurane and sacrificed by decapitation. Trunk blood was collected in labeled 1.5 ml EDTA-coated microcentrifuge tubes (Sarstedt, Germany) and kept on ice until centrifugation. After centrifugation (4 °C, 8000 rpm for 1 min) the plasma was removed and transferred to new, labeled tubes and stored at −20 °C until hormone quantification. For mRNA analysis, brains were removed, snap-frozen in isopentane at −40 °C, and stored at −80 °C for ISH. For protein analysis, brains were removed and placed inside a brain matrix with the hypothalamus facing upwards (spacing 1 mm, World Precision Instruments, Berlin, Germany). Starting from the middle of the chiasma opticum, a 1 mm thick brain slice was removed. The PVN was further isolated by cutting the slice on both sides of the PVN along the fornices (parallel to the 3rd ventricle) as a landmark and a horizontal cut between the reuniens and the thalamic nucleus. Finally, the slice containing the third ventricle was bisected, and the distal part discarded. The remaining part (containing the PVN) was immediately shocked frozen and stored at −80 °C until protein analysis [27]. The adrenals and thymus glands were dissected from fat and weighed.

Hormone assessment

CORT and ACTH concentrations were determined by radioimmunoassay using a corticosterone double-antibody ¹²⁵I RIA kit (sensitivity: 12.5 ng/ml, MP Biomedicals Inc.) and adrenocorticotrophic double-antibody hormone ¹²⁵I RIA kit (sensitivity: 10 pg/ml, MP Biomedicals Inc.) and were used following the manufacturers' instructions. Radioactivity of the pellet was measured with a gamma counter (Packard Cobra II Auto Gamma; Perkin-Elmer). Fifteen-minute post-stress analysis of ACTH concentrations was analyzed by using ACTH ELISA (IBL international GmbH, RE53081) and the ELISA was performed as recommended by the manufacturer. Final CORT and ACTH levels were derived from the standard curve.

In situ hybridization (ISH)

ISH was used to analyze mRNA expression of the major stress markers, *Fkbp5*, *Gr*, *Crh*, and *Avp*. Therefore, frozen

brains were sectioned at -20°C in a cryostat microtome at $20\ \mu\text{m}$, thaw mounted on Super Frost Plus slides, dried, and stored at -80°C . The ISH using ^{35}S UTP labeled ribonucleotide probes was performed as described previously [28, 29]. All primer details are available upon request. Briefly, sections were fixed in 4% paraformaldehyde and acetylated in 0.25% acetic anhydride in 0.1 M triethanolamine/HCl. Subsequently, brain sections were dehydrated in increasing concentrations of ethanol. The antisense cRNA probes were transcribed from a linearized plasmid. Tissue sections were saturated with $100\ \mu\text{l}$ of hybridization buffer containing approximately $1.5 \times 10^6\ \text{cpm}$ ^{35}S labeled riboprobe. Brain sections were coverslipped and incubated overnight at 55°C . On the next day, the sections were rinsed in $2 \times \text{SSC}$ (standard saline citrate), treated with RNase A (20 mg/l). After several washing steps with SSC solutions at room temperature, the sections were washed in $0.1 \times \text{SSC}$ for 1 h at 65°C and dehydrated through increasing concentrations of ethanol. Finally, the slides were air-dried and exposed to Kodak Biomax MR films (Eastman Kodak Co., Rochester, NY) and developed. Autoradiographs were digitized, and expression was determined by optical densitometry utilizing the freely available NIH ImageJ software. The mean of four measurements of two different brain slices was calculated for each animal. The data were analyzed blindly, always subtracting the background signal of a nearby structure not expressing the gene of interest from the measurements. For *Fkbp5*, exemplary slides were dipped in Kodak NTB2 emulsion (Eastman Kodak Co., Rochester, NY) and exposed at 4°C for representative pictures; exposure time was adjusted to average expression level. Slides were developed and examined with a light microscope with darkfield condensers to show mRNA expression.

RNAscope analysis and cell counting

For the RNAscope experiments, C57Bl/6 male mice were obtained from The Jackson Laboratory (Bar Harbor, ME, USA). All procedures conformed to National Institutes of Health guidelines and were approved by McLean Hospital Institutional Animal Care and Use Committee. Mice were housed in a temperature-controlled colony in the animal facilities of McLean Hospital in Belmont, MA, USA. All mice were group-housed and maintained on a 12:12 h light/dark cycle (lights on at 7 a.m.). Food and water were available ad libitum unless specified otherwise. Mice were 12 weeks at the time of tissue collection. Animals were allowed to acclimate to the room for 1 week before the beginning of the experiment. During the experiment, mice were either left undisturbed (ctrl) or subjected to 14 h (overnight) of food deprivation prior to sacrifice. During the stress procedure, animals were kept in their home cages and

had free access to tap water. All mice were sacrificed by decapitation in the morning (08:00 to 08:30 a.m.) following quick anesthesia by isoflurane. Brains were removed, snap-frozen in isopentane at -40°C , and stored at -80°C . Frozen brains were sectioned in the coronal plane at -20°C in a cryostat microtome at $18\ \mu\text{m}$, mounted on Super Frost Plus slides, and stored at -80°C . The RNA Scope Fluorescent Multiplex Reagent kit (cat. no. 320850, Advanced Cell Diagnostics, Newark, CA, USA) was used for mRNA staining. Probes used for staining were; mm-Avp-C3, mm-Crh-C3, mm-Fkbp5-C2, mm-Oxt-C3, mm-Sst-C3, and mm-Trh-C3. The staining procedure was performed according to the manufacturer's specifications. Briefly, sections were fixed in 4% paraformaldehyde for 15 min at 4°C . Subsequently, brain sections were dehydrated in increasing concentrations of ethanol. Next, tissue sections were incubated with protease IV for 30 min at room temperature. Probes (probe diluent (cat. no. 300041 used instead of C1-probe), Fkbp5-C2, and one of the above C3-probes) were hybridized for 2 h at 40°C followed by four hybridization steps of the amplification reagents 1–4. Next, sections were counterstained with DAPI, cover-slipped, and stored at 4°C until image acquisition. Images of the PVN (left and right side) were acquired by an experimenter blinded to the condition of the animals. Sixteen-bit images of each section were acquired on a Leica SP8 confocal microscope using a $40\times$ objective ($n = 3$ animals per marker and condition). For every individual marker, all images were acquired using identical settings for laser power, detector gain, and amplifier offset. Images of both sides were acquired as a z-stack of 3 steps of $1.0\ \mu\text{m}$ each. *Fkbp5* mRNA expression and co-expression were analyzed using ImageJ with the experimenter blinded to the condition of the animals. *Fkbp5* mRNA was counted manually and each cell containing 1 mRNA dot was counted as positive.

Single-cell sequencing. Tissue dissociation

Single-cell sequencing was performed on PVN tissue dissected from male C57Bl/6 mice aged between 8 and 12 weeks. Therefore, mice were anesthetized lethally using isoflurane and perfused with cold PBS. Brains were quickly dissected, transferred to ice-cold oxygenated artificial cerebral spinal fluid (aCSF), and kept in the same solution during dissection. Sectioning was performed using a $0.5\ \text{mm}$ stainless steel adult mouse brain matrix (Kent Scientific) and a Personna double edge prep razor blade. A slide (approximately $-0.58\ \text{mm}$ Bregma to $-1.22\ \text{mm}$ Bregma) was obtained from each brain and the extended PVN was manually dissected under the microscope. The PVN from five different mice was pooled and dissociated using the Papain dissociation system (Worthington) following the manufacturer's instructions. All solutions were

oxygenated with a mixture of 5% CO₂ in O₂. After this, the cell suspension was filtered with a 30 µm filter (Partec) and kept in cold and oxygenated aCSF.

Cell capture, library preparation, and high-throughput sequencing

Cell suspensions of PVN with ~1,000,000 cells/µL were used. Cells were loaded onto two lanes of a 10X Genomics Chromium chip per factory recommendations. Reverse transcription and library preparation was performed using the 10X genomics single-cell v2.0 kit following the 10X genomics protocol. The library molar concentration and fragment length were quantified by qPCR using KAPA Library Quant (Kapa Biosystems) and Bioanalyzer (Agilent high sensitivity DNA kit), respectively. The library was sequenced on a single lane of an Illumina HiSeq4000 system generating 100 bp paired-end reads at a depth of ~340 million reads per sample.

Quality control and identification of cell clusters

Pre-processing of the data was done using the 10X genomics cell ranger software version 2.1.1 in default mode. The 10X genomics supplied reference data for the mm10 assembly and corresponding gene annotation was used for alignment and quantification. All further analysis was performed using SCANPY version 1.3.7 [30]. A total of 5.113 cells were included after filtering gene counts (<750 and >6.000), UMI counts (>25.000), and the fraction of mitochondrial counts (>0.2). Combat [31] was used to remove chromium channels as batch effects from normalized data. The 4.000 most variable genes were subsequently used as input for Louvain cluster detection. Cell types were determined using a combination of marker genes identified from the literature and gene ontology for cell types using the web-based tool: mousebrain.org (<http://mousebrain.org/genesearch.html>).

Western blot analysis

Protein extracts were obtained by lysing cells in RIPA buffer (150 mM NaCl, 1% IGEPAL CA-630, 0.5% Sodium deoxycholate, 0.1% SDS 50 mM Tris (pH8.0)) freshly supplemented with protease inhibitor (Merck Millipore, Darmstadt, Germany), benzonase (Merck Millipore), 5 mM DTT (Sigma Aldrich, Munich, Germany), and phosphatase inhibitor cocktail (Roche, Penzberg, Germany). Proteins were separated by SDS-PAGE and electro-transferred onto nitrocellulose membranes. Blots were placed in Tris-buffered saline, supplemented with 0.05% Tween (Sigma Aldrich) and 5% non-fat milk for 1 h at room temperature, and then incubated with primary antibody (diluted in TBS/0.05% Tween)

overnight at 4 °C. The following primary antibodies were used: Actin (1:5000, Santa Cruz Biotechnologies, sc-1616), GR (1:1000, Cell Signaling Technology, #3660), p-GR Ser211 (1:500, Sigma, SAB4503820), p-GR Ser226 (1:1000, Sigma, SAB4503874), p-GR 203 (1:500, Sigma, SAB4504585), FKBP51 (1:1000, Bethyl, A301-430A).

Subsequently, blots were washed and probed with the respective horseradish peroxidase or fluorophore-conjugated secondary antibody for 1 h at room temperature. The immuno-reactive bands were visualized either using ECL detection reagent (Millipore, Billerica, MA, USA) or directly by excitation of the respective fluorophore. Determination of the band intensities was performed with BioRad, ChemiDoc MP. For quantification of phosphorylated GR, the intensity of phosphor-GR was always referred to as the signal intensity of the corresponding total GR.

Chromatin preparation for chromatin immunoprecipitation (ChIP) analysis

The GR ChIP was performed as previously described [32]. We added 1 mM AEBSF or 0.1 mM PMSF, 5 mM Na⁺-Butyrate (NaBut), and PhosSTOP phosphatase inhibitor cocktail tablets (1 per 10 ml; Roche, Burgess Hill, UK) to all solutions unless otherwise stated. Briefly, hypothalamus tissues from four mice were cross-linked for 10 min in 1% formaldehyde in PBS. Crosslinking was terminated by adding glycine (5 min, final concentration 200 µM) and centrifuged (5 min, 6000 g, 4 °C). Pellets were washed three times with ice-cold PBS. Next, the pellets were re-suspended in ice-cold Lysis Buffer [50 mM Tris-HCl pH 8, 150 mM NaCl, 5 mM EDTA pH 8.0, 0.5% v/v Igepal, 0.5% Na-deoxycholate, 1% SDS, 5 mM NaBut, 2 mM AEBSF, 1 mM Na₃VO₄, complete ultra EDTA-free protease inhibitor tablets and PhosSTOP phosphatase inhibitor cocktail tablet (both 1 per 10 ml, Roche, Burgess Hill, UK)] and rotated for 15 min at 4 °C. Samples were aliquoted, sonicated (high power; 2 × 10 cycles; 30 s ON, 60 s OFF) using a water-cooled (4 °C) Bioruptor Pico (Diagenode, Liège, Belgium) and centrifuged (10 min, 20,000 g, 4 °C). Supernatants (containing the sheared chromatin) were recombined and re-aliquoted into fresh tubes for subsequent ChIP analysis and for assessment of Input DNA (i.e., the starting material). Chromatin was sonicated to a length of ~500 base pairs.

For ChIP analysis

Aliquots of chromatin were diluted ten-times in ice-cold Dilution Buffer [50 mM Tris-HCl pH 8.0, 150 mM NaCl, 5 mM EDTA pH 8.0, 1% v/v Triton, 0.1% Na-deoxycholate 5 mM NaBut, 1 mM AEBSF, complete ultra EDTA-free protease inhibitor tablets and PhosSTOP phosphatase inhibitor

cocktail tablet (both 1 per 10 ml, Roche)]. 10 μ l of GR antibody (ProteinTech, USA) was added to each sample, and tubes were rotated overnight at 4 °C. Protein A-coated Dynabeads® (Life Technologies) were washed once in ice-cold 0.5% BSA/PBS before blocking overnight at 4 °C. Pre-blocked beads were washed once in ice-cold Dilution buffer, re-suspended in the antibody:chromatin mix, and allowed to incubate for 3 h at 4 °C to allow binding of beads to antibody:chromatin complexes. After 3 h, the samples were placed in a magnetic stand to allow the beads (with the Bound fraction bound) to separate from the liquid “Unbound” fraction. Beads carrying the Bound chromatin were washed three times with ice-cold RIPA buffer [10 mM Tris-HCl pH 7.5, 1 mM EDTA pH 7.5, 0.1% SDS, 0.5 mM EGTA, 1% Triton, 0.1% Na-Deoxycholate, 140 mM NaCl + inhibitors] and washed twice with ice-cold Tris-EDTA buffer. Bound DNA was eluted in two steps at room temperature; first with 200 μ l Elution buffer 1 (10 mM Tris-HCl pH 7.4, 50 mM NaCl, 1.5% SDS) and second with 100 μ l Elution buffer 2 (10 mM Tris-HCl pH 7.4, 50 mM NaCl, 0.5% SDS). Crosslinks were reversed by the addition of NaCl (final concentration 200 mM) and overnight incubation at 65 °C. The next day, samples were incubated first with RNase A (60 μ g/ml, 37 °C, 1 h), followed by incubation with proteinase K (250 μ g/ml, 37 °C, 3.5 h). DNA was purified using a QIAquick PCR purification kit (Qiagen) as per the manufacturer’s instructions. Input samples were incubated overnight at 65 °C with 200 mM NaCl to reverse crosslinks, incubated with RNase A and proteinase K (overnight), and DNA was purified using a Qiagen PCR purification kit. All samples (bounds and inputs) were diluted to a standardized concentration with nuclease-free water and analyzed by qPCR as described below using primers/probes (forward: 5′-TGTC AATGGACAAGTCATAAGAAACC; reverse: 5′-GAATCTCACATCCAATTATATCAACAGAT; probe: 5′-TTCCATTTTCGGGCTCGTTGACGTC). The binding of GR was expressed as a percentage of input DNA, i.e., % Input, which is a measure of the enrichment of steroid receptor bound to specific genomic sequences.

qPCR analysis

Mastermix for qPCR was prepared to contain 900 nM forward and reverse primers, 200 nM probe, 1X TaqMan fast mastermix (Life Technologies, Paisley, UK), and nuclease-free water. Primers and dual-labeled probes with 6-FAM as the fluorescent dye and TAMRA as the quencher were designed using Primer Express software (Version 3.0.1, Life Technologies). Standard curves were performed for each primer pair and the qPCR efficiency was calculated using the equation: $E = ((10 - 1/\text{slope}) - 1) \times 100$ (where E is qPCR efficiency and the slope is the gradient of the standard curve). Only primer pairs with efficiencies greater

than 90% were used. Quantitative PCR was performed using a StepOne Plus machine (Life Technologies, Paisley, UK). Taq enzymes were activated at 95 °C for 20 s, then 40 cycles of 95 °C (1 s) to 60 °C (20 s) were performed to amplify samples.

Electrophysiology

A separate cohort of CRH-ires-CRE/Ai9 mice (Fkbp5^{CRHOE} $n = 4$, Control $n = 4$) was used for electrophysiology experiments. Mice underwent surgery as described above. After 3–4 weeks of recovery, mice were anesthetized with isoflurane and decapitated. The brain was rapidly removed from the cranial cavity and, using a vibratome (HM650V, Thermo Scientific), 350 μ m-thick coronal slices containing the PVN were cut in an ice-cold carbonated gas (95% O₂/5% CO₂)-saturated solution consisting of (in mM): 87 NaCl, 2.5 KCl, 25 NaHCO₃, 1.25 NaH₂PO₄, 0.5 CaCl₂, 7 MgCl₂, 10 glucose, and 75 sucrose. Slices were incubated in carbonated physiological saline for 30 min at 34 °C and, afterward, for at least 30 min at room temperature (23–25 °C). The physiological saline contained (in mM): 125 NaCl, 2.5 KCl, 25 NaHCO₃, 1.25 NaH₂PO₄, 2 CaCl₂, 1 MgCl₂, and 10 glucose. Using infrared video microscopy, somatic whole-cell voltage-clamp recordings from control and FKBP51-overexpressing PVN neurons (identified by fluorescence imaging; seal resistance >1 G Ω ; holding potential –70 mV, corrected for a liquid junction potential of 10 mV) were performed with an EPC 10 amplifier (HEKA) at room temperature in physiological saline (2–3 ml/min flow rate) containing picrotoxin (100 μ M) and TTX (1 μ M). Patch pipettes (3–4 M Ω open tip resistance) were filled with a solution consisting of (in mM): 125 CsCH₃SO₃, 8 NaCl, 10 HEPES, 0.5 EGTA, 4 Mg-ATP, 0.3 Na-GTP, and 20 Na₂-phosphocreatine (pH adjusted to 7.2 with CsOH). Five minutes after a break-in to the cell, AMPA receptor-mediated miniature excitatory postsynaptic currents (mEPSCs) were recorded for 5 min. Offline analysis of mEPSCs was conducted using the Mini Analysis Program (Synaptosoft). Recordings, where series resistance changed by more than 10%, were excluded from the analysis.

Statistical analysis

The data presented are shown as means \pm SEM and sample sizes are indicated in the figure legends. All data were analyzed by the commercially available software SPSS 17.0 and GraphPad 8.0. When two groups were compared, the unpaired student’s t -test was applied. If data were not normally distributed the non-parametric Mann–Whitney test (MW-test) was used. For four group comparisons, a two-way analysis of variance (ANOVA) was performed,

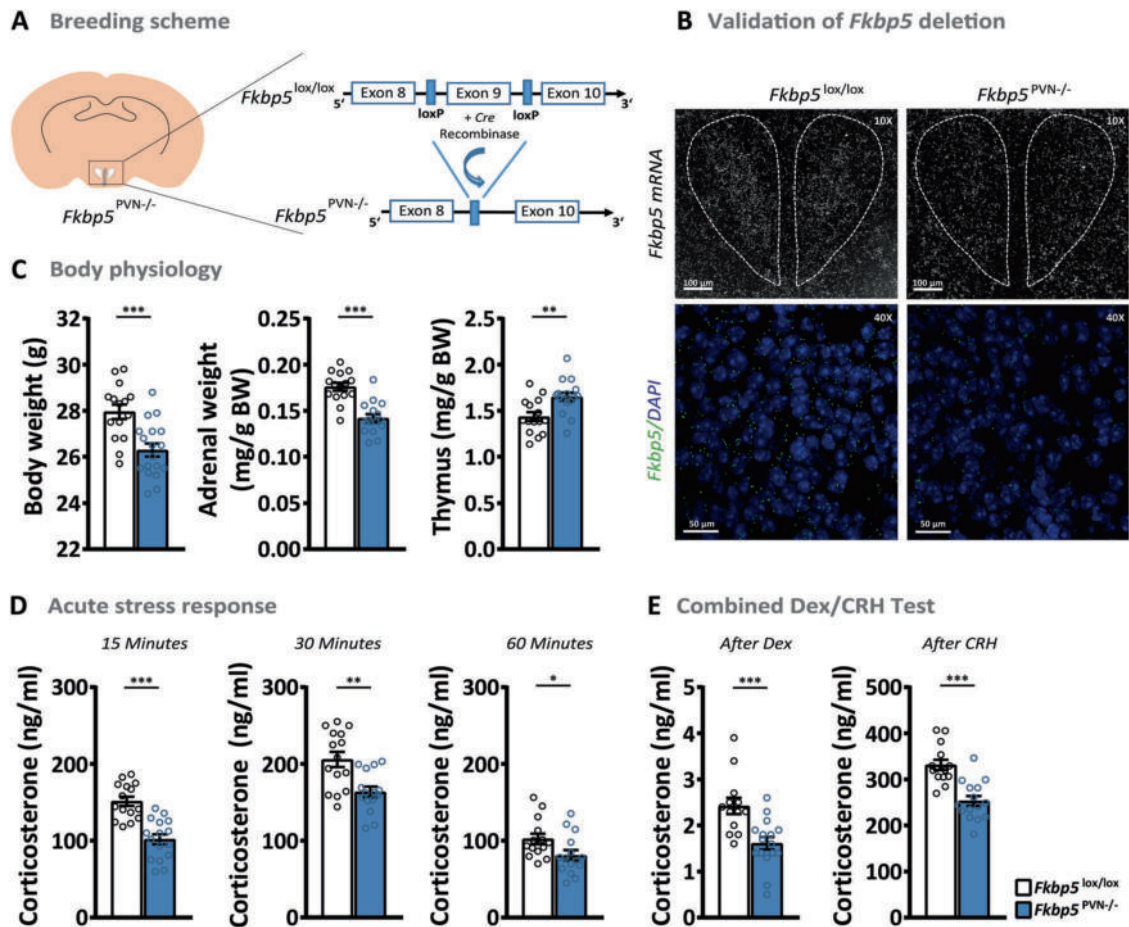


Fig. 1 Loss of *Fkbp5* in the PVN alters HPA axis physiology. **A** Cre-LoxP based generation of the *Fkbp5*^{PVN-/-} mouse line. **B** Validation of *Fkbp5* mRNA expression in the PVN via in situ hybridization (ISH) and RNAscope (for mRNA quantification see Supplementary Fig. 1A). **C** *Fkbp5*^{PVN-/-} mice ($n = 16$) presented reduced body weight, lowered adrenal weights, and increased thymus weights under non-stressed conditions compared to their WT littermates ($n = 15$). **D** Corticosterone levels were significantly reduced

following a 15 min restraint stress until at least 60 min after stress onset. **E** A combined Dex/CRH test showed a significantly pronounced response to a low dose of dexamethasone as well as a dampened response to CRH injection. Data are received from mice between 16 and 20 weeks of age and are presented as mean \pm SEM. All data were analyzed with a student's *t*-test. * $p < 0.05$, ** $p < 0.01$, and *** $p < 0.001$.

followed by a posthoc test, as appropriate. *P* values of less than 0.05 were considered statistically significant. The sample size was chosen such that with a type 1 error of 0.05 and a type 2 error of 0.2 the effect size should be at least 1.2-fold of the pooled standard deviation. All data were tested for outliers using the Grubbs test.

Results

Loss of *Fkbp5* in the PVN alters HPA axis physiology

To study the effects of *Fkbp5* in the PVN, we first generated PVN-specific conditional *Fkbp5* knockout mice (*Fkbp5*^{PVN-/-}) by crossing *Fkbp5*^{lox/lox} mice (generated in-house; for details see methods) with the Sim1-Cre mouse line, which expresses *Cre* recombinase in Sim1⁺

neurons mostly concentrated within the PVN (Fig. 1A). The successful deletion of *Fkbp5* in the PVN was assessed by mRNA and protein analysis (Fig. 1B and Supplementary Fig. 1). Under basal conditions, adult mice (16–20 weeks of age) lacking *Fkbp5* in the PVN showed significantly lower body-, and adrenal weights and higher thymus weights compared to their WT littermates (Fig. 1C). Interestingly, *Fkbp5*^{PVN-/-} mice in young adolescence (8 weeks of age) showed no significant differences in body weight, adrenal, or thymus weights (Supplementary Fig. 2), indicating an age-dependent phenotype of *Fkbp5* in the HPA-axis' response.

As PVN *Fkbp5* mRNA levels are highly responsive to an acute stressor [10], we hypothesized that *Fkbp5*^{PVN-/-} mice have an altered stress response following an acute challenge. Under basal conditions during the circadian trough,

no differences in corticosterone secretion were detected in young and adult mice (Supplementary Figs. 1 and 2). However, already after 15 min of restraint stress adult and young *Fkbp5*^{PVN-/-} mice displayed significantly reduced plasma corticosterone levels compared to the control group (Fig. 1D). The dampened stress response was persistent for 60 min in adult mice, while the effect has vanished in young mice already 30 min after stress onset (Fig. 1D and Supplementary Fig. 2). Levels of the adrenocorticotrophic hormone (ACTH) were not altered under basal or acute stressed conditions (Supplementary Fig. 1).

To further investigate the effect of *Fkbp5* on GR sensitivity, we performed combined dexamethasone (Dex, a synthetic GC)—corticotropin-releasing hormone (CRH) test on adults *Fkbp5*^{PVN-/-} mice. The combined Dex/CRH test is a method to analyze HPA axis (dys)function in depressed individuals or animals, measuring the responsiveness of the body's stress response system through suppression (by Dex injection) and stimulation (by CRH injection) of the HPA axis [33]. The injection of a low dose of Dex (0.05 mg/kg) resulted in a reduction in blood corticosterone levels compared to the evening corticosterone levels in both groups. Interestingly, mice lacking *Fkbp5* in the PVN showed 1.5-fold lower levels of corticosterone compared to their WT littermates. Following CRH stimulation (0.15 mg/kg) *Fkbp5*^{PVN-/-} mice showed a significantly lower reaction to CRH than control mice (Fig. 1E). These data indicate that specific deletion of *Fkbp5* in the PVN dampens HPA axis response and enhances GR sensitivity.

Overexpression of *Fkbp5* in the PVN induces a stress-like phenotype in C57Bl/6 mice under basal conditions

Chronic or acute stress upregulates *Fkbp5* in distinct brain regions, such as the PVN [10]. Therefore, we were interested to explore whether selective overexpression of *Fkbp5* in the PVN would be sufficient to affect body physiology and stress system regulation. To do so, we bilaterally injected 200 nl of an adeno-associated virus (AAV) containing an *Fkbp5* overexpression vector into the PVN of 10–12 weeks old C57Bl/6 mice (*Fkbp5*^{PVN OE}, Fig. 2A, B). The AAV-mediated overexpression resulted in a (fourfold) increase in *Fkbp5* mRNA and protein levels (*Fkbp5*) in the PVN (Supplementary Fig. 3).

Intriguingly, *Fkbp5* overexpression altered the physiology of stress-responsive organs. *Fkbp5*^{PVN OE} animals showed a significantly reduced thymus weight and increased adrenal weights compared to their littermates (Fig. 2C), the hallmark of chronically stressed animals [34, 35]. Furthermore, overexpression of *Fkbp5* affected the circadian rhythm of corticosterone secretion, indicated by increased blood corticosterone levels in the morning as well

as the evening (Fig. 2D). Consequently, ACTH levels of *Fkbp5*^{PVN OE} animals were also increased under non-stressed conditions (Supplementary Fig. 3). Next, we analyzed distinguished stress markers under basal conditions in order to determine whether consequences of PVN-specific *Fkbp5* overexpression are also detectable at the molecular level. *Nr1c3* and *Crh* mRNA expression in the PVN were increased in *Fkbp5*^{PVN OE} animals under basal conditions; however, to a lesser extent than the increase of *Fkbp5* mRNA due to viral overexpression. *Avp* mRNA levels were not altered (Supplementary Fig. 3). Together, these results are comparable to chronically stressed animals and demonstrate that local overexpression of *Fkbp5* in the PVN is sufficient to mimic a stress-like phenotype without physically challenging the animals.

In accordance with the knock-out studies of the *Fkbp5*^{PVN-/-} animals, we investigated the endocrinology of *Fkbp5*^{PVN OE} animals after an acute challenge. As expected, we detected higher blood corticosterone levels in *Fkbp5*^{PVN OE} mice 15 and 30 min after stress onset compared to the stressed controls (Fig. 2E). However, we could not detect any difference in ACTH release after stress (Supplementary Fig. 3). No differences between both groups were observed 60 and 90 min after restraint stress (Fig. 2E and Supplementary Fig. 3). These data show that *Fkbp5*^{PVN OE} mice have a hyperactive HPA axis response and are more vulnerable to acute stress exposure.

To further assess GR sensitivity in *Fkbp5* overexpressing animals, we again tested the response to a combined Dex/CRH test. While control animals showed a decline (<5 ng/ml) in blood corticosterone levels 6 h after Dex injection, *Fkbp5*^{PVN OE} mice showed almost no response to Dex treatment (Fig. 2F). Interestingly, the subsequent CRH injection resulted in a higher corticosterone release in *Fkbp5*^{PVN OE} mice compared to controls (Fig. 2F). These results suggest that excess levels of *Fkbp5* in the PVN lead to a decreased GR sensitivity and thereby to an altered HPA axis response. Taken together, animals overexpressing *Fkbp5* in the PVN show a hyperactive function of the HPA axis under basal and acute stress conditions, thereby mimicking the physiological hallmarks of chronic stress exposure and HPA axis hyperactivity, as observed in multiple stress-related diseases [36].

Reinstatement of endogenous *Fkbp5* in the PVN of global *Fkbp5* knock-out animals normalizes the body's stress response

Global loss of *Fkbp5* results in a more sensitive GR and better-coping behavior of mice after stress [8, 17, 28, 34], and our results demonstrated that *Fkbp5* in the PVN is necessary for an undisturbed stress system function. Thus, we were encouraged to test whether the reinstatement of

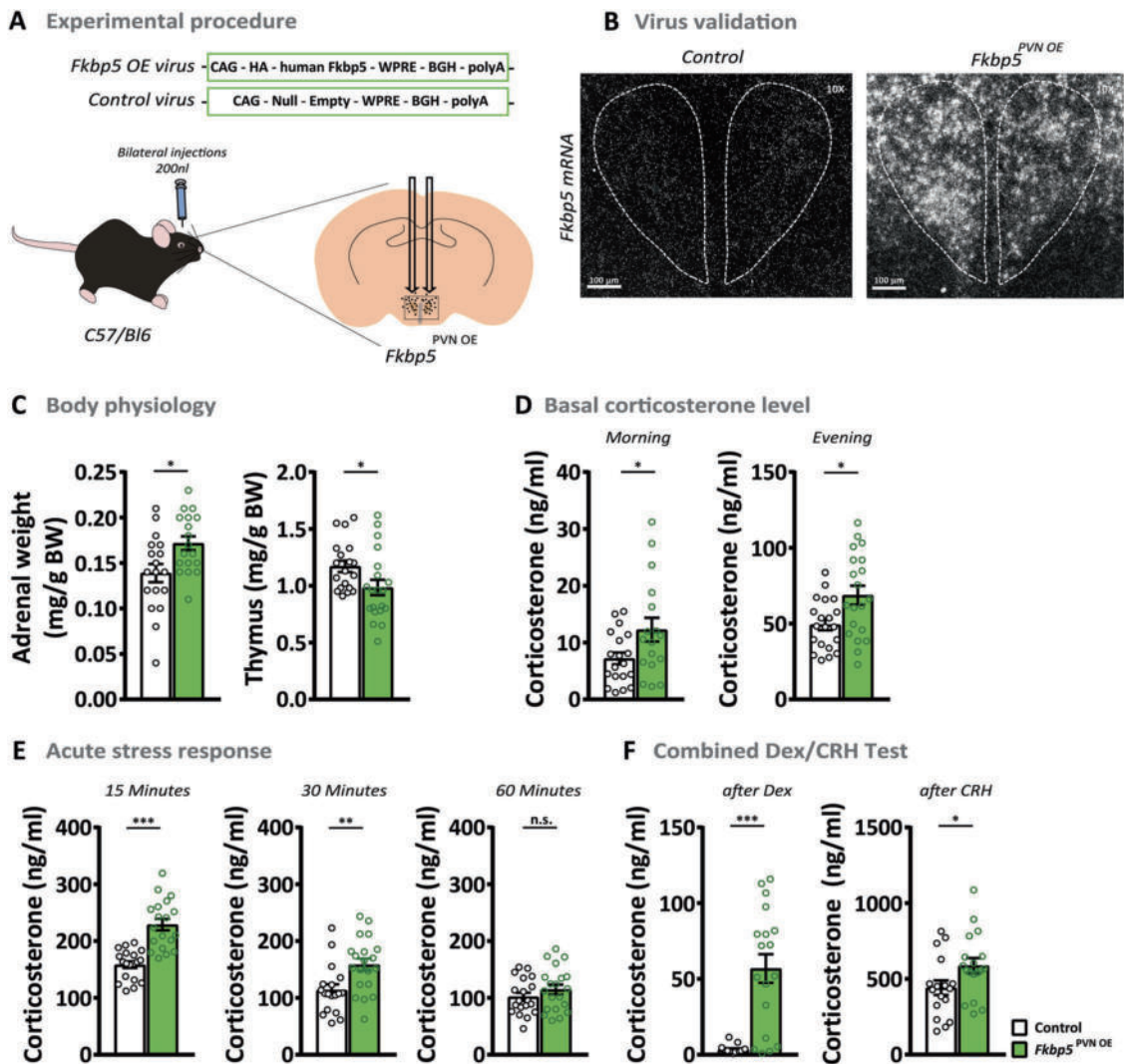


Fig. 2 The overexpression of *Fkbp5* in C57Bl/6 mice induces a stress-like phenotype under basal conditions. **A** Overexpression of *Fkbp5* in the PVN was achieved by bilateral viral injections. **B** Validation of *Fkbp5* mRNA overexpression in the PVN by ISH (see Supplementary Fig. 3A for mRNA quantification). **C** *Fkbp5*^{PVN OE} mice ($n = 20$) showed significantly increased adrenal weights and a reduced thymus weight under non-stressed conditions compared to the controls ($n = 20$). **D** *Fkbp5* overexpression resulted in heightened corticosterone levels during the day. **E** Fifteen and 30 min after stress

onset, *Fkbp5*^{PVN OE} mice displayed significantly higher corticosterone levels. **F** *Fkbp5*^{PVN OE} mice showed significantly elevated corticosterone 6 h after dexamethasone treatment. The following CRH injection further significantly increased the corticosterone release compared to controls. Data are presented as mean \pm SEM. All data were received from mice between 14 and 20 weeks of age and analyzed with student's *t*-test. * $p < 0.05$, ** $p < 0.01$, *** $p < 0.001$, *n.s.* not significant.

native *Fkbp5* expression only in the PVN is sufficient to push the HPA axis activity of global *Fkbp5* knock-out animals to a wildtype level. Therefore, we injected an Flp recombinase expressing virus into 12–14 weeks old *Fkbp5*^{Frt/Frt} mice. These mice carry an FRT flanked reporter selection (stop) cassette within the *Fkbp5* locus, leading to a disruption of the *Fkbp5* function. We compared *Fkbp5*^{Frt/Frt} mice to WT littermates and observed a similar HPA-axis phenotype to the well-established *Fkbp5* full KO lines ([8] and Supplementary Fig. 4). An Flp removes the stop cassette from the *Fkbp5* locus, resulting in endogenous *Fkbp5* re-expression (Fig. 3A, B, Supplementary Fig. 5). In

parallel to the two previous mouse models, we assessed body physiology, basal corticosterone levels, and the acute stress response. Interestingly, mice with re-instated *Fkbp5* expression (*Fkbp5*^{PVN Rescue}) showed significantly higher adrenal weights as compared to their control littermates (Fig. 3C). Furthermore, we observed that the reinstatement of *Fkbp5* in the PVN resulted in significantly increased blood CORT levels in the morning under basal conditions (Fig. 3D), with no effect on thymus weights, evening CORT, and ACTH levels (Supplementary Fig. 5). ISH analysis revealed significantly higher levels of *Crh* mRNA, but no changes in *Nr1c3* and *Avp* mRNA expression in the

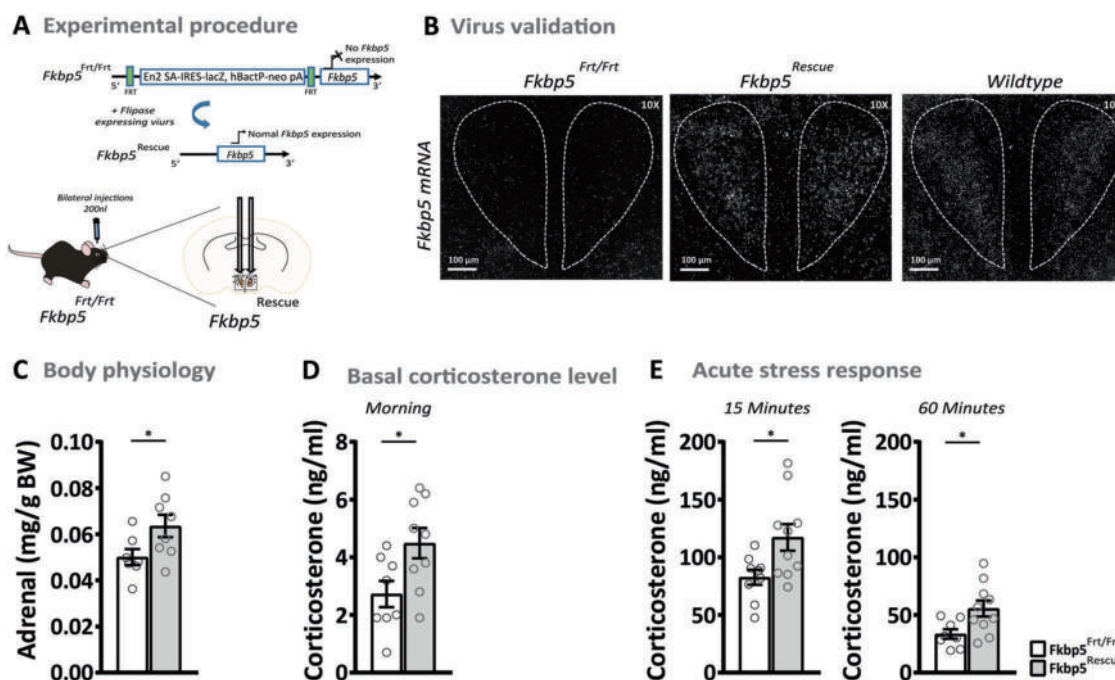


Fig. 3 The reinstatement of endogenous *Fkbp5* in the PVN of global *Fkbp5* knock-out animals. **A** Experimental procedure. **B** Validation of successful *Fkbp5* rescue by ISH (see Supplementary Fig. 5A for mRNA quantification) and comparable WT *Fkbp5* expression. **C** The reinstatement of *Fkbp5* in the PVN resulted in increased adrenal weights and elevated morning corticosterone levels

under basal conditions **D**. Furthermore, *Fkbp5* re-instated animals displayed a significantly higher corticosterone response after restraint stress **E**. For comparison of *Fkbp5*^{Frt/Frt} and WT see control experiments in Supplementary Fig. 4. Data are presented as mean \pm SEM. All data were received from mice between 16 and 20 weeks of age and analyzed with student's *t*-test. **p* < 0.05.

PVN under basal conditions (Supplementary Fig. 5). Next, we monitored blood corticosterone levels after 15 min of restraint stress. Here, we observed significantly higher corticosterone levels 15 and 60 min after stress onset (Fig. 3E). No differences were detected in the combined Dex/CRH test (Supplementary Fig. 5), which suggests that a PVN-driven over-activation of the HPA axis might be necessary for desensitization of GRs in the PVN and the pituitary. These rescue experiments underline the importance of *Fkbp5* in the acute stress response and demonstrate that *Fkbp5* in the PVN is necessary and sufficient to regulate HPA axis (re)activity.

***Fkbp5* manipulation directly affects GR phosphorylation**

It is well known that ligand-binding induced phosphorylation of GR plays an important role in response to hormone signaling [37]. The main phosphorylation sites involved in hormone signaling of GR are Serine (Ser)²⁰³ (mouse S²¹²), Ser²¹¹ (mouse Ser²²⁰), and Ser²²⁶ (mouse Ser²³⁴) and are associated with GR activity [37, 38]. Here, we tested the hypothesis that the co-chaperone *Fkbp5* regulates phosphorylation of GR in *Fkbp5*^{PVN-/-} and *Fkbp5*^{PVN OE} mouse lines. To do so, we dissected the PVN of *Fkbp5*^{PVN-/-} and

Fkbp5^{PVN OE} mice and measured the phosphorylation levels of Ser²⁰³, Ser²¹¹, and Ser²³⁴ under basal and stress conditions.

Under basal conditions, animals lacking *Fkbp5* in the PVN showed significantly less GR phosphorylation at Ser²⁰³ (Fig. 4A). Furthermore, *Fkbp5*^{PVN-/-} animals displayed higher phosphorylation of GR at Ser²³⁴ and Ser²¹¹ in comparison to their WT littermates (Fig. 4B, C). Under stressed conditions, deletion of *Fkbp5* had the same effects on pGR^{Ser211} and pGR^{Ser234} as we observed under basal conditions (Fig. 4B, C). Levels of pGR^{Ser203} were found to be unchanged in the *Fkbp5*^{PVN-/-} after acute stress compared to the basal levels. However, pGR^{Ser203} levels of the control group increased after stress (Fig. 4A).

Intriguingly, *Fkbp5*^{PVN OE} animals showed exactly the opposing phenotype at all three phosphorylation sites with less pGR^{Ser234} and pGR^{Ser211} and higher phosphorylation at Ser²⁰³ under basal conditions (Fig. 4E–G). In parallel to the unstressed condition, the overexpression of *Fkbp5* resulted in less GR phosphorylation at Ser²¹¹ and higher levels of pGR^{Ser203} compared to their control group after stress (Fig. 4E, F). Interestingly, levels of pGR^{Ser234} were unchanged after stress (Fig. 4G). Notably, total GR levels were not significantly altered in both experimental groups and conditions (Fig. 4D, H). Despite the altered GR phosphorylation, we could not detect any significant changes in

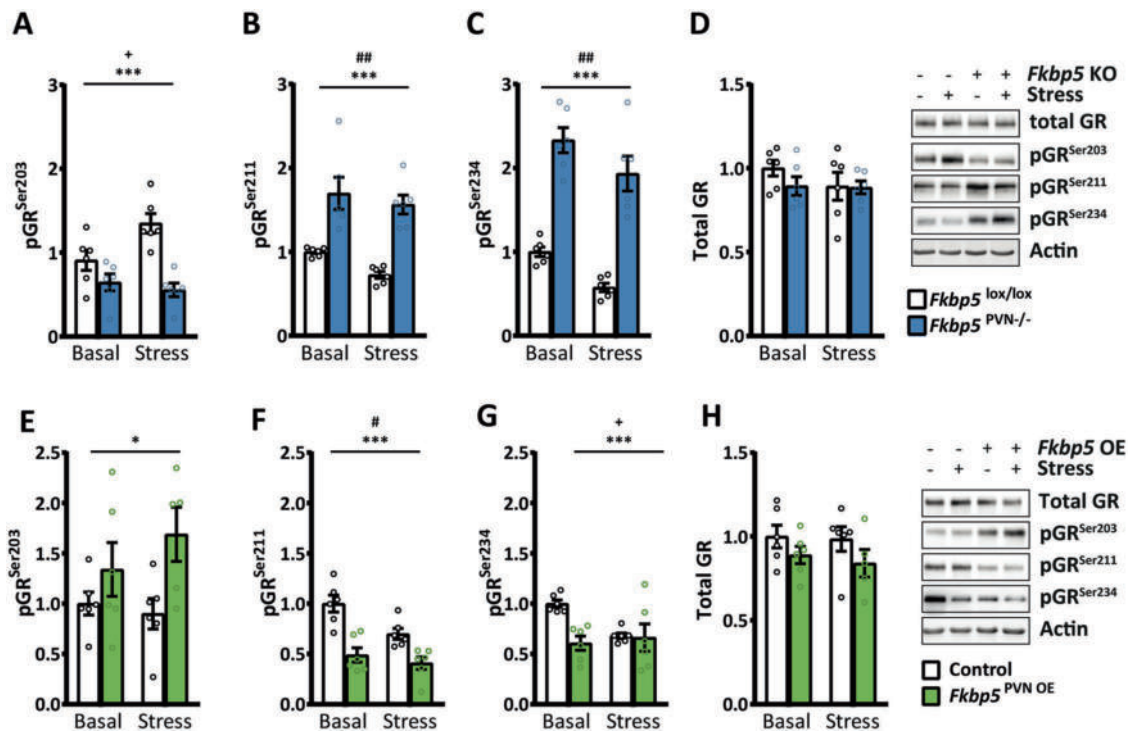


Fig. 4 Fkbp5 manipulation affects phosphorylation of the glucocorticoid receptor (GR). **A** Animals lacking Fkbp5 in the PVN showed significantly lower phosphorylation at pGR^{Ser203} and higher levels of **(B)** pGR^{Ser211} and **(C)** pGR^{Ser234} compared to the control animals. **D** Fkbp5^{PVN-/-} mice showed no differences in total GR. **E** Fkbp5^{PVN OE} animals showed the opposite effect on GR phosphorylation with higher phosphorylation on pGR^{Ser203}. **F** In addition, we observed significantly lower phosphorylation at the GR sites Ser²¹¹

and **(G)** Ser²³⁴. **H** Fkbp5 overexpression had no effect on total GR protein level. Representative blots are shown in **(D)** and **(H)**. Group size for **(A)–(H)**: 6 vs. 6. Data were received from animals between 16 and 20 weeks of age and are presented as relative fold change to control condition, mean ± SEM, and were analyzed with a two-way ANOVA. *significant genotype effect, (**p* < 0.05, ***p* < 0.01, ****p* < 0.001). +significant genotype × stress interaction (+*p* < 0.05), #significant stress effect (#*p* < 0.05, ##*p* < 0.01).

GR enrichment at the glucocorticoid response element (GRE) in the *Crh* gene after acute stress (Supplementary Fig. 6), which may be due to the use of an antibody that recognizes all GR molecules irrespective of its phosphorylation state.

Overall, our data demonstrate that *Fkbp5* manipulation in the PVN affects GR phosphorylation at all three major phosphorylation sites and thereby affects GR activity.

Fkbp5 in the PVN acts in a complex cellular context

To further unravel the expression profile of *Fkbp5* in the PVN and to detect cellular populations that might be mediating the effects of *Fkbp5* on HPA axis control, we used a single-cell RNA sequencing dataset consisting of 5113 single cells isolated from the PVN of C57Bl/6 male mice [39]. The single-cell expression data reveal a complex cellular composition, with the majority of cells identified as neurons (38%), ependymal cells (25%), and astrocytes (14%) (Fig. 5A–C). *Fkbp5* was found to be differentially and cell-type specifically expressed, with the biggest *Fkbp5*⁺ cell population found in GABAergic neurons (42%). A significant expression of *Fkbp5* was also detected

in neuronal populations known to be directly involved in HPA axis regulation, most prominently in *Crh* positive neurons (Fig. 5D). However, it is important to point out that the expression levels of *Fkbp5* are relatively low. Unfortunately, lowly expressed genes may not be detected using this technique [40] and therefore many *Fkbp5* positive cells may have remained undetected in this dataset. To circumvent this problem, we next performed a targeted co-expression study of *Fkbp5* with five major markers that are characteristic of the stress response oxytocin (*Oxt*), somatostatin (*Sst*), vasopressin (*Avp*), thyrotropin-releasing hormone (*Trh*), and *Crh* under basal and stress conditions (Fig. 5E, Supplementary Fig. 7). We observed a strong but not complete co-localization of *Fkbp5* expression with these neuropeptide-expressing cellular populations in the PVN under basal conditions. Interestingly, a detailed quantification of the change in co-expression following stress revealed that there was a significant increase in *Crh*-*Fkbp5* co-localization only in the *Crh*-expressing neurons (Fig. 5E, F and Supplementary Fig. 8).

These data reveal the complex cell-type-specific expression pattern of *Fkbp5* under stress and basal conditions in the PVN. The significant increase of FKBP51 in

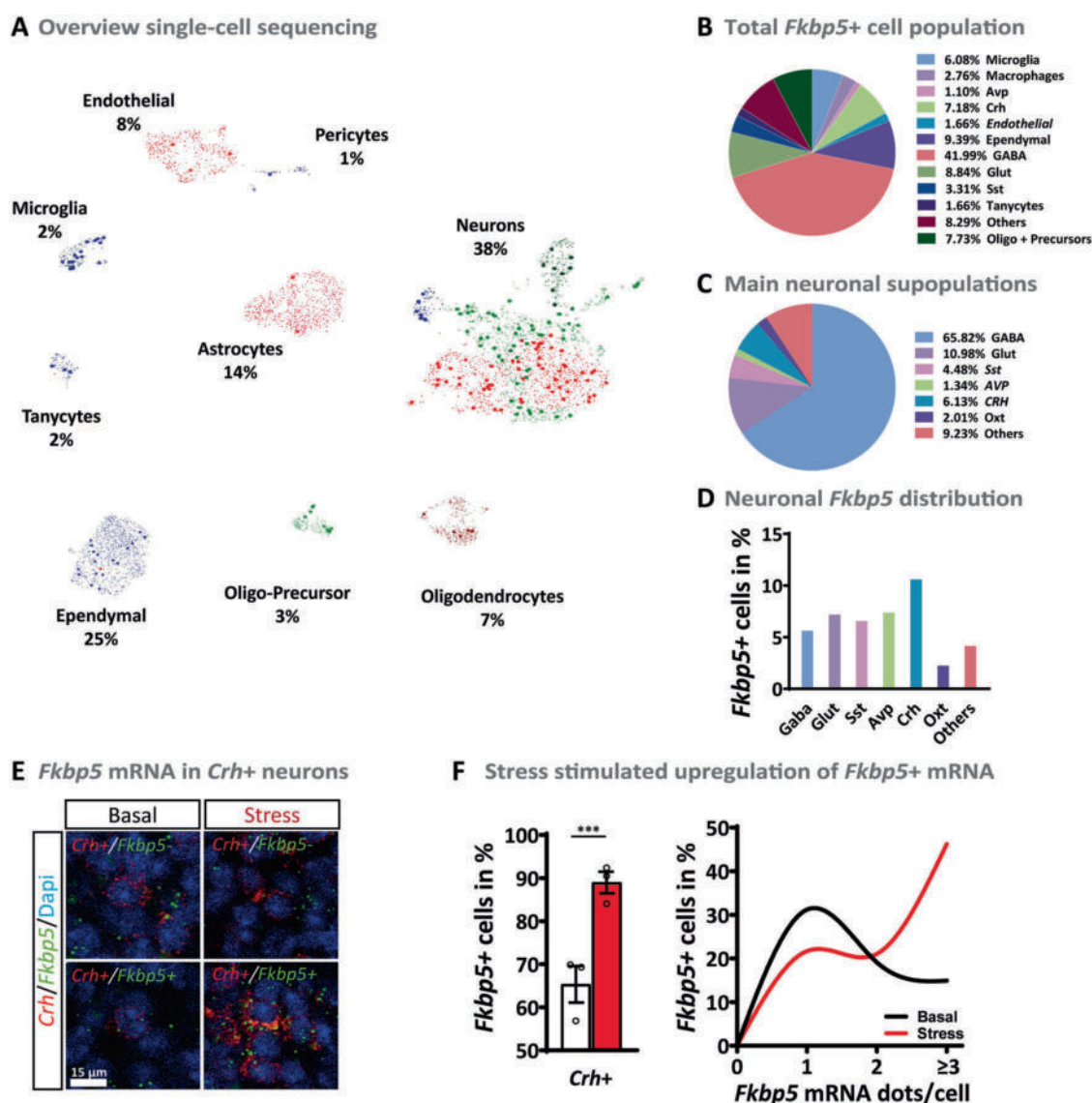


Fig. 5 Single-cell RNA sequencing of cells in the PVN of C57Bl/6 male mice under non-stressed conditions. **A** Single-cell sequencing depicted several different cell types. With the majority being neurons (38%), ependymal cells (25%), and astrocytes (14%). *Fkbp5*⁺ cells are highlighted. **B** Diversity of *Fkbp5*⁺ cell population. **C** Neurons could be divided mostly into GABAergic (66%) and glutamatergic (Glut, 11%) cells. Furthermore, the well-known stress markers corticotropin-releasing hormone (*Crh*, 6%), somatostatin (*Sst*, 5%), oxytocin (*Oxt*,

2%), and vasopressin (*Avp*, 1%) could be detected under basal conditions. **D** *Fkbp5*⁺ cells of selected neuronal subpopulations under basal conditions. **E** RNAscope validation of *Fkbp5* mRNA expression in *Crh*⁺ neurons. **F** Quantity of *Fkbp5*⁺ cells, as well as *Fkbp5* mRNA levels, are significantly increased after stress. Data were received from animals between 8 and 12 weeks of age and are presented as mean ± SEM. For (**E**): data were analyzed with student's *t*-test. ****p* < 0.001.

Crh positive neurons after an acute stress challenge encouraged us to specifically manipulated FKBP51 in *Crh* positive neurons.

***Crh*-specific overexpression of *Fkbp5* in the PVN alters HPA axis physiology and CRH neuronal activity**

Based on the observed increase in *Crh-Fkbp5* colocalization post-stress (Fig. 5E, F and Supplementary

Fig. 8), we were interested whether a *Crh*-specific *Fkbp5* overexpression in the PVN could drive the stress-like phenotype observed in the unspecific PVN overexpression (Fig. 2) and whether this neuron-specific manipulation alters CRH neuronal activity. Therefore, we bilaterally injected 200 nl of an AAV containing a Cre-dependent *Fkbp5* overexpression vector into the PVN of adult (26 weeks) CRH-ires-CRE/Ai9 mice expressing tdTomato specifically in CRH neurons (*Fkbp5*^{CRH OE}) (Fig. 6A). Cre-dependent AAV mediated overexpression resulted in a

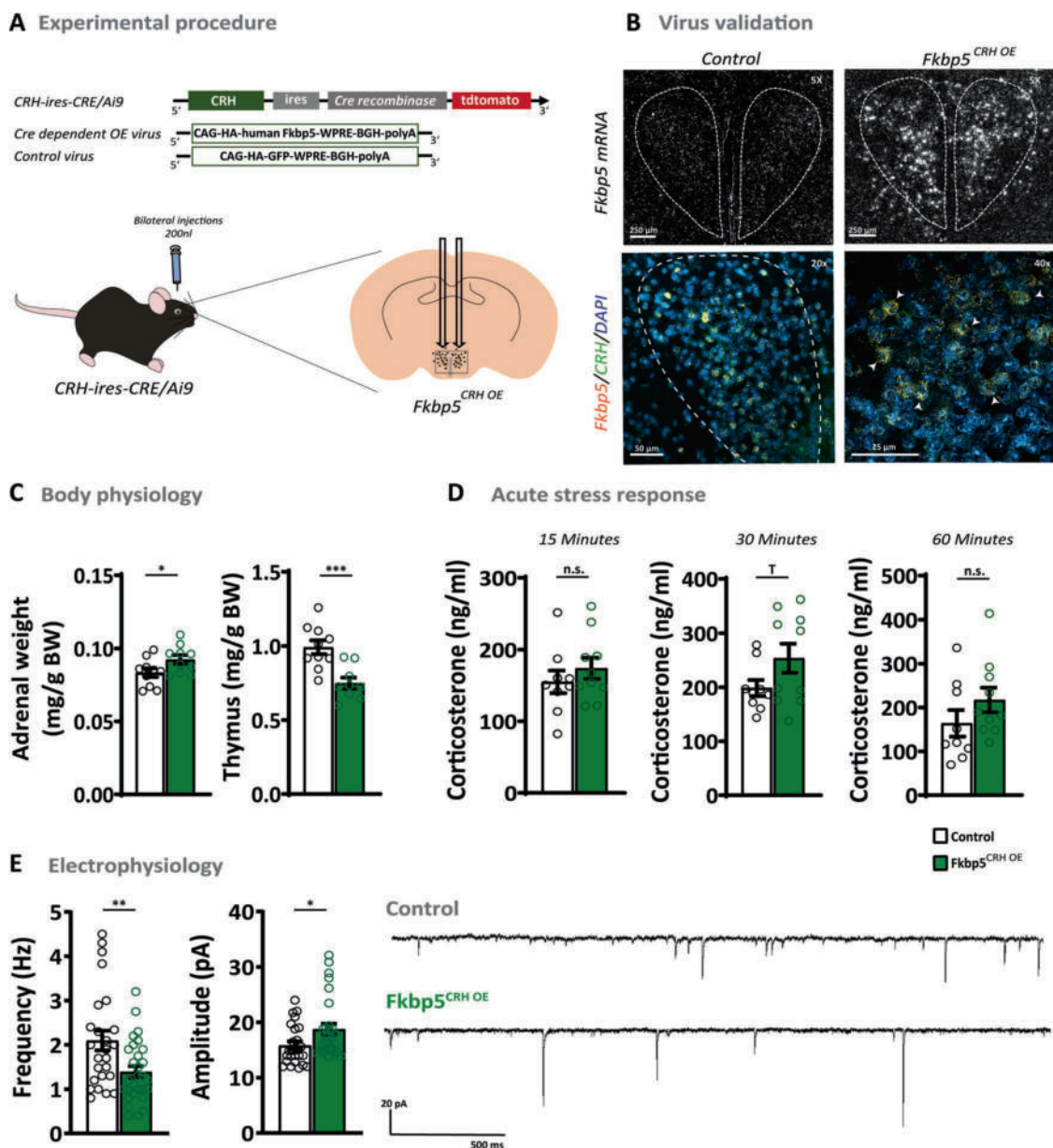


Fig. 6 The *Crh*-specific overexpression of *Fkbp5* in the PVN. **A** *Crh*-specific overexpression of *Fkbp5* in the PVN was achieved by bilateral injections of a Cre-dependent *Fkbp5* overexpression virus in the PVN of CRH-ires-CRE/Ai9 mice. **B** Validation of *Crh*-specific *Fkbp5* mRNA overexpression in the PVN by ISH and RNAscope. Arrowheads pointing at viral *Fkbp5* expressing *Crh*⁺ neurons (For mRNA quantification see Supplementary Fig. 9D). **C** *Fkbp5*^{CRH OE} mice showed significantly increased adrenal weights ($n = 10$) and reduced thymus weights ($n = 9$) under non-stressed conditions compared to the controls ($n = 10$). **D** Corticosterone levels were mildly,

but not significantly increased in *Fkbp5*^{CRH OE} at 15, 30, and 60 min post-stress (*Fkbp5*^{CRH OE} $n = 10$; Control $n = 9$). **E** *Fkbp5*^{CRH OE} mice displayed a decrease in CRH neuronal mEPSC frequency accompanied by an increased amplitude (*Fkbp5*^{CRH OE} $n_{\text{mouse}} = 4$; $n_{\text{neuron}} = 29$; Control $n_{\text{mouse}} = 4$; $n_{\text{neuron}} = 25$), which is reflected in two representative recording traces. Data are presented as mean \pm SEM. All data were received from animals between 30 and 34 weeks of age and analyzed with the student's *t*-test. * $p < 0.05$, ** $p < 0.01$, *** $p < 0.001$, $T = 0.05 < p < 0.1$, *n.s.* not significant.

fourfold increase of *Fkbp5* mRNA level in the PVN and *Crh* specificity of *Fkbp5* overexpression was successfully confirmed by RNAscope (Fig. 6B and Supplementary Fig. 9E). Under basal conditions, *Fkbp5*^{CRH OE} mice displayed significantly increased adrenal weights and reduced thymus weights compared to the control group (Fig. 6C),

indicative of chronic hyperactivity of the HPA axis. Surprisingly, the circadian rhythm of corticosterone secretion (Supplementary Fig. 9A), as well as stress-induced corticosterone level (Fig. 6D), were unaffected by the *Crh*-specific *Fkbp5* overexpression. Further, basal and 15 min post-stress ACTH level and DEX/CRH corticosterone level

remained unaffected in *Fkbp5*^{CRH OE} mice (Supplementary Fig. 9B–D). To further assess the impact of *Fkbp5* overexpression on neuronal activity in *Crh* positive (*Crh*⁺) neurons in the PVN, we recorded AMPA receptor-mediated mEPSCs in these cells using cell patch-clamp recordings in a separate cohort. *Fkbp5* overexpression decreased the frequency of mEPSC frequency while increasing amplitude (Fig. 6E). This data shows that the *Fkbp5* expression level in *Crh*⁺ neurons can steer CRH neuronal activity within the PVN, whereas the baseline- and stress phenotype of *Fkbp5*^{CRH OE} mice is mostly unaffected by the manipulation, identifying *Crh*⁺ neurons as one important but not the only driver of the observed stress-like *Fkbp5*^{PVN OE} phenotype.

Discussion

FKBP5 was first associated with stress-related disorders in 2004 [13] and has been studied extensively over the past 15 years with regard to stress regulation and sensitivity. However, detailed cell-type and region-specific manipulations of Fkbp5 in the brain are still lacking. In this study, we highlight the importance of this co-chaperone in the regulation of the acute stress response through the combined analysis of deletion, overexpression, and rescue of *Fkbp5* exclusively in the PVN.

Fkbp5 is a stress-responsive gene and past research has shown that its main effects occur after chronic or acute stress [8, 18, 28, 32, 41]. Given that deletion of *Fkbp5* in the PVN mimics the previously described phenotype of *Fkbp5* KO mice [28, 41], with regard to their basal neuroendocrine profile and HPA axis function, our data illustrate that the functional contribution of *Fkbp5* to HPA axis activity is centered in the PVN. In addition, reinstatement of native basal *Fkbp5* expression in the PVN of *Fkbp5* KO mice was sufficient to normalize HPA axis function. Interestingly, the phenotype of intensified HPA axis suppression due to the loss of *Fkbp5* in the PVN emerges only in adult animals, excluding developmental effects and underlining the previously reported importance of Fkbp5 in aging [42, 43].

Further, our results highlight the essential role of Fkbp5 in stress adaptation, as PVN-specific Fkbp5 excess is sufficient to reproduce all physiological and endocrinological hallmarks of a chronic stress situation [29, 44]. Interestingly, the results of our *Fkbp5*^{PVN OE} cohort are comparable to the neuroendocrine effect of GR deletion in the PVN [45] and are in line with the high PVN-specific FKBP5 expression in rats with a hyperactive HPA axis [20]. The consequence of a heightened *Fkbp5* expression in the PVN is twofold. Firstly, it leads to direct changes in GR sensitivity and downstream GR signaling directly in the PVN. Secondly, PVN *Fkbp5* overexpression dramatically affects GR sensitivity and feedback at the level of the pituitary, as

demonstrated by the inability of a low Dex dose (that does not cross the blood-brain barrier and acts predominantly at the level of the pituitary [26]) to suppress corticosterone secretion. This secondary effect is likely due to the constant overproduction of CRH in the PVN and very similar to the effects of HPA hyperactivity observed in many depressed patients [33, 46].

Mechanistically, we explored the role of Fkbp5 in modulating GR phosphorylation. The status of GR phosphorylation at Ser²¹¹, Ser²⁰³, and Ser²³⁴ is associated with transcriptional activity, nuclear localization, and ability to associate with GRE containing promoters [37]. Whereas higher levels of phosphorylation at Ser²¹¹ are associated with full transcriptional activity and localization in the nucleus, increased phosphorylation of Ser²⁰³ is linked to a transcriptionally inactive form of GR within the cytoplasm and thereby less active GR [38, 47, 48]. In our experiments, overexpression of Fkbp5 resulted in dephosphorylation at Ser²¹¹ and higher phosphorylation at Ser²⁰³, suggesting that the GR is mostly located in the cytoplasm and less active. Deletion of Fkbp5 showed the opposing effect, indicating a more active GR in *Fkbp5*^{PVN^{-/-}} animals. Unfortunately, we were not able to analyze the GR phosphorylation in our *Fkbp5*^{PVN Rescue} animals due to technical and breeding issues and therefore can only speculate that FKBP5^{PVN Rescue} animals might have elevated levels of pGRSer203 and decreased levels of pGRSer211 and pGRSer234. It has previously been reported that GR phosphorylation is regulated by several kinases, including CDK5 and ERK [37, 49], and Fkbp5 has also been shown to be associated with CDK5 in the brain [50]. Therefore, we hypothesize that Fkbp5 also interacts with CDK5 to phosphorylate GR at multiple phosphorylation sites, thereby directly affecting ligand-dependent GR activity.

Given the complexity of the different cell types with highly specialized functions in the brain, it is essential to gain a deeper understanding of the cellular architecture of the PVN and the specific function of Fkbp5 in this context. Previously, it was assumed that Fkbp5 is quite widely expressed in most cell types of the nervous system [51]. However, our current data suggest that while *Fkbp5* is indeed expressed in the PVN, it is enriched in specific subpopulations, including for example GABAergic neurons, *Crh*⁺ neurons, and microglia, but largely absent in others, such as astrocytes and endothelial cells. Interestingly, when quantifying Fkbp5 regulation, we identified a highly selective regulation of *Fkbp5* in *Crh*⁺ neurons, further supporting the central role of Fkbp5-controlled GR feedback in this neuronal subpopulation.

To further disentangle the role of *Fkbp5* within *Crh* positive neurons in the acute stress response and HPA-axis feedback regulation, we selectively overexpressed *Fkbp5* in *Crh*⁺ cells within the PVN and assessed baseline- and

stress-induced phenotypes paralleled by selective patch-clamp recordings from *Crh*⁺ neurons. *Fkbp5* overexpression enhanced the amplitude of mEPSCs in *Crh*⁺ cells indicating a postsynaptic and, thus, the direct effect of our *Fkbp5* manipulation on excitatory neurotransmission onto these neurons. This effect, which was accompanied by a diminished rate of mEPSC, potentially arises from accelerated recycling of internalized AMPA receptors to the postsynaptic density [52] and suggests an increased activity of *Crh*⁺-cells. However, *Fkbp5* overexpression only partially recapitulating the HPA-axis phenotype observed in the *Fkbp5*^{PVN OE} mice. The unselective *Fkbp5* overexpression in *Fkbp5*^{PVN OE} animals targeted a broad range of *Fkbp5* expressing cell populations within the PVN, amongst which are oxytocin and vasopressin. Their essential contribution to the initiation and termination of the HPA-axis is well established, with vasopressin (together with CRH) inducing ACTH release from the pituitary [53] and oxytocin enhancing the negative feedback helping to dampen the stress response [54]. Hence, our data suggest that *Fkbp5* might play an essential role in at least one further neuronal subpopulation of the PVN driving the observed stress-like phenotype of *Fkbp5*^{PVN OE} mice in concert with CRH neurons.

The current study also comes with a number of limitations. Importantly, only male animals were used and the conclusions should therefore only be drawn with respect to male HPA axis regulation. Furthermore, given the fact that we did not observe differences in ACTH levels after stress, we cannot exclude that *Fkbp5* manipulations in the PVN also drive changes in adrenal sensitivity, e.g., via alterations of sympathetic adrenal innervation [55]. Furthermore, the time course of CRH and ACTH release is quite different from the CORT response, so our measures may have missed a differential regulation. In fact, a modest increase in circulating ACTH at certain times of the circadian rhythm can indeed lead to adrenal hypertrophy and increased sensitivity, thereby contributing to increased CORT secretion even following comparable ACTH levels. Finally, the lack of ACTH data in the Dex/CRH test was technically unavoidable but also limits the conclusions with regard to the involved mechanism.

In summary, this study is the first to specifically manipulate *Fkbp5* in the PVN and underlines its central importance in shaping HPA axis regulation and the acute stress response. The results have far-reaching implications for our understanding of stress physiology and stress-related disorders.

Acknowledgements The authors thank Claudia Kühne, Mira Jakovcevski, Daniela Harbich, and Bianca Schmid (Max Planck Institute of Psychiatry, Munich, Germany) for their excellent technical assistant and support. We thank Stefanie Unkmeir, Sabrina Bauer, and the scientific core unit *Genetically Engineered Mouse Models* for

genotyping support. Further, we want to thank Alina Tontsch and the core unit *BioPrep* (Biomaterial Processing and Repository) for ELISA analysis of ACTH samples. This work was supported by the “OptiMD” grant of the Federal Ministry of Education and Research (01EE1401D; MVS), the BioM M4 award “PROCERA” of the Bavarian State Ministry (MVS), the “Kids2Health” grant of the Federal Ministry of Education and Research (01GL1743C; MVS) and by a NARSAD Young Investigator Grant from the Brain and Behavior Research Foundation (JH).

Author contributions ASH, and MVS: conceived the project and designed the experiments. JMD: provided scientific expertise for establishing *Fkbp5* mouse lines. ASH and LMB managed the mouse lines and genotyping. ASH, MLP, LR, and LMB performed animal experiments and surgeries. RS: performed CORT and ACTH hormone assays and analysis. J-PL, SR, and EB: performed single-cell sequencing experiments and analysis. JMHMR, and HMG: Performed and analyzed GR-CHIP experiments. ASH, JH, LMB, and CE: performed and designed RNAscope experiments and manual counting of cells. NCG, TB, and KH: Performed protein analysis. ME and DM: designed, performed, and analyzed single-cell patch-clamp experiments. KJR and AC: supervised and revised the manuscript. ASH: wrote the initial version of the manuscript. MVS: Supervised the research and all authors revised the manuscript.

Funding Open Access funding enabled and organized by Projekt DEAL.

Compliance with ethical standards

Conflict of interest The authors declare no competing interests.

Publisher's note Springer Nature remains neutral with regard to jurisdictional claims in published maps and institutional affiliations.

Open Access This article is licensed under a Creative Commons Attribution 4.0 International License, which permits use, sharing, adaptation, distribution and reproduction in any medium or format, as long as you give appropriate credit to the original author(s) and the source, provide a link to the Creative Commons license, and indicate if changes were made. The images or other third party material in this article are included in the article's Creative Commons license, unless indicated otherwise in a credit line to the material. If material is not included in the article's Creative Commons license and your intended use is not permitted by statutory regulation or exceeds the permitted use, you will need to obtain permission directly from the copyright holder. To view a copy of this license, visit <http://creativecommons.org/licenses/by/4.0/>.

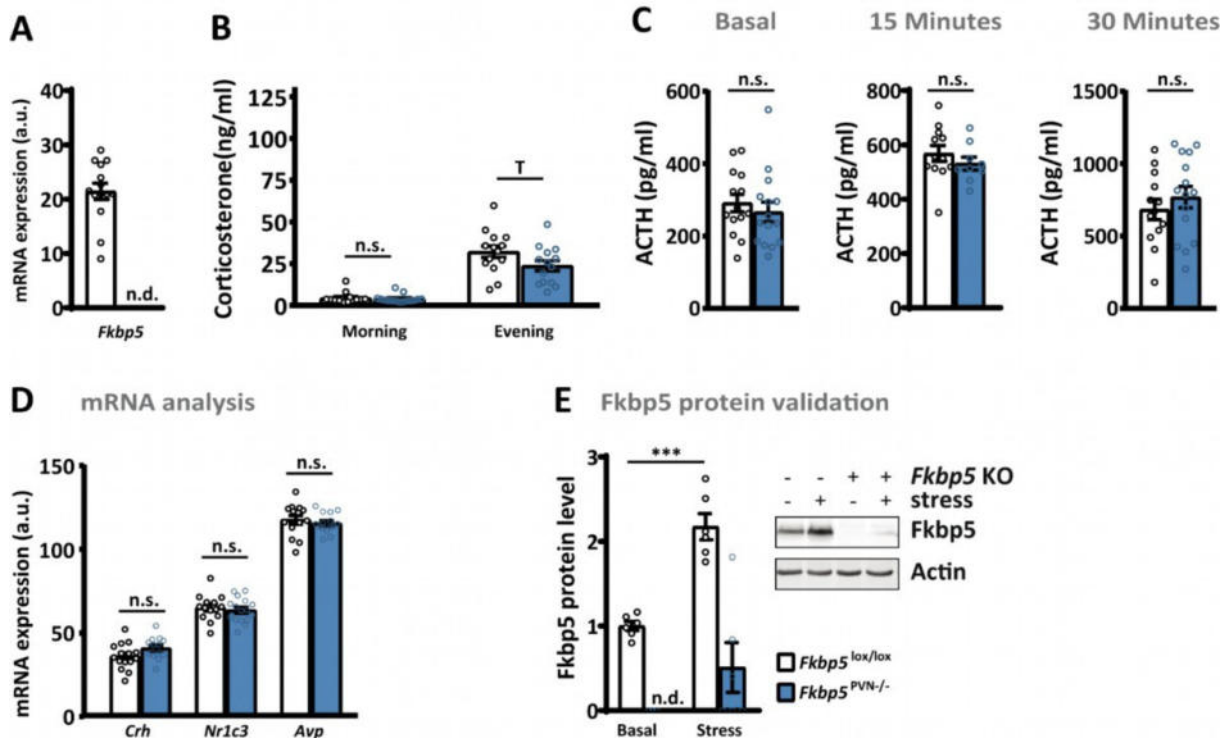
References

1. De Kloet ER, Joëls M, Holsboer F. Stress and the brain: from adaptation to disease. *Nat Rev Neurosci*. 2005;6:463–75.
2. Sinars CR, Cheung-Flynn J, Rimerman RA, Scammell JG, Smith DF, Clardy J. Structure of the large FK506-binding protein FKBP51, an Hsp90-binding protein and a component of steroid receptor complexes. *Proc Natl Acad Sci USA*. 2003;100:868–73.
3. Wochnik GM, Rüegg J, Abel GA, Schmidt U, Holsboer F, Rein T. FK506-binding proteins 51 and 52 differentially regulate dynein interaction and nuclear translocation of the glucocorticoid receptor in mammalian cells. *J Biol Chem*. 2005;280:4609–16.
4. Scammell JG, Denny WB, Valentine DL, Smiths DF. Overexpression of the FK506-binding immunophilin FKBP51 is the

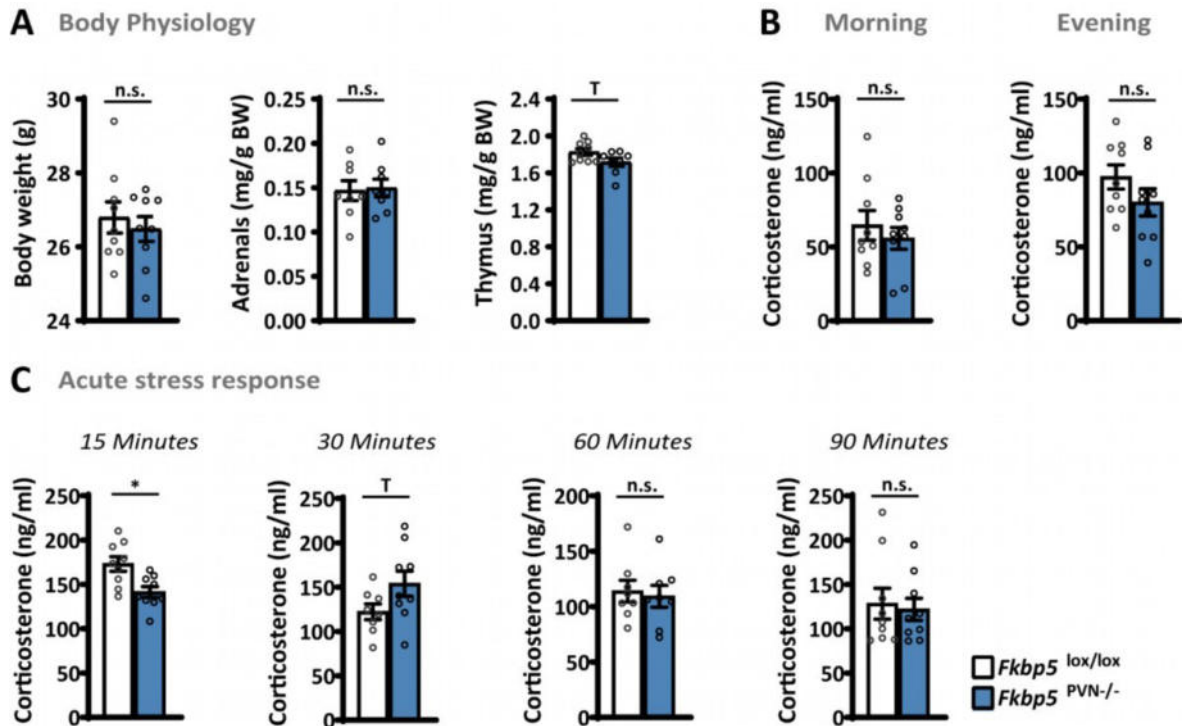
- common cause of glucocorticoid resistance in three new world primates. *Gen Comp Endocrinol.* 2001;124:152–65.
5. Binder EB, Bradley RG, Liu W, Epstein MP, Deveau TC, Mercer KB, et al. Association of FKBP5 polymorphisms and childhood abuse with risk of posttraumatic stress disorder symptoms in adults. *JAMA.* 2008;299:1291–305.
 6. Denny WB, Valentine DL, Reynolds PD, Smith DF, Scammell JG. Squirrel monkey immunophilin FKBP51 is a potent inhibitor of glucocorticoid receptor binding. *Endocrinology.* 2000;141:4107–13.
 7. Ising M, Depping AM, Siebertz A, Lucae S, Unschuld PG, Kloiber S, et al. Polymorphisms in the FKBP5 gene region modulate recovery from psychosocial stress in healthy controls. *Eur J Neurosci.* 2008;28:389–98.
 8. Touma C, Gassen NC, Herrmann L, Cheung-Flynn J, Bli DR, Ionescu IA, et al. FK506 binding protein 5 shapes stress responsiveness: modulation of neuroendocrine reactivity and coping behavior. *Biol Psychiatry.* 2011;70:928–36.
 9. Westberry JM, Sadosky PW, Hubler TR, Gross KL, Scammell JG. Glucocorticoid resistance in squirrel monkeys results from a combination of a transcriptionally incompetent glucocorticoid receptor and overexpression of the glucocorticoid receptor co-chaperone FKBP51. *J Steroid Biochem Mol Biol.* 2006;100:34–41.
 10. Scharf SH, Liebl C, Binder EB, Schmidt MV, Müller MB. Expression and regulation of the *Fkbp5* gene in the adult mouse brain. *PLoS ONE.* 2011;6:1–10.
 11. Zannas AS, Binder EB. Gene-environment interactions at the FKBP5 locus: sensitive periods, mechanisms and pleiotropism. *Genes Brain Behav.* 2014;13:25–37.
 12. Matosin N, Halldorsdottir T, Binder EB. Understanding the molecular mechanisms underpinning gene by environment interactions in psychiatric disorders: the FKBP5 model. 2018. <https://doi.org/10.1016/j.biopsych.2018.01.021>.
 13. Binder EB, Salyakina D, Lichtner P, Wochnik GM, Ising M, Pütz B, et al. Polymorphisms in FKBP5 are associated with increased recurrence of depressive episodes and rapid response to antidepressant treatment. *Nat Genet.* 2004;36:1319–25.
 14. Klengel T, Mehta D, Anacker C, Rex-Haffner M, Pruessner JC, Pariante CM, et al. Allele-specific FKBP5 DNA demethylation mediates gene-childhood trauma interactions. *Nat Neurosci.* 2013;16:33–41.
 15. Young KA, Thompson PM, Cruz DA, Williamson DE, Selemo LD. BA11 FKBP5 expression levels correlate with dendritic spine density in postmortem PTSD and controls. *Neurobiol Stress.* 2015;2:67–72.
 16. Sinclair D, Fillman SG, Webster MJ, Weickert CS. Dysregulation of glucocorticoid receptor co-factors FKBP5, BAG1 and PTGES3 in prefrontal cortex in psychotic illness. *Sci Rep.* 2013;3:1–10.
 17. Gassen NC, Hartmann J, Zschocke J, Stepan J, Hafner K, Zellner A, et al. Association of FKBP51 with priming of autophagy pathways and mediation of antidepressant treatment response: evidence in cells, mice, and humans. *PLoS Med.* 2014;11:e1001755.
 18. Hartmann J, Wagner KV, Gaali S, Kirschner A, Kozany C, Ruhter G, et al. Pharmacological inhibition of the psychiatric risk factor FKBP51 has anxiolytic properties. *J Neurosci.* 2015;35:9007–16.
 19. Herman JP, McKlveen JM, Ghosal S, Kopp B, Wulsin A, Makinson R, et al. Regulation of the hypothalamic-pituitary-adrenocortical stress response. *Compr Physiol.* 2016;6:603–21.
 20. Walker SE, Zanoletti O, Guillot de Suduiraut I, Sandi C. Constitutive differences in glucocorticoid responsiveness to stress are related to variation in aggression and anxiety-related behaviors. *Psychoneuroendocrinology.* 2017. <https://doi.org/10.1016/j.psyneuen.2017.06.011>.
 21. Rodríguez CI, Buchholz F, Galloway J, Sequerra R, Kasper J, Ayala R, et al. High-efficiency deleter mice show that *FLPe* is an alternative to *Cre-loxP*. *Nat Genet.* 2000;25:139–40.
 22. Balthasar N, Dalgaard LT, Lee CE, Yu J, Funahashi H, Williams T, et al. Divergence of melanocortin pathways in the control of food intake and energy expenditure. *Cell.* 2005;123:493–505.
 23. Dedic N, Kühne C, Jakovcevski M, Hartmann J, Genewsky AJ, Gomes KS, et al. Chronic CRH depletion from GABAergic, long-range projection neurons in the extended amygdala reduces dopamine release and increases anxiety. *Nat Neurosci.* 2018;21:803–7.
 24. Schmidt MV, Schulke J-P, Liebl C, Stiebs M, Avrabos C, Bock J, et al. Tumor suppressor down-regulated in renal cell carcinoma 1 (*DRR1*) is a stress-induced actin bundling factor that modulates synaptic efficacy and cognition. *Proc Natl Acad Sci USA.* 2011;108:17213–8.
 25. Paré WP, Glavin GB. Restraint stress in biomedical research: a review. *Neurosci Biobehav Rev.* 1986;10:339–70.
 26. Karssen AM, Meijer OC, Berry A, Sanjuan Piñol R, De Kloet ER. Low doses of dexamethasone can produce a hypocortisosteroid state in the brain. *Endocrinology.* 2005;146:5587–95.
 27. Jakovcevski M, Schachner M, Morellini F. Susceptibility to the long-term anxiogenic effects of an acute stressor is mediated by the activation of the glucocorticoid receptors. *Neuropharmacology.* 2011;61:1297–305.
 28. Hartmann J, Wagner KV, Liebl C, Scharf SH, Wang XD, Wolf M, et al. The involvement of FK506-binding protein 51 (*FKBP5*) in the behavioral and neuroendocrine effects of chronic social defeat stress. *Neuropharmacology.* 2012;62:332–9.
 29. Schmidt MV, Sterlemann V, Ganea K, Liebl C, Alam S, Harbich D, et al. Persistent neuroendocrine and behavioral effects of a novel, etiologically relevant mouse paradigm for chronic social stress during adolescence. *Psychoneuroendocrinology.* 2007;32:417–29.
 30. Alexander Wolf F. PA and FJT. SCANPY: large-scale single cell data analysis. *Genome Biol.* 2017;19:2926–34.
 31. Johnson WE, Li C, Rabinovic A. Adjusting batch effects in microarray expression data using empirical Bayes methods. *Biostatistics.* 2007;8:118–27.
 32. Mifsud KR, Reul JM. Acute stress enhances heterodimerization and binding of corticosteroid receptors at glucocorticoid target genes in the hippocampus. *Proc Natl Acad Sci USA.* 2016;113:11336–41.
 33. Ising M, Holsboer F. Genetics of stress response and stress-related disorders. *Dialogues Clin Neurosci.* 2006;8:433–44.
 34. Wagner KV, Marinescu D, Hartmann J, Wang XD, Labermaier C, Scharf SH, et al. Differences in FKBP51 regulation following chronic social defeat stress correlate with individual stress sensitivity: influence of paroxetine treatment. *Neuropsychopharmacology.* 2012;37:2797–808.
 35. Nestler EJ, Barrot M, DiLeone RJ, Eisch AJ, Gold SJ, Monteggia LM. Neurobiology of depression. *Neuron.* 2002;34:13–25.
 36. Tsigos C, Chrousos GP. Hypothalamic-pituitary-adrenal axis, neuroendocrine factors and stress. *J Psychosom Res.* 2002;53:865–71.
 37. Gallier-Beckley AJ, Cidlowski JA. Emerging roles of glucocorticoid receptor phosphorylation in modulating glucocorticoid hormone action in health and disease. *IUBMB Life.* 2009;61:979–86.
 38. Wang Z, Frederick J, Garabedian MJ. Deciphering the phosphorylation ‘code’ of the glucocorticoid receptor in vivo. *J Biol Chem.* 2002;277:26573–80.
 39. Dourmes C, Dine J, Lopez J-P, Brivio E, Anderzhanova E, Roeh S, et al. Hypothalamic glucocorticoid receptor in CRF neurons is essential for HPA axis habituation to repeated stressor. *BioRxiv.* 2020:2020.11.30.402024.
 40. Luecken MD, Theis FJ. Current best practices in single-cell RNA-seq analysis: a tutorial. *Mol Syst Biol.* 2019;15:e8746.

41. Hoeijmakers L, Harbich D, Schmid B, Lucassen PJ, Wagner KV, Schmidt MV, et al. Depletion of FKBP51 in female mice shapes HPA axis activity. *PLoS ONE*. 2014. <https://doi.org/10.1371/journal.pone.0095796>.
42. Sabbagh JJ, O'Leary JC, Blair LJ, Klengel T, Nordhues BA, Fontaine SN, et al. Age-associated epigenetic upregulation of the FKBP5 gene selectively impairs stress resiliency. *PLoS ONE*. 2014;9:e107241.
43. O'Leary JC, Dharia S, Blair LJ, Brady S, Johnson AG, Peters M, et al. A new anti-depressive strategy for the elderly: ablation of FKBP5/FKBP51. *PLoS ONE*. 2011;6:e24840.
44. Klein F, Lemaire V, Sandi C, Vitiello S, Van der Logt J, Laurent PE, et al. Prolonged increase of corticosterone secretion by chronic social stress does not necessarily impair immune functions. *Life Sci*. 1992;50:723–31.
45. Laryea G, Arnett M, Muglia LJ. Ontogeny of hypothalamic glucocorticoid receptor-mediated inhibition of the hypothalamic-pituitary-adrenal axis in mice. *Stress*. 2015. <https://doi.org/10.3109/10253890.2015.1046832>.
46. De Kloet ER. Hormones and the stressed brain. *Ann N Y Acad Sci*. 2004;1018:1–15.
47. Blind RD, Garabedian MJ. Differential recruitment of glucocorticoid receptor phospho-isoforms to glucocorticoid-induced genes. *J Steroid Biochem Mol Biol*. 2008;109:150–7.
48. Krstic MD, Rogatsky I, Yamamoto KR, Garabedian MJ. Mitogen-activated and cyclin-dependent protein kinases selectively and differentially modulate transcriptional enhancement by the glucocorticoid receptor. *Mol Cell Biol*. 1997;17:3947–54.
49. Kino T, Ichijo T, Amin ND, Kesavapany S, Wang Y, Kim N, et al. Cyclin-dependent kinase 5 differentially regulates the transcriptional activity of the glucocorticoid receptor through phosphorylation: clinical implications for the nervous system response to glucocorticoids and stress. *Mol Endocrinol*. 2007;21:1552–68.
50. Gassen NC, Hartmann J, Zannas AS, Kretschmar A, Zschocke J, Maccarrone G, et al. FKBP51 inhibits GSK3 β and augments the effects of distinct psychotropic medications. *Mol Psychiatry*. 2016;21:277–89.
51. Scharf SH, Schmidt MV. Animal models of stress vulnerability and resilience in translational research. *Curr Psychiatry Rep*. 2012;14:159–65.
52. Blair LJ, Criado-Marrero M, Zheng D, Wang X, Kamath S, Nordhues BA, et al. The disease-associated chaperone FKBP51 impairs cognitive function by accelerating AMPA receptor recycling. *ENeuro*. 2019;6:ENEURO.0242–18.
53. Sapolsky RM, Romero LM, Munck AU. How do glucocorticoids influence stress responses? Integrating permissive, suppressive, stimulatory, and preparative actions. *Endocr Rev*. 2000;21:55–89.
54. Winter J, Jurek B. The interplay between oxytocin and the CRF system: regulation of the stress response. *Cell Tissue Res*. 2019.
55. Leon-Mercado L, Chao DHM, Basualdo M del C, Kawata M, Escobar C, et al. The arcuate nucleus: a site of fast negative feedback for corticosterone secretion in male rats. *ENeuro*. 2017. <https://doi.org/10.1523/ENEURO.0350-16.2017>.

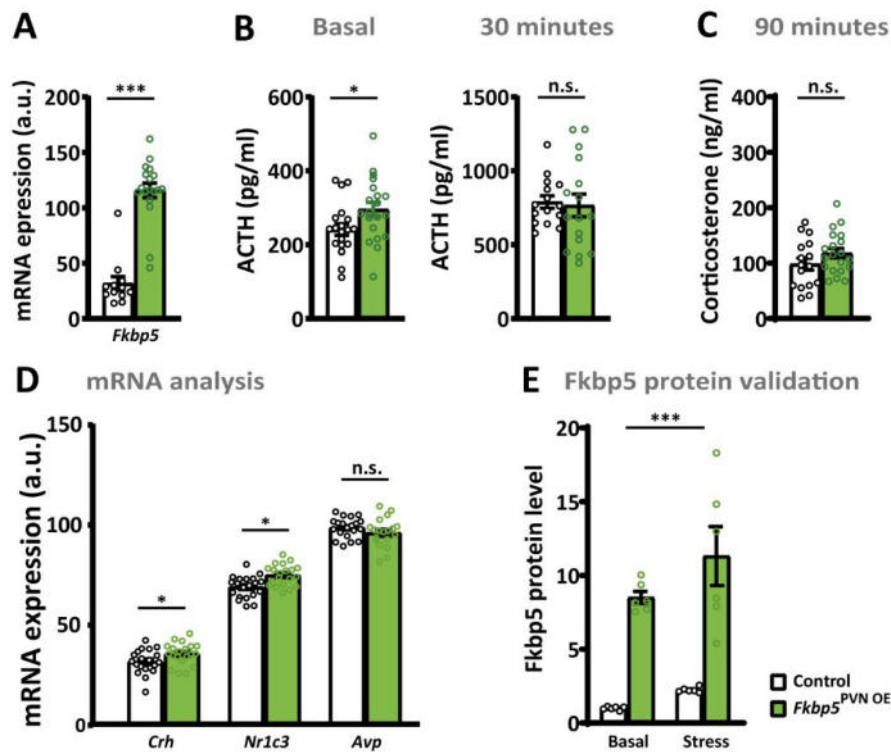
Supplementary figures.



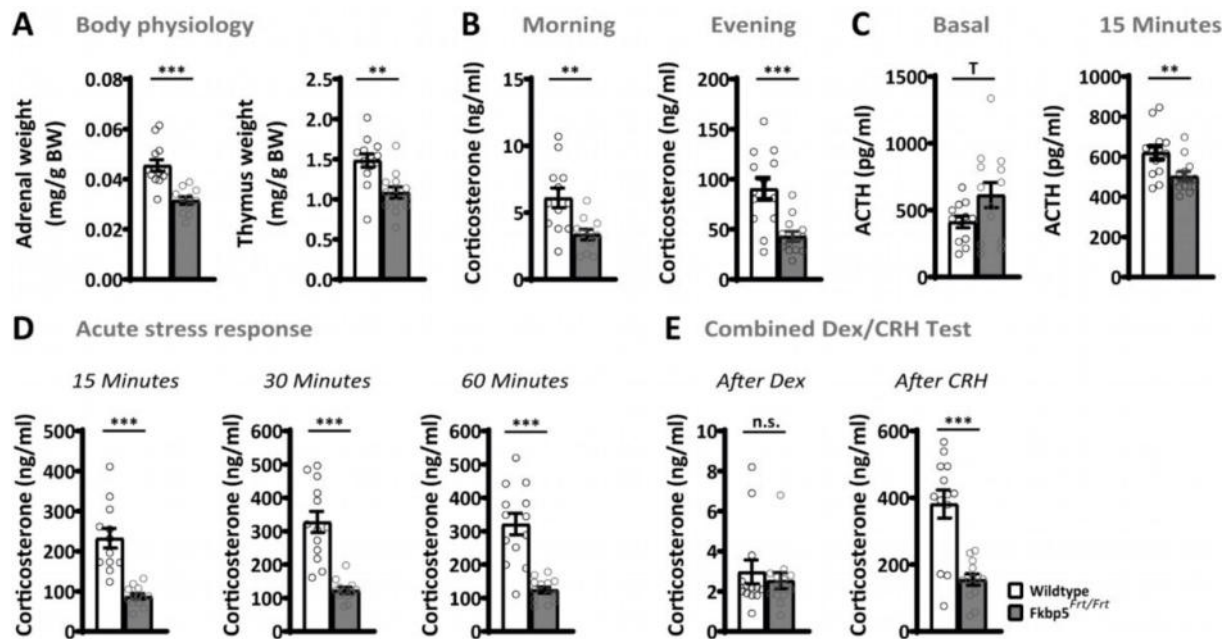
Supplementary Figure 1: Corticosterone and ACTH levels of *Fkbp5*^{PVN-/-} mice (16-20 weeks of age). (A) Validation of the *Fkbp5* deletion in *Fkbp5*^{PVN-/-} animals (*Fkbp5*^{PVN-/-} n = 16; *Fkbp5*^{lox/lox} n =15). (B) *Fkbp5* deletion in the PVN has no effect on basal CORT levels (*Fkbp5*^{PVN-/-} n = 16; *Fkbp5*^{lox/lox} n =15). (C) ACTH levels under basal,15 and 30 minutes after stress onset were unaltered (*Fkbp5*^{PVN-/-} n = 9-16; *Fkbp5*^{lox/lox} n =12-15). (D) mRNA changes of stress responsive genes within the PVN under basal conditions (*Fkbp5*^{PVN-/-} n = 16; *Fkbp5*^{lox/lox} n =15). (E) Fkbp5 protein levels under basal and stress conditions (*Fkbp5*^{PVN-/-} n = 6; *Fkbp5*^{lox/lox} n = 6 for stressed and non-stressed group). All data were received from mice between 16 and 20 weeks of age and are presented as mean ± SEM and were analyzed with a student's t-test (A-D) or with a two way ANOVA (E). n.d. = not detectable; n.s. = not significant; T = 0.05 < p < 0.1; *** = p < 0.001.



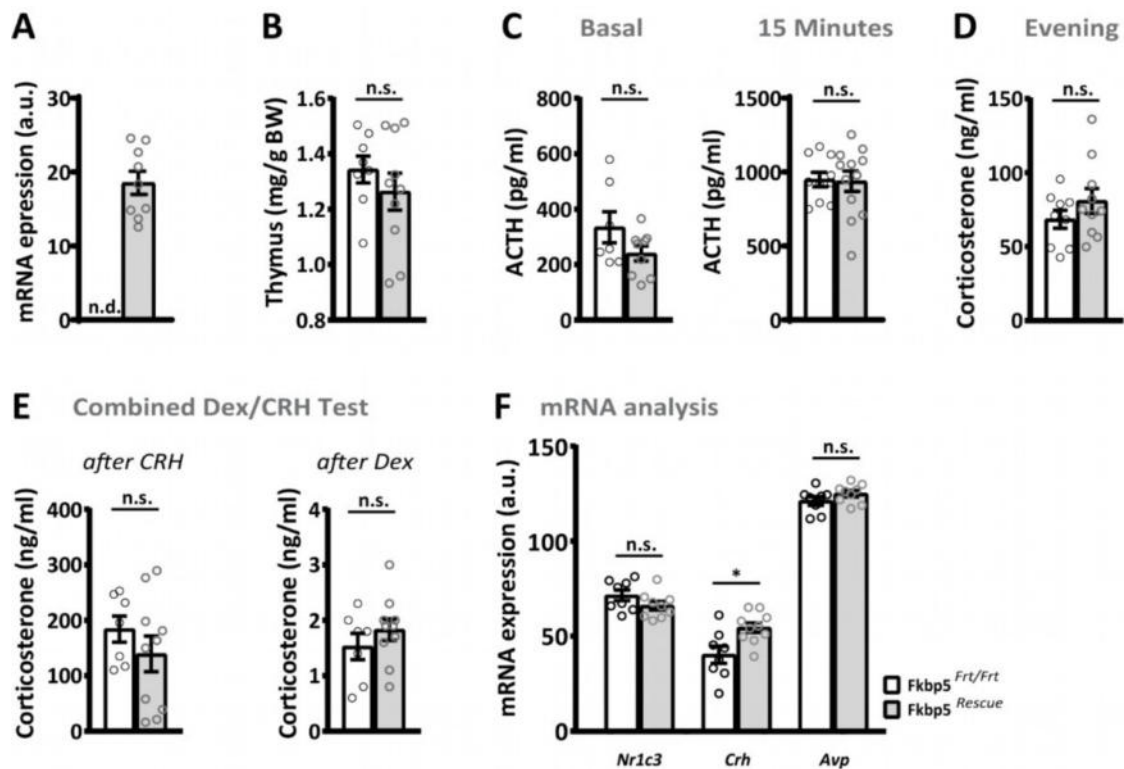
Supplementary Figure 2: Young mice with *Fkbp5* deletion in the PVN. (A) Animals with an age of 8-10 weeks had no alterations in body physiology. (B) Morning and evening corticosterone levels were unchanged. (C) FKBP51^{PVN-/-} animals had significantly lower corticosterone levels 15 minutes after stress onset compared to the control group (group size for A-C: *Fkbp5*^{PVN-/-} n = 9; *Fkbp5*^{lox/lox} n = 9). All data were received from mice between 8 and 10 weeks of age and are presented as mean ± SEM. Data were analyzed with a student's t-test. n.s. = not significant; T = 0.05 < p < 0.1; * = p < 0.05.



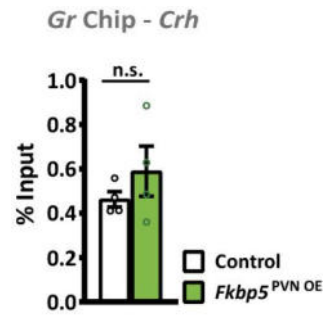
Supplementary Figure 3: Overexpression of *Fkbp5* in the PVN affected ACTH and mRNA levels. (A) *Fkbp5* overexpression resulted in a significant increase of *Fkbp5* mRNA (n (control) = 12 vs n (*Fkbp5*^{PVN OE}) = 18). **(B)** ACTH levels were significantly higher in *Fkbp5*^{PVN OE} mice under basal conditions (n = 20 vs. 20) and unchanged 30 minutes after stress onset (n = 12 vs. 12) compared to their controls. **(C)** We did not detect any differences in corticosterone levels 60 minutes after stress onset (n = 20 vs. 20). **(D)** mRNA levels of *Nr1c3* and *Crh* and *Avp* under basal conditions (n = 20 vs. 20). **(E)** Viral overexpression resulted in a 4-fold *Fkbp5* protein upregulation (n = 6 vs. 6 for stress and non-stressed groups). All data were received from mice between 14-20 weeks of age and are presented as mean \pm SEM and were analyzed with a student's t-test (A-D) or with a two way ANOVA (E). n.s. = not significant; * = $p < 0.05$, *** = $p < 0.001$.



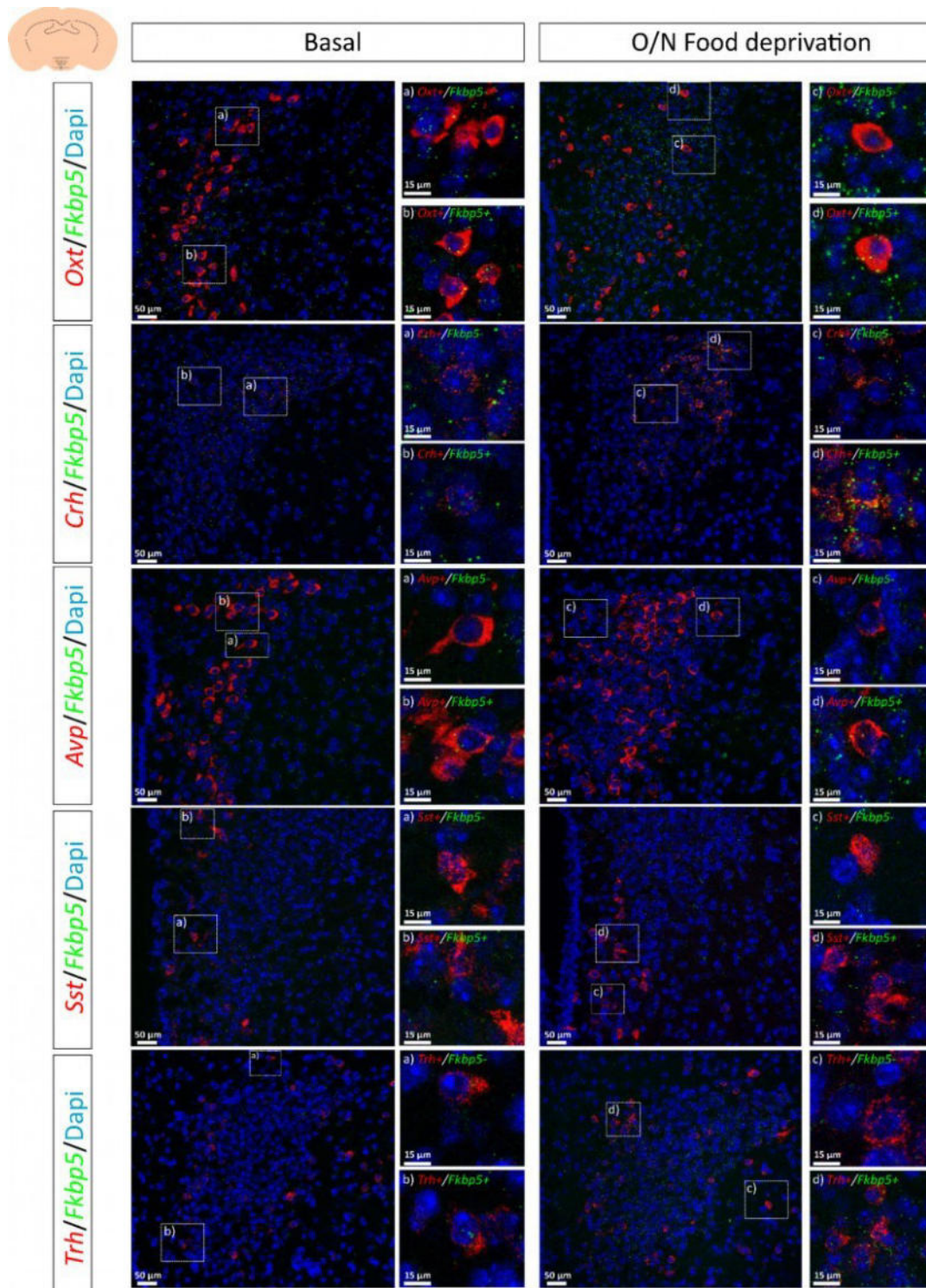
Supplementary Figure 4: Validation of the *Fkbp5^{Frt/Frt}* mouse line in comparison to wildtype littermates. (A) Adrenal and thymus weights on sacrifice day. **(B)** Morning and evening corticosterone levels. **(C)** ACTH under basal conditions and 15 minutes after stress onset. **(D)** Corticosterone after 15 minutes of restraint stress. **(E)** Combined Dex/CRH test. For all groups, n (wildtype) = 12 vs. n (*Fkbp5^{Frt/Frt}*) = 11. All data were received from mice of 16-24 weeks of age and are presented as mean \pm SEM and were analyzed with a student's t-test. n.s. = not significant; T = 0.05 < p < 0.1; ** = p < 0.01, *** = p < 0.001.



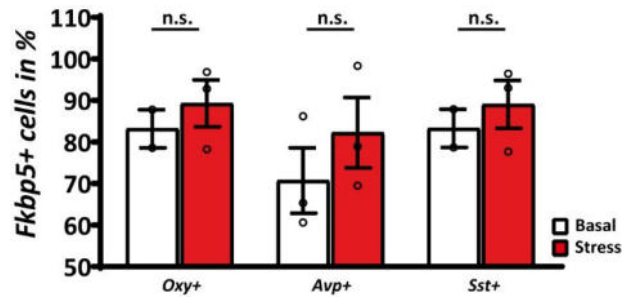
Supplementary Figure 5: Corticosterone and ACTH levels of $Fkbp5^{Rescue}$ mice. (A) Validation of $Fkbp5$ mRNA expression compared to $Fkbp5^{Frt/Frt}$. (B) $Fkbp5$ reinstatement had no effect on thymus weights. (C) ACTH hormone levels were unaltered under basal and 15 minutes after stress. (D) Evening corticosterone. (E) Rescue of endogenous $Fkbp5$ in global knock-out animals had no significant effect on the Dex/CRH test. (F) mRNA levels of stress responsive genes under basal conditions. Group sizes for A-F: $Fkbp5^{Rescue}$ $n = 10$; $Fkbp5^{Frt/Frt}$ $n = 9$). All data were received from mice between 16 and 20 weeks of age and are presented as mean \pm SEM and were analyzed with a student's t-test. n.s. = not significant; n.d. = not detectable; * = $p < 0.05$.



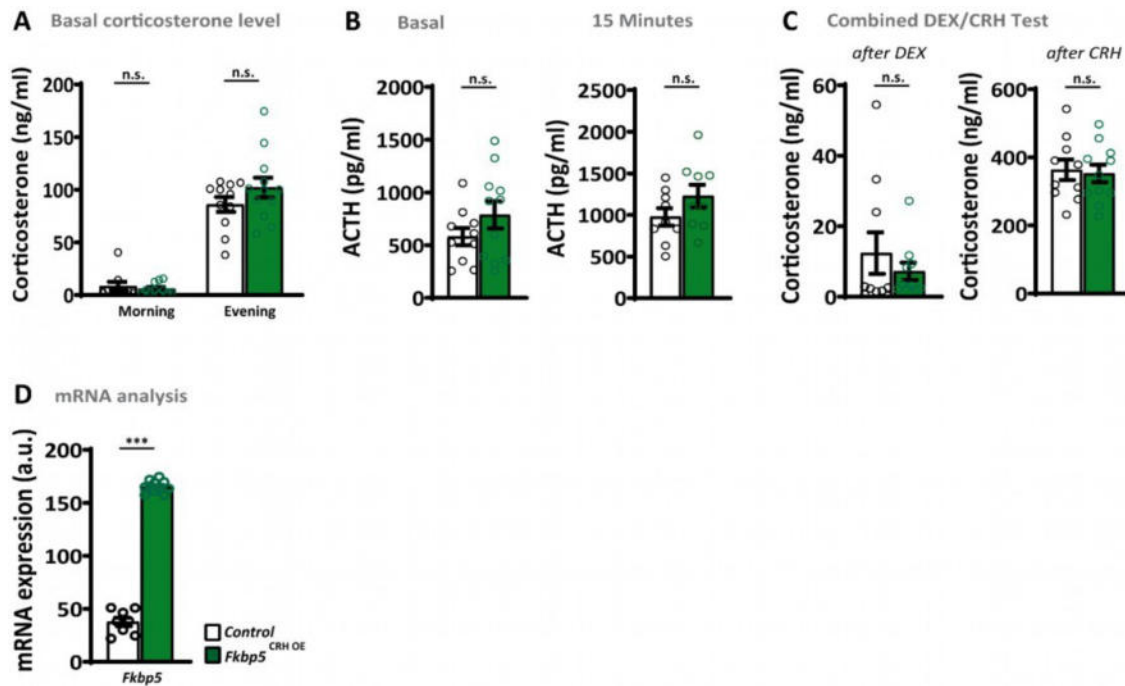
Supplementary Figure 6: GR to GRE binding within the *Crh* gene after stress. Mice were sacrificed 30 minutes after stress onset. Every n consists of a pool of 4 individual hypothalami. All data were received from mice aged between 12-16 weeks and are indicated as mean ± SEM and were analyzed with a student's t-test; (n = 4 vs. 4); n.s. = not significant.



Supplementary Figure 7: RNA scope analysis of *Fkbp5* expression in stress response neuronal cell populations of C57Bl/6 under basal and stressed conditions. In comparison to single-cell sequencing, RNA scope revealed a significant higher co-localization ratio of *Fkbp5* in oxytocin (*Oxt*), corticotropin-releasing hormone (*Crh*), vasopressin (*Avp*), somatostatin (*Sst*) and thyronine releasing hormone (*Trh*) neurons. Overnight food deprivation increased *Fkbp5* mRNA in all cell populations.



Supplementary Figure 8: Quantification of *Fkbp5* co-localization in stress response markers under basal and stress conditions. Under basal conditions *Fkbp5* mRNA signal was detected in 83% of *Oxy+* neurons, 68% in *Avp+* and 84% of *Sst+* neurons. We monitored a non-significant increase in *Fkbp5* mRNA expression in all neuronal populations. Each n represents an average of the detected *Fkbp5* mRNA expression in all neuronal populations. Each n represents an average of the detected *Fkbp5* cells within six z-stacks of 1um each (3 per PVN side). Data were received from animals between 8-12 weeks of age and are presented as mean \pm SEM and were analyzed with a student's t-test. n.s. = not significant.



Supplementary Figure 9: Corticosterone and ACTH levels of $Fkbp5^{CRH OE}$ mice. (A) *Fkbp5* overexpression in CRH neurons within the PVN had no effect on basal morning ($Fkbp5^{CRH OE}$ $n = 11$; Control $n = 9$) and evening ($Fkbp5^{CRH OE}$ $n = 12$; Control $n = 11$) CORT level. **(B)** ACTH level were unaltered at baseline ($Fkbp5^{CRH OE}$ $n = 11$; Control $n = 10$) and 15 minutes post stress ($Fkbp5^{CRH OE}$ $n = 9$; Control $n = 9$). **(C)** In the combined Dex/CRH test CORT level were unaltered in $Fkbp5^{CRH OE}$ ($n_{after DEX} = 10$; $n_{after CRH} = 11$) compared to controls ($n = 10$) **(D)** *Fkbp5* mRNA expression level. All data are presented as mean \pm SEM and were analyzed with a student's t-test. n.s. = not significant; *** = $p < 0.001$.

4. General discussion

The co-chaperone FKBP51 is a highly stress-inducible protein to finetune the impact of glucocorticoids via a negative feedback loop on the GR. Alterations of FKBP51 signaling and SNPs within the *FKBP5* gene are associated with a dysfunctional HPA axis and mental disorders like PTSD and MD⁵³. During the last decade, multiple new interaction partners of FKBP51 were discovered besides GR, and FKBP51 emerged as a novel regulator controlling metabolism. In addition, polymorphisms within *FKBP5* have been associated with traits of T2D^{152,153}. However, the underlying molecular and region-specific mechanisms of FKBP51 are still largely unknown. This thesis investigated the nucleus and tissue-specific role of FKBP51 in regulating whole-body metabolism and the acute stress response.

The first study illustrated that total loss of FKBP51 improved the metabolic phenotype of adult mice and protected against diet-induced body weight gain, accompanied by improved glucose metabolism. We could pinpoint the beneficial phenotype of FKBP51 deficient mice to enhanced insulin signaling and increased energy expenditure. Mechanistically, we discovered an active role of FKBP51 within the PI3K-AKT2-AS160 signaling pathway to regulate glucose uptake in skeletal muscle. Next, we antagonized FKBP51 acutely and chronically with SAFit2, a selective FKBP51 antagonist, to investigate the therapeutic potential of FKBP51. These experiments revealed that SAFit2 is able to restore the beneficial phenotype of FKBP51 deficient mice and demonstrated that effects on glucose metabolism are independent of the reduction of body weight.

The second study addressed the function of hypothalamic FKBP51 in the control of whole-body metabolism. We manipulated FKBP51 expression by viral deletion and overexpression in the MBH and revealed a novel role of central FKBP51 in managing body weight. Whereas deletion of hypothalamic FKBP51 led to massive obesity within a few weeks after surgery under a regular chow diet, overexpression resulted in a lean phenotype under HFD conditions. We suggested that differences in food intake and altered sympathetic outflow to peripheral tissues caused these changes in body weight. Acute FKBP51 manipulation impacted metabolism differently than total loss of FKBP51 and emphasized the tissue-specificity of FKBP51. Mechanistically, we discovered a new regulatory role of

FKBP51 on autophagy signaling in response to metabolic stressors by altering the balance between the two central energy sensors in the MBH, AMPK and mTORC1 (Chapter 3.2).

The third study investigated the function of FKBP51 within the PVN and demonstrated the fundamental role of FKBP51 within the acute stress response (Chapter 3.3). We showed that loss of FKBP51 in the PVN increased GR sensitivity, while FKBP51 overexpression resulted in a stress-like phenotype with a chronic increase in glucocorticoids. Next, we studied the expression profile of FKBP51 within the PVN and revealed a distinct pattern of FKBP51 expression under baseline and stress conditions, with the highest FKBP51 induction in CRH⁺ neurons after acute stress. Surprisingly, CRH-specific overexpression of FKBP51 did not affect the HPA axis response after acute challenges, suggesting a rather collective action of FKBP51 in multiple neuronal subpopulations within the acute stress response.

In summary, this thesis extends the knowledge about the hypothalamic- and muscle-specific action of FKBP51 in regulating the acute stress response and whole-body metabolism. The novel data provide substantial evidence of the importance of FKBP51 on stress and metabolic relevant pathways, such as the insulin and autophagy pathways, to regulate systemic homeostasis.

4.1. FKBP51 in the control of metabolism

4.1.1. Total loss of FKBP51 improves metabolic health in mice

FKBP51 is a stress-inducible co-chaperone acting as a primary regulator of the HPA axis by altering GR sensitivity. GR is widely expressed in relevant metabolic tissues and regulates molecular processes like gluconeogenesis, lipolysis, and proteolysis⁴⁶. Therefore, it seems plausible that FKBP51 might also play a role in regulating metabolism. First studies on conventional FKBP51 knockout (KO) mice, which carry a deletion of FKBP51 in all tissues from conception, on chronic social defeat stress (CSDS) demonstrated that FKBP51 KO mice are leaner than their WT littermates under a regular chow diet⁵⁷. However, research on FKBP51's role in metabolism is still rare, and the focus, so far, was on the stress response. In the central part of this thesis, we therefore attempted to investigate the role of FKBP51 in controlling whole-body metabolism.

First, we characterized FKBP51 KO mice under chow and high-fat diet (HFD) conditions (Chapter 3.1). We could demonstrate that FKBP51 KO mice are protected from high-fat diet-induced weight gain with improved glucose tolerance on chow and HFD conditions. Furthermore, the beneficial health of FKBP51 KO mice was accompanied by increased lean and reduced fat mass. There are multiple causes for body weight loss, but the most obvious is a shift in energy homeostasis, a tightly regulated balance between energy intake and energy expenditure (Chapter 1.3). Intriguingly, we could not observe any effects of FKBP51 deletion on food intake (Chapter 3.1). Thus, we suggested that changes in energy expenditure are a critical factor contributing to the reduced body weight of FKBP51 KO mice. Indeed, loss of FKBP51 resulted in an increased total energy expenditure (TEE), which was assessed by indirect calorimetry.

A recent study by Stechschulte and colleagues, which also investigated the role of FKBP51 in energy homeostasis in a non-related strain of conventional FKBP51 KO mice, strengthens our findings. They observed similar beneficial effects of FKBP51 KO mice on a standard chow diet and a robust resistance to HFD induced body weight gain. The authors concentrated on the role of FKBP51 in adipose tissue and discovered that FKBP51 KO mice exhibit reduced WAT mass accompanied by smaller adipocytes

compared to WT littermates^{30,153}. Small adipocytes are a vital characteristic of healthy adipose tissue because they counteract metabolic decline and lower the susceptibility to developing diabetes¹⁵⁴.

Adipose tissue has a profound influence on energy storage and systemic metabolic homeostasis. During obesity, adipose depots expand massively in 2 ways: 1) existing adipocytes increase in size (so-called hypertrophy) or 2) preadipocytes differentiate into new adipocytes (so-called hyperplasia)¹⁵⁴. Interestingly, FKBP51 is highly induced in the early stages of adipocyte differentiation, and loss of FKBP51 completely inhibits adipocyte differentiation *in-vitro*^{153,155}. The key transcriptional factor of adipocyte differentiation is PPAR γ , which is highly activated upon fat expansion to promote the terminal stage of preadipocyte differentiation and lipid storage in mature adipocytes¹⁵⁶. Stechschulte et al. built on this knowledge and concluded that FKBP51 KO mice were resistant to WAT expansion caused by a deficiency in adipogenesis, which they confirmed by showing reduced expression of PPAR γ responsive genes¹⁵⁷.

The study further revealed significantly higher levels of BAT mass as a decisive characteristic of FKBP51 KO mice and an increased rate of WAT browning (beige fat cells). BAT and beige fat cells derive from different cell lineages and are known to burn energy through thermogenesis. A crucial driver of thermogenesis is the uncoupling protein 1 (UCP1), which is highly expressed in brown or beige fat cells¹⁵⁸. Our study and the study by Stechschulte observed significantly increased thermogenic genes, such as PGC-1 α (PPAR γ coactivator 1-alpha), UCP-1, and PRDM16 (PR domain containing 16), which might explain the increased energy expenditure¹⁵⁷. However, the underlying molecular mechanism causing increased UCP-1 expression and higher rates of BAT mass was not yet investigated and should be addressed in future studies.

In addition to the adipose-specific effects of FKBP51 observed by Stechschulte et al., we could identify a unique role of FKBP51 in skeletal muscle. In FKBP51 KO mice, reduced scaffolding of PHLPP to AKT resulted in hyperactivation of AKT2 and AS160. Hyperactivation of the AKT2-AS160 complex resulted in enhanced GLUT4 translocation and thereby increased glucose uptake in muscle tissue (Chapter 3.1). Furthermore, we could reveal that deletion of FKBP51 did not affect insulin release under fasted and glucose-stimulated conditions, suggesting a hormone-independent role of FKBP51. These

observations and the hyperactive insulin pathway in skeletal muscle, one of the major tissues regulating insulin-induced glucose utilization, indicate that the enhanced glucose metabolism in FKBP51 KO mice accounts for the improved insulin sensitivity.

Overall, these data suggest a prominent role of FKBP51 in whole-body metabolism with a critical regulatory role in glucose metabolism, adipogenesis, and browning of WAT. Furthermore, the data indicate that the observed effects cause the lean phenotype of FKBP51 KO mice despite the lack of food intake alterations and that peripheral FKBP51 might be the driving factor of the metabolic phenotype of FKBP51 KO mice.

4.1.2. Hypothalamic FKBP51 manipulation affects food intake and body weight control

The effects of FKBP51 in the brain on metabolism are barely studied despite its high upregulation after metabolic challenges, such as food deprivation and HFD^{60,129}. We were encouraged to gain a deeper understanding of the central role of FKBP51 and investigated the function of FKBP51 in the MBH (Chapter 3.2), one of the critical areas integrating peripheral signals to regulate energy homeostasis (Chapter 1.3.2).

To test the hypothesis that hypothalamic FKBP51 regulates whole-body metabolism, we used an AAV viral approach to delete and overexpress FKBP51 in the MBH. We demonstrated that central FKBP51 deletion (FKBP51^{MBH-KO}) resulted in massive obesity on a standard research diet, whereas FKBP51 overexpression (FKBP51^{MBH-OE}) protected against induced weight gain following an HFD regimen. In contrast to our experiments with conventional FKBP51 KO animals (Chapter 3.1), we observed changes in food intake. In fact, we monitored reduced food intake in FKBP51^{MBH-OE} mice and increased food intake in FKBP51^{MBH-KO} mice (Chapter 3.2). As an underlying mechanism, we hypothesized that FKBP51 regulates food intake and sympathetic outflow by balancing the two primary energy sensors AMPK and mTOR, and thereby autophagy signaling (see 4.2.2 for detailed mechanism). Intriguingly, we observed reduced AMPK and increased mTOR signaling in the MBH of FKBP51^{MBH-KO} and FKBP51^{MBH-OE} mice despite opposing phenotypes on food intake and body weight. The different behavioral outcomes may derive from several reasons.

First, the hypothalamus is a very heterogeneous brain region with multiple nuclei controlling different metabolic functions within the body. In our experiments, however, we targeted FKBP51 in all neurons within the MBH. These neuronal populations have opposing functions on food intake and energy expenditure. There is evidence that autophagy or mTOR signaling have antagonistic roles in different neuronal subpopulations. In more detail, whereas neuron-specific deletion of autophagy signaling in POMC neurons results in hyperphagia and obesity¹⁴⁵, deletion of autophagy in AgRP neurons is associated with lean mice and reduced food intake in response to fasting¹⁴⁴. In contrast, mice fed with a chronic HFD showed impaired autophagy in the arcuate nucleus, and a deletion of ATG7 in the MBH resulted in hyperphagia and increased body weight gain¹⁴². In addition, while chronic activation of

mTOR in POMC neurons caused hyperphagic obesity¹⁵⁹, activation of mTOR in multiple nuclei of the MBH reduced food intake and body weight gain¹⁶⁰. Second, we observed profound differences in peripheral autophagy and mTOR signaling in adipose tissue and skeletal muscle between FKBP51^{MBH-KO} and FKBP51^{MBH-OE} mice. While FKBP51^{MBH-OE} mice showed increased autophagy and reduced mTOR signaling, FKBP51^{MBH-KO} mice displayed an opposing phenotype. Fat and muscle are crucial mediators of whole-body metabolism and dysregulation of mTOR or autophagy in either of those tissues alone can alter body weight in mice. In fact, increased mTOR signaling in skeletal and adipose tissue is associated with obesity and insulin resistance¹⁶¹. We attributed the molecular changes in peripheral tissues to dampened sympathetic outflow in FKBP51^{MBH-OE} mice. We did not monitor sympathetic outflow in FKBP51^{MBH-KO} mice, but several studies indicate that obesity and hyperphagia are associated with increased sympathetic nervous system activity¹⁶²⁻¹⁶⁴. Thus, it might be worth speculating that FKBP51^{MBH-KO} mice have increased sympathetic nervous system activity and that the combined inhibition of central and peripheral autophagy is contributing to the obese phenotype. Third, hypothalamic FKBP51 manipulation may affect different pathways in the MBH, and subsequent changes in food intake alone can have a tremendous effect on circulating adipose tissue hormones, such as leptin and insulin¹⁶⁵. Both hormones are stimulated by the SNS and act in the MBH to mediate changes in food intake⁸⁹. Several studies demonstrated that leptin and insulin affect the AMPK and mTOR (p70S6K) signaling pathways in the hypothalamus. For instance, leptin inhibits AMPK in the arcuate nucleus to reduce food intake¹⁶⁶. Interestingly, FKBP51^{MBH-KO} mice showed a hyperactive insulin pathway within the MBH, which might affect insulin sensitivity and glucose uptake in the brain. Stechschulte and colleagues found that conventional FKBP51 KO mice have elevated adiponectin levels, which is known to activate AMPK in the ARC to promote food intake^{157,166}. We did not assess these hormones in our study, but central FKBP51 manipulation is likely to directly or indirectly affect signaling hormones or associated downstream signaling pathways to alter central hormone responsiveness. These hormonal changes might be a crucial factor contributing to the obese and lean phenotype of FKBP51^{MBH-KO} mice and FKBP51^{MBH-OE} mice, respectively.

Our results highlight the decisive role of FKBP51 in the MBH to regulate body weight but also raises the question of which nucleus or neuronal subpopulation is the main driver. It was recently shown that

FKBP51 is expressed in POMC neurons within the ARC, but the study did not find any differences in body weight on chow diet ¹⁶⁷. These findings are not surprising given the stress-responsive nature of FKBP51. Therefore, the biological relevance of FKBP51 in POMC neurons might be more pronounced after a metabolic challenge, such as an HFD. In addition, FKBP51 manipulation in a single neuronal population may not be sufficient to provoke long-lasting changes in whole-body metabolism. This hypothesis is in line with our study in Chapter 3.3, where we demonstrated that FKBP51 overexpression in all neurons within the PVN resulted in a stress-like phenotype with hypercortisolemia, but CRH-specific overexpression alone was not sufficient to recapitulate this phenotype. Preliminary experiments from our lab suggested that FKBP51 is not only expressed in POMC but also AgRP neurons and has a very distinct expression pattern within several nuclei of the hypothalamus, including the VMH and lateral hypothalamus. Both nuclei are known to regulate food intake and sympathetic nervous system activity ^{80,94}. Therefore, it might be possible that manipulation of FKBP51 in different or multiple neuronal subpopulations under certain environmental conditions is necessary to trigger a metabolic phenotype.

In our third study, where we addressed the PVN-specific role of FKBP51 in regulating the acute stress response, we observed that the conditional deletion of FKBP51 in *Sim1*⁺ neurons reduced body weight on a standard research diet (Chapter 3.3). This finding might be due to decreased corticosterone signaling. Despite high corticosterone levels, a PVN-specific overexpression had no effect on body weight, arguing against a corticosterone-mediated body weight phenotype. The study, however, aimed to explore the stress system and not the consequences of FKBP51 PVN deletion on metabolism. Nevertheless, these findings are exciting and should be explored in more detail in the future.

In summary, we present profound evidence that hypothalamic FKBP51 significantly affects food intake, sympathetic outflow to peripheral tissues, and thus whole-body metabolism in mice. Future studies are needed to investigate whether FKBP51 drives the observed phenotype via the AMPK-mTOR axis or an additional pathway not yet discovered.

4.2. Underlying molecular mechanism regulated by FKBP51

4.2.1. FKBP51 regulates AKT in skeletal and adipose tissue

In 2009, Pei et al. identified FKBP51 as a negative regulator of all 3 isoforms of AKT (AKT1, AKT2, and AKT3) by scaffolding the recruitment of the phosphatase PHLPP to AKT²⁸. Within the AKT-PHLPP complex, PHLPP dephosphorylates AKT at Ser473 to reduce AKT stability and activity¹⁶⁸. This milestone study further demonstrated that downregulation of FKBP51 diminished the interaction of PHLPP with AKT and thereby increased AKT activity²⁸. In general, AKT activity is regulated by the phosphorylation and dephosphorylation status at Ser473 and Thr308. Whereas Thr308 phosphorylation is required for AKT activity, phosphorylation of Ser473 is not. In fact, phosphorylation of AKT at Ser473 stabilizes and strengthens the duration of Thr308 phosphorylation. Importantly, PHLPP interacts with AKT independent of FKBP51¹⁶⁸. Thus, the role of FKBP51 might be of regulatory nature by regulating the overall efficiency of PHLPP-AKT signaling. Pei and colleagues identified the mechanism in cancer cells, but all three AKT isoforms are widely expressed throughout the body and regulate several signaling pathways important for metabolic control.

We used this knowledge in our first study and investigated the potential role of FKBP51 in muscle tissue, the main tissue for glucose utilization, as a possible underlying mechanism causing the beneficial glucose metabolism of FKBP51 KO mice (Chapter 3.1). We found that AKT2 signaling is increased in skeletal muscle of FKBP51 KO mice, which was caused by hyperactivation of AKT2, and resulted in heightened translocation of GLUT4 to the plasma membrane and elevated glucose uptake into muscle cells. A crucial molecule in regulating GLUT4 trafficking from the intracellular compartment to the plasma membrane is AS160, which is activated by AKT2¹⁶⁹. Our co-immunoprecipitation studies revealed that FKBP51 is in complex with PHLPP, AKT2, and AS160 (Chapter 3.1, Figure 8), building a heterocomplex to inactivate AKT2 signaling and GLUT4 vesicle translocation to the membrane. In parallel to our KO studies, we treated obese WT mice with the FKBP51 antagonist SAFit2, which disrupted the PHLPP-AS160-AKT2 heterocomplex and improved glucose metabolism (Chapter 3.1). We further demonstrated that this AKT2 hyperactivation of the PHLPP-AS160-AKT2 heterocomplex is limited to muscle tissue.

Independent of our results, Stechschulte and colleagues used the FKBP51-PHLPP-AKT-axis and found an unknown role of FKBP51 in controlling adipogenesis and lipolysis in WAT via the p38 kinase. Naturally, activated p38 translocates to the nucleus and phosphorylates GR α at Ser220 and Ser234 to induce lipogenesis genes. Simultaneously, active p38 kinase inhibits PPAR γ by phosphorylation at Ser112 to reduce adipogenesis. Stechschulte showed that FKBP51 diminishes p38 kinase activity via two mechanisms: 1) FKBP51 directly binds to PPAR γ and GR α via Hsp90, which hinders both receptors from translocating to the nucleus, and 2) via the suppression of the p38 activator AKT^{153,157,170}. Consequently, *in vivo* FKBP51 knockout activated p38 kinase in WAT, which resulted in increased lipolysis and reduced adipogenesis and lipid storage in adipose tissue¹⁵⁷. The authors claim that these mechanisms inhibit fat expansion in FKBP51 KO mice under chow and HFD conditions. This mechanism could also be responsible for phosphorylation changes of GR in the PVN, as we observed in our study (Chapter 3.3, Figure 8).

The above-described mechanisms raise the question of why FKBP51 acts in a tissue-specific manner. FKBP51 is a co-chaperone with strong competition for target binding sites. For instance, the most critical “competitor” for FKBP51 is FKBP52, which is best known as a positive regulator of GR²⁴. Our data suggest that the FKBP52 expression level might be significant for the differences in FKBP51 mediated inhibition of AKT2 in muscle cells. FKBP51 and FKBP52 show a distinct expression profile across WAT and skeletal muscle. While FKBP51 is highly expressed in muscle and low in adipose tissue, FKBP52 is highly expressed in fat and low in muscle. Both proteins co-immunoprecipitated with AKT and AS160, but FKBP52 has not the ability to interact with PHLPP1. Moreover, FKBP52 overexpression abolished the effects of FKBP51 overexpression on AKT2 signaling, indicating that high FKBP52 levels in WAT block FKBP51 mediated AKT2 inhibition. Thus, the balance between FKBP51 and FKBP52 is essential for the physiological outcome in muscle, fat, and most probably other tissues. Importantly, FKBP52 might not be the only molecular counterpart of FKBP51. Thus, the role of competing proteins should be accounted for more frequently in the future.

4.2.2. FKBP51 regulates autophagy by balancing AMPK and mTOR signaling

Our second study (Chapter 3.2) demonstrated that hypothalamic FKBP51 regulates autophagy and metabolism in a dose-dependent manner. Autophagy is controlled by the systemic energy sensors AMPK and mTOR, which work in coordination to regulate anabolic and catabolic pathways in response to nutritional challenges. Nutrient depletion activates AMPK by LKB1 mediated phosphorylation of T172¹⁷¹. Increased LKB1/AMPK signaling activates the TSC1/TSC2 complex, which in turn inhibits mTOR activity¹⁷². Bakula and colleagues established that the WIPI protein family members WIPI3 and WIPI4 are essential scaffolders of the LKB1/AMPK/TSC1/2 signaling network in response to metabolic stress¹⁷³. The authors revealed that glucose starvation signals via the LKB1/AMPK-related kinase circuit to WIPI4. The study further illustrated that WIPI3 interacts with the activated TSC1/TSC2 complex and, therefore, is a crucial scaffold for the AMPK-induced inhibition of mTORC1.^{173,174}

FKBP51 is highly induced upon starvation within the hypothalamus, and our second study manifested that FKBP51 is essential in starvation-induced autophagy. Furthermore, our co-immunoprecipitation studies exposed that FKBP51 directly interacts with LKB1, AMPK (subunits $\alpha 1$, $\gamma 2$ and $\beta 1$), WIPI4, WIPI3, and TSC2. These results align with previous reports that proposed interactions of FKBP51 with LKB1²² and WIPI4¹⁷³. Mechanistically, our data suggest that FKBP51 recruits LKB1 to the WIPI4-AMPK regulatory platform to induce AMPK phosphorylation at T172. In addition, FKBP51 associates with the TSC2/WIPI3 heterocomplex to co-regulate mTOR signaling. Finally, we demonstrate that FKBP51 expression directly correlates with the degree of autophagy signaling in an inverted u-shaped manner. Whereas moderate FKBP51 induces autophagy, exaggerated expression and deletion of FKBP51 level inhibit it while supporting AKT1/mTORC1 signaling (Chapter 3.2, Figure 8).

A study by Gassen and colleagues in 2014 deciphered an additional mechanism in which FKBP51 regulates autophagy signaling in response to antidepressant treatment. The authors showed that FKBP51 regulates the activity and expression level of Beclin1 by FKBP51 mediated inhibition of AKT, which facilitates inhibitory phosphorylation of BECN1 and reduces SKP2 activity. Interestingly, the authors could show that dexamethasone enhanced autophagy in wildtype cells and FKBP51 deletion blocks this

effect^{29,175}. Thus, it is possible that FKBP51 mediates the effects of stress on autophagy via the AMPK-mTOR or PHLPP-AKT axis.

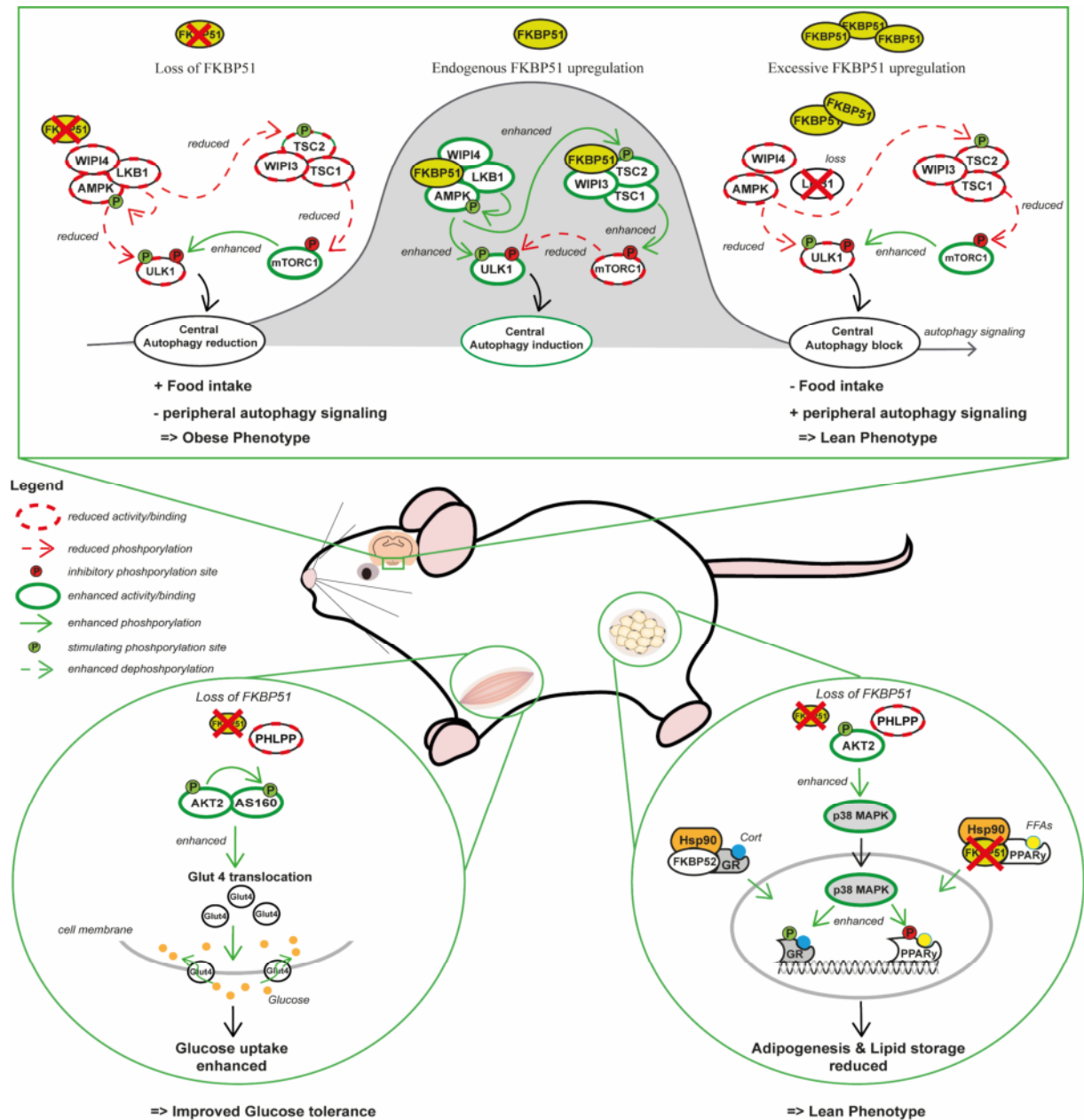


Figure 8: Possible underlying molecular mechanism contributing to the observed effects of FKBP51 on metabolism. FKBP51 regulates metabolism in a tissue-specific manner. Within the mediobasal hypothalamus, FKBP51 regulates autophagy in an inversed u-shaped manner and the activity of the sympathetic nervous system to regulate food intake and body weight. In the periphery, FKBP51 acts in muscle tissue to mediate glucose uptake by regulating the insulin signaling pathway. In adipose tissue, FKBP51 regulates the induction of GR and PPAR γ mediated translation of lipolysis and adipogenesis genes. Consequently, in-vivo deletion of FKBP51 resulted in improved glucose uptake in muscle and reduced adipogenesis and lipid storage in fat resulting in a lean phenotype.

In summary, this thesis provides further compelling data that position FKBP51 as a central regulatory switch between autophagy initiation and mTOR signaling. We and others have demonstrated that FKBP51 interacts with several heterocomplexes within the autophagy pathway, which are critical to nutrient sensing and cellular energy homeostasis. In addition, FKBP51 is in complex with AKT and PHLPP within the insulin signaling pathway, which favors mTOR signaling. Thus, FKBP51 fine-tunes the AMPK-mTOR-AKT regulatory network on multiple levels upon stress exposure, which can be in the form of either metabolic, physiological, or psychological stress. Importantly, FKBP51 expression itself is controlled by stress hormones.

The balance between autophagy and mTOR signaling is vital for cellular health, and stress can cause dysregulation of this homeostasis, which is associated with a range of (patho-) physiological conditions, including infectious disease, cancer, neurodegeneration, psychiatric disorders, obesity, and diabetes. Consequently, a better grasp of the newly discovered interactions under different gene and environmental conditions is crucial to further understand the complex interaction between metabolic and mental diseases.

4.3. Translation to humans - FKBP51 a marker for psychiatric and metabolic disorders?

Preclinical studies present accumulating evidence of the importance of FKBP51 in regulating metabolic and stress-related pathways and diseases. In fact, animal data indicate that FKBP51 is highly upregulated after metabolic stress, such as a HFD, especially in muscle and adipose tissue, and that central FKBP51 levels are associated with an increased body weight gain ^{129,176}. Thus, reducing FKBP51 expression under some circumstances might be beneficial. However, to fully elaborate on its potential as a drug target, the most critical question is whether our and other data are transferable to humans. Unfortunately, only a handful of studies investigated the molecular mechanism of FKBP51 regarding metabolic disorders in humans. These studies mainly concentrated on human adipose tissue and revealed that SNPs within the human *FKBP5* gene are associated with T2D and linked to insulin resistance ^{177–179}.

Several SNPs within the *FKBP5* gene (e.g., rs1360780) are associated with increased FKBP51 protein levels. A study by Hartmann and colleagues exhibited that obese individuals carrying the rs1360780 gene had reduced weight loss after bariatric surgery. More importantly, the study showed that these patients did not differ in basal body weight compared to the non-allele carrier ¹⁸⁰. In addition, Pereira et al. reported that FKBP51 is highly induced in the adipose tissue upon dexamethasone treatment and that increased FKBP51 protein levels are correlated with the magnitude of insulin resistance. At the same time, the study did not find any differences in body weight under baseline conditions. Sidibeh and colleagues demonstrated that FKBP51 was increased in fat tissue of patients with T2D ¹⁷⁸. These data support the hypothesis that elevated FKBP51 is crucial in body weight regulation and glucose metabolism, especially after environmental stimuli, such as metabolic stress, chronic stress, or psychological trauma.

Numerous studies have already identified complementary biology between stress and energy metabolism. Although acute stress often triggers a protective and adaptive mechanism to prepare for the future, chronic stress evokes cellular changes with potentially harmful consequences. Not surprisingly, chronic stress is a major risk factor in the development of various diseases, such as PTSD, depression, obesity and associated diseases, such as T2D ¹⁸¹. The association of SNPs within the *FKBP5* gene (e.g.,

rs1360780) with depression and PTSD was already shown in multiple independent studies. In more detail, those SNPs are associated with higher FKBP51 expression in blood cells, elevated cortisol, GR resistance and consequently an impaired HPA axis reactivity⁵⁶. However, clinical studies investigating the effect of *FKBP5* polymorphism and the prevalence of traits of the metabolic syndrome in large cohorts of patients suffering from mental illness diseases are still elusive.

Genetic studies revealed a positive correlation between FKBP51 expression and antidepressant treatment response⁵⁶. A significant metabolic problem associated with many psychiatric therapies is unwanted body weight changes during medication. While antidepressants might improve mental health, they might also cause adverse effects on multiple biological pathways, such as inflammation or oxidative stress, caused by medication-induced weight gain¹⁸². In addition, weight gain can further impact the self-esteem and psychological health of individuals already suffering from mental disorders. As a consequence, patients might relapse or develop resistance to treatment¹⁸². Several conventional antidepressants, such as paroxetine, are associated with a substantial increase in body weight¹⁸³. A study by Gassen et al. demonstrated that FKBP51 deletion positively affects paroxetine treatment. More importantly, they have monitored body weight during a 3-week paroxetine treatment and discovered that FKBP51 deletion significantly reduced paroxetine-induced body weight gain compared to wild-type mice²⁹. Unfortunately, the study did not assess other metabolic parameters, such as blood glucose and triglyceride levels, all elevated upon paroxetine treatment¹⁸³. Nevertheless, FKBP51 expression might play a crucial role in body weight control during antidepressant treatment and might function as a marker to predict unwanted body weight changes upon treatment. Thus, co-medication of FKBP51 antagonists with antidepressants, at least in some cases, might be a potential option to stabilize body weight during psychiatric therapies and prevent relapse or treatment resistance.

Taken together, the current literature presents profound evidence that alterations in FKBP51 expression might contribute to an increased risk for a vast number of mental disorders. However, little data on the effect of FKBP51 polymorphisms on metabolic diseases are available. Longitudinal human studies examining FKBP51 polymorphisms with obese patients comorbid with mental illnesses or vice versa would be exciting and could further advance the field.

4.4. FKBP51 - a therapeutic option for stress-related and metabolic disorders?

Since the whole-body deletion of FKBP51 had no adverse effects on general health nor any physiological parameter in mice, the publication of the next generation of the induced-fit FKBP51 antagonists, SAFit2 and SAFit1 was very exciting²⁷. The most promising antagonist is SAFit2, which is able to cross the BBB and therefore acts in the brain as well as in the periphery. So far, our and other preclinical studies present promising data on body weight reduction, glucose metabolism, and chronic pain without any side effects during or after the treatment with SAFit2^{184,185}. In this thesis, we investigated whether FKBP51 antagonism by SAFit2 affects the health of FKBP51 deficient mice. To do so, we administered SAFit2 over different time frames, namely 24-h, 10-day, and 30-day periods. Chronic treatment with SAFit2 resulted in reduced body weight and improved glucose tolerance and recapitulated the effects of complete FKBP51 deletion in mice. Furthermore, during our acute SAFit2 treatment, we observed that the glucose tolerance improvement was independent of the body weight changes (Chapter 2 and 3.1).

Given the newly discovered role of central FKBP51 in developing obesity, targeting FKBP51 only in the periphery could be an exciting approach. The most promising target organs in the periphery are muscle and adipose tissue, which show the highest FKBP51 expression^{101,177}. Therefore, tissue-specific drug delivery might be a feasible strategy and would prevent unwanted inhibition of FKBP51 in the brain. For instance, FKBP51 antagonists could be packed in nanoparticles with the physical and chemical properties that enable them to target specific organs¹⁸⁶. However, current FKBP51 antagonists are still too big and must be reduced in size to be functionally packed in any suitable delivery system.

The difficulties in the breakthrough of FKBP51 as a ready-to-use drug target might lie in its own abilities as a co-chaperone, assisting tens, maybe hundreds of proteins interactions, which might differ from organ to organ. In addition, inhibiting FKBP51 and potentially interacting proteins might cause side effects not yet discovered. For example, it was also shown that FKBP51 deletion is associated with muscle loss, and FKBP51 KO mice show delayed muscle regeneration¹⁷⁰. Furthermore, FKBP51 is a multi-domain protein, and each domain regulates different protein cascades adding to the complexity of developing a suitable antagonist for each specific pathway. Consequently, it should be noted that there

is still a long way to go. Laboratories and researchers focusing on FKBP51 must further gather a substantial amount of animal and human data to fill missing knowledge gaps. In addition, it will be essential to develop new generations of FKBP51 antagonists in the future.

Taken together, FKBP51 might have the potential as a drug target, but research also showed that the current antagonists might not yet be sufficient. Importantly, there is accumulating evidence that the relevance of FKBP51 in the development of certain diseases is dependent on the combined appearance of genotype (specific carriers of *FKBP5* polymorphisms) and environmental factors, such as stress. Therefore, further data collection in multiple preclinical and clinical studies will be necessary to capture these gene x environment connections scientifically. These data will provide novel molecular and physiological insights, which can advance current FKBP51 antagonists and might fully deploy FKBP51's potential as a drug target for stress-related or metabolic diseases.

4.5. Conclusion

FKBP51 is a multifunctional protein that emerged as a regulator of various physiological and molecular processes in maintaining body homeostasis. This thesis emphasizes the tissue specificity of FKBP51 and provides compelling evidence of the importance of FKBP51 in the regulation of the acute stress response, body weight control, and glucose metabolism. Furthermore, it presents FKBP51 as a complex co-chaperone beyond the well-established function as a negative GR regulator. The newly discovered ability of FKBP51 to regulate the activity of AKT, AMPK, and mTOR, here and elsewhere^{28–30,152,157,187}, might open promising treatment avenues for metabolic disorders, such as obesity, T2D, psychiatric diseases, and cancer. In the future, it will be necessary to advance the knowledge of FKBP51 with a particular emphasis on tissue specificity, human clinical studies, and advancements in the development of FKBP51 antagonists to carefully target single pathways more accurately. However, only the combined analysis and interpretation of preclinical and clinical data together with advanced FKBP51 antagonists can finally route the way to success.

5. References

1. Rothe, J., Buse, J., Uhlmann, A., Bluschke, A. & Roessner, V. Changes in emotions and worries during the Covid-19 pandemic: an online-survey with children and adults with and without mental health conditions. *Child Adolesc. Psychiatry Ment. Heal.* 2021 151 **15**, 1–9 (2021).
2. Pancani, L., Marinucci, M., Aureli, N. & Riva, P. Forced Social Isolation and Mental Health: A Study on 1,006 Italians Under COVID-19 Lockdown. *Front. Psychol.* **0**, 1540 (2021).
3. Santomauro, D. F. *et al.* Global prevalence and burden of depressive and anxiety disorders in 204 countries and territories in 2020 due to the COVID-19 pandemic. *Lancet* **0**, (2021).
4. Kumar, A. & Nayar, K. R. COVID 19 and its mental health consequences. *J. Ment. Health* **30**, 1–2 (2021).
5. Cullen, W., Gulati, G. & Kelly, B. D. Mental health in the COVID-19 pandemic. *QJM An Int. J. Med.* **113**, 311–312 (2020).
6. Kola, L. *et al.* COVID-19 mental health impact and responses in low-income and middle-income countries: reimagining global mental health. *The Lancet Psychiatry* **8**, 535–550 (2021).
7. World Health Organization. Depression and Other Common Mental Disorders Global Health Estimates. (2017).
8. Popkin, B. M. *et al.* Individuals with obesity and COVID-19: A global perspective on the epidemiology and biological relationships. *Obes. Rev.* **21**, e13128 (2020).
9. Stefan, N., Birkenfeld, A. L. & Schulze, M. B. Global pandemics interconnected — obesity, impaired metabolic health and COVID-19. *Nat. Rev. Endocrinol.* 2021 173 **17**, 135–149 (2021).
10. World Health Organization. Obesity and overweight. *Fact Sheet* (2017). Available at: <https://www.who.int/news-room/fact-sheets/detail/obesity-and-overweight>. (Accessed: 2nd October 2021)

11. Stunkard, A. J. *et al.* Depression and obesity. *Biol. Psychiatry* **54**, 330–337 (2003).
12. Faith, M. S., Matz, P. E. & Jorge, M. A. Obesity–depression associations in the population. *J. Psychosom. Res.* **53**, 935–942 (2002).
13. Lindberg, L., Hagman, E., Danielsson, P., Marcus, C. & Persson, M. Anxiety and depression in children and adolescents with obesity: a nationwide study in Sweden. *BMC Med.* *2020* **181** **18**, 1–9 (2020).
14. Milaneschi, Y., Simmons, W. K., van Rossum, E. F. C. & Penninx, B. W. Depression and obesity: evidence of shared biological mechanisms. *Mol. Psychiatry* *2018* **241** **24**, 18–33 (2018).
15. Saibil, H. Chaperone machines for protein folding, unfolding and disaggregation. *Nat. Rev. Mol. Cell Biol.* *2013* **1410** **14**, 630–642 (2013).
16. Pirkl, F. & Buchner, J. Functional analysis of the hsp90-associated human peptidyl prolyl Cis/Trans isomerases FKBP51, FKBP52 and cyp40. *J. Mol. Biol.* **308**, 795–806 (2001).
17. Barik, S. Immunophilins: For the love of proteins. *Cell. Mol. Life Sci.* **63**, 2889–2900 (2006).
18. Riggs, D. L. *et al.* The Hsp90-binding peptidylprolyl isomerase FKBP52 potentiates glucocorticoid signaling in vivo. *EMBO J.* **22**, 1158–67 (2003).
19. Schmidt, M. V., Paez-Pereda, M., Holsboer, F. & Hausch, F. The Prospect of FKBP51 as a Drug Target. *ChemMedChem* **7**, 1351–1359 (2012).
20. Young, J. C., Obermann, W. M. J. & Hartl, F. U. Specific binding of tetratricopeptide repeat proteins to the C-terminal 12-kDa domain of hsp90. *J. Biol. Chem.* **273**, 18007–18010 (1998).
21. Sinars, C. R. *et al.* Structure of the large FK506-binding protein FKBP51, an Hsp90-binding protein and a component of steroid receptor complexes. *Proc. Natl. Acad. Sci. U.S.A* **100**, 868–873 (2003).
22. Taipale, M. *et al.* A quantitative chaperone interaction network reveals the architecture of cellular protein homeostasis pathways. *Cell* **158**, 434–448 (2014).

23. Luo, K. *et al.* USP49 negatively regulates tumorigenesis and chemoresistance through FKBP51-AKT signaling. *EMBO J.* **36**, 1434 (2017).
24. Storer, C. L., Dickey, C. A., Galigniana, M. D., Rein, T. & Cox, M. B. FKBP51 and FKBP52 in signaling and disease. *Trends Endocrinol. Metab.* **22**, 481–490 (2011).
25. Fries, G. R., Gassen, N. C. & Rein, T. The FKBP51 glucocorticoid receptor co-chaperone: Regulation, function, and implications in health and disease. *International Journal of Molecular Sciences* **18**, (2017).
26. Hähle, A., Merz, S., Meyners, C. & Hausch, F. The many faces of FKBP51. *Biomolecules* **9**, (2019).
27. Gaali, S. *et al.* Selective inhibitors of the FK506-binding protein 51 by induced fit. *Nat. Chem. Biol.* **11**, 33–37 (2015).
28. Pei, H. *et al.* FKBP51 Affects Cancer Cell Response to Chemotherapy by Negatively Regulating Akt. *Cancer Cell* **16**, 259–266 (2009).
29. Gassen, N. C. *et al.* Association of FKBP51 with Priming of Autophagy Pathways and Mediation of Antidepressant Treatment Response: Evidence in Cells, Mice, and Humans. *PLoS Med.* **11**, e1001755 (2014).
30. Stechschulte, L. A. *et al.* FKBP51 Reciprocally Regulates GR α and PPAR γ Activation via the Akt-p38 Pathway. *Mol. Endocrinol.* (2014). doi:10.1210/me.2014-1023
31. Cannon, W. B. ORGANIZATION FOR PHYSIOLOGICAL HOMEOSTASIS. *Physiol. Rev.* **9**, 399–431 (1929).
32. Chrousos, G. P. Stress and disorders of the stress system. *Nature Reviews Endocrinology* **5**, 374–381 (2009).
33. Ulrich-Lai, Y. M. & Herman, J. P. Neural regulation of endocrine and autonomic stress responses. *Nat.Rev.Neurosci.* **10**, 397–409 (2009).

34. Selye, H. A Syndrome produced by Diverse Nocuous Agents. *Nat. 1936 1383479* **138**, 32–32 (1936).
35. Szabo, S., Tache, Y. & Somogyi, A. The legacy of Hans Selye and the origins of stress research: A retrospective 75 years after his landmark brief ‘letter’ to the Editor# of Nature. *Stress* (2012). doi:10.3109/10253890.2012.710919
36. McEwen, B. S. Physiology and neurobiology of stress and adaptation: Central role of the brain. *Physiological Reviews* (2007). doi:10.1152/physrev.00041.2006
37. McEwen, B. S. & Akil, H. Revisiting the Stress Concept: Implications for Affective Disorders. *J. Neurosci.* **40**, 12 (2020).
38. De Kloet, E. R. Hormones and the stressed brain. *Ann. N. Y. Acad. Sci.* **1018**, 1–15 (2004).
39. Richter-Levin, G. & Sandi, C. Title: “Labels Matter: Is it stress or is it Trauma?” *Transl. Psychiatry 2021 111* **11**, 1–9 (2021).
40. Sapolsky, R. M., Romero, L. M. & Munck, a. U. How Do Glucocorticoids Influence Stress Responses ? Preparative Actions *. *Endocr. Rev.* **21**, 55–89 (2000).
41. Papadimitriou, A. & Priftis, K. N. Regulation of the hypothalamic-pituitary-adrenal axis. *Neuroimmunomodulation* **16**, 265–271 (2009).
42. Benjannet, S., Rondeau, N., Day, R., Chrétien, M. & Seidah, N. G. PC1 and PC2 are proprotein convertases capable of cleaving proopiomelanocortin at distinct pairs of basic residues. *Proc. Natl. Acad. Sci. U. S. A.* (1991). doi:10.1073/pnas.88.9.3564
43. Herman, J. P. *et al.* Regulation of the Hypothalamic-Pituitary-Adrenocortical Stress Response. in *Comprehensive Physiology* **6**, 603–621 (John Wiley & Sons, Inc., 2016).
44. Gillies, G. E., Linton, E. A. & Lowry, P. J. Corticotropin releasing activity of the new CRF is potentiated several times by vasopressin. *Nature* (1982). doi:10.1038/299355a0
45. Whitnall, M. H. Stress selectively activates the vasopressin-containing subset of corticotropin-releasing hormone neurons. *Neuroendocrinology* (1989). doi:10.1159/000125302

46. De Kloet, E. R., Joëls, M. & Holsboer, F. Stress and the brain: From adaptation to disease. *Nat. Rev. Neurosci.* **6**, 463–475 (2005).
47. Herman, J. P. *et al.* 13 Neurochemical Systems Regulating the Hypothalamo– Pituitary– Adrenocortical Axis. *Handb. Neurochem. Mol. Neurobiol.* (2007).
48. Gjerstad, J. K., Lightman, S. L. & Spiga, F. Role of glucocorticoid negative feedback in the regulation of HPA axis pulsatility. <https://doi.org/10.1080/10253890.2018.1470238> **21**, 403–416 (2018).
49. Tasker, J. G. Rapid glucocorticoid actions in the hypothalamus as a mechanism of homeostatic integration. *Obesity (Silver Spring)*. **14 Suppl 5**, 259–265 (2006).
50. Di, S., Malcher-Lopes, R., Marcheselli, V. L., Bazan, N. G. & Tasker, J. G. Rapid Glucocorticoid-Mediated Endocannabinoid Release and Opposing Regulation of Glutamate and γ -Aminobutyric Acid Inputs to Hypothalamic Magnocellular Neurons. *Endocrinology* **146**, 4292–4301 (2005).
51. Mora, F., Segovia, G., Del Arco, A., De Blas, M. & Garrido, P. Stress, neurotransmitters, corticosterone and body-brain integration. *Brain Res.* **1476**, 71–85 (2012).
52. Vandevyver, S., Dejager, L. & Libert, C. On the Trail of the Glucocorticoid Receptor: Into the Nucleus and Back. *Traffic* **13**, 364–374 (2012).
53. Zgajnar, N. R. *et al.* Biological Actions of the Hsp90-binding Immunophilins FKBP51 and FKBP52. *Biomolecules* **9**, (2019).
54. Denny, W. B., Valentine, D. L., Reynolds, P. D., Smith, D. F. & Scammell, J. G. Squirrel monkey immunophilin FKBP51 is a potent inhibitor of glucocorticoid receptor binding. *Endocrinology* **141**, 4107–4113 (2000).
55. Wochnik, G. M. *et al.* FK506-binding proteins 51 and 52 differentially regulate dynein interaction and nuclear translocation of the glucocorticoid receptor in mammalian cells. *J. Biol. Chem.* **280**, 4609–16 (2005).

56. Binder, E. B. The role of FKBP5, a co-chaperone of the glucocorticoid receptor in the pathogenesis and therapy of affective and anxiety disorders. *Psychoneuroendocrinology* **34**, 186–195 (2009).
57. Hartmann, J. *et al.* The involvement of FK506-binding protein 51 (FKBP5) in the behavioral and neuroendocrine effects of chronic social defeat stress. *Neuropharmacology* **62**, 332–339 (2012).
58. Criado-Marrero, M. *et al.* Hsp90 and FKBP51: Complex regulators of psychiatric diseases. *Philosophical Transactions of the Royal Society B: Biological Sciences* (2018). doi:10.1098/rstb.2016.0532
59. Wagner, K. V. *et al.* Differences in FKBP51 regulation following chronic social defeat stress correlate with individual stress sensitivity: Influence of paroxetine treatment. *Neuropsychopharmacology* **37**, 2797–2808 (2012).
60. Scharf, S. H., Liebl, C., Binder, E. B., Schmidt, M. V. & Müller, M. B. Expression and regulation of the *Fkbp5* gene in the adult mouse brain. *PLoS One* **6**, 1–10 (2011).
61. Touma, C. *et al.* FK506 binding protein 5 shapes stress responsiveness: Modulation of neuroendocrine reactivity and coping behavior. *Biol. Psychiatry* **70**, 928–936 (2011).
62. Willour, V. L. *et al.* Family-based association of FKBP5 in bipolar disorder. *Mol. Psychiatry* **14**, 261–268 (2009).
63. Brent, D. *et al.* Association of FKBP5 polymorphisms with suicidal events in the Treatment of Resistant Depression in Adolescents (TORDIA) study. *Am. J. Psychiatry* **167**, 190–197 (2010).
64. Supriyanto, I. *et al.* Association of FKBP5 gene haplotypes with completed suicide in the Japanese population. *Prog. Neuro-Psychopharmacology Biol. Psychiatry* **35**, 252–256 (2011).
65. Klengel, T. *et al.* Allele-specific FKBP5 DNA demethylation mediates gene-childhood trauma interactions. *Nat. Neurosci.* **16**, 33–41 (2013).
66. R, Y. *et al.* Gene expression patterns associated with posttraumatic stress disorder following exposure to the World Trade Center attacks. *Biol. Psychiatry* **66**, 708–711 (2009).

67. Binder, E. B. *et al.* Polymorphisms in FKBP5 are associated with increased recurrence of depressive episodes and rapid response to antidepressant treatment. *Nat. Genet.* **36**, 1319–1325 (2004).
68. Schwartz, M. W., Woods, S. C., Porte, D., Seeley, R. J. & Baskin, D. G. Central nervous system control of food intake. *Nature* **404**, 661–671 (2000).
69. Cutler, D. M., Glaeser, E. L. & Shapiro, J. M. Why have Americans become more obese? *Journal of Economic Perspectives* (2003). doi:10.1257/089533003769204371
70. NCD Risk Factor Collaboration (NCD-RisC). Worldwide trends in body-mass index, underweight, overweight, and obesity from 1975 to 2016: a pooled analysis of 2416 population-based measurement studies in 128·9 million children, adolescents, and adults. *Lancet* **390**, 2627–2642 (2017).
71. NCD Risk Factor Collaboration (NCD-RisC). Trends in adult body-mass index in 200 countries from 1975 to 2014: a pooled analysis of 1698 population-based measurement studies with 19·2 million participants. *Lancet* **387**, 1377–1396 (2016).
72. Berrington de Gonzalez, A. *et al.* Body-mass index and mortality among 1.46 million white adults. *N. Engl. J. Med.* **363**, 2211–2219 (2010).
73. Fontaine, K. R., Redden, D. T., Wang, C., Westfall, A. O. & Allison, D. B. Years of Life Lost Due to Obesity. *JAMA* **289**, 187–193 (2003).
74. Hackett, R. A. & Steptoe, A. Type 2 diabetes mellitus and psychological stress — a modifiable risk factor. *Nat. Rev. Endocrinol.* **2017 139** **13**, 547–560 (2017).
75. M, R. *et al.* Low-dose leptin reverses skeletal muscle, autonomic, and neuroendocrine adaptations to maintenance of reduced weight. *J. Clin. Invest.* **115**, 3579–3586 (2005).
76. Blüher, M. Obesity: global epidemiology and pathogenesis. *Nat. Rev. Endocrinol.* **2019 155** **15**, 288–298 (2019).
77. Blüher, M. Metabolically Healthy Obesity. *Endocr. Rev.* **41**, 405–420 (2020).

78. Bray, G. A., Kim, K. K. & Wilding, J. P. H. Obesity: a chronic relapsing progressive disease process. A position statement of the World Obesity Federation. *Obes. Rev.* **18**, 715–723 (2017).
79. KENNEDY, G. C. The role of depot fat in the hypothalamic control of food intake in the rat. *Proc. R. Soc. London. Ser. B, Biol. Sci.* (1953). doi:10.1098/rspb.1953.0009
80. Morton, G. J., Meek, T. H. & Schwartz, M. W. Neurobiology of food intake in health and disease. *Nat. Rev. Neurosci.* **15**, 367–378 (2014).
81. Gibbs, J., Young, R. C. & Smith, G. P. Cholecystokinin decreases food intake in rats. *J. Comp. Physiol. Psychol.* **84**, 488–495 (1973).
82. Ley, R. E. Obesity and the human microbiome. *Curr. Opin. Gastroenterol.* **26**, 5–11 (2010).
83. Cryan, J. F. *et al.* The microbiota-gut-brain axis. *Physiol. Rev.* **99**, 1877–2013 (2019).
84. Myers, M. G., Cowley, M. A. & Münzberg, H. Mechanisms of Leptin Action and Leptin Resistance. *Annu. Rev. Physiol.* **70**, 537–556 (2008).
85. Ingalls, A. M., Dickie, M. M. & Snell, G. D. Obese, a new mutation in the house mouse. *J. Hered.* **41**, 317–318 (1950).
86. Zhang, Y. *et al.* Positional cloning of the mouse obese gene and its human homologue. *Nat.* **372**, 425–432 (1994).
87. Farooqi, I. S. *et al.* Effects of recombinant leptin therapy in a child with congenital leptin deficiency. *N. Engl. J. Med.* (1999). doi:10.1056/NEJM199909163411204
88. El-Haschimi, K., Pierroz, D. D., Hileman, S. M., Bjørnbæk, C. & Flier, J. S. Two defects contribute to hypothalamic leptin resistance in mice with diet-induced obesity. *J. Clin. Invest.* **105**, 1827–1832 (2000).
89. Friedman, J. M. Leptin and the endocrine control of energy balance. *Nat. Metab.* **2019 18 1**, 754–764 (2019).

90. Pan, W. W. & Myers, M. G. Leptin and the maintenance of elevated body weight. *Nat. Rev. Neurosci.* 2018 192 **19**, 95–105 (2018).
91. Chua, S. C. *et al.* Phenotypes of Mouse diabetes and Rat fatty Due to Mutations in the OB (Leptin) Receptor. *Science (80-.).* **271**, 994–996 (1996).
92. Chen, H. *et al.* Evidence That the Diabetes Gene Encodes the Leptin Receptor: Identification of a Mutation in the Leptin Receptor Gene in db/db Mice However, db/db mice fail to respond to recombinant. *Cell* **84**, 491–495 (1996).
93. Flak, J. N. & Myers, M. G. Minireview: CNS mechanisms of leptin action. *Molecular Endocrinology* (2016). doi:10.1210/me.2015-1232
94. Myers, M. G. & Olson, D. P. Central nervous system control of metabolism. *Nature* **491**, 357–363 (2012).
95. Schwartz, M. W. & Porte, D. Diabetes, obesity, and the brain. *Science (80-.).* **307**, 375–379 (2005).
96. Kahn, S. E., Hull, R. L. & Utzschneider, K. M. Mechanisms linking obesity to insulin resistance and type 2 diabetes. *Nature* **444**, 840–846 (2006).
97. Woods, S. C., Lotter, E. C., McKay, L. D. & Porte, D. Chronic intracerebroventricular infusion of insulin reduces food intake and body weight of baboons [12]. *Nature* **282**, 503–505 (1979).
98. Obici, S., Feng, Z., Karkanias, G., Baskin, D. G. & Rossetti, L. Decreasing hypothalamic insulin receptors causes hyperphagia and insulin resistance in rats. *Nat. Neurosci.* 2002 56 **5**, 566–572 (2002).
99. Kleinridders, A., Ferris, H. A., Cai, W. & Kahn, C. R. Insulin action in brain regulates systemic metabolism and brain function. *Diabetes* **63**, 2232–2243 (2014).
100. Taniguchi, C. M., Emanuelli, B. & Kahn, C. R. Critical nodes in signalling pathways: Insights into insulin action. *Nat. Rev. Mol. Cell Biol.* **7**, 85–96 (2006).

101. Baughman, G., Widerrecht, G. J., Chang, F., Martin, M. M. & Bourgeois, S. Tissue distribution and abundance of human FKBP51, and FK506-binding protein that can mediate calcineruin inhibition. *Biochem. Biophys. Res. Commun.* **232**, 437–443 (1997).
102. Hetherington, A. W. & Ranson, S. W. Hypothalamic lesions and adiposity in the rat. *Anat. Rec.* (1940). doi:10.1002/ar.1090780203
103. Hetherington, A. W. & Ranson, S. W. The relation of various hypothalamic lesions to adiposity in the rat. *J. Comp. Neurol.* (1942). doi:10.1002/cne.900760308
104. ANAND, B. K. & BROBECK, J. R. Hypothalamic control of food intake in rats and cats. *Yale J. Biol. Med.* (1951).
105. Timper, K. & Brüning, J. C. Hypothalamic circuits regulating appetite and energy homeostasis: Pathways to obesity. *DMM Dis. Model. Mech.* **10**, 679–689 (2017).
106. Zhang, X. & van den Pol, A. N. Hypothalamic arcuate nucleus tyrosine hydroxylase neurons play orexigenic role in energy homeostasis. *Nat. Neurosci.* **19**, 1341–1347 (2016).
107. Jais, A. *et al.* PNOCARC Neurons Promote Hyperphagia and Obesity upon High-Fat-Diet Feeding. *Neuron* **106**, 1009-1025.e10 (2020).
108. Jais, A. & Brüning, J. C. Arcuate nucleus-dependent regulation of metabolism - pathways to obesity and diabetes mellitus. *Endocr. Rev.* (2021). doi:10.1210/ENDREV/BNAB025
109. Voss-Andreae, A. *et al.* Role of the central melanocortin circuitry in adaptive thermogenesis of brown adipose tissue. *Endocrinology* **148**, 1550–1560 (2007).
110. Balthasar, N. *et al.* Divergence of melanocortin pathways in the control of food intake and energy expenditure. *Cell* (2005). doi:10.1016/j.cell.2005.08.035
111. Huszar, D. *et al.* Targeted disruption of the melanocortin-4 receptor results in obesity in mice. *Cell* **88**, 131–141 (1997).
112. Ollmann, M. M. *et al.* Antagonism of Central Melanocortin receptors in vitro and in vivo by agouti-related protein. *Science* (80-.). **278**, 135–138 (1997).

113. Cowley, M. A. *et al.* Leptin activates anorexigenic POMC neurons through a neural network in the arcuate nucleus. *Nature* (2001). doi:10.1038/35078085
114. Spanswick, D., Smith, M. A., Mirshamsi, S., Routh, V. H. & Ashford, M. L. J. Insulin activates ATP-sensitive K⁺ channels in hypothalamic neurons of lean, but not obese rats. *Nat. Neurosci.* 2000 38 **3**, 757–758 (2000).
115. Williams, K. W. *et al.* Segregation of Acute Leptin and Insulin Effects in Distinct Populations of Arcuate Proopiomelanocortin Neurons. *J. Neurosci.* **30**, 2472–2479 (2010).
116. Quarta, C. *et al.* POMC neuronal heterogeneity in energy balance and beyond: an integrated view. *Nat. Metab.* **3**, 299–308 (2021).
117. Campbell, J. N. *et al.* A molecular census of arcuate hypothalamus and median eminence cell types. *Nat. Neurosci.* 2017 203 **20**, 484–496 (2017).
118. Shimizu, N., Oomura, Y., Plata-Salamán, C. R. & Morimoto, M. Hyperphagia and obesity in rats with bilateral ibotenic acid-induced lesions of the ventromedial hypothalamic nucleus. *Brain Res.* **416**, 153–156 (1987).
119. Dhillon, H. *et al.* Leptin directly activates SF1 neurons in the VMH, and this action by leptin is required for normal body-weight homeostasis. *Neuron* **49**, 191–203 (2006).
120. Majdic, G. *et al.* Knockout mice lacking steroidogenic factor 1 are a novel genetic model of hypothalamic obesity. *Endocrinology* **143**, 607–614 (2002).
121. Sternson, S. M., Shepherd, G. M. G. & Friedman, J. M. Topographic mapping of VMH → arcuate nucleus microcircuits and their reorganization by fasting. *Nat. Neurosci.* **8**, 1356–1363 (2005).
122. Morrison, S. F. & Nakamura, K. Central neural pathways for thermoregulation. *Front. Biosci. (Landmark Ed.* **16**, 74–104 (2011).
123. JA, D. & DV, Z. The dorsomedial hypothalamus: a new player in thermoregulation. *Am. J. Physiol. Regul. Integr. Comp. Physiol.* **292**, (2007).

124. Bellinger, L. L. & Bernardis, L. L. The dorsomedial hypothalamic nucleus and its role in ingestive behavior and body weight regulation: Lessons learned from lesioning studies. *Physiol. Behav.* **76**, 431–442 (2002).
125. Rezai-Zadeh, K. *et al.* Leptin receptor neurons in the dorsomedial hypothalamus are key regulators of energy expenditure and body weight, but not food intake. *Mol. Metab.* **3**, 681–693 (2014).
126. Bi, S., Robinson, B. M. & Moran, T. H. Acute food deprivation and chronic food restriction differentially affect hypothalamic NPY mRNA expression. *Am. J. Physiol. Regul. Integr. Comp. Physiol.* **285**, (2003).
127. Bi, S., Ladenheim, E. E., Schwartz, G. J. & Moran, T. H. A role for NPY overexpression in the dorsomedial hypothalamus in hyperphagia and obesity of OLETF rats. *Am. J. Physiol. Regul. Integr. Comp. Physiol.* **281**, (2001).
128. Chao, P. T., Yang, L., Aja, S., Moran, T. H. & Bi, S. Knockdown of NPY Expression in the Dorsomedial Hypothalamus Promotes Development of Brown Adipocytes and Prevents Diet-Induced Obesity. *Cell Metab.* **13**, 573–583 (2011).
129. Yang, L. *et al.* Hypothalamic Fkbp51 is induced by fasting, and elevated hypothalamic expression promotes obese phenotypes. *AJP Endocrinol. Metab.* **302**, E987–E991 (2012).
130. Galluzzi, L. *et al.* Molecular definitions of autophagy and related processes. *EMBO J.* **36**, 1811–1836 (2017).
131. Boya, P., Reggiori, F. & Codogno, P. Emerging regulation and functions of autophagy. *Nat. Cell Biol.* **15**, 713–720 (2013).
132. Tsukada, M. & Ohsumi, Y. Isolation and characterization of autophagy-defective mutants of *Saccharomyces cerevisiae*. *FEBS Lett.* (1993). doi:10.1016/0014-5793(93)80398-E
133. Choi, A. M. K., Ryter, S. W. & Levine, B. Mechanisms of Disease Autophagy in Human Health and Disease. *n engl j med* **7**, 651–62 (2013).

134. Levine, B. & Kroemer, G. Biological Functions of Autophagy Genes: A Disease Perspective. *Cell* **176**, 11–42 (2019).
135. Kitada, M. & Koya, D. Autophagy in metabolic disease and ageing. *Nat. Rev. Endocrinol.* **2021** 1–15 (2021). doi:10.1038/s41574-021-00551-9
136. Klionsky, D. J. *et al.* Autophagy in major human diseases. *EMBO J.* **40**, e108863 (2021).
137. Zhang, Y., Sowers, J. R. & Ren, J. Targeting autophagy in obesity: From pathophysiology to management. *Nature Reviews Endocrinology* **14**, 356–376 (2018).
138. Gesta, S., Tseng, Y. H. & Kahn, C. R. Developmental Origin of Fat: Tracking Obesity to Its Source. *Cell* **131**, 242–256 (2007).
139. Singh, R. *et al.* Autophagy regulates lipid metabolism. *Nature* **458**, 1131–1135 (2009).
140. An, L. *et al.* Role for serotonin in the antidepressant-like effect of a flavonoid extract of Xiaobuxin-Tang. *Pharmacol. Biochem. Behav.* **89**, 572–580 (2008).
141. Zhang, Y. *et al.* Adipose-specific deletion of autophagy-related gene 7 (*atg7*) in mice reveals a role in adipogenesis. *Proc. Natl. Acad. Sci. U. S. A.* **106**, 19860–5 (2009).
142. Meng, Q. & Cai, D. Defective hypothalamic autophagy directs the central pathogenesis of obesity via the I κ B kinase β (IKK β)/NF- κ B pathway. *J. Biol. Chem.* **286**, 32324–32332 (2011).
143. He, C. *et al.* Exercise-induced BCL2-regulated autophagy is required for muscle glucose homeostasis. *Nature* **481**, 511–515 (2012).
144. Kaushik, S. *et al.* Autophagy in hypothalamic AgRP neurons regulates food intake and energy balance. *Cell Metab.* **14**, 173–83 (2011).
145. Kaushik, S. *et al.* Loss of autophagy in hypothalamic POMC neurons impairs lipolysis. *EMBO Rep.* **13**, 258–265 (2012).
146. Yang, L., Li, P., Fu, S., Calay, E. S. & Hotamisligil, G. S. Defective Hepatic Autophagy in Obesity Promotes ER Stress and Causes Insulin Resistance. *Cell Metab.* **11**, 467–478 (2010).

147. Singh, R. Autophagy in the control of food intake. *Adipocyte* **1**, 75–79 (2012).
148. Yamamoto, S. *et al.* Autophagy Differentially Regulates Insulin Production and Insulin Sensitivity. *Cell Rep.* **23**, 3286–3299 (2018).
149. Kim, J., Kundu, M., Viollet, B. & Guan, K. L. AMPK and mTOR regulate autophagy through direct phosphorylation of Ulk1. *Nat. Cell Biol.* **13**, 132–141 (2011).
150. Klionsky, D. J. *et al.* Guidelines for the use and interpretation of assays for monitoring autophagy (3rd edition). *Autophagy* **12**, 1–222 (2016).
151. Kim, K. H. & Lee, M. S. Autophagy - A key player in cellular and body metabolism. *Nature Reviews Endocrinology* **10**, 322–337 (2014).
152. Gassen, N. C. *et al.* SKP2 attenuates autophagy through Beclin1-ubiquitination and its inhibition reduces MERS-Coronavirus infection. *Nat. Commun.* **10**, (2019).
153. Stechschulte, L. A. *et al.* FKBP51 controls cellular adipogenesis through p38 kinase-mediated phosphorylation of GR α and PPAR γ . *Mol. Endocrinol.* **28**, 1265–1275 (2014).
154. Ghaben, A. L. & Scherer, P. E. Adipogenesis and metabolic health. *Nat. Rev. Mol. Cell Biol.* **2018 204** **20**, 242–258 (2019).
155. Yeh, W. C. *et al.* Identification and characterization of an immunophilin expressed during the clonal expansion phase of adipocyte differentiation. *Proc. Natl. Acad. Sci.* **92**, 11081–11085 (1995).
156. Rosen, E. D. & Spiegelman, B. M. What we talk about when we talk about fat. *Cell* **156**, 20–44 (2014).
157. Stechschulte, L. A. *et al.* FKBP51 Null Mice Are Resistant to Diet-Induced Obesity and the PPAR γ Agonist Rosiglitazone. *Endocrinology* **157**, 3888–3900 (2016).
158. Nedergaard, J. & Cannon, B. The Browning of White Adipose Tissue: Some Burning Issues. *Cell Metab.* **20**, 396–407 (2014).

159. Kim, J. G. & Horvath, T. L. mTOR Signaling Fades POMC Neurons during Aging. *Neuron* **75**, 356–357 (2012).
160. Cota, D. *et al.* Hypothalamic mTOR signaling regulates food intake. *Science* **312**, 927–30 (2006).
161. Khamzina, L., Veilleux, A., Bergeron, S. & Marette, A. Increased activation of the mammalian target of rapamycin pathway in liver and skeletal muscle of obese rats: Possible involvement in obesity-linked insulin resistance. *Endocrinology* **146**, 1473–1481 (2005).
162. Lambert, G. W., Schlaich, M. P., Eikelis, N. & Lambert, E. A. Sympathetic activity in obesity: a brief review of methods and supportive data. *Ann. N. Y. Acad. Sci.* **1454**, 56–67 (2019).
163. Esler, M. *et al.* Sympathetic nervous system and insulin resistance: From obesity to diabetes. *Am. J. Hypertens.* **14**, 304S-309S (2001).
164. Tentolouris, N., Liatis, S. & Katsilambros, N. Sympathetic System Activity in Obesity and Metabolic Syndrome. *Ann. N. Y. Acad. Sci.* **1083**, 129–152 (2006).
165. Morton, G. J., Cummings, D. E., Baskin, D. G., Barsh, G. S. & Schwartz, M. W. Central nervous system control of food intake and body weight. *Nature* **443**, 289–295 (2006).
166. Hardie, D. G. AMPK: positive and negative regulation, and its role in whole-body energy homeostasis. *Curr. Opin. Cell Biol.* **33**, 1–7 (2015).
167. Brix, L. M. *et al.* The co-chaperone FKBP51 modulates HPA axis activity and age-related maladaptation of the stress system in pituitary proopiomelanocortin cells. *Psychoneuroendocrinology* **138**, 105670 (2022).
168. Wang, L. FKBP51 regulation of AKT/protein kinase B phosphorylation. *Curr. Opin. Pharmacol.* **11**, 360–364 (2011).
169. Sakamoto, K. & Holman, G. D. Emerging role for AS160/TBC1D4 and TBC1D1 in the regulation of GLUT4 traffic. *Am. J. Physiol. - Endocrinol. Metab.* **295**, 29–37 (2008).
170. Smedlund, K. B., Sanchez, E. R. & Hinds, T. D. FKBP51 and the molecular chaperoning of metabolism. *Trends Endocrinol. Metab.* **32**, 862–874 (2021).

171. Hardie, D. G. AMP-activated/SNF1 protein kinases: Conserved guardians of cellular energy. *Nature Reviews Molecular Cell Biology* **8**, 774–785 (2007).
172. Shackelford, D. B. & Shaw, R. J. The LKB1-AMPK pathway: Metabolism and growth control in tumour suppression. *Nature Reviews Cancer* **9**, 563–575 (2009).
173. Bakula, D. *et al.* WIPI3 and WIPI4 β -propellers are scaffolds for LKB1-AMPK-TSC signalling circuits in the control of autophagy. *Nat. Commun.* **8**, (2017).
174. Bakula, D., Mueller, A. J. & Proikas-Cezanne, T. WIPI β -propellers function as scaffolds for STK11/LKB1-AMPK and AMPK-related kinase signaling in autophagy. *Autophagy* **14**, 1082–1083 (2018).
175. Gassen, N. C., Hartmann, J., Schmidt, M. V & Rein, T. FKBP5/FKBP51 enhances autophagy to synergize with antidepressant action. *Autophagy* **11**, 578–580 (2015).
176. Balsevich, G. *et al.* Interplay between diet-induced obesity and chronic stress in mice: Potential role of FKBP51. *J. Endocrinol.* **222**, 15–26 (2014).
177. Pereira, M. J. *et al.* FKBP5 expression in human adipose tissue increases following dexamethasone exposure and is associated with insulin resistance. *Metabolism* **63**, 1198–1208 (2014).
178. Sidibeh, C. O. *et al.* FKBP5 expression in human adipose tissue: potential role in glucose and lipid metabolism, adipogenesis and type 2 diabetes. *Endocrine* **62**, 116–128 (2018).
179. Ortiz, R., Joseph, J. J., Lee, R., Wand, G. S. & Golden, S. H. Type 2 diabetes and cardiometabolic risk may be associated with increase in DNA methylation of FKBP5. *Clin. Epigenetics* **10**, 82 (2018).
180. Hartmann, I. B. *et al.* The FKBP5 polymorphism rs1360780 is associated with lower weight loss after bariatric surgery: 26 months of follow-up. *Surg. Obes. Relat. Dis.* **12**, 1554–1560 (2016).
181. Marcovecchio, M. L. & Chiarelli, F. The effects of acute and chronic stress on diabetes control. *Sci. Signal.* **5**, (2012).

182. Lopresti, A. L. & Drummond, P. D. Obesity and psychiatric disorders: commonalities in dysregulated biological pathways and their implications for treatment. *Prog. Neuropsychopharmacol. Biol. Psychiatry* **45**, 92–99 (2013).
183. McIntyre, R. S. *et al.* The Association between Conventional Antidepressants and the Metabolic Syndrome. *CNS Drugs* **24**, 741–753 (2012).
184. Hartmann, J. *et al.* Pharmacological Inhibition of the Psychiatric Risk Factor FKBP51 Has Anxiolytic Properties. *J. Neurosci.* **35**, 9007–9016 (2015).
185. Maiarù, M. *et al.* The stress regulator FKBP51 drives chronic pain by modulating spinal glucocorticoid signaling. *Sci. Transl. Med.* **8**, 325ra19 (2016).
186. Manzari, M. T. *et al.* Targeted drug delivery strategies for precision medicines. *Nat. Rev. Mater.* **6**, 351–370 (2021).
187. Gassen, N. C. *et al.* FKBP51 inhibits GSK3 β and augments the effects of distinct psychotropic medications. *Mol. Psychiatry* **21**, 277–89 (2016).

Curriculum Vitae

Name	Alexander Häußl
Current Position	Project and Business Development at Biophyll GmbH
Date of Birth	*11.12.1987, Munich, Germany

Education:

Since 10/2015	PhD candidate, Max-Planck Institute of Psychiatry, Munich
10/2012 – 09/2015	Master of Science, Ludwig-Maximilians-University, Munich
02/2014 – 07/2014	University of Queensland, Brisbane, Australia
07/2013 – 11/2013	James Cook University, Townsville, Australia
10/2009 – 08/2012	Bachelor of Science, Maximilians-University, Munich
09/1998 – 07/2008	Abitur, Gymnasium Pfarrkirchen

Research and work Experience:

03/2019 – Current	Biophyll GmbH Project and Business Development
10/2015 – 2019	Max-Planck-Institute of Psychiatry, Munich Research Group of Dr. Mathias Schmidt, Neurobiology of Stress Resilience Focus on FKBP51 in the regulation of stress and metabolic disorders
02/2012 – 09/2015	Max-Planck-Institute of Neurobiology, Munich, Research Group of Moritz Helmstaedter Mapping of neocortical circuits
05/2015 – 07/2015	Weizmann Institute of Science, Rehovot, Israel Research Group of Prof. Alon Chen The effect of stress on hypothalamic neurogenesis
10/2014 – 03/2015	Max-Planck-Institute of Psychiatry, Munich Research Group of Dr. Mathias Schmidt, Neurobiology of Stress Resilience

04/2012 – 03/2013 Master Thesis: The role of hypothalamic FBKP51 in metabolism
Max-Planck-Institute of Psychiatry, Munich
Research Group of Dr. Mathias Schmidt, Neurobiology of Stress Resilience
Bachelor Thesis: Homer1 in reward seeking behavior

Grants, Awards and Scholarships:

2017 The 47th Meeting of European Brain Behaviour Society (EBBS), **Travel Grant**

2016 Helmholtz-Nature Medicine Diabetes Conference, Munich Germany,
Nature Reviews Endocrinology Abstract Prize, 4th

2015 EBPS Workshop 2015

Rehovot, Israel, **Weizmann Institute of Science Travel Award**

List of Publications

2022 T Bajaj, AS Häusl, MV Schmidt and NC Gassen: **FKBP5/FKBP51 on weight watch: central FKBP5 links regulatory WIPI protein networks to autophagy and metabolic control.**

Autophagy, 19 April 2022,

AS Häusl, T Bajaj, LM Brix, ML Pöhlmann, K Hafner, M de Angelis, J Nagler, F. Dethloff, G Balsevich, KW Schramm, P Giavalisco, A Chen, MV Schmidt, NC Gassen: **Mediobasal hypothalamic FKBP51 acts as a molecular switch linking autophagy to whole-body metabolism.**

Science Advances, Vol 8, Issue 10, March 2022:

Lea M Brix, **Alexander S. Häusl**, Irmak Toksöz, Joeri Bordes, Lotte van Doeselaar, Clara Engelhardt, Sowmya Narayan, Margherita Springer, Vera Sterlemann, Jan M. Deussing, Alon Chen, Mathias V. Schmidt: **The co-chaperone FKBP51 modulates HPA axis activity and age-related maladaptation of the stress in pituitary proopiomelanocortin cells.**

Psychoneuroendocrinology, Volume 138, April 2022,

2021 Clara Engelhardt, Fiona Tang, Radwa Elkhateib, Joeri Bordes, Lea Maria Brix, Lotte van Doeselaar, **Alexander S Häusl**, Max L Pöhlmann, Karla Schraut, Huanqing Yang, Alon Chen, Jan M. Deussing, and Mathias V. Schmidt: **FKBP51 in the Oval Bed Nucleus of the Stria Terminalis Regulates Anxiety-Like Behavior.**

eNeuro. 2021 Nov-Dec; 8(6): ENEURO-0425-21.2021.

Gassen, Nils C. and Stepan, Jens and Heinz, Daniel E. and Dethloff, Frederik and Bajaj, Tomas and Hafner, Kathrin and Wiechmann, Svenja and Ebert, Tim and Martinelli, Silvia and **Häusl, Alexander S.** and Pöhlmann, Max L. and Hermann, Anke and Pavenstädt, Hermann and Schmidt, Mathias V. and Philipsen, Alexandra and Turck, Christoph W. and Deussing, Jan M. and Kuster, Bernhard and Wehr, Michael C. and Kremerskothen, Joachim and Wotjak, Carsten T: **Hippo-Released WWC1 Primes Ampa Receptor Regulatory Complexes for Hippocampal Learning.**

Cell Reports <https://ssrn.com/abstract=3831460> or <http://dx.doi.org/10.2139/ssrn.3831460>

- AS Häusl**, LM Brix, J Hartmann, ML Pöhlmann, JP Lopez, D Menegaz, E Brivio, C Engelhardt, S Roeh, T Bajaj, L Rudolph, R Stoffel, K Hafner, HM Gross, JMHM Reul, JM Deussing, M Eder, KJ Ressler, NC Gassen, A Chen, MV Schmidt: **The co-chaperone Fkbp5 shapes the acute stress response in the paraventricular nucleus of the hypothalamus of male mice.**
Molecular Psychiatry, March 2021,
- 2019** **AS Häusl**, G Balsevich, NC Gasse, MV Schmidt: **Focus on FKBP51: A molecular link between stress and metabolic disorders.**
Molecular metabolism, 2019, 29: 170-181.
- 2018** ML Pöhlmann, **AS Häusl**, D Harbich, G Balsevich, C Engelhardt, X Feng, M Breitsamer, F Hausch, G Winter, MV Schmidt: **Pharmacological modulation of the psychiatric risk factor FKBP51 alters efficiency of common antidepressant drugs.**
Front. Behav. Neurosci., 2018, 12:262.
- 2017** Georgia Balsevich*, **Alexander S. Häusl***, Carola W. Meyer, Stoyo Karamihalev, Xixi Feng, Max L. Pöhlmann, Carine Dournes, Andres Uribe-Marino, Sara Santarelli, Christiana Labermaier, Kathrin Hafner, Tianqi Mao, Michaela Breitsamer, Marily Theodoropoulou, Chrisitan Namendorf, Manfred Uhr, Marcelo Paez-Pereda, Gerhard Winter, Felix Hausch, Alon Chen, Mathias H. Tschöp, Theo Rhein, Nils C. Gassen, and Mathias V. Schmidt: **Stress-responsive FKBP51 regulates AKT2-AS160 signaling and metabolic function.**
Nature Communication 8, Article number 1725 (2017). * shared first authorship.
- 2015** J Hartmann, KV Wagner, S Gaali, A Kirschner, C Kozany, G Rührter, N Dedic, **AS Häusl**, L Hoeijmakers, S Westerholz, C Namendorf, T Gerlach, M Uhr, A Chen, JM Deussing, F Holsboer, F Hausch, MV Schmidt: **Pharmacological inhibition of the psychiatric risk factor FKBP51 has anxiolytic properties.**
Journal of Neuroscience, 2015, 35 (24): 9007-9016

KV Wagner, J Hartmann, C. Labermaier, **AS Häusl**, G Zhao, D. Harbich, B Schmid, XD Wang, S Santarelli, C Kohl, NC Gassen, N Matosin, M Schieven, C Webhofer, CW Turck, L Lindemann, G Jascke, JG Wettstein, T Rein, MB Müller, MV Schmidt: **Homer1/mGluR5 activity moderates vulnerability to chronic social stress.**
Neuropharmacology, 2015, 40(5): 1222-1233

2014 KV Wagner, **AS Häusl**, ML Pöhlmann, J Hartmann, C Labermaier, MB Müller, MV Schmidt: **Hippocampal Homer1 levels influence motivational behavior in an operant conditioning task.**
PLOS ONE, 2014; 9(1): e85975

Acknowledgement

This thesis carries my name, but all the experiments and new data would not have been possible without the tremendous help and support of my colleagues, family, and friends. So now I want to thank them.

Mathias, thank you for everything you have done during the last 10 (!!!) years, since I started my Bachelor thesis in your lab. You are an amazing supervisor in science and also a great tutor in life. You gave me the scientific freedom to conduct and design my experiments and stopped me when my enthusiasm got the best of me.

Nils, thank you for your support and a lot of fresh ideas during my thesis. It is always fun working with you on new projects, and I hope we will continue to do so in the future. The next whisky session is due!

Special thanks go to my shared first authors, Lea, Georgia, and Thommy. All of you are fantastic scientists and have become good friends over the years. Without your ideas, hard work, and efforts, this thesis would not have been possible. Thank you!

Dani, Bianca, and Lisa, it was great to have you on my side. You are the best in the lab, and I am grateful that you shared your wisdom with me and that I got to learn from you. Thank you for being so supportive!

I also want to thank Jakob and Klaus, who were there from the beginning and supported me with open eyes and ears. Furthermore, I would like to thank all the other former and current lab members that contributed to my work directly or indirectly: Clara Engelhardt, Joeri Bordes, Karla Schraut, Kathrin Hafner, Lotte van Doeselaar, Maya Reinhardt, and Xiao-Dong Wang.

Max, it was a pleasure sharing an office with you. We always supported each other with our experiments, data analysis, and everything else. We might work together again in the future but for sure will stay best friends!

My parents guided me throughout my life and supported my every step. I sincerely want to thank my dad, who stayed patient and gave me the time to finish this thesis during my daily job.

Last but not least, I would like to thank my wife, Conny, and my newborn son, Jakob. I know it was not always easy for us to do so many things simultaneously, but I think it turned out very well. I am very grateful to have you two on my side. Conny, we went through all the ups and downs together, and without your patience and understanding, it would not have been possible to finish this thesis. Jakob, you are just one and a half years old, but your curiosity and happiness is a daily inspiration for me. I am looking forward to enjoying every day together with my little family.

Declaration of Contribution

Chapter 3.1: Stress responsive FKBP51 regulates AKT2-AS160 signaling and metabolic function

Georgia Balsevich*, Alexander S. Häusl*, [...], Theo Rhein, Nils C. Gassen and Mathias V. Schmidt. *Nature Communications*, 1725 (2017).

*contributed equally

Contributions:

G.B. conceived the project and designed the experiments in cooperation with **A.S.H.**, N.C.G., M.V.S

G.B. performed the following experiments:	A.S.H.: performed the following animal and cell culture experiments:
- All FKBP51 KO vs. WT experiments	- acute SAfit2 treatment (Fig. 3a-e, Fig. S4a-e)
- 10 d SAfit2 treatment	- Cell culture experiments (Fig. 4c, Fig. 5a-b, in cooperation with N.C.G.)
- Molecular characterization of FKBP51	- Isolation of Primary EDL myotubes + experiments (Fig. 4d, Fig. 5c-f in cooperation with N.C.G)
- Cell culture experiments	
A.S.H. and G.B performed together:	
- chronic SAfit2 treatment (Fig. 3H-I) Fig. S5A-G)	

G.B.: Data analysis, in cooperation with NCG, and SK

G.B.: Wrote initial version of the manuscript, in cooperation with MVS and ASH

We hereby confirm the above statements.

.....

Alexander Häusl

.....

Georgia Balsevich

.....

PD. Dr. Mathias Schmidt

Chapter 3.2: Mediobasal hypothalamic FKBP51 acts as a molecular switch linking autophagy to whole-body metabolism

Alexander S. Häusl*, Thomas Bajaj*, [...], Mathias V. Schmidt and Nils C. Gassen

Published in Science Advances. *contributed equally

Contributions:

A.S.H conceived and designed the research project in cooperation with M.V.S., N.C.G, and T.B.

A.S.H. designed and performed the following animal experiments, surgeries, and data analysis:	T.B designed and analyzed the following molecular experiments and data analysis:
- Data analysis, Figure design (Fig. 2A – H, Fig. 3)	- Human and murine metabolomics analysis (Fig. 1A-B, Fig. S1, Fig. S2)
- In-Vivo autophagic flux HFD vs Chow (Fig. S6A-D, molecular analysis by N.C.G, Fig. S6E-H)	- Design and creation of Crispr-CAS murine FKBP51 KO cells (Fig. S2A-C)
- FKBP51 overexpressing experiments (Fig. 4D-G, Fig. 5, Fig. S7, S8, molecular analysis by N.C.G)	- Autophagic flux in FKBP51 KO cells (Fig. 2I – 2J, Fig. S3H-I), TFEB nuclear localization (Fig. 2K-L)
- FKBP51 deletion Fig. S7, S8 (experiments by L.M.B, data analysis by A.S.H)	- Hypusination of eIF5A (Fig. S4)
- Figure design of Fig. 5 (molecular analysis by N.C.G, statistics by A.S.H.)	- Blots and analysis of Fig. S9
- In-Vivo alpha-MPT injections and turnover rate calculations + protein statistics (Fig. S6, Fig. S8 Catecholamine measurements by M.D.A, J.N.)	

A.S.H. wrote the initial version of the manuscript in cooperation with MVS and N.C.G., and T.B.,

We hereby confirm the above statements.

.....

Alexander Häusl

.....

Thomas Bajaj

.....

PD. Dr. Mathias Schmidt

Chapter 3.3: The co-chaperone Fkbp5 shapes the acute stress response in the paraventricular nucleus of the hypothalamus of male mice

Alexander S. Häusl*, Lea M. Brix*, [..], and Mathias V. Schmidt.

Published in *Molecular Psychiatry* 26, 3060-3076 (2021).

*contributed equally

Contributions:

A.S.H conceived and designed the research project in cooperation with M.V.S., and L.M.B.

A.S.H and L.M.B. managed the mouse lines and genotyping together.

A.S.H. designed and performed the following animal experiments, surgeries, and data analysis:	L.M.B designed and performed the following animal experiments, surgeries, and data analysis:
- FKBP51 specific PVN deletion (Fig. 1A-1E, Fig-S1A-E, S2A-C)	- CRH specific FKBP51 overexpression, (Fig. 6A-6D, Fig. S9 A-D)
- FKBP51 overexpression experiments (Fig. 2A-2F, Fig. S3A-E)	- Representative pictures of ISH and RNAscope imaging and analysis
- FKBP51 rescue (Fig. 3A, 3C-3E, Fig. S5A-F)	- ISH experiments, imaging and analysis, FKBP51 rescue (Fig. 3B)
- Animal work for GR phosphorylation (molecular analysis by N.C.G, statistic by A.S.H.)	- FKBP51 rescue control experiments (Fig. S4A-E)
- Single cell sequencing Figure design (Fig. 5A-D, data from JP.L. and analysis by JP. L and S.R.)	- FKBP51 rescue surgeries + ACTH measurements (Fig. S5C)
- mRNA scope cell counting + analysis (Fig. 5E, 5F, Fig. S7, S8, pictures provided by J.H.)	

A.S.H. wrote the initial version of the manuscript in cooperation with MVS and L.M.B

We hereby confirm the above statements.

.....

Alexander Häusl

.....

Lea M. Brix

.....

PD. Dr. Mathias Schmidt

Eidesstattliche Erklärung

Ich versichere hiermit an Eides statt, dass die vorgelegte Dissertation von mir selbständig und ohne unerlaubte Hilfe angefertigt ist.

München, den **19.05.2022**

..... **Alexander Häusl**

(Unterschrift)

Erklärung

Hiermit erkläre ich, *

- dass die Dissertation nicht ganz oder in wesentlichen Teilen einer anderen Prüfungskommission vorgelegt worden ist.
- dass ich mich anderweitig einer Doktorprüfung ohne Erfolg **nicht** unterzogen habe.
- ~~dass ich mich mit Erfolg der Doktorprüfung im Hauptfach
und in den Nebenfächern
bei der Fakultät für der
(Hochschule/Universität)
unterzogen habe.~~
- ~~dass ich ohne Erfolg versucht habe, eine Dissertation einzureichen oder mich der Doktorprüfung zu unterziehen.~~

München, den..... **19.05.2022**

..... **Alexander Häusl**

(Unterschrift)

*) Nichtzutreffendes streichen